GLIDING PROPERTIES OF THE FLEXOR TENDON IN ZONE 2: TENDON REPAIR AND PULLEY RESECTION

Thesis submitted for the degree of
Doctorate of Medicine
at the University of Leicester

by

Miss Ladan Hajipour
MB ChB, FRCS (Tr & Orth)
Department of Health and Science
University of Leicester
2016

Very little grows

On jagged rocks.

Be Ground.

Be Crumbled.

So wildflowers will

come up

Where you are.

-Rumi

To

Gabriel, for his presence.

Sathi, for his endurance.

Kobra and Ali, for their prayers.

Mr Kershaw, for his support.

Professor Dias, for his patience.

Professor Harper, for his vision.

Abstract

Title: Gliding properties of the flexor tendon in zone 2: Tendon repair and pulley resection

Author: L. Hajipour

Flexor tendon injuries can lead to significant morbidity and the repair of such injuries in zone 2 is technically demanding. Technical skills from bench models transfer very well to practical use, and many mechanical simulators have been developed for investigating optimal flexor tendon repairs.

Embalmed cadavers are markedly different from fresh human tissue, and the latter is becoming increasingly difficult to obtain due to public concern over the handling of tissue removed from cadavers and the risk of transmissible diseases. Pig and chicken tendons have previously been used due to their similar anatomy to human tendons, to allow basic repair and mechanical testing of suture techniques. Turkey tendons are larger than chicken tendons, allowing for better handling but have not been studied or used routinely for flexor tendon studies.

The outcome of flexor tendon repairs relies heavily on post-operative rehabilitation and a strong, trigger free tendon repair that can withstand active movements. The surface changes of a repaired tendon can lead to increased friction and therefore an increased risk of rupture. There are currently no studies in the literature that have looked at: 1) the anatomy of turkey feet and their relevance in tendon repair research; 2) surface changes to the flexor tendon following tendon repair; and 3) the effect of pulley resection following tendon repair in paired specimens from the same animal. There are no strong studies in the literature that show whether paired tendons from the same animal exhibit the same gliding properties under experimental settings. This research aims to answer these questions.

Aims

As the structure of the thesis corresponds closely to its aim they are listed at the start. There are 6 areas for investigation in this study.

1. To study the animal model, turkey feet structure and tendons, and assess their suitability with regards to flexor tendon experimentation.

2. To study the gliding surfaces of the flexor tendon (volar) and the corresponding pulley under electron microscopy before and after a tendon repair in order to evaluate the effect of the tendon repair technique on the gliding surfaces.

3. To determine if the gliding resistance of paired tendons from the same animal behave in the same manner by measuring their gliding resistance and coefficient of friction.

4. To evaluate the effect of a full tendon repair on the gliding resistance and coefficient of friction (at the A2 pulley level) when compared to the intact tendon for paired specimens, and to understand the effect of increasing the flexion angle and load following tendon repair.

5. To evaluate the effect of sequential pulley resection on the gliding resistance and coefficient of friction (at the A2 pulley level) when compared to the intact tendon for paired specimens, and to understand the effect of increasing the flexion angle and load.

6. To evaluate the individual effect of a suture knot and peripheral suture on the gliding resistance and coefficient of friction at the A2 pulley level and to understand the effect of increasing the flexion angle and load.

7. To understand which component of a tendon injury and repair has the most significant effect on the coefficient of friction and gliding resistance.

Acknowledgements

I would like to thank: Professor Dias for his supervision, tremendous patience and expert guidance throughout this research; Mr Bhowal for his time, support and close supervision of the research work; Mr Ullah for taking me through the first few steps of starting this research; and my good friends Mr Gulihar and Mr Kennedy, for their assistance in the laboratory.

I would also like to thank Mr John Baker for his ingenious engineering of the control board, Miss Natalie Allcock in the University of Leicester Electron Microscopy laboratory for her work on preparing the specimens and excellent images, Professor Philip Scarf (University of Salford) and Mr Nick Taub (University of Leicester) for their help in the statistical analysis, and Leicestershire Fresh Turkey Farm for their kind and meticulous preparation of the specimens.

Finally, I would like to thank my Gabriel for growing up and understanding me as I completed this research, Sathi for his daily motivation and support throughout, and most importantly, my mum and dad for making me what I am.

Table of Contents

List of Tables

List of Figures

List of Abbreviations

CF	Coefficient of Friction
CGRP	Calcitonin Gene-Related Peptide
CPD	Critical Point Drying
DBO	Dorsal Blocking Orthosis
DIPJ	Distal Inter-Phalangeal Joint
ECM	Extra Cellular Matrix
FDI	*Flexor digitorum intermediate*
FDP	*Flexor digitorum profundus*
FDS	*Flexor digitorum superficialis*
FPB	*Flexor policis brevis*
FPL	*Flexor policis longus*
GAG	Glycosaminoglycan
GR	Gliding Resistance
HA	Hyaluronic Acid
HMDS	Hexemethyldisilazane
IPJ	Inter-Phalangeal Joint
MCPJ	Metacarpophalangeal Joint
MGH	Massachusetts General Hospital
MK	Modified Kessler
MMP	Matrix Metalloproteinases
MTJ	Muscle-Tendon Junction
N	Newton
OTJ	Osseo-Tendon Junction
PDS	Polydioxanon
PIPJ	Proximal Inter-phalangeal Joint
SEM	Surface Electron Microscopy

Chapter 1 - Introduction

1.1 Epidemiology and Cost Analysis of Flexor Tendon Injuries

Based on a recent epidemiological study by Clayton and Court-Brown (2008), tendon injuries of the hand and forearm account for 20.3% of all soft tissue injuries per year. Of these, 4.5% are flexor tendon injuries, which are commonest in males in their second and third decades (unimodal distribution), with the incidence steadily declining with age thereafter, whereas they remain low in women for all different age groups. This difference has been thought to be related to higher industrial-related occupational activities in male patients (72% of all injuries) (Clayton and Court-Brown, 2008).

Rosberg et al. (2003) investigated the cost of flexor tendon repairs in zone 2, within and outside the healthcare sector in Sweden. Of the 135 patients that were evaluated, 68% were employed at the time of their injury, and the little finger was found to be the most frequently injured (43%), usually with a knife (46%), whilst 30% of the injuries were work related, with the *Flexor digitorum superficialis* (FDS) being the most commonly injured (28%). The average cost of healthcare per person with active mobilisation was estimated at €6,000, whereas for complete immobilisation rehabilitation there were higher rates of complications and secondary surgery (40%), and the average time away from work was 73 days. The cost outside the healthcare sector, defined as the loss of production activity, was measured as €10,100 per person, with treatment complications leading to a 57% increase in the total cost (Rosberg et al., 2003).

In the UK, over £100 million is spent each year in treating hand injuries, including flexor tendon injuries. However, the indirect expense to patients and the consequences of permanent disability are seldom considered (Dias and Garcia-Elias, 2006).

1.2 Anatomy of the Flexor Tendon in the Human Hand

The forearm muscles provide digital motion in the hand by means of the flexor tendons which connect the muscle to the small bones of the fingers. The FDS has two heads; the humero-ulnar and radial, and four long tendons come off this muscle near the wrist and travel through the carpal tunnel. The *Flexor digitorum profundus* (FDP) originates in the upper 3/4 of the anterior forearm and lies deep to the FDS muscle, fanning out into four tendons, one to each finger (index to little fingers).

There are three phalanxes to each finger (proximal, middle and distal phalanx) and two to the thumb (proximal and distal phalanx). The FDS and FDP insert at the base of the middle and distal phalanx, respectively. At the base of the fingers the FDS tendon divides (chiasma), allowing the FDP tendon to pass through in order to reach the distal phalanx. The *Flexor policis longus* (FPL) and *Flexor policis brevis* (FPB) are inserted into the distal and proximal phalanx of the thumb, respectively. Contraction of the FDS and FDP in the forearm leads to flexion of the proximal inter-phalangeal joint (PIPJ) and distal inter-phalangeal joint (DIPJ), respectively (Drake and Vogl, 2014). However, FDP contraction leads to PIPJ and DIPJ flexion, as the tendon crosses both joints.

Finger flexor tendons are covered by a synovial sheath extending from the proximal edge of the A1 pulley to the DIPJ. The sheath is multi-layered, functions as an ultra-filtration membrane, produces synovial fluid (rich in hyaluronate), and provides nutrition to the tendon and also lubrication for tendon gliding (Doyle, 1989, Lundborg and Myrhage, 1977). Other non-synovial tendons are surrounded by loose areolar connective tissue called paratenon, lined on the inner surface by synovial cells (Jozsa and Balint, 1978, Williams, 1986). Paratenon allows for the free movement of a tendon against the surrounding tissues (Hess et al., 1989) and is composed of type I and type III collagen and elastic fibrils (Kvist et al., 1985).

Under the paratenon or tendon sheath, the entire tendon is surrounded by a fine connective tissue sheath called the epitenon (Figure 1.1). On the outer surface, the epitenon is adjacent to the paratenon and on the inner surface to the endotenon. The endotenon is a thin network of connective tissue inside the tendon, which has a well-developed crisscross pattern of collagen fibrils that binds all the individual fibres, and

in larger units, the fibre bundles together (Elliott, 1965, Jozsa et al., 1991, Kastelic et al., 1978, Rowe, 1985). This allows fibre groups to glide past each other and carries blood vessels, nerves, and lymphatics to the deeper portion of the tendon (Elliott, 1965, Hess et al., 1989).

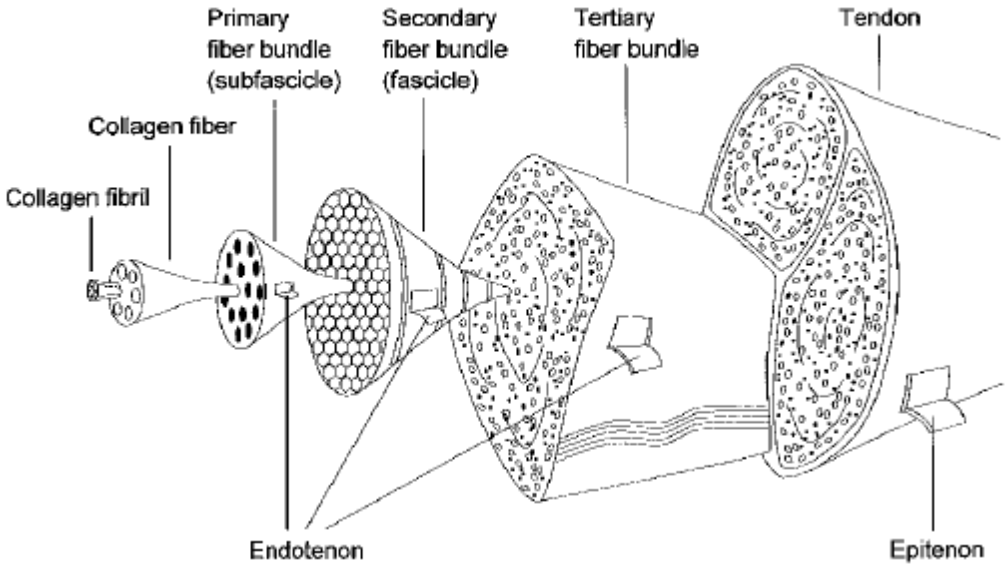

Figure 1.1: The structure of a tendon

With permission from: Kannus (2000)

At the muscle-tendon junction (MTJ), tendinous collagen fibrils are inserted into deep recesses formed by myocyte processes, allowing the tension generated by intracellular contractile proteins of the muscle fibres to be transmitted to the collagen fibrils. This complex architecture reduces the tensile stress exerted on the tendon during muscle contraction, although due to this structural architecture it remains the weakest point of the muscle-tendon unit (Kvist et al., 1991). The osseo-tendon junction (OTJ), where the tendon inserts onto the bone, is composed of four zones: a dense tendon zone, fibro-cartilage, mineralised fibro-cartilage, and bone (Benjamin and Ralphs, 1998). The specialised structure of the OTJ prevents collagen fibre from bending, fraying, shearing and failure (Evans et al., 1990).

1.3 Tendon Structure

1.3.1 Tendon Cells

Tendons vary in form and can be rounded cords, strap-like bands or flattened ribbons (Benjamin and Ralphs, 1998). When healthy, tendons appear brilliant white and have a fibro-elastic texture, with 70% of the tendon dry mass being composed of water. The dry component of the tendon, 30% of the total tendon mass, is composed of tenoblasts and tenocytes, lying within the extracellular matrix (ECM) between the collagen fibres and along the long axis of a tendon (O'Brien, 1997, Williams, 1986). Tenoblasts are immature tendon cells and are spindle-shaped, with numerous cytoplasmic organelles reflecting their high metabolic activity. As they age, tenoblasts become elongated and transform into tenocytes, with a lower nucleus-to-cytoplasm ratio than tenoblasts and decreased metabolic activity. Together, tenoblasts and tenocytes account for 90-95% of the cellular elements of tendons (Kannus et al., 2000). Under pathological conditions, many other cell types, such as inflammatory cells, macrophages, and myofibroblasts, can be observed within tendon tissue (Jozsa and Kannus, 1997).

The remaining 5-10% of the cellular elements of tendons consist of chondrocytes at the bone attachment and insertion sites, synovial cells of the tendon sheath, and vascular cells, including capillary endothelial cells and smooth muscle cells of arterioles (Sharma and Maffulli, 2005).

Tenocytes synthesise collagen and all components of the ECM, and they are active in energy generation (O'Brien, 1997). Oxygen consumption by tendons and ligaments is 7.5 times lower than in skeletal muscles (Vailas et al., 1978). The energy generation processes, the aerobic Krebs cycle and anaerobic glycolysis, both occur in human tenocytes (Jozsa et al., 1979, Kvist et al., 1987, Tipton et al., 1975b, Tipton et al., 1975), although with increasing age, the metabolic pathways shift from aerobic to more anaerobic energy production (Kannus and Jozsa, 1991). The low metabolic rate and well-developed anaerobic energy generation capacity allow tendons to carry loads and maintain tension for long periods of time, whilst avoiding the risk of ischemia and

subsequent necrosis. However, a low metabolic rate results in slow healing after injury (Williams, 1986).

1.3.2 Collagen

At least 28 different types of collagens occur within vertebrates (numbered I-XXVIII; some with common names), together with a large group of collagen-like proteins (Myllyharju and Kivirikko, 2001). However, type I collagen is the most abundant and is the principal component of bone, tendons, skin, and ligaments, as well as in the cornea. It is also found in most interstitial connective tissues, where it provides tensile strength to tissues, regulates cell adhesion, and facilitates cell migration (Kadler et al., 2007).

Collagens contain three polypeptide chains, which are held together by inter-chain hydrogen bonds and arranged in hierarchical levels of increasing complexity, beginning with tropocollagen (a triple-helix polypeptide chain). Soluble tropocollagen molecules form cross-links to create insoluble collagen molecules, which then aggregate progressively into microfibrils and then subsequently into collagen fibrils (diameters of ~25–500 nm) which are clearly visible via scanning electron microscopy (SEM) (Gelse et al., 2003, Kadler et al., 2007, Shoulders and Raines, 2009). A bunch of collagen fibrils forms a collagen fibre, which is the basic unit of a tendon (Figure 1.1) (Jozsa and Kannus, 1997). A collagen fibre is the smallest tendon unit which is visible using a light microscope and is aligned from end to end within a tendon (Curwin, 1997). Although collagen fibres are mainly oriented longitudinally, fibres also run transversely and horizontally, forming spirals and plaits (Chansky and Iannotti, 1991, Jozsa et al., 1991).

The main composition of a tendon matrix is type I collagen, which accounts for 65-80% of a tendon's dry mass, with small amounts of type III and IV collagen (Curwin, 1997, Hess et al., 1989, Jozsa et al., 1989, Kirkendall and Garrett, 1997, O'Brien, 1997, Tipton et al., 1975). Tendon-to-tendon variation is present, and within a tendon there is site-to-site variation with regards to collagen content and type distribution (Fan et al., 1997).

Elastic fibres account for approximately 1–2% of the dry mass of a tendon and only 10% of healthy human tendons (Carlstedt, 1987, Jozsa and Balint, 1978), whereas in

the aorta, elastic fibres make up 30–60% of the dry weight (Kirkendall and Garrett, 1997). The fibrocartilage and mineralised fibrocartilage zones of the oseotendinous junction contain elastic fibres (Becker and Krahl, 1978). In some pathological conditions, such as Ehlers-Danlos syndrome and chronic uraemia, the number and volume of the tendinous elastic fibres is increased (Jozsa and Balint, 1978, Jozsa et al., 1979). Although the function of elastic fibres is not entirely clear, they are thought to contribute to the recovery of the wavy configuration of collagen fibres after tendinous stretching (Butler et al., 1978).

In human tendons the diameter of the tertiary bundles varies from 1000-3000 nm and the secondary bundles from 150-1000 nm. The diameter of both bundle types is directly related to the macroscopic size of the tendon, so that the lowest values are seen in the smaller tendons, such as the flexors and extensors of the fingers and toes, and the largest diameters in the bigger tendons, such as the Achilles and tibialis anterior tendons (Jozsa and Kannus, 1997).

1.3.3 Extra Cellular Matrix

The ground substance of the ECM, which surrounds the collagen and the tenocytes, is composed of proteoglycans, glycosaminoglycans (GAG), glycoproteins and several other small molecules (Kannus, 2000) (Figure 1.2).

Proteoglycans are composed of a core protein with multiple GAG attachments, and is attached to hyaluronic acid (HA) via a linker protein. The strongly hydrophilic nature of proteoglycans enables the rapid diffusion of water soluble molecules and the migration of cells. Proteoglycans can vary in consistency depending on the relative proportions of HA and chondroitin sulphate present (Karpakka, 1991). The major biological function of proteoglycans is derived from the GAG component of the molecule, which provides hydration and swelling pressure to the tissue, thus enabling it to withstand compressional forces. Proteoglycans are also involved in cell and tissue activities, for example decorin, which is present in many connective tissues, may have a role in regulating collagen fibril formation (Yanagishita, 1993).

Tendon tissue contains various non-collagenous proteins, such as glycoproteins, which are macromolecules and have possess the ability to bind other macromolecules or cell

surfaces together (Kannus et al., 1998). Adhesive glycoproteins, such as fibronectin and thrombospondin, participate in the repair and regeneration processes within tendons (Jozsa et al., 1991). Tenascin-C, another tendon ECM component, is thought to play a role in collagen fibre alignment and orientation, and is found in the tendon body and at the OTJ and MTJ (Kannus et al., 1998, Mackie and Ramsey, 1996).

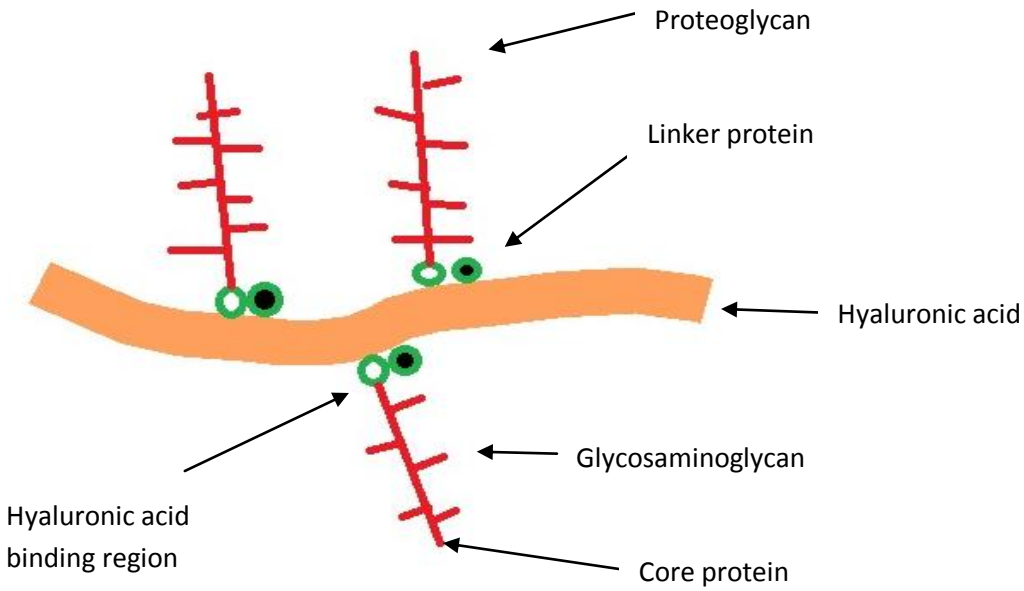

Figure 1.2: The structure of proteoglycan

Within tendons, many inorganic components involved in growth, development, and normal metabolism of musculoskeletal structures have been detected, and these form less than 0.2% of the tendon dry mass (Lappalainen et al., 1982, Schor et al., 1973). The most abundant is calcium, which is 0.001–0.01% of the tendon dry weight in the tensional area of a normal tendon, and 0.05–0.1% in the insertion zone. In pathological conditions, such as calcifying tendinopathy, a 10 to 20-fold increase in the local calcium level can be detected (Jozsa et al., 1989). Other components that have been identified include magnesium, manganese, cadmium, cobalt, copper, zinc, nickel, lithium, lead, fluoride, phosphor, and silicon. Copper has been determined to have an important role in the formation of collagen cross-linking, while manganese is required for several enzymatic reactions during the synthesis of connective tissue molecules, and calcium has a key role in the development of the OTJs, with all required for the tendon healing process (Minor, 1980).

1.3.4 Tendon Blood Supply

Tendons receive their blood supply from two main sources: the intrinsic systems at the MTJ and OTJ, and from the extrinsic system via the paratenon or the synovial sheath (Carr and Norris, 1989). The ratio of blood supplied from the intrinsic and extrinsic systems varies from tendon to tendon (Sharma and Maffulli, 2006). For example, the central third of a rabbit's Achilles tendon receives 35% of its blood supply from the extrinsic system (Naito and Ogata, 1983). At the MTJ, perimyseal vessels are unlikely to extend beyond the proximal third of a tendon, while the blood supply from the OTJ is limited to the insertion zone, although it communicates with periosteal vessels (Carr and Norris, 1989).

In tendons enveloped by sheaths, branches from major vessels pass through the vincula (mesotenon) to reach the visceral layer of the synovial sheath, where they form a plexus that supplies the superficial and deep parts of a tendon (Jozsa and Kannus, 1997). These penetrating vessels travel in the endotenon septae, and form a connection between the peri- and intra-tendinous vascular networks. In the absence of a synovial sheath, the extrinsic paratenon vessels course transversely, and branch repeatedly to form a complex and deep vascular network (Field, 1971, Kannus, 2000, Reynolds and Worrell, 1991) .

Tendon vascularity is compromised at the junctional zones and sites of torsion, friction or compression. A zone of hypovascularity is present on the dorsal surface of the FDP tendon adjacent to the volar plate and within 1 cm of the tendon insertion (Leversedge et al., 2002). In general, tendon blood flow declines with increasing age and mechanical loading (Astrom, 2000). During peak exercise peritendinous blood flow reaches only approximately 20% of the maximal blood flow capacity in that area (Boushel et al., 2000).

1.3.5 Tendon Innervations

Tendons are innervated from cutaneous, muscular, and peritendinous nerve trunks. At the MTJ nerve fibres enter at the paratenon level, branch into the epitenon and terminate as nerve endings on its surface. Myelinated nerve fibres function as specialised mechanoreceptors (Golgi tendon organs) to detect changes in pressure or

tension, and are most numerous at the insertion of tendons into the muscle (Lephart et al., 1997). Golgi tendon organs are a delicate capsule of connective tissue that enclose a group of large myelinated nerve fibres, which terminate between bundles of collagen fibres of a tendon (Barr and Kiernan, 1988).

Un-myelinated nerve endings act as nociceptors (sense and transmit pain), and both sympathetic and para-sympathetic fibres are present within tendons and control blood flow into a tendon (Ackermann et al., 2001).

1.3.6 Tendon Biomechanics

Tendons transmit the force generated by muscle to the bone, and absorb part of the external forces thus limiting muscle damage (Best and Garrett, 1994). Tendons are viscoelastic tissues, which display stress relaxation (the time dependent decrease in applied stress that is required to maintain a constant elongation) and creep (the time dependent elongation of tissue when subjected to a constant stress) (Viidik, 1996).

The mechanical behaviour of collagen is dependent upon the number and types of intra- and inter-molecular bonds (Fyfe and Stanish, 1992). This is best demonstrated by the stress-strain curve of a tendon as shown in Figure 1.3. At rest, collagen fibres and fibrils display a crimped configuration (Diamant et al., 1972). The initial concave portion of the curve (toe region), where a tendon is strained up to 2%, represents flattening of this crimped pattern (Butler et al., 1978). Beyond this point, a tendon deforms in a linear fashion due to intra molecular sliding of collagen triple helices, and the fibres become more aligned (Mosler et al., 1985). If the strain remains below 4%, a tendon behaves in an elastic fashion, and returns to its original length when unloaded (Curwin and Stanish, 1984). However, when the strain exceeds 4%, there is microscopic failure within a tendon due to intra-fibril damage caused by molecular slippage (Sasaki et al., 1999). X-ray diffraction studies have demonstrated that molecular elongation initially leads to collagen fibril elongation, but as stress increases, the gap between molecules increases, eventually leading to slippage of the lateral adjoining molecules, and complete failure occurs rapidly as the fibres recoil at the ruptured end (Best and Garrett, 1994).

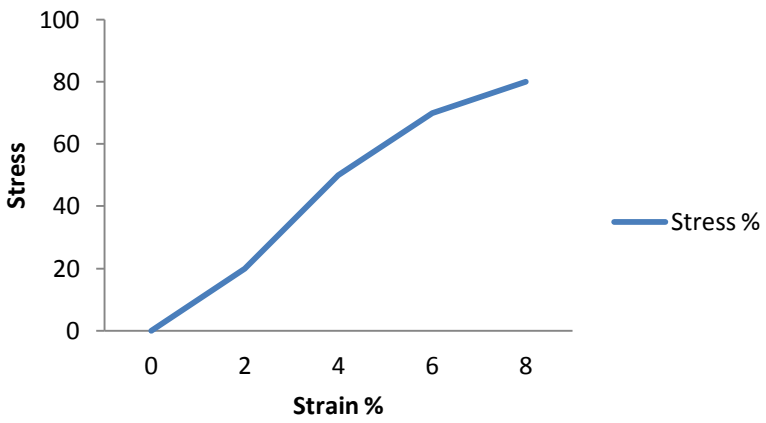

Figure 1.3: Stress-strain curve for a tendon

With permission from: Sharma and Maffulli, (2006)

The tensile strength of a tendon is related to the thickness and collagen content, and a tendon with an area of 1 cm^2 is capable of bearing 500-1000 kg (Shadwick, 1990). In the human Achilles tendon, forces of 9 KN, corresponding to 12.5 times body weight, have been recorded during running (Komi et al., 1992).

Tendons are at the highest risk of rupture if tension is applied quickly, thereby reducing the time for stress relaxation, and the highest forces are seen during eccentric muscle contraction, when there is muscle elongation despite active contraction (Fyfe and Stanish, 1992).

1.3.7 Physiological Responses of Tendons

Physical training in animal experiments has been shown to lead to an improvement in tensile strength, elastic stiffness, weight and the cross-sectional area of tendons (Kannus et al., 1997). These findings were found to correlate with an increase in collagen and ECM synthesis by tenocytes. Little data exists on the effect of exercise on human tendons; however, intensively trained athletes are reported to have thicker Achilles tendons than control subjects (Archambault et al., 1995, Maffulli and King, 1992).

Research has shown that lower tensile strength and strain at the point of failure in rabbit patellar tendons following injury and prolonged immobilisation was due to tendon atrophy (Yamamoto et al., 1999). However, due to a low metabolic rate and

vascularity, these changes occur slowly (Maffulli and King, 1992, Maganaris et al., 2006). With age, tendon and muscle properties, such as function and strength, decline due to aging tenocytes and the reduced production of collagen and its cross-linking, leading to tendon stiffness (Macaluso and De Vito, 2004). However resistance training in old age can partly reverse some of these ageing effects (Bailey et al., 1974, Maganaris et al., 2004, Reeves et al., 2003).

1.3.8 Tendinopathy

Tendon injuries can be acute or chronic, and caused by intrinsic or extrinsic factors, either alone or in combination. Intrinsic factors, such as alignment and biomechanical faults, are thought to be the cause in two-thirds of athletes with Achilles tendon disorders (Kvist, 1994). Excessive loading of tendons during vigorous physical training is the main stimulus for degeneration, and in the presence of intrinsic risk factors can lead to a greater risk of inducing tendinopathy (Selvanetti et al., 1997).

Tendons respond to repetitive injury with either inflammation of their sheath, degeneration of their body, or a combination of both. Although the aetiology of tendinopathy remains unclear, hypoxia, ischemic damage, oxidative stress, hyperthermia, impaired apoptosis, inflammatory mediators, fluoroquinolones, and a matrix metalloproteinase imbalance have all been implicated as mechanisms of tendon degeneration (Benazzo et al., 2000, Bestwick and Maffulli, 2004, Birch et al., 1997, Goodship et al., 1994, Yuan et al., 2003). Macroscopically, tendons lose their normal white appearance and become grey or brown (Khan et al., 1999). Histologically, there is a picture of disordered and haphazard healing with the absence of inflammatory cells, non-inflammatory intra tendinous collagen degeneration, fibre disorientation and thinning, hyper-cellularity, scattered vascular in-growth, and increased inter-fibrillar GAG (Jozsa and Kannus, 1997). Frank inflammatory lesions and granulation tissue are mostly associated with tendon rupture (Maffulli et al., 2000).

1.3.9 Tendon Healing after Acute Injuries

1.3.9.1 Cellular Response

Tendon healing can occur intrinsically, via the proliferation of epitenon and endotenon tenocytes, or extrinsically, through the invasion of cells from the surrounding sheath/ synovium, and this combination of healing makes tendon healing of zone 2 injuries different to other tendons (Boyes, 1970, Gelberman et al., 1984, Lister et al., 1977, Matthews and Richards, 1976, Phillips et al., 1985, Potenza, 1963, Tang et al., 2013).

During intrasynovial flexor tendon healing, the recruitment of wound repair cells may involve diffusion from the tendon sheath, migration via an intact vinculum, and neo-vascularisation within the tendon itself. In addition, synovial fluid may bathe the intra-synovial tendon with nutrients and encourage the capacity to heal intrinsically (Abrahamsson et al., 1989). Although this form of healing is ideal, a combination of extrinsic and intrinsic healing usually occurs within injured tendons.

Despite receiving minimal injury, synovial fibroblasts in the synovial lining proliferate to a greater extent than endotenon fibroblasts (Khan et al., 1999, Riederer-Henderson et al., 1983). The dividing cells are fibroblasts, as macrophages only occasionally divide outside the bone marrow (Territo and Cline, 1975). Epitenon tenoblasts also initiate the repair process through proliferation and migration (Gelberman et al., 1986, Manske et al., 1985). Internal tenocytes secrete larger and more mature collagen than epitenon cells and the relative contribution of each cell type may be influenced by the type of trauma sustained, tendon location, presence of a synovial sheath, and the amount of load induced by motion following tendon repair (Fujita et al., 1992, Koob, 2002). Tenocyte function varies depending on their origin, and those from the tendon sheath produce less collagen and GAG compared to epitenon and endotenon cells. Intrinsic healing leads to improved biomechanics, fewer complications and better gliding properties within the tendon sheath in contrast to extrinsic healing, where the scar tissue results in adhesion formation and the disruption of tendon gliding (Koob and Summers, 2002, Strickland, 1997).

1.3.9.2 Tendon Healing Phases

Tendon healing occurs in three overlapping phases.

1) In the initial inflammatory phase peak cellular apoptosis occurs within the tendons (first week), followed by progressive tenocyte proliferation (second and third weeks) (Lui et al., 2007). The site of injury is infiltrated by erythrocytes and inflammatory cells (neutrophils), and phagocytosis of necrotic materials by macrophages occurs in the first 24 hours (Wong et al., 2006). Released vasoactive and chemotactic factors lead to increased vascular permeability, the initiation of angiogenesis, tenocyte proliferation, and the recruitment of further inflammatory cells (Murphy et al., 1994). Tenocytes migrate to a wound and during this stage the strength of a repair is solely through a surgical suture and possibly a fibrin clot.

2) After a few days the modelling stage begins with peak type III collagen synthesis. Water content and GAG concentrations remain high during this stage, which lasts for a few weeks (Oakes, 2003). Repair is highly cellular at this stage and tendon strength is increased by the synthesis of the ECM, despite the random organisation of collagen (Greiling and Clark, 1997).

3) The re-modelling stage commences after approximately 6 weeks, when the healing tissue is resized and reshaped, while collagen, GAG synthesis and cellularity is decreased. The re-modelling stage can be divided into the consolidation and maturation stages (Tillman and Chasan, 1996). During the consolidation stage (weeks 6-10) the repair tissue changes from cellular to fibrous, with tenocyte metabolism remaining high with the synthesis of more type I collagen, and tenocytes become aligned with the collagen fibres in the direction of stress. The newly synthesised collagen fibres are re-organised longitudinally and change from collagen type III to collagen type I in the final remodelling stage (Abrahamsson, 1991, Hooley et al., 1980, Woo et al., 2000). The maturation stage begins after 10 weeks, with a gradual change in the fibrous tissue to scar-like tendon tissue over the course of a year. Tenocyte metabolism and tendon vascularity decline during the last half of this stage (Amiel et al., 1987).

1.3.9.3 Effect of the Healing Process on Tenocytes

Early healing stages:

Peak apoptosis is followed by the gradual proliferation of tenocytes is noted during this stage. In a chicken model, tenocyte apoptosis was high several days after an injury was sustained, followed by an increase in the proliferation of tenocytes (2 to 4 weeks) accompanied by the activation of molecular events that inhibited apoptosis (Wu and Tang, 2013).

Middle and late healing stage:

Persistent apoptosis with the reduced proliferation of tenocytes is observed during this stage, with a higher percentage of apoptotic tenocytes on the surface of a tendon compared to within the core, indicating a greater need for cellular clearance and surface remodelling in the middle to late periods (Wu and Tang, 2013).

The total cell population was found not start to decline until after day 56, and cell apoptosis remained at a relatively high level on the tendon surface even at 3 months but declined in the core region after 2 months. These findings indicate that active tendon surface remodelling persists through the very late tendon healing period. The proliferation of tenocytes declined drastically after week 4 in contrast to increased tenocyte apoptosis, which is considered to be a major biological event in the remodelling and restoration of the gliding surface. Tenocyte apoptosis was shown to be greater at the junction sites of a surgical repair and tendon surface, where it is responsible for clearing excess cells and providing a smooth gliding surface by remodelling adhesions, but was still lower than in the first few days after surgery (Wu and Tang, 2013) (Figure 1.4).

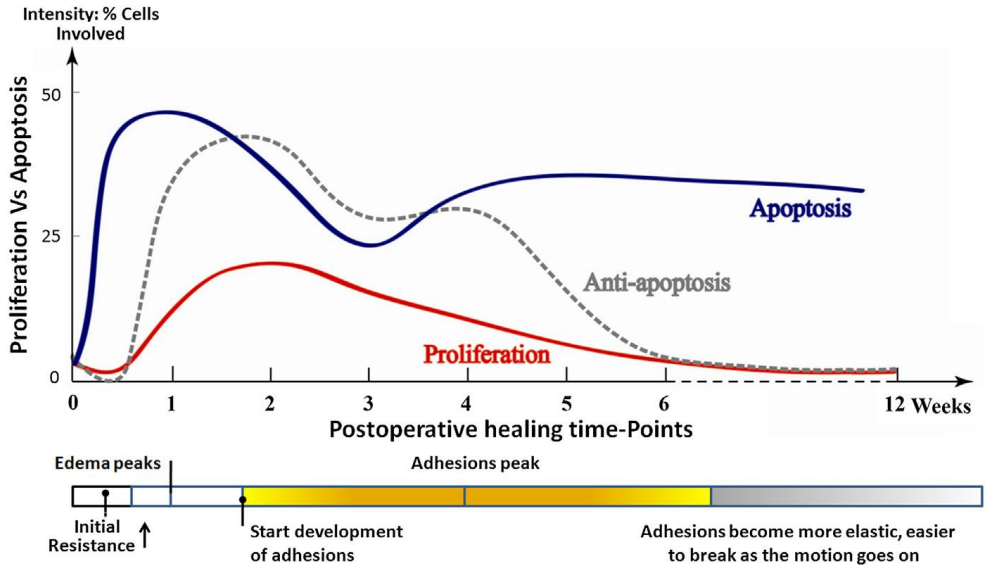

Figure 1.4: Proliferation and apoptosis of tenocytes

With permission from: Wu and Tang, (2013)

1.3.9.4 Cellular Apoptosis in Adhesions

The extent of apoptosis in a repaired digital flexor tendon of a chicken 3 weeks after immobilisation has been investigated. The percentage of apoptotic cells was found to increase from the tendon core to the tendon surface, and the adhesion-tendon interface. Apoptosis was found to be highest level in the adhesion core (Wu and Tang, 2013). The percentages of apoptotic cells in adhesions, at the adhesion-tendon gliding interface, and over the junction sites of the tendon ends were 50%, 65% and 69%, respectively. Tendons with more severe adhesions or a lower excursion, exhibited greater apoptosis in their adhesions and adhesion-tendon interfaces. It has therefore been concluded that cellular apoptosis may contribute to the fate of adhesions and the outcome of tendon injuries. Similar findings have been reported for a mouse tendon model and it is believed that the increases in cellular apoptosis at the adhesion and the tendon-adhesion interface are associated with the effect of deformation induced by early mobilisation; therefore, increased apoptosis at the tendon repair site would accelerate the recovery of the smooth gliding surface (Wong et al., 2006).

1.3.9.5 Micro Dynamics of Adhesions

Wong and colleagues (2009) demonstrated that the structure of the adhesions (plasticity and strength) can vary substantially in the course of tendon healing and

from the middle to late healing stages the ability of adhesion tissues to resist tension decrease and tissue flexibility increases. With persistent apoptosis of the adhesion cells, the adhesions break more easily when a tendon is loaded during the early range of motion. The authors suggested that digital motion is transferred to shear force over the adhesion-tendon gliding interface, leading to continuous stimulation of cellular apoptosis. It is therefore concluded that early motion will break up the adhesion fibres and reduce their density and strength in the late healing stage.

1.3.9.6 Remodelling Responses

Modulators of healing, such as matrix metalloproteinases (MMP), are important regulators of ECM remodelling, and their local levels at an injury site affect collagen formation and degradation at different stages of tendon healing (Riley et al., 2002). Inflammation provokes the release of growth factors and cytokines from platelets, leukocytes, macrophages and other inflammatory cells, which in turn can induce neo-vascularisation, stimulate fibroblast and tenocytes proliferation, and promote collagen synthesis (Evans, 1999, Molloy et al., 2003).

Nitric oxide is a short-lived free radical, which is bactericidal, can induce apoptosis in inflammatory cells, and causes angiogenesis and vasodilatation (Evans et al., 1996, Ziche et al., 1994). Nitric oxide synthase is responsible for synthesising nitric oxide from L-arginine (an amino acid), and studies have shown that levels of nitric oxide synthase peak 7 days after, and return to baseline 14 days, after tenotomy of a rat Achilles tendon (Murrell et al., 1997). Inhibition of nitric oxide synthase has been shown to reduce tendon healing, decrease the cross-sectional area of a tendon, and reduced a tendon's load to failure (Murrell et al., 1997).

Substance P and calcitonin gene-related peptide (CGRP) are pro-inflammatory substances, and are also forms of MMP, that peak during the proliferative phase of tendon healing and cause vasodilation and protein extravasation (Brain et al., 1985, Nakamura-Craig and Smith, 1989).

1.4 Tendon Sheath

All flexor tendons in the hand are covered by a double layered tendon sheath. The layer in contact with the tendon and the pulley are called the visceral and parietal layers, respectively. The granular structure of the visceral layer is found to be responsible for the production and removal of synovial fluid (Inoue et al., 1976), which improves the gliding properties and provides nutrition to intact or injured intra-synovial tendons (Tang, 2013). Studies have shown that an autogenous tendon sheath graft, in the presence of both tendon and tendon sheath injury, can lead to better tendon healing, a lower in-growth rate of adhesions from the damaged tendon sheath, and therefore lower friction at the tendon-pulley interface (Tang et al., 2013, Tang et al., 1990, Tang et al., 1993).

1.5 Pulley Anatomy

Doyle and Blyth's work in 1975 identified four annular and three cruciate pulleys but this was later revised by Hunter (Ochiai et al., 1979) with the addition of an extra annular pulley. Pulleys are fibrous bands with either a ring or cruciform configuration. The A1, A3, and A5 pulleys originate from the volar plate and the adjacent bones of the MCPJ, PIPJ and DIPJ, respectively.

The A2 and A4 pulleys span over the diaphyseal section of the proximal and middle phalanges, respectively. They are stiffer, broader and shorten less during finger flexion than other pulleys, reflecting their function in keeping the flexor tendons close to the axis of joint motion (Lin et al., 1989). The average lengths of the annular pulleys are 7.9 mm (A1), 16.8 mm (A2), 2.8 mm (A3), 6.7 mm (A4), and 4.1 mm (A5) (Doyle, 1989).

The cruciate pulleys are C1 (at the end of the A2 pulley), C2 (between the A3 and A4 pulleys) and C3 (at the distal end of the A4 pulley) (Figure 1.5). The cruciate pulleys are composed of oblique fibres that inter-digitate with the adjacent annular pulleys. They are relatively flexible, which allows them to shorten or collapse during finger flexion in order to protect the annular pulleys (Dy and Daluiski, 2013).

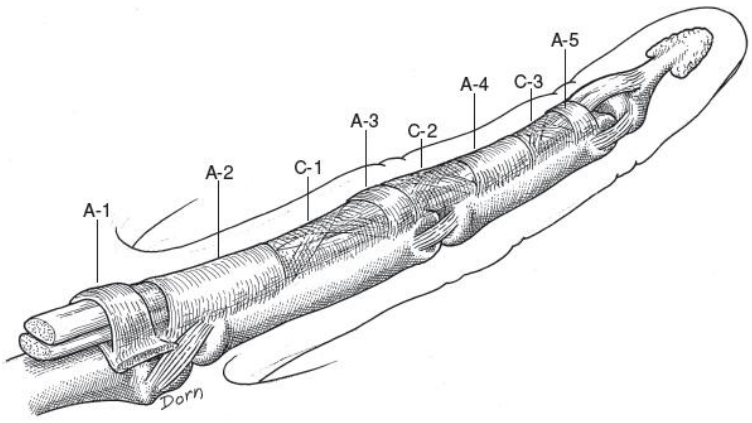

Figure 1.5: Pulley structures in a human finger

With permission from: Zidel, (2007)

The pulley system maintains the flexor tendon close to the bone, allowing the conversion of the linear motion of the flexor tendon to the angular movement of the digit. The annular pulleys minimise the amount of tendon excursion that is required for finger flexion, therefore avoiding bowstringing of the tendon during digital flexion. However the A2 and A4 pulleys are most important for optimal efficiency of the flexor tendons (Clark et al., 2010, Doyle, 1988, Peterson et al., 1986, Rispler et al., 1996).

A pulley consists of three layers, with the inner layer secreting HA to promote tendon gliding and characterised by collagen bundles parallel to the flexor tendon (Figure 1.6A). Electron microscopy investigations of this layer have revealed cartilaginous and glandular cells to be present among the collagen fibres (Sbernardori et al., 2007) (Figure 1.7A).The middle layer is characterised by a large amount of elastin fibrils, in addition to densely packed collagen fibres that are arranged perpendicular to the axis of the flexor tendon (Figure 1.6B). This layer provides structural support to the pulley and does not produce HA. The outer layer is composed of loosely arranged areolar tissue with numerous fine capillary networks, and this layer provides nutrition to the pulley and does not contain any elastic fibres or HA (Ellis et al., 1995).

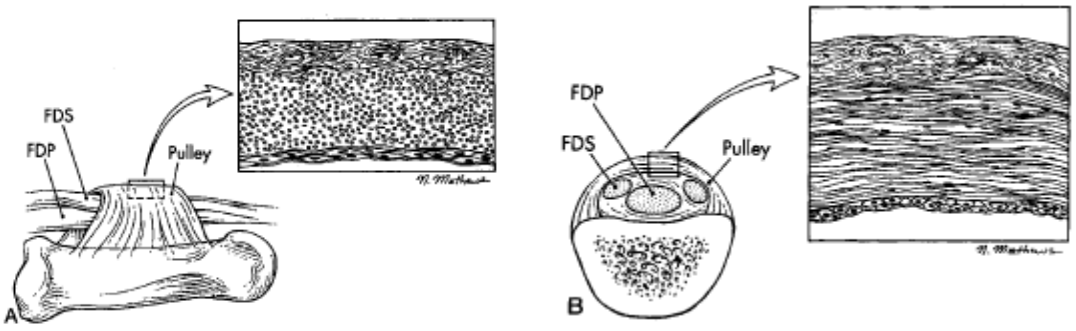

A B

Figure 1.6: Cross section of the annular pulley

A: Longitudinal, B: Transverse.

With permission from: Ellis et al. (1995)

In the pathological condition of trigger finger, abnormal mechanical forces between the tendon and the pulley or an abnormality in the tendon can lead to impingement of the tendon as it tries to slide under the proximal ridge of the pulley, leading to significant fragmentation of the deep layer (Bilos et al., 1977, Gordon, 1981, Schlenker et al., 1981) (Figure 1.7B).

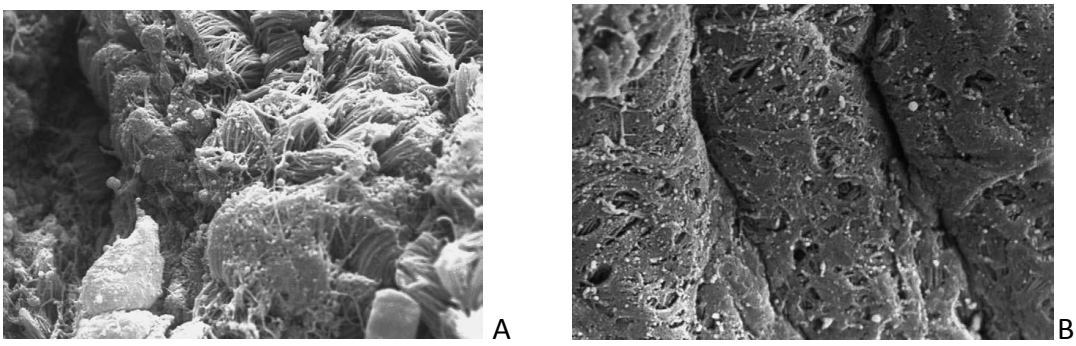

A B

Figure 1.7: SEM of a pulley

A) normal pulley (×400), B) pathological pulley (×200)

With permission from: Sbernardori et al. (2007)

Although any compromise of the A2 or A4 pulley raises the risk of bowstringing, recent studies have suggested that these pulleys can be partially incised without substantial effects on the work of flexion or tendon excursion (Mitsionis et al., 1999, Savage, 1990, Tang, 1995, Tomaino et al., 1998).

Mitsionis et al. (1999) demonstrated using a cadaveric model that 25% of both the A2 and A4 pulleys can be released, either alone or in conjunction, without a significant loss of finger flexion. They suggested that more aggressive release of up to 75% may still provide finger motion that is clinically acceptable. In animal models complete incision of the A2 pulley has been shown to improve tendon excursion and decrease the work of flexion compared with an intact or expanded A2 pulley (Tang et al., 2001, Tang et al., 2007). A further study has shown that complete release of the A4 pulley does not substantially increase the work of flexion or tendon excursion in a cadaveric model (Franko et al., 2011).

These biomechanical studies have been supported by clinical reports advocating the intentional release of the A4 pulley to facilitate flexor tendon repair and have provided important knowledge for surgeons during difficult acute flexor tendon repair and insight into the available options for flexor pulley reconstruction (Tang et al., 2007). There seems to be a leniency within the flexor pulley system that was not previously appreciated and patients may be able to tolerate some compromise of their pulley system, even within the A2 and A4 pulleys, thereby allowing them to avoid pulley reconstruction (Dy and Daluiski, 2013).

Although this developing knowledge does not change current practice and the indications for flexor pulley reconstruction, it allows a surgeon to tailor the approach to the number of pulleys that are required to be released following acute tendon repair or reconstructed at a later date.

1.6 Flexor Tendon Zones

Verdan (1972) described five flexor tendon zones in the hand based on anatomic factors and the outcome of tendon treatments: zone 1 is distal to the insertion of the FDS tendon and only contains the FDP tendon; zone 2 begins at the proximal margin of the A1 pulley and extends to the FDS insertion at the base of the middle phalanx; zone 3 is between the distal margin of the carpal tunnel and the proximal margin of the A1 pulley; zone 4 is within the carpal tunnel; and zone 5 is proximal to the carpal tunnel (Figure 1.8).

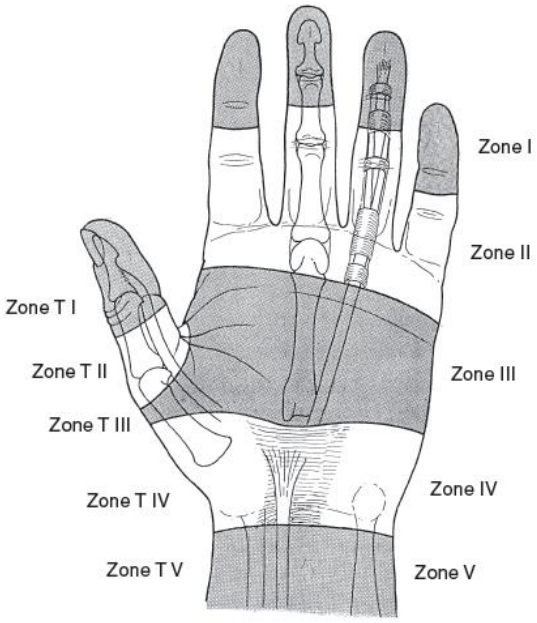

Figure 1.8: The five zones of flexor tendon

With permission from: Zidel, (2007)

Bunnell (1956) described zone 2 as ' No man's land' in order to emphasise the poor outcome for these injuries following surgery. Tang (1990) has revised this zone into four subdivisions: 2A, from the distal margin of the FDS insertion to the proximal margin of the insertion; 2B, from the proximal margin of the FDS insertion to the distal border of the A2 pulley; 2C, the area covered by the A2 pulley; and 2D, from the proximal border of the A2 pulley to the proximal margin of zone 2. The 2D zone is the narrowest part of the pulley system (Figure 1.9).

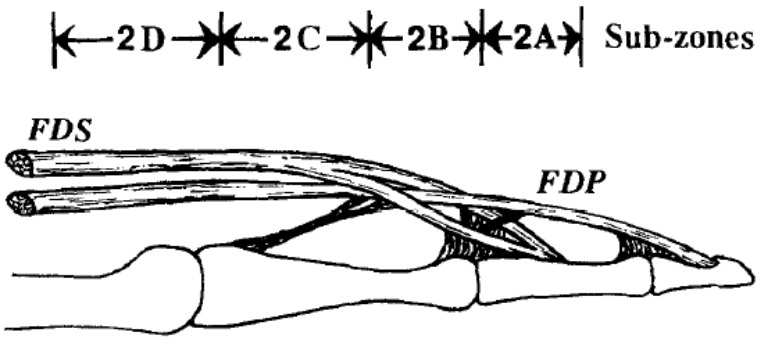

Figure 1.9: Subdivision of zone 2, 'No man's Land'

With permission from: Tang, (1990)

The A2 and A4 pulleys are found to be stiffer and less deformable when loaded, until failure (Lin et al., 1990). Tendon repair where the pulley is at the narrowest and the stiffest can lead to tendon triggering, gap formation from excess friction, tendon adhesion, subsequent tendon rupture, and therefore a poor outcome.

1.7 Flexor Tendon Repair

The aim of flexor tendon repair is to achieve the early restoration of active digital flexion, while avoiding complications, such as excess friction at the repair site, rupture of the repaired tendon and formation of adhesions or joint contracture (see Section 1.10).

Although current repair methods may vary, some principles are universal, such as using strong core sutures, ensuring knot security, achieving secure suture-tendon junctions, creating a tighter tension over the repair site, ensuring sufficient core suture purchase (1.0 cm) and pulley venting to avoid triggering of the repaired tendon at the entry and exit site to the pulley (Tang, 2012, Tang et al., 2005, Wu and Tang, 2012).

1.7.1 Suture Materials and their Properties

Two factors are involved in producing a strong mechanical tendon repair: the suture material used and the technique. The ideal suture material for a tendon repair should possess the following six characteristics (Trail et al., 1989):

1. High tensile strength.
2. Easily knotted, with minimal loss of strength after knotting.
3. Inextensible, to prevent ‘gapping’. Gapping is a phenomenon that occurs in a sutured tendon when the divided ends separate under load, without mechanical failure of the repair itself.
4. Minimal tissue response to the suture material.
5. Absorbable later, maintaining tensile strength in the early phases of healing but disappearing when tendon repair is complete.
6. Easy to use.

In the past two decades both braided polyester (McLarney et al., 1999, Savage, 1985, Silfverskiold and Andersson, 1993, Trail et al., 1992) and monofilament nylon

(Greenwald et al., 1994, Komanduri et al., 1996, Tang et al., 2001, Wagner et al., 1994) have been used for core tendon repair. Both sutures, for the same suture calibre, have a relatively high load to failure when unknotted, ~19N and 12N, respectively. Both suture materials are suitable for tying a surgeon's knot (Figure 1.10) and for the security of the knot an additional three throws for a braided polyester suture and three to four throws for monofilament nylon are recommended. However, when knotted the load to failure is significantly reduced, ~10N and 8N, respectively, with monofilament nylon being the weakest suture material when knotted (Trail et al., 1989).

Muffly et al. (2009) investigated the end length of a suture distal to the knot. Knots with an end length of 0 mm were found to come untied significantly more often than either 3 or 10 mm knots; and coated suture materials were more prone to untying than uncoated sutures due to the presence of a silicon cover.

Figure 1.10: The surgeon's knot

With permission from: Trail et al. (1989)

Trail et al. (1989) demonstrated that braided polyester sutures gave the least elongation at failure (~33 mm) compared to monofilament nylon (~60 mm). In addition, monofilament nylon sutures led to increased gapping at the repair site following tendon loading, which can have an adverse effect on tendon healing.

Any suture material used in tendon repair should elicit a minimal inflammatory response in order to reduce the amount of adhesions and subsequent friction at the tendon-pulley interface. Srugi and Adamson (1972) investigated the inflammatory response of different suture materials within canine flexor tendons. Nylon resulted in the smallest inflammatory response, while other suture materials, such as stainless steel, polyester and chromic catgut, produced between 2-2.5 times the response to

nylon, with silk sutures causing the most intense cellular reaction (14 times that of nylon).

The time required for a repaired human flexor tendon to achieve sufficient tensile strength to allow it to be independent of a suture repair is unknown, and it is for this reason that absorbable sutures are avoided by many surgeons. Bourne et al. (1988) found that the tensile strength of a strong absorbable suture constructed from polydioxanone (PDS) only lasted for six weeks, and therefore was unable to maintain its tensile strength during the crucial healing stage (up to 12 weeks).

Finally, different surgeons prefer different suture materials based on their ease of use.

1.7.2 Core Suture Techniques

Primary or delayed primary repair is standard practice in digital flexor tendon repair. Direct end-to-end repair using a multi-strand core suture (2-strand, 4-strand, 6-strand, or 8-strand repair) can be used (Figure 1.11), and the repair strength can be increased by increasing the number of strands bridging the repair, with numerous techniques having been developed to achieve this (Al-Qattan and Al-Turaiki, 2009, Angeles et al., 2002, Aoki et al., 1995, Dinopoulos et al., 2000, Gill et al., 1999, Kusano et al., 1999, Lee, 1990, Manchio et al., 2009, Savage, 1985, Shaieb and Singer, 1997, Viinikainen et al., 2007). However, multi-strand repairs are complex, time-consuming and involve repetitive tendon handling, with the repeated passage of needles and sutures through a tendon leading to a significant iatrogenic injury to an already injured tendon.

It has been shown that a larger diameter suture is stronger (Taras et al., 2001), that locking loops have a stronger hold on a tendon (Xie and Tang, 2005, Xie et al., 2005), that better suture purchase has an effect (Cao et al., 2006, Tan and Tang, 2004), and that a running finishing stitch improves gap resistance (Lin et al., 1988). It has also been demonstrated that low profile repairs where there is less suture material visible on the surface of a tendon, such as the modified Kessler (MK) repair, have less gliding resistance (GR) than high profile repairs (Zhao et al., 2001), and that monofilament suture materials, such as nylon, have less GR than braided suture materials, however they can lead to larger gap formation. A size 3-0 or 4-0 suture is recommended for core sutures during flexor tendon repairs (Tang, 2012). Core sutures are better applied

on the volar 2/3 of a flexor tendon to avoid injury to the vincula and on the dorsal region of a tendon.

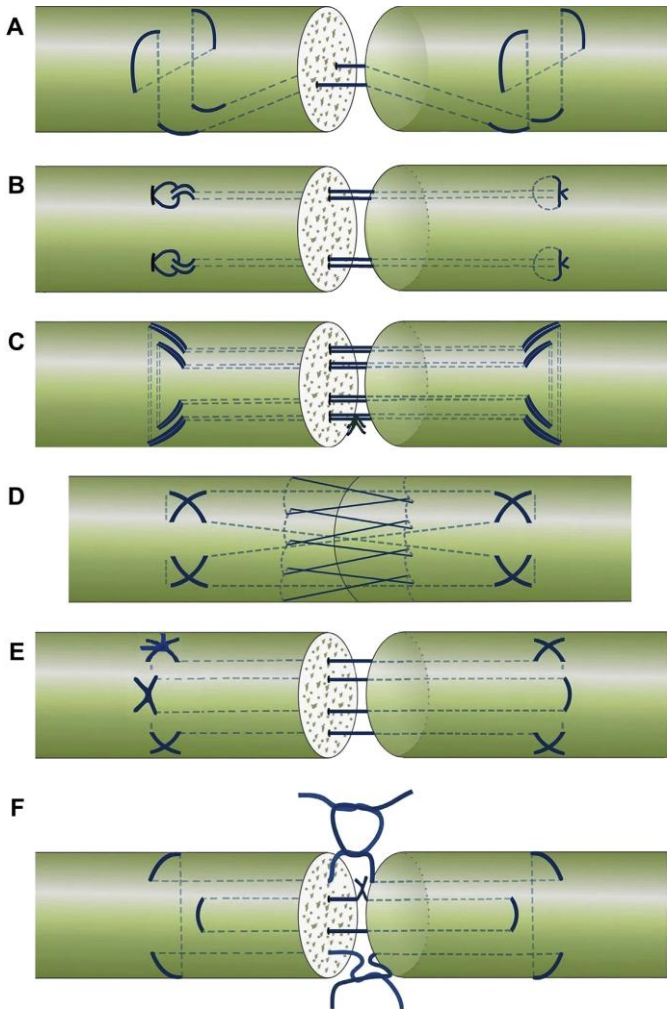

Figure 1.11: Different core suture methods

(A) modified Pennington suture, (B) 4-strand double Tsuge suture. Both (A) and (B) are used in the Mayo Clinic. (C) Eight-strand Gelberman-Winters suture used in Washington University in St Louis (MO). (D) Cruciate repair used in the Hospital of Special Surgery, New York (NY). (E) A modified Strickland, a 4-strand repair made up of a locking Kessler repair and a horizontal mattress suture, used in the Stanford University Medical Centre. (F) Strickland suture.
With permission from: Tang et al. (2013)

The effect of the core suture technique on the GR during cyclic motion following flexor tendon repair has been studied. A comparison between the Modified Kessler (MK) suture and the Massachusetts General Hospital (MGH) repair (Figure 1.12) demonstrated that the MGH repair had a higher GR and lower load to failure irrespective of the suture calibre and material (Moriya et al., 2010). This may be

directly related to the presence of suture knots and excess suture material on the gliding surface of the flexor tendon. For this reason the locked Kessler suture technique was recommended for core sutures in preference to MGH suture.

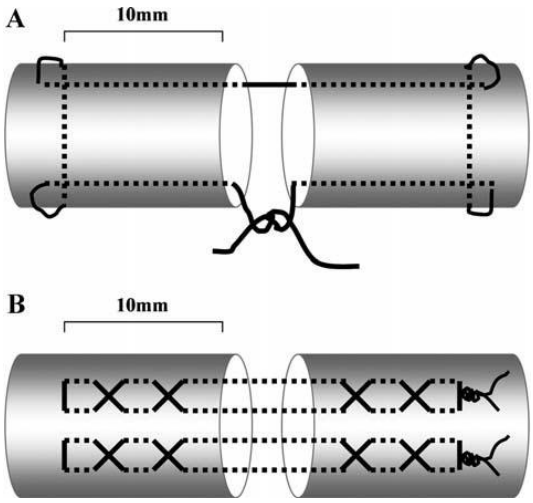

Figure 1.12: Core suture techniques

(A) Modified Kessler core suture, (B) Massachusetts General Hospital Suture Technique.

With permission from: Moriya et al. (2012)

1.7.3 Circumferential Suture Techniques

A shortcoming of a core suture used in isolation is that a gap can form at the tendon ends without slippage of the suture anchor points, owing to concertinaing of the tendon ends, which predisposes the tendon edges to snag when gliding under the pulley. This gap formation and snagging can be corrected by a peripheral suture (Diao et al., 1996, Merrell et al., 2003, Nelson et al., 2012, Sandow and McMahon, 2011). The 'simple' peripheral suture (Figure 1.13A) was introduced by Kleinert as a method of smoothing and tidying-up the tendon ends, and a size 6-0 suture is recommended for peripheral sutures in flexor tendon repairs (Tang, 2012).

Wade et al. (1989) showed that the forces required to create an initial gap following tendon repair in human flexor tendons were as follows:

1. Two-strand MK core suture alone, 3.4 N (0.34 kg).
2. Two-strand core suture with a simple running peripheral suture, 22 N (a six-fold increase).

3. Two-strand core suture with a Halsted peripheral suture, 39 N (a 10-fold increase from the core suture alone).

Silfverskiold and Andersson (1993) confirmed the mechanical benefit of a simple peripheral suture and described a cross-stitch peripheral suture (Figure 1.13B) with greater strength (50 N for a 2 mm gap and 60 N at ultimate failure) for sheep flexor tendons with no core suture. An improvement of the cross stitch with interlocking anchor points (Figure 1.13C) prevented the narrowing of the transverse strands and provided an additional 26% strength (Dona et al., 2003).

Hirpara et al. (2007) studied core sutures without a peripheral suture in pig flexors: the two-strand, four-strand and six-strand core sutures, using 4-0 polyester (Ethibond; Ethicon, Somerville, NJ, USA). In a second series of experiments a Silfverskiöld peripheral suture (using 6- 0 nylon) was added to each core suture. There was little difference in bulking related to the core sutures alone, with a slight increase when a Silfverskiöld peripheral suture was added. The force to produce a 3 mm gap in the two strand, four strand and 6 strand repairs was 2 N, 2 3N and 44 N, respectively. With the addition of a Silfverskiöld peripheral suture the results were 38 N, 58 N and 82 N, respectively. The ultimate force was larger for the core and peripheral suture, but was recognised as a pointless measurement in relation to clinical practice because at this point the repair was stretched and functionally useless. The authors commented that any repair in which less than 40 N produced a 3 mm gap in a static test was inadequate for early active mobilisation.

The effect of a different circumferential suture has been studied by Gulihar et al. (2012). Thirty flexor tendons and A2 pulleys were harvested from turkey toes and the GR was measured for all intact tendons and following 50% laceration and repair. The study used the MK technique for the core suture and three different peripheral suture techniques: Silfverskiold, Halsted and a simple running suture. The increase in GR following a full tendon repair compared to the intact tendon was 100% with the Halsted repair, 80% with the Silfverskiold repair and 60% with a running suture ($p = 0.05$). The authors concluded that a simple running suture had a lower GR compared to the other techniques.

However, a recent study has shown that a strong core suture with appropriate tension over the repair site may be strong enough to avoid the need for peripheral sutures and that strengthened but simpler sutures, appropriate pulley venting and early rehabilitation is the way forward in treating these injuries (Elliot and Giesen, 2013).

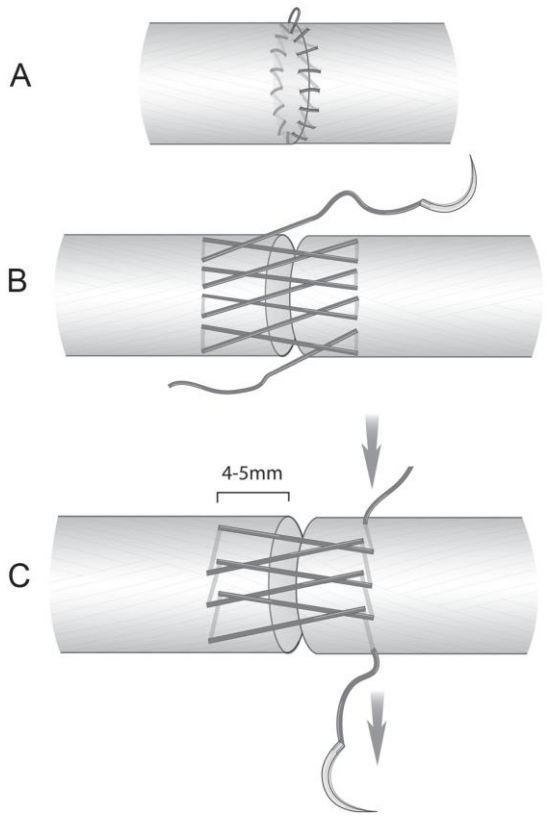

Figure 1.13: Peripheral sutures

(A) Simple running, (B) Silfverskiöld cross stitch, (C) Interlocking horizontal mattress.

With permission from: Savage (2014)

1.7.4 The Cellular Effect of Sutures on Tendons

Wong et al. (2006) studied the effect of a single interrupted suture on a tendon at the cellular level and demonstrated an 'acellular zone' at days 1, 3, 5, 7 and 14 after a suture was inserted which persisted over 14 days. The placement of an untied suture in a tendon did not produce this effect but applying the tied knot did. The authors explained that the rapidity of onset suggests that cells move from the zone of injury and strain into less mechanically strained tissue. This phenomenon highlights biological events that must be considered in parallel with the current trend for multi-strand locking flexor tendon suture repairs.

1.8 Pulley Venting

In the past 10 years theories concerning the treatment of the pulleys have changed. When the level of tendon repair is within a pulley or when a repaired tendon cannot be moved passively through its full excursion without triggering on the edge of a pulley, then partial pulley venting is required.

Preservation of the entire A2 pulley can be harmful when there are oedematous tendon ends. Pulley venting leads to improved tendon gliding, reduced repair site loading during rehabilitation, allows room for post-operative tendon oedema, and reduces the work of flexion (Franko et al., 2011, Tang et al., 2009, Zhao et al., 2000). However, excessive pulley resection can lead to inefficient flexor tendon function and subsequent tendon bowstringing. The exact amount for safe pulley resection that allows a low GR and friction at the level of a tendon repair and pulley interface is not clear. Tanaka et al. (2004) used a human cadaveric study to show that up to 50% of the A2 pulley, in the presence of other intact annular pulleys, can be incised to facilitate exposure, tendon repair and improve tendon gliding with little increase in GR (Figure 1.14). In one study resection of 25% of the A2 pulley and 75% of the A4 pulley was found to be safe without resulting in a significant effect on angular rotation (Tomaino et al., 1998).

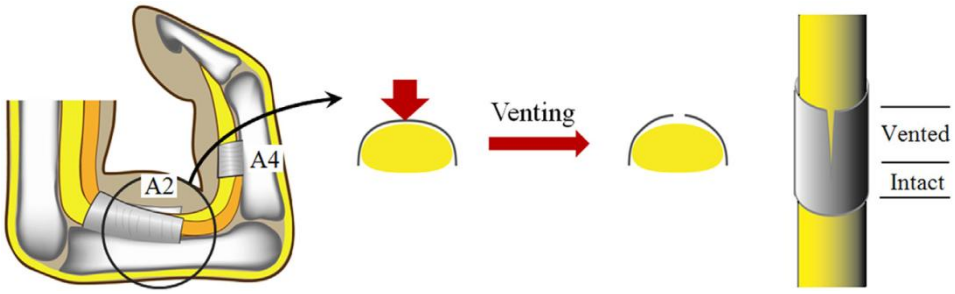

Figure 1.14: Venting major pulleys

With permission from: Wu and Tang (2013)

Kwai Ben and Elliot (1998) looked at 126 fingers with complete division of one or more tendons in zones 2A and 2B. After completion of the repair the finger was moved passively through a full range of motion and the repair was observed for catching on the proximal edge of the A4 or distal edge of the A3 pulleys. When this occurred, the

pulley was vented along the lateral edge (Figure 1.15) for as much of its length as was necessary to allow a full and trigger free range of motion of the repair. In total, 81 (64%) of repairs required some degree of venting of either the A2 or A4 pulley. During this study it was noted that the length of the FDS insertion and its relationship with the A4 pulley was variable, and 27% of the fingers had an FDS insertion completely proximal, while 73% showed the expected pattern whereby the FDS insertion was partially beneath the A4 pulley. These observations make it apparent that the A4 pulley and the FDS insertion cannot both be used to define the boundary between zones 1 and 2. Zone 1 must be considered as the area distal to the FDS insertion (Verdan, 1972), and not the whole length of the A4 pulley as the level of attachment of the FDS tendon under the A4 pulley is variable.

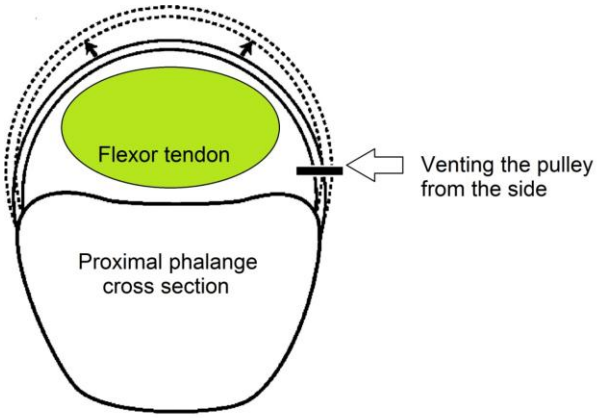

Figure 1.15: Lateral pulley venting

With permission from: Dona and Walsh (2006)

1.9 Post-Operative Rehabilitation

Mobilisation following tendon repair is required to avoid tendon adhesions and subsequent friction at the tendon-pulley interface. Studies have shown that early mobilisation of tendons can improve the healing process, the strength of the repair, and encourage more rapid tendon healing under the influence of longitudinal forces (Duran and Houser, 1975, Gelberman et al., 1991, Seyfer and Bolger, 1989, Strickland, 2005, Strickland and Glogovac, 1980, Tanaka et al., 2005).

Early passive motion (EPM) protocols were designed based on the theory of Duran and Houser (1975), that 3 to 5 mm of tendon excursion can decrease tendon adhesion

formation. Both passive and active rehabilitation regimes begin with basic wound care, oedema control, and a custom-fabricated dorsal blocking orthosis (DBO). The difference between the active and passive rehabilitation groups is that in active motion rehabilitation, active contraction of a muscle unit leads to the excursion of the tendon with the absolute and relative excursion of the tendons being greater than the passive motion (Korstanje et al., 2012). Combined active-passive motion regimes are the mainstay of current post-operative care, but the details of the exercise protocols are variable and in practice purely early passive motion has declined. An adequate and strong tendon repair is necessary before an active post-operative rehabilitation program is recommended to avoid tendon gap and rupture during rehabilitation.

There are four tendon rehabilitation programmes:

1. Complete immobilisation

This protocol is used in children from birth to 10 years old and for patients who cannot cognitively comprehend and comply with the rehabilitation process. The period of immobilisation is case dependent and is overseen by both a hand therapist and surgeon.

2. Duran regime (passive flexion and extension)

This protocol (Duran and Houser, 1975) originally used a DBO with rubber band traction. In modified versions of the Duran protocol a strap is used (Figure 1.16) to hold the digits (instead of the rubber band traction), thereby keeping the fingers in extension when not exercising (20° of wrist flexion, 70° of metacarpophalangeal joint (MCPJ) flexion and the inter-phalangeal joints (IPJ) in neutral). Once oedema is controlled a patient can complete repetitions of PIP and DIP passive flexion/extension, inside the DBO, every two waking hours. At 3.5 weeks the patient is allowed active finger flexion/extension in the DBO and at 4.5 weeks wrist and digital flexion/extension exercises are completed outside the DBO. At 5.5 weeks the DBO is discontinued and at 6 weeks passive extension stretching and proximal blocking exercises are added to the treatment regimen, finally at 8 weeks resisted exercises are introduced. This modified Duran protocol is still used in many units in the US (Clancy and Mass, 2013).

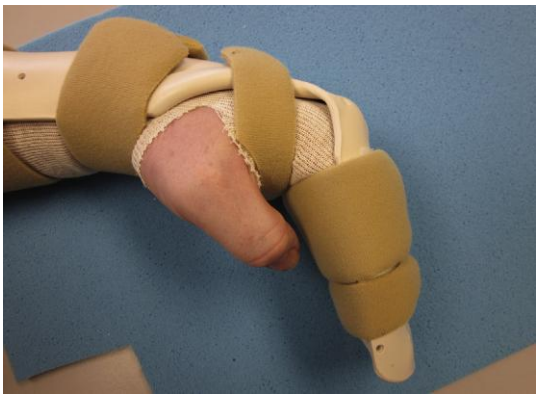

Figure 1.16: Modified Duran dorsal blocking orthosis

With permission from: Clancy and Mass (2013)

3. Kleinert regime (passive flexion and active extension)

The original Kleinert regime was introduced in 1967. A dorsal protective splint was applied after flexor tendon repair with the wrist flexed to 45°, and the MCPJ and PIPJ flexed to 20° for 4 weeks. Elastic traction was applied from the fingernail to the volar forearm to allow for active extension and passive flexion of the finger. Exercises were recommended twice daily with 6-8 repetitions. At week 5 the splints were discontinued for the wrist cuff with elastic traction, allowing gentle active extension/ passive flexion of the fingers, and at week 6, all splints were removed and active motion was commenced. However, this regime led to poor mobilisation of the DIPJ (Kleinert et al., 1975) and was therefore modified. The changes included placing a palmar bar to position the DIPJ into composite flexion, increasing the exercises to hourly, gradual correction of the wrist flexion to neutral in the DBO and application of a night splint to prevent flexion contracture. Light resistive exercises commenced with progression to work simulation in the eighth week. The application of the Kleinert protocol requires good custom orthotic fabrication skills and experience of recognising tendon adhesions. The use of a rubber band leads to digital joint flexion contracture and due to its complexity increasingly fewer surgeons use this protocol (Clancy and Mass, 2013).

4. Belfast protocol (early active flexion and extension)

The early active motion protocol was first introduced by a group of surgeons in Belfast (Small et al., 1989), and it has been confirmed that the absolute and relative excursion of the tendons was greater with active motion protocols (Korstanje et al., 2012). In this

regime a dorsal blocking splint is applied at day 2 after surgery with the wrist in full flexion minus 30°, MCPJ at 90° flexion and IPJ at 0°. More recent modifications of this regime have a less extreme flexion posture. Early active exercises commence 2 hourly with two active flexion movements in the air (PIPJ to 30° and DIPJ to 5-10°), then two passive flexion movements into the palm, and two active extension movements back into the splint. At 6 weeks the splint is discontinued and active flexion exercises are commenced. At 8 weeks, strengthening and passive extension exercises are instituted as needed and at 12 weeks a patient may return to work and unrestricted activities.

There are many early active protocols described in the literature which attempt to control the active motion by different means. (Gratton, 1993, Pettengill, 2005, Silfverskiold and May, 1994). The series reported by Silfverskiold and May (1994) from Gotenburg in Sweden, show the best results from a civilian unit anywhere in the world, and features of Kleinert, Duran–Houser and the Belfast techniques of mobilisation are used in combination.

1.10 Complications

Any surgical procedure performed on the hand carries the risk of infection, wound breakdown, scar sensitivity, injury to blood vessels and nerves, joint swelling and stiffness, and chronic regional pain syndrome. With regards to flexor tendon repair, there are three additional potential complications and the aim of treatment is to reduce the risk of gap formation, tendon rupture and adhesion formation.

1.10.1 Tendon Rupture

Harris et al. (1999) reported 3-6% flexor tendon rupture after primary repair and early active mobilisation. The ability of a tendon suture to withstand early active motion forces was considered the most important factor in avoiding tendon rupture. However, a patient's behaviour in the early post-operative period had a strong correlation with the rate of tendon rupture. More than half of the tendon ruptures were reported to have occurred following an act of stupidity (while wearing the splint), following activities that they were advised to avoid and up to 9 weeks following surgery. The authors advised that:

a) The current practice of wearing a splint continuously for 4-5 weeks should be continued.
b) Light grasping activities should start only after 8 weeks.
c) Heavy manual labour should be avoided until 12 weeks after surgery.

1.10.2 Gap Formation

The presence of a gap between the ends of the repaired tendon following rehabilitation can lead to tendon rupture, healing with an increased length, adhesion formation, increased friction, loss of movement and poor outcomes. When considering that 1.3 mm of tendon movement equates to 10° of angular joint movement, a 5 mm lengthening could cause a 65° loss of movement (Ejeskar, 1982, McGrouther and Ahmed, 1981).

Small tendon gaps of 1 mm or less have little effect, but gaps of 3 mm or more can completely block tendon motion beyond the limits of any repair strength (Drape et al., 1996, Gelberman et al., 1999, Silfverskiold et al., 1992). Current research indicates that a core suture and a full circumferential suture, specifically of an interlocking style, has better strength under cyclic loading with a lower risk of gap formation (Takeuchi et al., 2010, Takeuchi et al., 2011).

1.10.3 Adhesion

An adhesion is a tissue bridge formed between a flexor tendon and the surrounding tissue following an injury or repair. Adhesions lead to gliding restrictions and higher frictional forces, therefore a larger force is required to move a tendon, which in turn can be higher than the load to failure of a freshly repaired tendon.

Branford et al. (2011) showed that the quality of adhesions is highly dependent upon the level of post-operative mobilisation. The authors noted a statistically significant increase in structural stiffness and load to failure of immobilised adhesions (140% and 160%, respectively) compared to that for mobilised adhesions. This confirms the previous understanding of the cellular changes that occur following early mobilisation, leading to cellular apoptosis at the adhesion site.

1.11 Gliding Resistance and the Coefficient of Friction

Friction is a force measured in Newtons and presents as various types, e.g. static, kinetic, and rolling. Friction is essentially an electrostatic force between two surfaces, only responding to motion and acting in parallel to the surfaces that are moving with respect to each other. Friction is dependent on the types of materials that are in contact (μ - the coefficient of friction) and the net force pressing the two surfaces together (N) but is independent of the total surface area of contact if both surfaces are constructed from the same material.

The GR between a tendon and pulley reflects the roughness of the tendon surface after tendon repair, as well as any disruption of the tendon size or shape due to injury or repair (Zhao et al., 2001). It is measured by subtracting the forces at the two ends of the tendon (GR=F2-F1).

1.11.1 Uchiyama Method for Measuring Friction

Uchiyama et al. (1995) developed a method for measuring the GR of a tendon *in vitro* and therefore the coefficient of friction (CF) of the tendon-pulley interface. Measuring tendon friction is relatively straightforward. If a tendon is sliding under a pulley against a fixed load, then the force on the distal end of the tendon between the load and the pulley is equal to the load, while on the proximal side of the pulley, the force on the tendon (if it is moving) is equal to the load plus friction, so it is therefore a higher value. By attaching load transducers to a tendon proximal and distal to the pulley followed by applying a fixed load, it is possible to measure the frictional force while the tendon glides under the pulley (Figure 1.17) (An et al., 1993, Uchiyama et al., 1995).

In Figure 1.17 the proximal phalanx and its attached A2 pulley are mounted in the centre of the experiment frame, and the FDP tendon passes through the pulley at a proximal angle of 30° and a distal angle of 20°. Force transducers are attached to the proximal and distal ends of the tendon. The proximal transducer F2 is attached to a mechanical actuator, which can pull the tendon proximally or release it to move distally under the influence of a distal load. The distal transducer F1 is attached between the tendon and the load. When the tendon is moved towards the actuator

the force recorded at F1 is equal to the load, and the force at F2 is equal to the load plus the friction force.

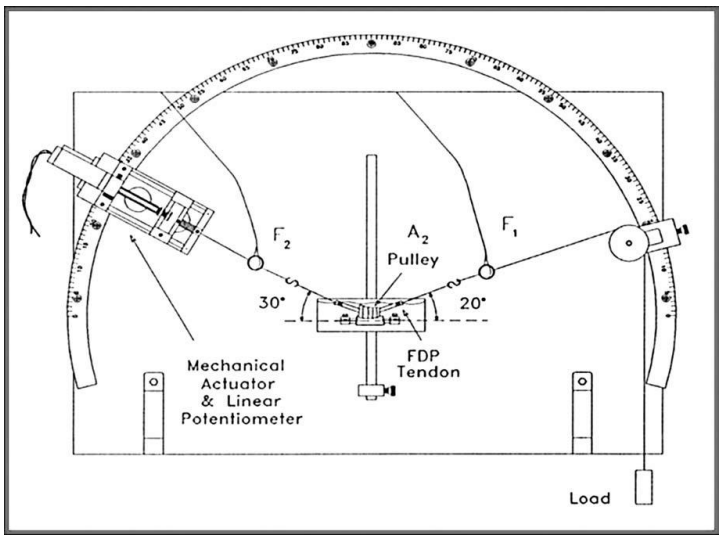

Figure 1.17: Tendon friction testing device

With permission from: Uchiyama et al. (1995).

A tendon sliding through a curved pulley is similar to a belt wrapped around a fixed mechanical pulley, where the total arc of contact between the cable and the pulley is φ and the tensions in the belt are F1 and F2 on each end (Figure 1.18). If the motion of the cable is from F1 to F2, then F2 is greater than F1 due to friction (f), and f=F2-F1. When excursion of the tendon cable is in the direction of M, F_2 is greater than F_1 and is equal to F_1 plus the GR of the tendon (f).

$$F2 = F1 + f$$

Tension F_2 is related to F_1 as a function of the CF (μ) and the arc of contact (ϕ).

$$F2 = F1e^{\mu\varphi}$$

From these two equations the frictional force can be obtained from F_1.

$$f = F2 - F1 = F1\,(e^{\mu\varphi} - 1)$$

The frictional co-efficient can be measured by taking the natural logarithm of the ratio of F_2 and F_1.

$$\mu = Ln[(F2\ /\ F1)]/\varphi$$

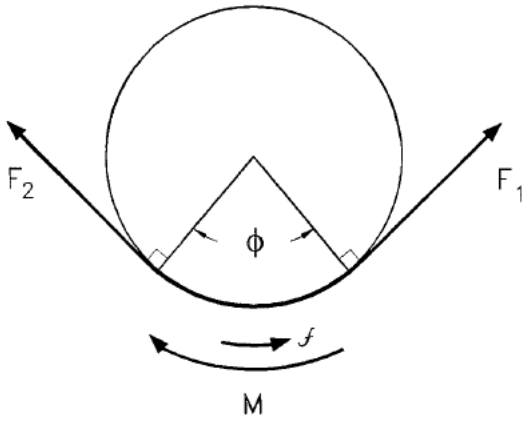

Figure 1.18: Diagram of a belt around a pulley

With permission from: Uchiyama et al. (1995).

Normally, the friction between a human finger flexor tendon and a pulley is very low, about 0.1 N, or 10 g of force (Uchiyama et al., 1995). This is the amount of force that is needed to move the tendon, over and above the tension needed to counter the weight of the moving part (a phalanx, finger, or hand, as the case may be). This frictional force is less at lower angles of tendon–pulley contact, and higher at greater angles because the frictional force is proportional to the load applied to the pulley, which increases as the arc of contact increases (Uchiyama et al., 1995).

While the CF, a property of the interacting materials, in this case a tendon and pulley, does not change, the total frictional force is greater in a flexed digit (e.g. 90° at PIPJ) than an extended digit. The tendon gliding surface in zone 2 has a CF of about 0.03, not very different to that of metal on ice (0.02) or cartilage on cartilage (roughly 0.01) (Uchiyama et al., 1995). Depending on the location of the laceration and the type of repair, following a tendon repair the force necessary to move the tendon and overcome friction increases to as much as 6 N (about 600 g per tendon), due to tendon adhesion and oedema (Momose et al., 2000, Strick et al., 2004, Tanaka et al., 2003, Tanaka et al., 2004, Zhao et al., 2002, Zhao et al., 2004, Zhao et al., 2001).

The GR at the tendon-pulley interface reflects the roughness of the tendon surface after a tendon repair, as well as any disruption to the tendon size or shape due to an injury or repair (Zhao et al., 2001).

1.12 Animal Model

Turkey toes were used in this research, as they were readily available from a local farm. These specimens required health and safety approval due to a previous outbreak of avian influenza. The anatomy of turkey toes resembles that of human fingers, and the specimens are of sufficient size to allow for complex tendon repair procedures to be carried out. In addition they are cheap and do not require ethical or Home Office approval. Cadaveric human, canine, rat, rabbit, pigs and chicken tendons have been used previously for studies on flexor tendon repairs. Table 1.1 illustrates the similarities and differences between these animal models (Farkas et al., 1974, Smith et al., 2005, Syed et al., 2013, Uchiyama et al., 2008).

Table 1.1: Anatomical differences for available animal models.

	Pigs	Chicken	Turkey
Phalanx	3	4 (in the 3rd digit)	4 (in the 3rd digit)
Tendon	2	3	3
Pulley	5	7	7
Tendon Sheath	present	present	present
Average Range of flexion (middle long toe)	Not recorded	IPJ1=50.8° IPJ2=43.5° IPJ3=18° (average : 112.3°)	IPJ1=38° IPJ2=32° IPJ3=42° (average=112°) (Figure 1.19)

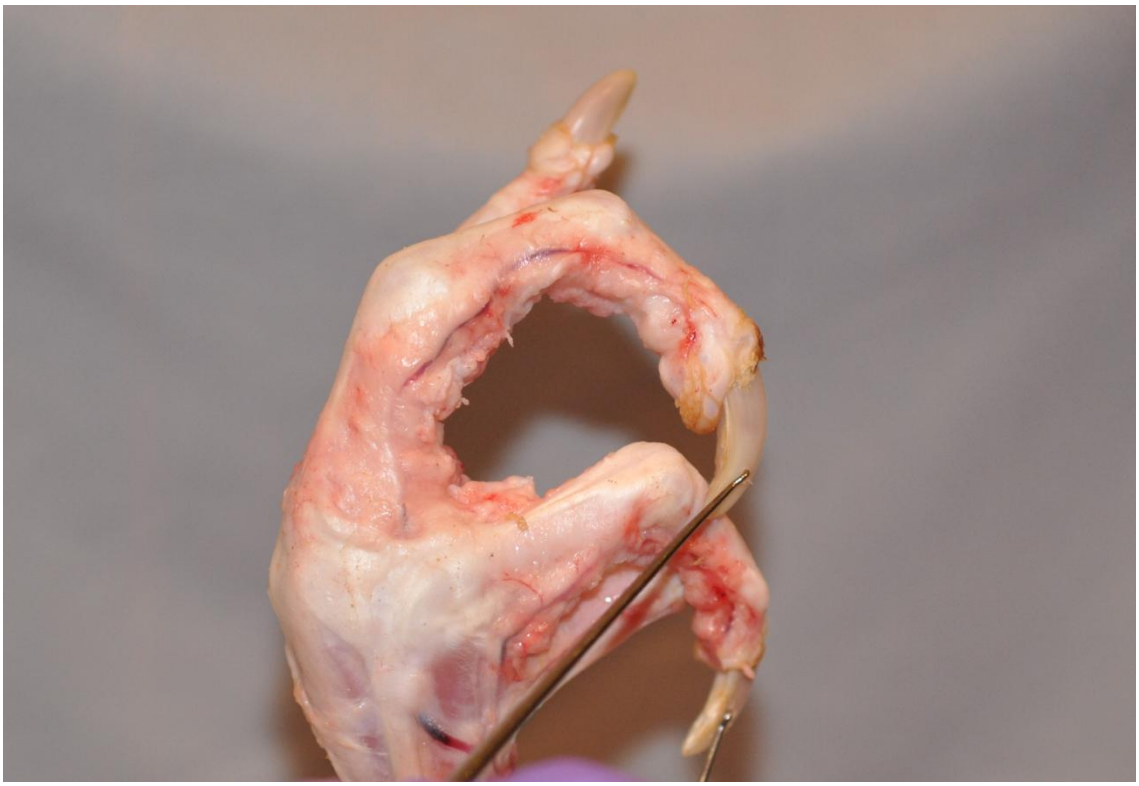

Figure 1.19: Range of motion for the middle toe of a turkey specimen

Table 1.2 indicates the reasons why turkey toes were used for this research instead of pig's trotters or chicken toes.

Table 1.2: Reasons for choosing a turkey animal model

Pigs trotters	Phalanxes are small. The tendon at the distal end of the A2 pulley is too short to allow for attachment to the apparatus. The A2 pulley is short (16mm) (Syed et al., 2013), making the sequential pulley resection prone to inaccuracy.
Chicken toes	All structures are similar to the human bone-tendon-pulley complex but are smaller, even in a mature birds aged 9 months.
Turkey toes	Mature birds have larger and longer tendons that allow for better tissue handling and the application of experimental surgical treatment. The average range of motion in the joints is similar to those of chicken toes.

Chapter 2 - Anatomy of Turkey Feet

2.1 External Anatomy

The structural similarity between the turkey toe and the human finger anatomy make these specimens a suitable alternative to use in order to study the biomechanical properties of the flexor tendons in human fingers.

There is no detailed anatomy of these structures available in the literature. Therefore, these anatomical findings and illustrations are the first recorded images of the anatomy of turkey feet. All images in this chapter unless indicated otherwise are produced by the main author.

All the specimens were provided by the slaughter house following disarticulation at the level of the mid-leg (the black arrow in

Figure 2.1), across the joint that resembles the knee joint in humans. This joint allows a forwardly directed flexion, and therefore the forward propagation of the animal, unlike the human knee which provides a backward flexion.

Figure 2.1: Forward flexion of the turkey's lower leg

With permission from Professor Thomas Roberts, Brown University, Rhode Island, USA. (Courage, 2011).

The lower half of the leg resembles a human forearm, as there are three long digits and a small rudimentary digit, which is similar to the human thumb. During weight

bearing all the digits are kept in extension by the bird's weight, despite the stronger flexion force in the toes.

The dorsal surface of the foot and the lower leg is covered by hard scale (Figure 2.2) and the plantar surface by glabrous skin (Figure 2.3). The heel pad consists of hardened skin resembling the heel pad in the human foot. It has small degree of mobility and flexibility but remains adherent to the underlying deep structures via a fibrous septum (Figure 2.4).

For the purpose of this study the innermost digit (the smallest) is labelled as digit 1, the adjacent digit as 2; the longest digit as 3; and the outermost digit as 4 (Figure 2.2 and Figure 2.3).

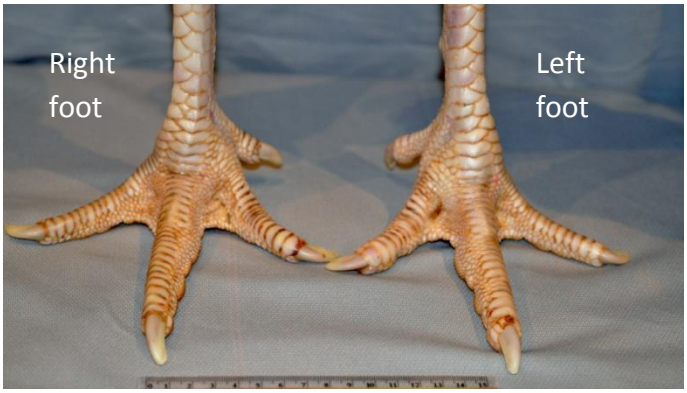

Figure 2.2: Scaley dorsal skin present on turkey feet

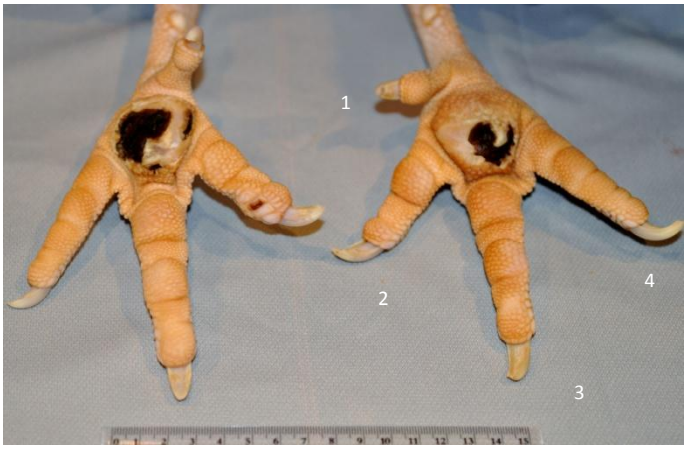

Figure 2.3: Glabrous skin on the plantar surface

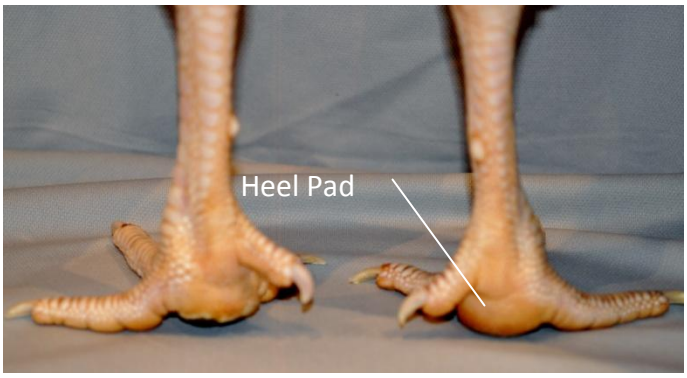

Figure 2.4: Weight bearing views and appearance of heel pad

2.2 Superficial Dissection

The left foot was dissected for the purpose of this anatomical investigation. All the deep structures on the extensor surface are covered by a thick layer of fascia (Figure 2.5). On the plantar surface the fascia is reinforced by a thick layer of fatty adipose tissue in the heel area (heel pad) and on the digits over the IPJ (Figure 2.6). This fatty tissue appears to provide padding for the areas of ground contact while the bird is weight bearing. In humans this area of fatty tissue overlies the concave part of the phalanxes where it provides protection for the neurovascular and deeper structures.

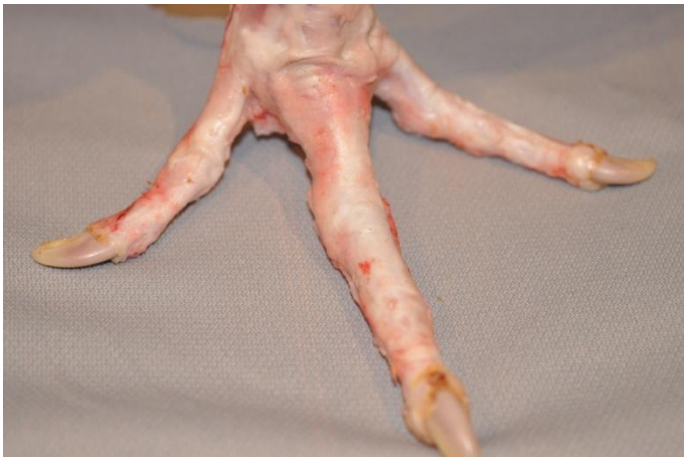

Figure 2.5: Fascia over the dorsum of the foot

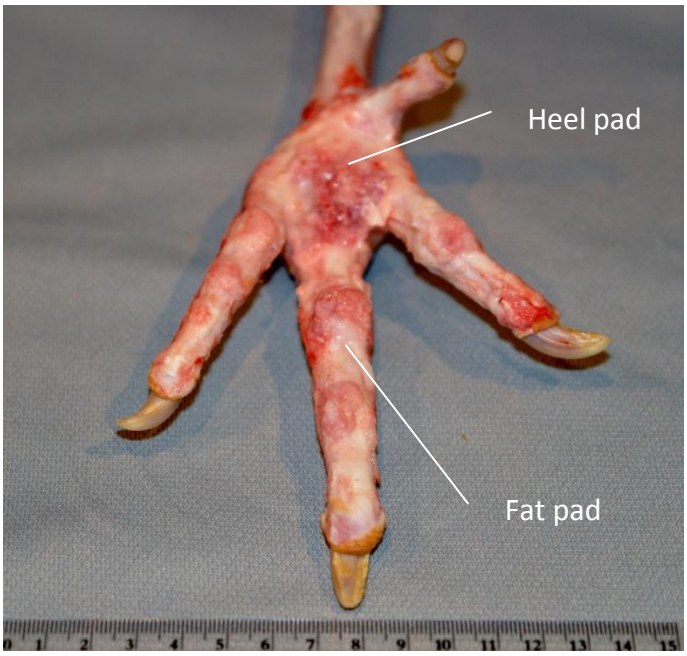

Figure 2.6: Plantar surface of the turkey foot

2.3 Plantar Structures

The three long digits are orientated in one plane. Digit 1 (the smallest) is suspended from the lower leg bone about 60° from the horizontal plane, and is maintained in this position by a different joint configuration and two sagital bands (A and B) which reinforce the base of digit 1 to the base of digit 2 and 4 respectively. These extend from the plantar surface of digit 1 to the extensor surface of both digit 2 and 4 (Figure 2.7 and Figure 2.8). A third sagital band extends from the base of the second digit (extensor and medial surface) in the plantar direction to the base of the third digit (extensor and lateral surface) (Figure 2.8). This is thought to provide constrained approximation of the digits during weight bearing.

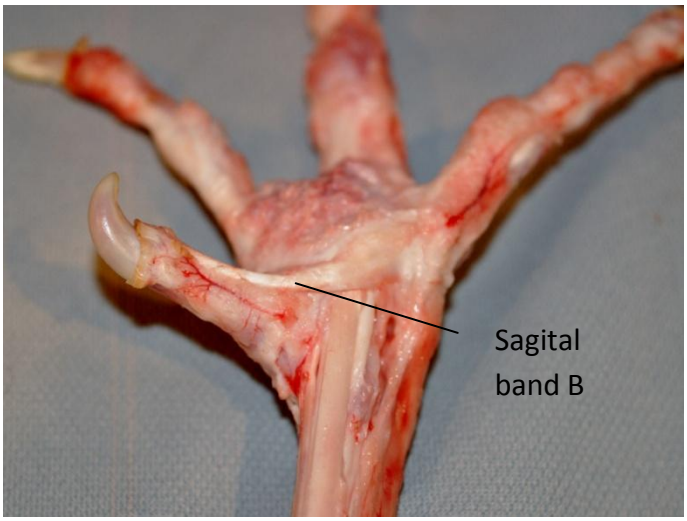

Figure 2.7: Sagital band from the plantar surface

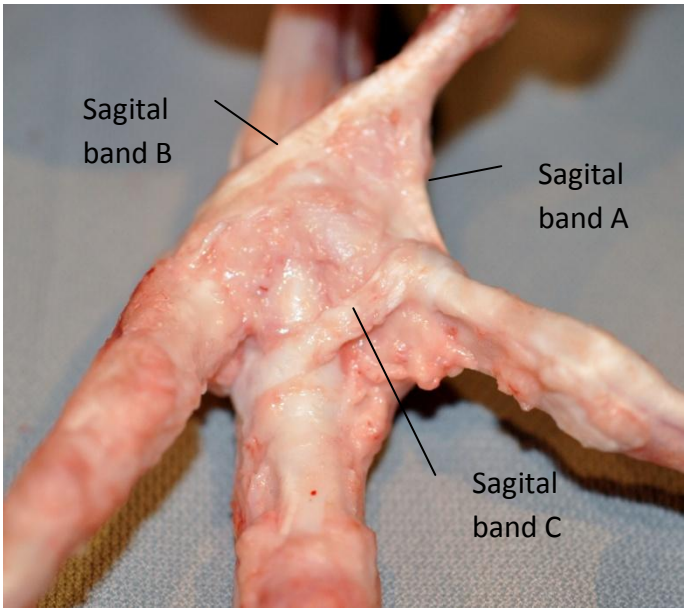

Figure 2.8: Sagital bands A, B and C

There are three phalanxes to digits 1 and 2, four phalanxes to digit 3 and five phalanxes to digit 4. The nail is an extension of the most distal phalanx where the longest flexor tendon inserts (Figure 2.9). For the purpose of this study all the IPJ are named after the most proximal phalanx involved. The most superficial flexor tendon is named the same as the equivalent human tendon, the FDS, and the deepest tendon, the FDP. There is an additional tendon in turkey digit due to the presence of an extra phalanx. This tendon will be called the *Flexor digitorum intermediate* (FDI).

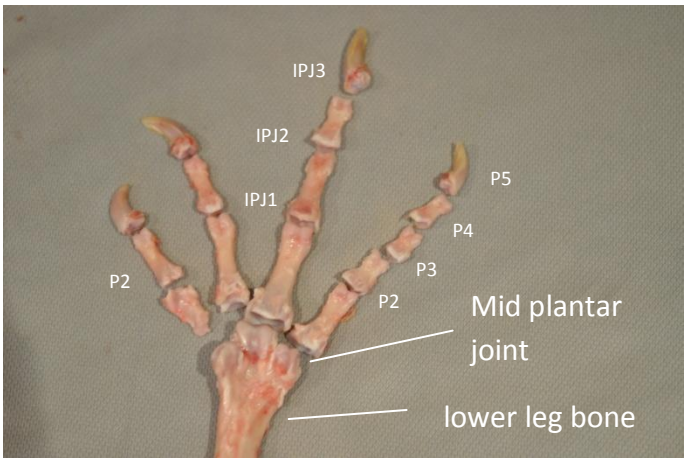

Figure 2.9: Bony structure of the turkey foot

There are two flexor tendons to digit 1, leading to the flexion of this digit to a 90° angle in relation to the other digits. FDS and FDP insert to the base of P2 and P3, respectively. The FDS has been removed in Figure 2.10 to reveal the FDP tendon.

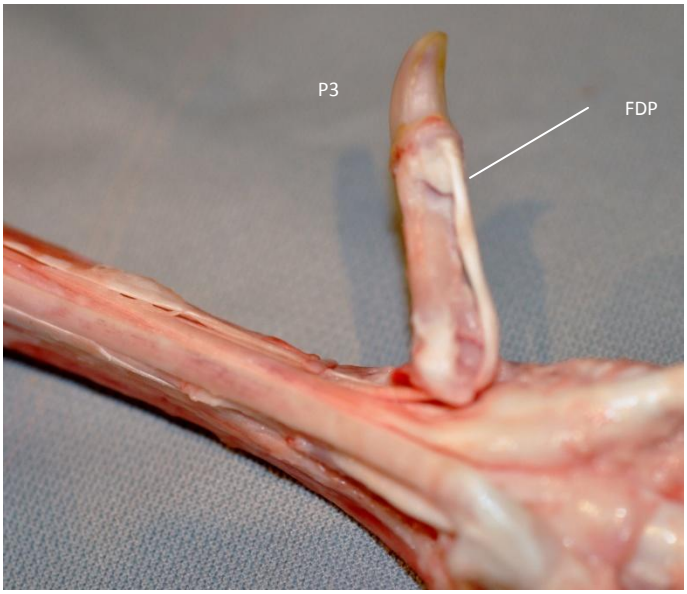

Figure 2.10: FDP to digit 1 with insertion to P3

The annular pulley systems in the turkey digits are very similar to those in human fingers and for the purpose of this study a similar nomenclature has been used to describe them. The most proximal annular pulley (A1) overlies the volar aspect of the flexor tendons at the region of the joint between the lower leg bone and the most proximal phalanx (mid plantar joint) (Figure 2.11). The A2, A3, A4, A5, A6 and A7 pulleys overlie the flexor tendons at the level of the main body of P1, IPJ1, the main body of P2, IPJ2, and the main body of P3 and IPJ3, respectively in the third digit. There

are two additional pulleys, A8 and A9 over P4 and IPJ4, respectively in the fourth digit as this digit contains one extra phalanx (Figure 2.12).

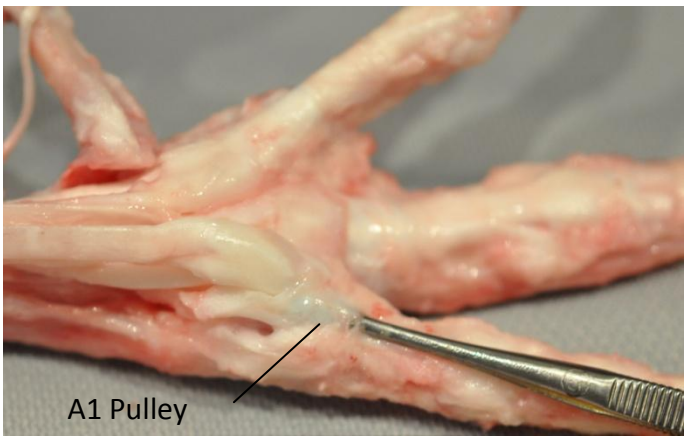

Figure 2.11: A1 pulley

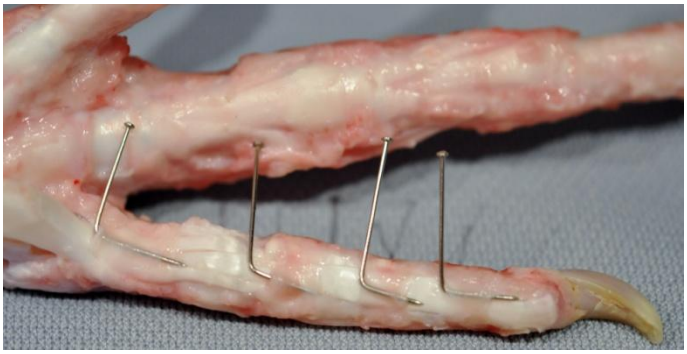

Figure 2.12: Annular pulley system in digit 4

The A1, A3, A5, A7 and A9 pulleys are excised. Pins indicate A2, A4, A6 and A8 pulleys from proximal to distal.

In addition to the digital annular pulley, there are three extra mid plantar pulley systems that are proximal to the A1 pulley, which contain and restrain the flexor tendons in relation to the lower leg bone. These are mid plantar pulleys and are named according to the underlying digit (Figure 2.13 and Figure 2.14). At this level there are interconnections between the deep and superficial flexor tendons. This means that the contraction or pull of one tendon also activates the contraction of the adjacent tendon in the same digit (Figure 2.15).

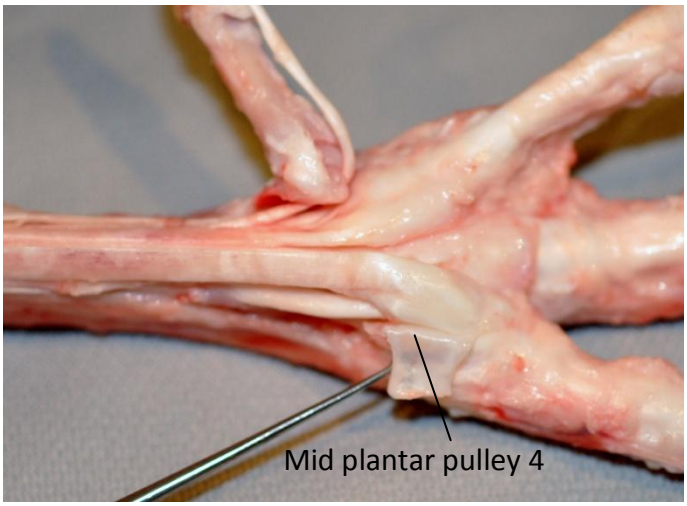

Figure 2.13: Mid plantar pulley 4

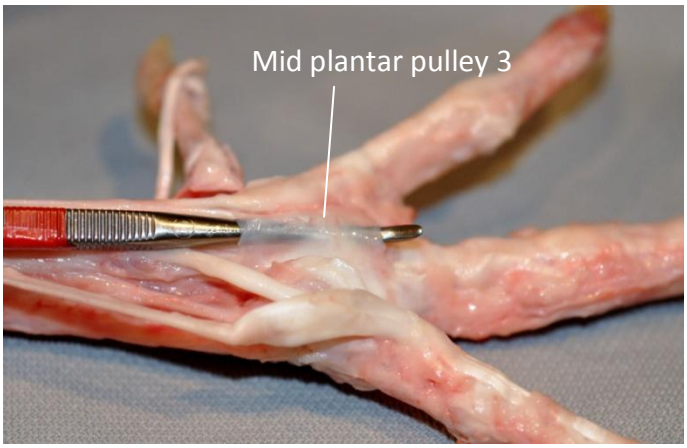

Figure 2.14: Mid plantar pulley 3

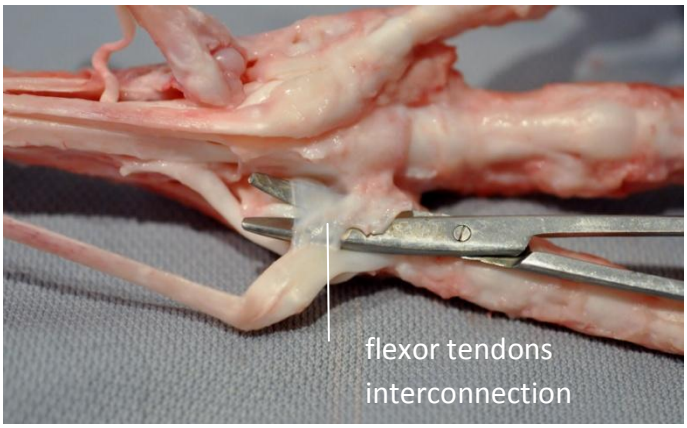

Figure 2.15: Flexor tendon interconnections

There are three flexor tendons to the digit 3. FDS, the most superficial tendon, is flat at the mid plantar region and inserts to the distal third of P1, on both sides of the midline. FDI, the intermediate flexor tendon, inserts on the distal third of the P2 and FDP, the deepest tendon, inserts on P4 in the midline direction; P3 has no tendon attachments (Figure 2.16). There are three vascular connections from the volar plates to the FDP tendon which provide nutrition to the tendon. This also assists in flexion of the IPJ during tendon contraction (Figure 2.17). FDS, FDI and FDP tendon contraction leads to mid plantar, IPJ1 and IPJ2 flexion, respectively (Figure 2.18, Figure 2.19 and Figure 2.20).

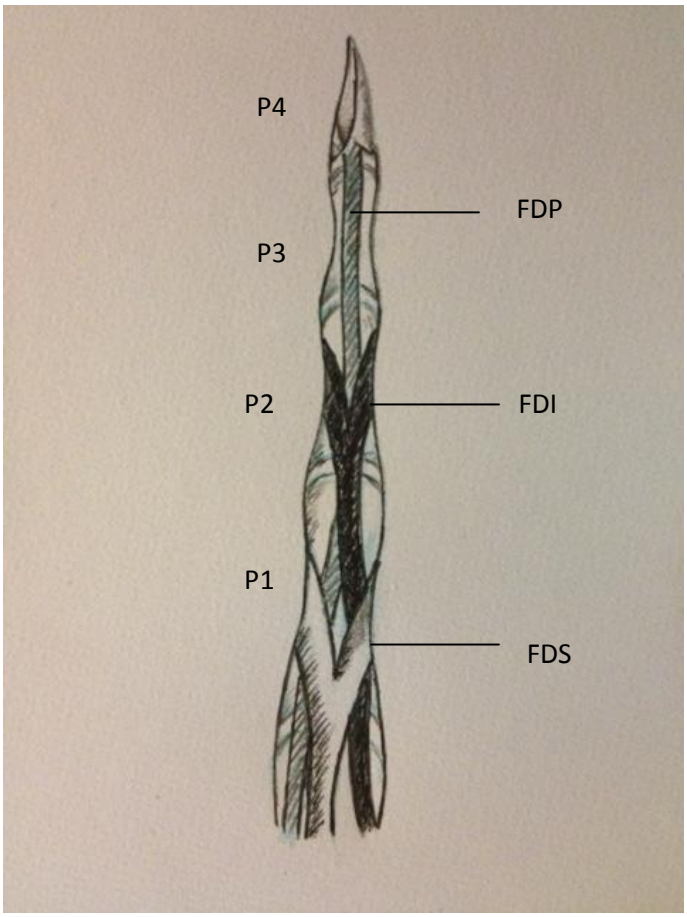

Figure 2.16: Flexor tendon configuration (plantar view)

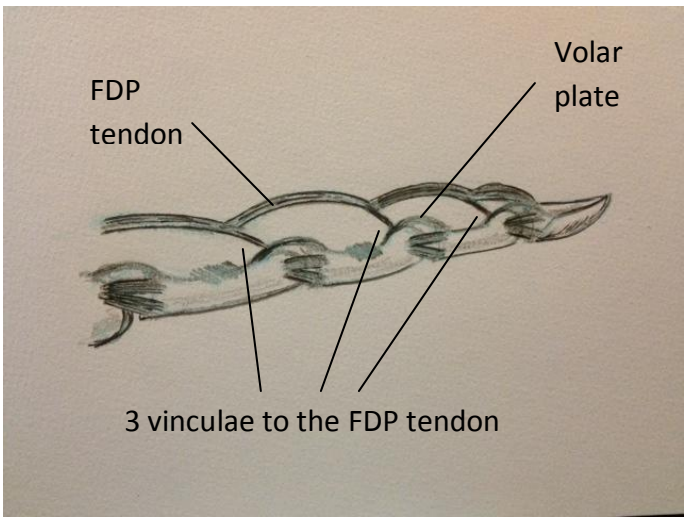

Figure 2.17: FDP and the relevant vinculae and their relationship to the volar plate

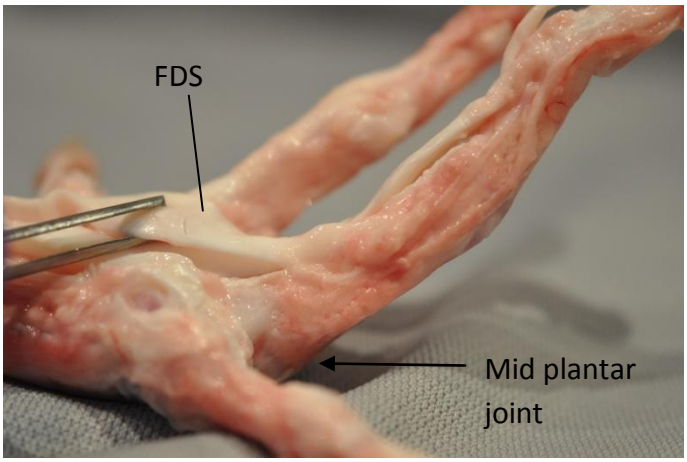

Figure 2.18: FDS contraction and flexion of the mid plantar joint

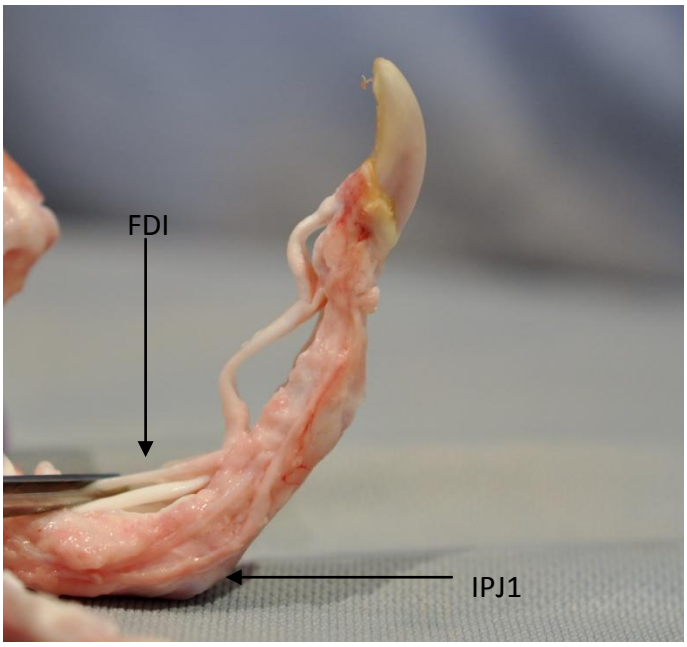

Figure 2.19: Contraction of FDI and flexion of IPJ1

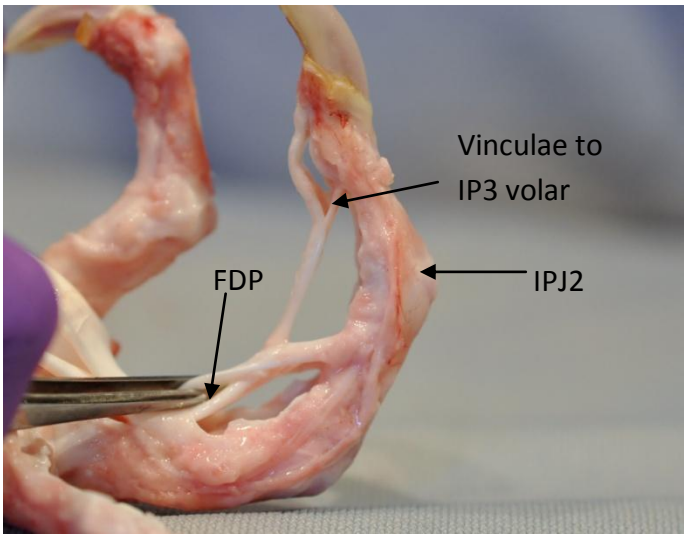

Figure 2.20: Contraction of the FDP and flexion of IPJ2 via the distal vinculae

The vascular structures run on both sides of the digit, at the junction of dorsal 2/3 and plantar 1/3 on the side profile (Figure 2.21). There were no digital nerves identifiable at this level. The vessel is covered by a thick layer of fascia. Except for small superficial and dorsal veins, no other large vein was identified within the digit.

Collateral ligaments across the IPJ were identical to those in humans and consisted of two components: the main collateral ligament with horizontal alignment, was parallel to the axis of the digit; and an accessory component with an oblique orientation that inserts into the plantar plate, as well as the adjacent phalanx (Figure 2.22).

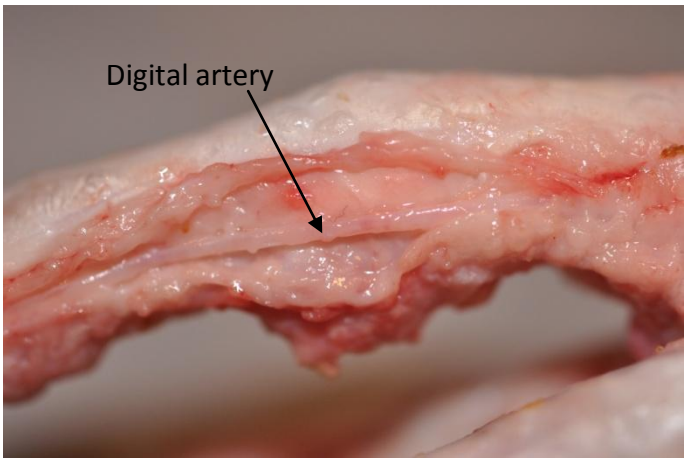

Figure 2.21: Digital vessel

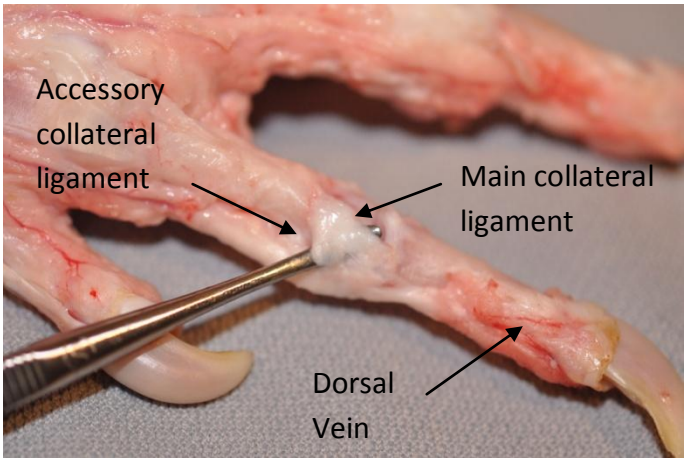

Figure 2.22: Collateral ligaments and dorsal veins

All FDS, FDI and FDP tendons arise from their individual muscle belly. These tendons changed at the mid plantar level from a flexible structure to a calcified structure and become adherent to the lower leg bone (Figure 2.23 and Figure 2.24); this is not observed in human tendons.

Deep to the tendons, the plantar plates (volar plates' equivalent structures) cover the IPJ and at the mid plantar level thick plantar plates provide cover over the mid plantar joints (Figure 2.25). These provide strong resistance against digital hyperextension at this level whilst the bird is weight bearing.

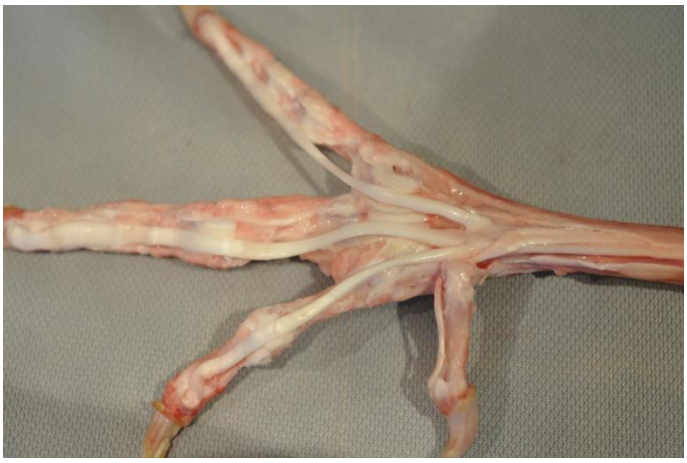

Figure 2.23: FDP tendon to all digits

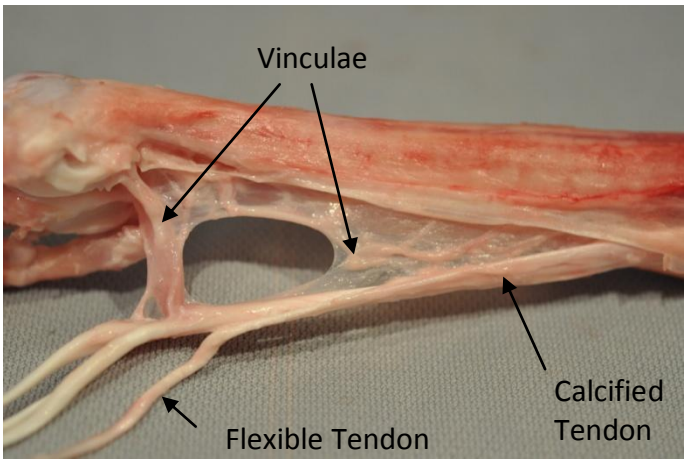

Figure 2.24: FDS tendon in the lower leg and associated vascular vinculae

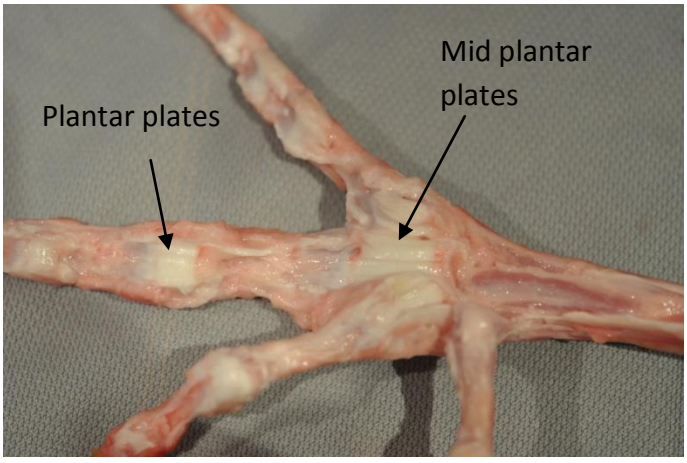

Figure 2.25: Plantar plates across the joints

2.4 Bony Anatomy

The lower half of the leg consists of two bones, resembling the tibia and fibula in human anatomy. For the purposes of this anatomical study the larger bone will be called the tibia and the smaller bone the fibula. The tibia is attached to the fibula at two levels, proximally at the articular level, and distally at the level of the middle and the distal third junction of the tibia. There are no articulations between these two bones, unlike those found in the human equivalents (Figure 2.26). The distal end of the tibia diverts to three condylar structures that form the mid plantar joints with the base of the proximal phalanxes (P1). The middle condyle is more distal compared with the adjacent condyles (Figure 2.27). There is a flat bony extension on the medial side, proximal to the medial condyle that provides an articulation surface for the proximal phalanx of the digit 1 (Figure 2.28).

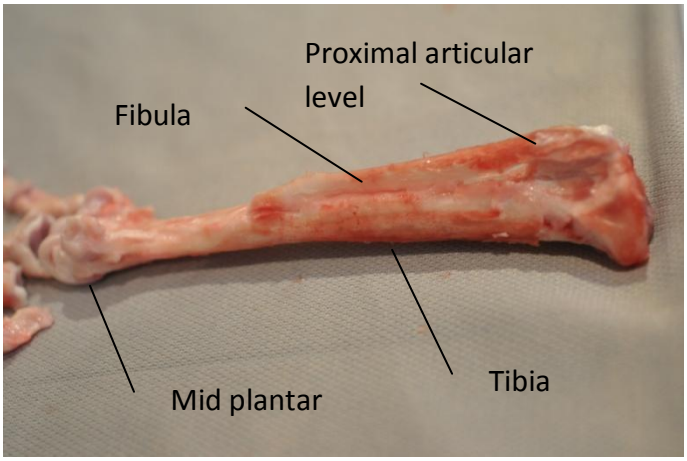

Figure 2.26: Lower leg bony structure

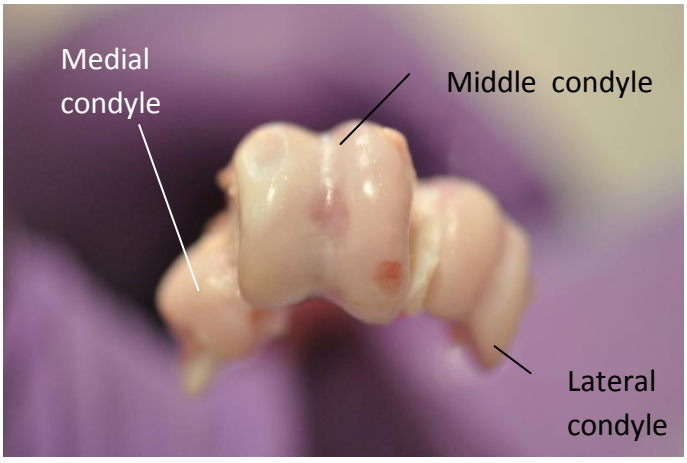

Figure 2.27: Distal tibia condylar alignment

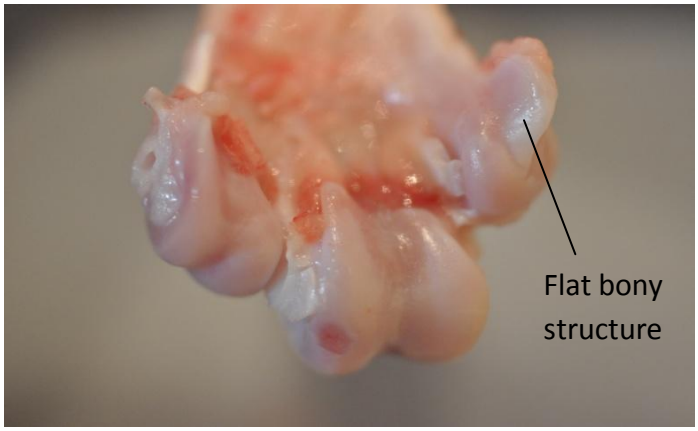

Figure 2.28: Medial condyle with flat bony component

2.5 Dorsal Structures

There are two layers of extensor tendons at the dorsal surface of the lower leg and digits. The deep extensor tendon inserts onto P1 of digit 3 only (Figure 2.29).

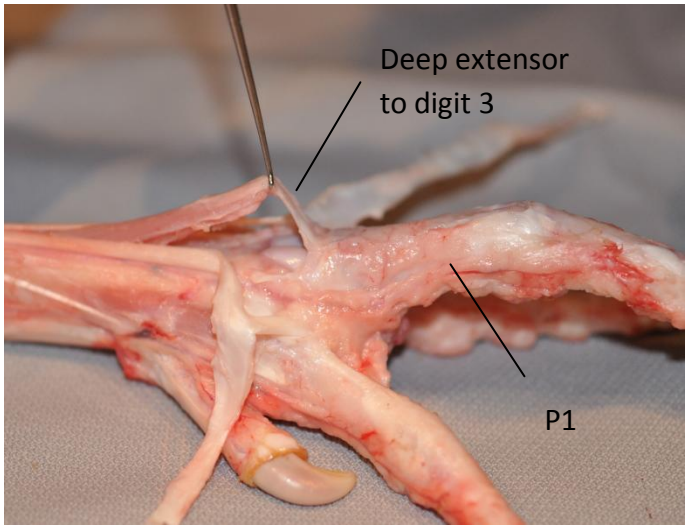

Figure 2.29: Deep extensor tendon to the digit 3, P1

One of the three superficial extensor tendons inserts on the distal phalanx of digit 1. This tendon inserts in a plane perpendicular to the plane of the tendon in the lower leg in the weight bearing bird (Figure 2.30). The other two superficial extensor tendons insert onto the other toes. These tendons are calcified structures in the lower leg with no flexibility and become flexible and tendon-like structure at the level of the mid plantar joints (similar to the flexor tendons). The most medial tendon provides

extension to digits 2 and 3, and the lateral extensor tendon provides extension to digits 3 and 4 (Figure 2.31and Figure 2.32).

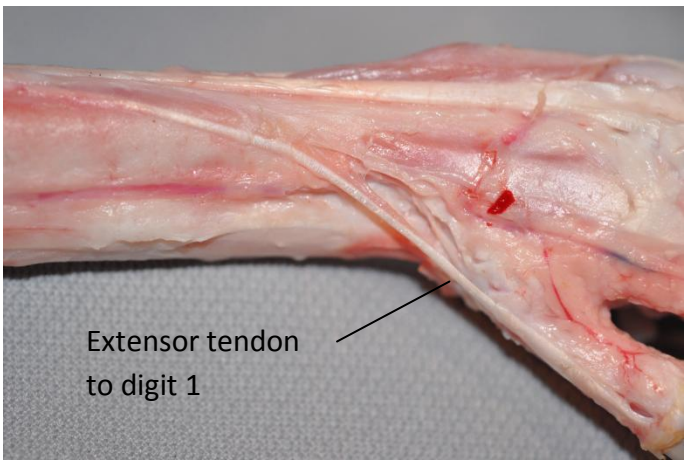

Figure 2.30: Isolated extensor tendon to digit 1

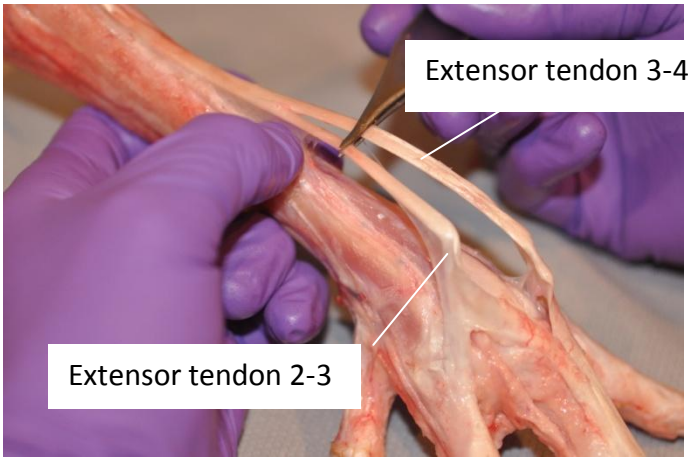

Figure 2.31: Two superficial extensor tendons

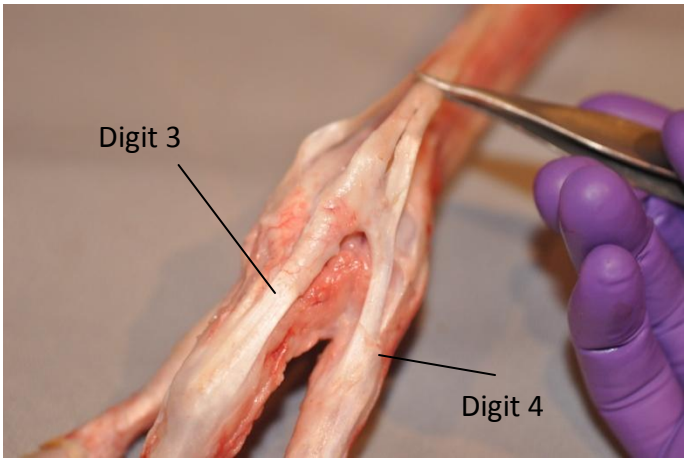

Figure 2.32: Extensor tendon 3-4

Extensor tendon 2-3 provides extensor slips to all phalanxes of digit 2 (Figure 2.33) and an extra slip to P2 in digit 3 (Figure 2.34). Extensor tendon 3-4 provides five tendon slips to all the phalanxes in digit 4 and two separate slips to P3 and P4 in digit 3 (Figure 2.34).

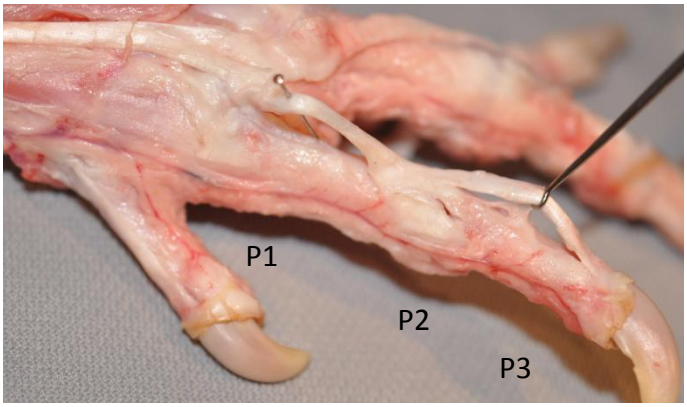

Figure 2.33: Extensor tendon 2-3

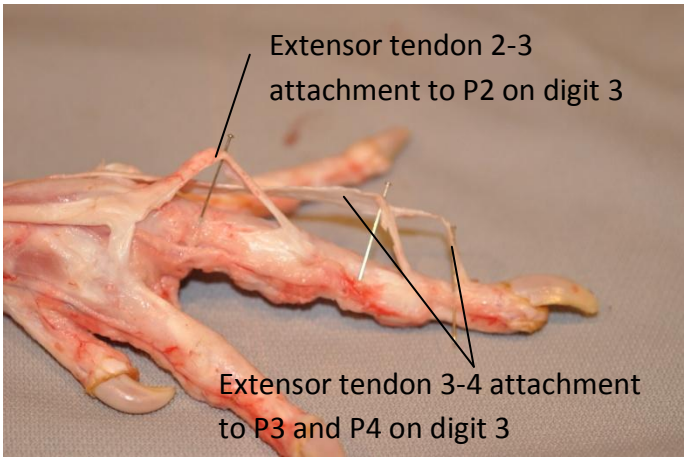

Figure 2.34: Extensor tendon 2-3

Chapter 3 - Specimen Dissection and Experimental Set-up

3.1 Initial Dissection

Paired turkey feet were collected on the day of animal slaughter from the Turkey Farm (Leicestershire Farm Fresh Turkey, Cold Newton Lodge, Cold Newton Rd, Leicester LE7 9DA) and cooled in a refrigerator to preserve the tissues for dissection the following day. All specimens were washed in cold water prior to dissection in order to remove dirt and debris. The dorsal surface of the long digit was incised at the mid lateral point to remove the dorsal scaly skin without damaging the extensor and flexor components, using a sharp size 10 surgical blade mounted on a blade handle for dissection (see Appendix 1, Figures W1 and W2) and toothed forceps to hold the dorsal skin away from the deeper structures (see Appendix 1, Figure W3); this allowed the better identification of the joints from the dorsal surface. The dorsal joint surface between the middle condyle (Figure 2.27) and the proximal phalanx was incised without interfering with the volar plate. The specimen was then turned to expose the plantar skin. The plantar skin and the fat pad were removed with care to avoid injury to the pulley complexes.

The digit was hyper-extended to pull as much flexor tendon into the pulley mechanism distally, in order to provide a longer length of the flexor tendon for use in the experiments, and all three flexor tendons were then divided proximally at the level of the middle condyle and proximal phalanx, on the volar surface. The mid plantar plate and collateral ligaments were divided at this point and the digit was removed from the foot. Proximal to this point all tendons were calcified and it was not possible to divide them using a surgical blade.

Stabilising the proximal part of the long digit with the help of an assistant, the long flexor tendon (FDP) was held using toothed forceps and divided at the DIPJ, using a size 15 surgical blade mounted on a blade handle (see Appendix 1, Figure W4). The distal phalanx was removed by disarticulation of the DIPJ. Protecting the tendon and pulling it to one side at the distal end, the pulleys were released on the opposite side to the pulled tendon to avoid lateral tendon injury. Using a size 15 blade, the pulleys

were released on both sides of the tendon, from inside to outside and in the distal to proximal direction, up to the mid-point of the A3 pulley. The distal half of the A3 pulley and all the dissected distal pulleys were removed fully. The long flexor tendon was released from the three connecting vinculae and was freely mobile at this point. The two flexor tendons were protected by flexing them away from the bone and PIPJ1 was extended to allow better visualisation of the volar plate at this level (Figure 3.1). The volar plate and the collateral ligaments were cut at the IPJ1, moving from the volar to the dorsal direction, to avoid injury to the flexor tendon.

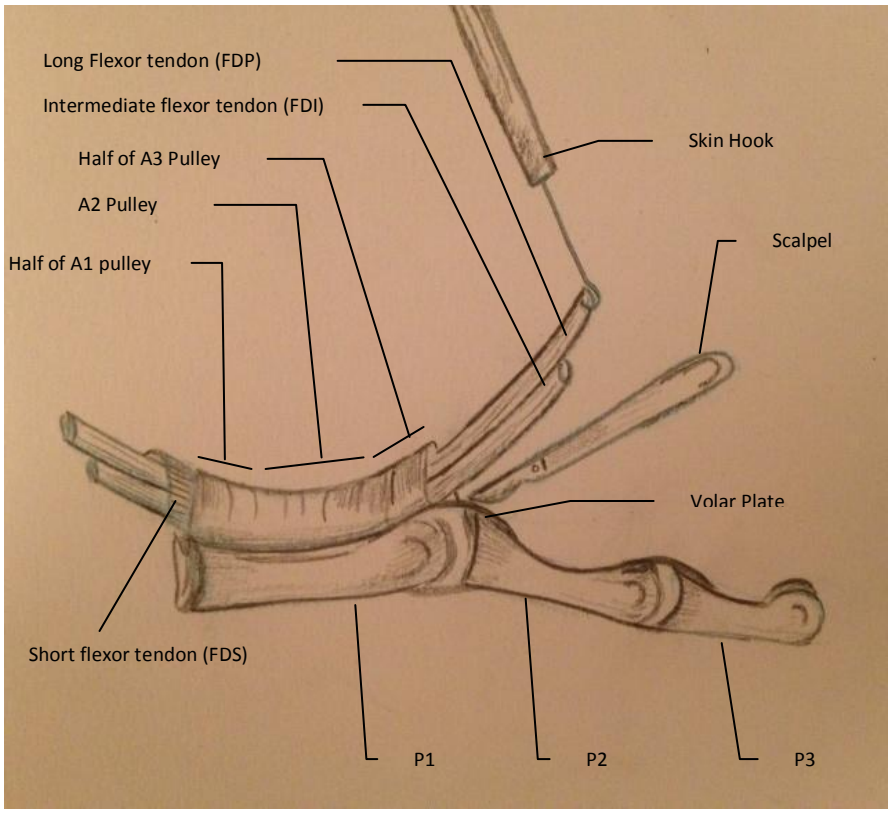

Figure 3.1: Release of the volar plate to free the specimen from the other phalanxes

The specimen at this point was composed of the proximal phalanx, A2 and half the A3 and A1 pulleys and all three flexor tendons. The specimens were then aligned individually on a piece of cling film with the tendons laid flat on the surface without bending, and then individually wrapped. The specimens were then frozen at -40° C (the lowest freezing point available in the departmental laboratory) to avoid the adverse effect of the freezing process on the gliding properties of the specimen (Douglas, 2013).

3.2 Second Stage Dissection

Before each experiment a 2mm drill hole (see Appendix 1, Figure W5) was made across the length of the bone from the proximal to distal direction. This was easier to accomplish when the specimen was frozen as it could be gripped better. The specimen could be very slippery and was prone to damage during this process if the drill holes were made after thawing. Each specimen was thawed in normal saline for 30 minutes and then using 3.5 magnification each specimen was dissected further. At the proximal end, the FDS tendon was divided at the proximal edge of the A2 pulley using a sharp blade. The FDI tendon was gently pulled out of the specimen, as it has no attachment in the proximal phalanx, while protecting the long flexor tendon at both ends. The synovial sheath that covers the FDP tendon was then removed using toothed forceps and tenotomy scissors (see Appendix 1, Figure W6). The proximal part of the A3 pulley that covers the distal condyle of P1 and the distal end of the A1 pulley that covers the proximal flare of P1 were removed to expose only the A2 pulley.

A 15 cm length of garden wire (see Appendix 1, Figure W7) was passed inside the bone through the drill hole and through the holes on each side of the experiment plate. The wire ends were then tightened underneath the experiment plate using pliers (see Appendix 1, Figure W8) to secure the specimen and avoid micro movement of the specimen during the experiments.

The specimen and the experiment plate (Figure 3.2) were mounted on the centre of the experiment frame (Figure 3.3) with the distal end of the FDP tendon at the actuator end.

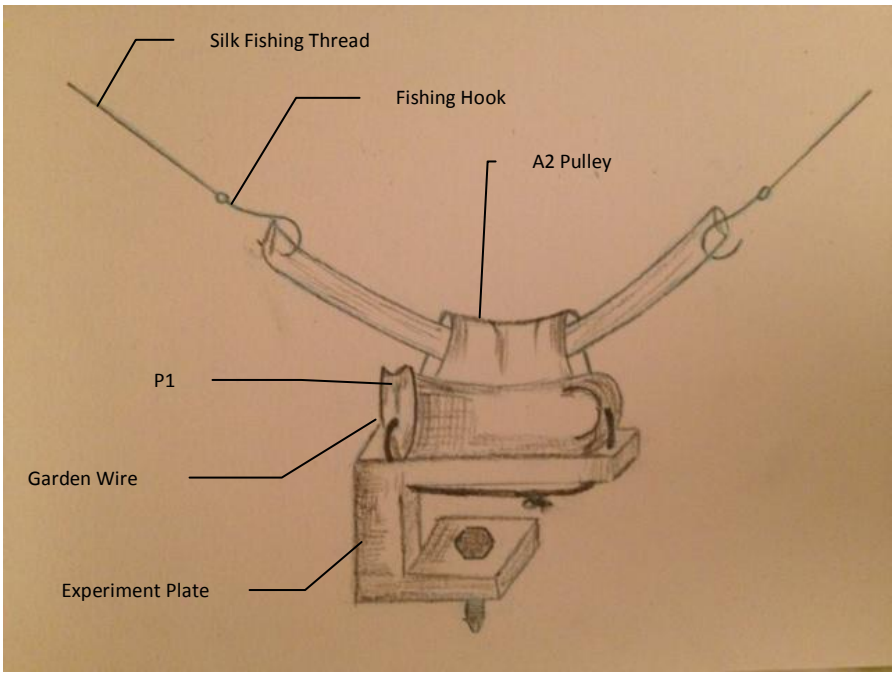

Figure 3.2: Specimen and the experiment plate

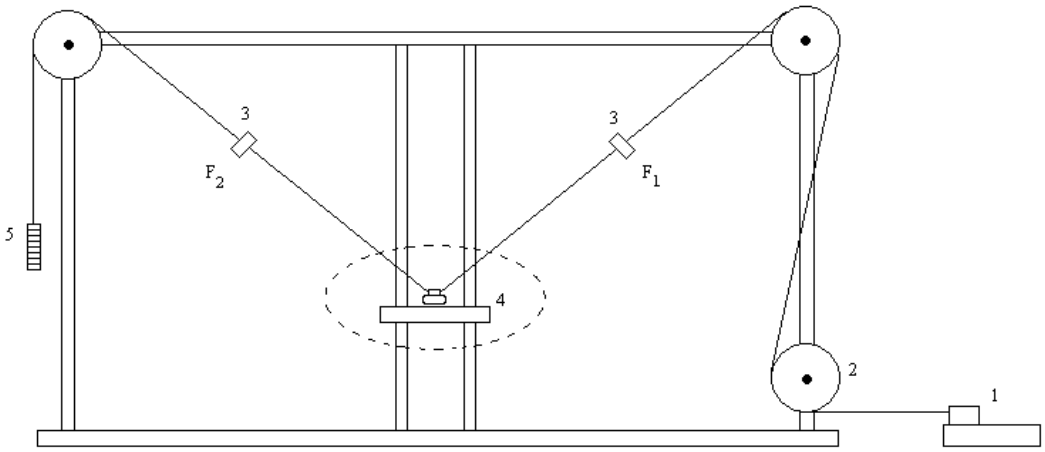

Figure 3.3: Experiment frame

1.Linear actuator 2. Ball Bearing Pulley 3. Force Transducers (measuring F_1 and F_2) 4. Specimen and the plate 5. Attached weight 200 or 400 g 6. Silk fishing thread.

With Permission from James A. Kennedy (Kennedy, 2011).

3.3 Experimental Set-up

The setup was supported by a steel frame to which three pulleys were attached to guide the fishing thread, for an accurate line of pull on the tendons (Figure 3.3).

Two fishing hooks attached to a fishing line cable were used to attach each end of the tendon to a load cell. The fishing hooks were inserted at the two ends of the tendon, and were positioned more than 10 mm from the tendon ends. This distance was chosen based on trial and error during the experiments. The fishing hook was found to pull out through the tendon end during an experiment if the distance was shorter than 10 mm.

On the left side of the apparatus, the load cell was connected to the proximal part of the tendon at one end and a weight on the other end. The thread carrying the weights (200 or 400 g, 2N or 4N, respectively) ran over a low friction ball bearing pulley, to allow for flexibility while the flexion angles were changed, and directed the weight to the tendon end at the correct angle with minimal friction.

On the right side of the apparatus, the load cell was connected to the distal end of the tendon at one end and a fishing thread on the other end, which ran over two pulleys before connecting to the actuator. This was to allow the horizontal movement of the actuator situated on the table to be converted to the angular pull at the end of the tendons.

The electronically controlled linear actuator was attached to the table on the right side of the apparatus using industrial Velcro. The actuator was controlled by a computer program to provide precise linear motions during the experiments.

3.3.1 Actuator

Device: ESZ3 Motorised Linear Slide, Oriental Motor UK Ltd., Basingstoke, Hampshire, UK (see Appendix 1, Figure W9).

Function: This device drives a roller ball screw system, providing a linear motion with repetitive positioning accuracy of ±0.02 mm, maximum distance of 850 mm, and maximum transportable mass, horizontal 60 kg / vertical 30 kg. An excursion of 40 mm

and a velocity of 30 mm/sec was used to allow full entry and exit of the marked flexor tendon under the full length of the A2 pulley and at a speed slow enough to allow for visual assessment of the excursion. Using a program called Slider (a custom designed program that allows full control of the actuator in terms of distance, speed, acceleration and deceleration), the actuator was programmed to produce repetitive excursions with identical velocities. The actuator was set up to complete the excursion cycle at the end of each experiment (60 seconds) with equal acceleration and deceleration velocities. The experiments and the subsequent data were therefore not affected by the direction of the excursion (Uchiyama et al., 1995).

3.3.2 Calliper

A digital calliper (see Appendix 1, Figure W10) with an accuracy of 0.00 mm was used to measure the length of the A2 pulleys after thawing.

3.3.3 Load cells

Device: Load cell. Model 31 Low Range Precision Miniature Load Cells, Sensotec Inc., Columbus, Ohio, USA (see Appendix 1, Figure W11).

Function: The strain forces applied at each end of the load cell leads to the resistance of an electrical conductor inside the load cell. Load cells with a range of 50 g to 500 g were chosen in this study as 200 g (1.962 N) and 400 g (3.924 N) loads were used. The values obtained by the load cells were therefore within the plateau phase of the transducer's recording.

A load cell was positioned at each end of the tendon, and when the tendon was pulled in and out of the pulley mechanism, the tensile forces were measured and recorded at both ends of the tendon. The output from the load cells was at a frequency of 100 Hz which was then amplified and converted to a voltage in the control board (2 amplifiers, analogue to digital converter, USB interface, power supply and actuator driver, custom design by UKELO technology, Punch X Ltd, Huddersfield, UK) before reaching an ATD converter (ATD Converter USB-1408FS, Measurement Computing Corporation, Norton Massachusetts, USA). Tracer DAQ software (version 2.1.1, Measurement Computing Corporation, Norton Massachusetts, USA) (see Appendix 1, Figure W12) recorded the

output (100 recordings / sec) for 60 seconds, displaying the results as a graph. In total, 6000 pieces of data were recorded per transducer, per experiment. These were saved as a .txt file and converted to a Microsoft Excel file (2007, Microsoft Corporation) for data handling and analysis.

3.3.4 Ball Bearing Pulley

Device: Dynaroll miniature precision motion control pulley, (see Appendix 1, Figure W13).

Function: This is a double-shielded ball bearing pulley, made of 400 series hardened stainless steel. This miniature precision motion control pulley, with a deep-groove ball bearing is designed for use in applications requiring low torque, smooth operation, low noise and creates lower friction. The pulley has a single groove on the outer raceway's surface that keeps the fishing thread in place, thereby preventing it from wearing down by rubbing against the sides of the pulley.

Rolling bearings use rolling elements to maintain the separation between moving parts in order to reduce rotational friction and support radial and axial loads. Sealed bearings are lubricated with oil or grease in the bearing factory, while open and shielded bearings should be lubricated in place, with periodic reapplication of lubrication, based on use. All the pulleys were therefore lubricated using a general lubricant, WD-40 before the start of the experiments. The pulleys were used to provide the appropriate line of pull for the correct angle of the tendon-A2 pulley, during the experiments.

3.3.5 Silk Fishing Thread

Device: Antares silk shock, 1.860 kg maximum weight, 0.12 mm thickness, Shimano, Japan (see Appendix 1, Figure W14).

Function: Silk shock technology has limited stretch and a high modulus of elasticity of 7 N/Tex, compared with 5.2 N/Tex for prolene and 5.5 N/ Tex for vicryl suture materials. It also has a high breaking strain and maximum smoothness. In these experiments this is important as the strain forces will not be wasted while stretching the line fibres, and

the smoothness of the line will lead to lower friction when in contact with the stainless steel pulley.

3.3.6 Fishing hook

Device: Gamakatsu Siwash Hooks, Japan (see Appendix 1, Figure W15).

Function: These size 24 fish hooks were used to suspend the tendon within the apparatus during the experiments. The sharp tips allowed for a smooth entry into the tendon about 10 mm from the tendon ends. The hooks have a deep throat bend, cutting point and anti-corrosion black chrome finish to allow for multiple use.

3.3.7 Weights

Device: Brass slotted laboratory weights, (see Appendix 1, Figure W16).

Function: These slotted weights are made from solid brass and each weighs 50 g. The weights were used to provide counter resistance to the movement of the tendon under the A2 pulley, initiated by the actuator movement. Two weights, 200 g (2 N) and 400 g (4 N), were used, attached via fishing thread over the ball bearing pulley, to the proximal tendon load transducer. These were used to reflect the effects of passive mobilisation of a tendon, based on other *in vivo* studies (Lieber et al., 1996, Schuind et al., 1992).

3.3.8 Experiment Plate and Centre Piece

The specimen as described in the dissection section was mounted on the central plate (Figure 3.2), at the middle of the frame using a bolt screw and nut which was fully tightened with a pair of pliers to avoid micro movement of the experiment plate during the experiments.

3.3.9 Tendon Moisturising Liquid

Device: Normal (0.9%) saline delivered via an adjustable flow rate giving set (see Appendix 1, Figure W17).

Function: Normal saline contains sterile water and 9 g/L of sodium chloride, and is a fluid routinely provided intravenously for the rehydration of patients. This fluid was

used during the experiments to maintain the moisture of the specimens, to provide a close to natural *in vivo* environment for the tendons, and to avoid surface drying which could lead to excess friction between the tendon and the A2 pulley. The normal saline bag and the giving set were positioned on the upper part of the frame and secured with tape. The giving set was secured using a wire at the centre of the frame to direct the giving set over the specimen where a steady dripping of the fluid over the specimen was maintained.

3.3.10 Suture Material

During the experiments where tendon repair was required, two different sutures were employed.

1. 4-0 Ethibond suture was used for the core tendon repair (see Appendix 1, Figure W18). This is a polyester, green (to improve visibility), braided, coated (to improve handling quality and gliding) and non-absorbable suture. Ethibond suture size 4-0 was used, as it was more consistent with the size of the turkey tendon.
2. 6-0 Ethilon was used for circumferential tendon repair (see Appendix 1, Figure W19). This is a non-absorbable (to provide prolonged tensile strength), mono filament (with a uniform and smooth surface), polyamide suture. It has a smooth surface with good handling and pliability characteristics that permits easy and secure knotting. This was used to finely suture the tendon edges following the core suture to provide a smooth edge at the laceration site and therefore reduce the GR during tendon excursion. Ethilon size 6-0 was used, as it was more consistent with the size of the turkey tendon.

3.3.11 Environment

Experiments were carried out in university laboratories in Leicester General Hospital and Leicester Royal Infirmary. Both laboratories were air conditioned at temperature controlled at 18° C.

3.3.12 Animal Model

Chicken feet digital flexor tendons have previously been used as a model for flexor tendon studies to investigate different surgical treatments for flexor tendon

lacerations (Cao et al., 2008, Farkas et al., 1974, Tang et al., 2007, Xie et al., 2008, Xu and Tang, 2003). For the purpose of these experiments, turkey feet have been used which have been shown to be similar to human fingers (Chapter 2). The turkey digits are larger than chicken digits and more similar to human digits in terms of the actual size.

3.3.13 System Calibration

Both load cells were calibrated to 0 and 50 g prior to the start of each experiment. This was performed by initially resting the sensor on a wooden table away from any metal object or magnetic field, and then by suspending the load cells from one end, against the 50 g weight at the other end.

The system was calibrated by adjusting the small screw on the control board for each load cell so that the value of 0 and 50 would appear as a flat line on the tracer DAQ software for each weight respectively.

The process of calibration required measurements of the gliding resistance for each ball bearing pulley and for combination of all three ball bearing pulleys without any tendon specimen. The values obtained by the load cells were lower than 0.0001 when all three pulleys were used together. It was concluded that the gliding resistance from the equipment was unlikely to result in a significant change in the final results.

3.3.14 Data Handling

Unlike Uchiyama, these experiments accounted for the forward and backward movement of the tendon in and out of the pulley. This meant that F1 and F2 had to be alternated depending on the direction of the tendon movement.

Calculation of the GR and CF required that motion was in the direction of F2, actual finger flexion with the flexor tendon being pulled towards the muscle part; therefore, F2 was greater than F1 at this point of time. The change of direction was identified from a force against time graph, using the ‘MAX’ and ‘MIN’ functions of Excel to identify F1 and F2.

F1 and F2 were recorded in volts and were used in the formula as volt values. The formula contains the natural logarithm of the forces divided and therefore the units cancel each other out to provide a value for CF, which has no unit.

Conversion of the arc of contact from degrees to radians was performed using the equation:

$$\text{Degrees} = \text{Radians} \times \frac{180}{\pi}.$$

Therefore an angle of 10° and 70° are converted to 0.1744 and 1.225 radians, respectively.

Chapter 4 - Surface Electron Microscopy of the Flexor Tendon and A2 Pulley

4.1 Background

There have been many reports of increased tendon repair strength using a variety of core and epitenon suture materials and designs (Greenwald et al., 1994, Haddad et al., 1988). Suture material used for the tendon repair and the zone of injury come into direct contact with the pulley mechanism during active and passive finger motion. Increased friction at this point can lead to higher GR and subsequent inflammation and greater adhesion formation (Zhao et al., 2001). This is therefore an important factor which affects the outcome of tendon repair.

To improve the gliding ability the surface modification of a tendon has been studied using surface lubricants, such as HA, lubricin, and phospholipids (Moro-oka et al., 2000, Sun et al., 2004, Taguchi et al., 2008, Tanaka et al., 2007). Analysis of the surface changes of the flexor tendon and pulley following tendon repair can identify areas of improvement within surgical techniques, and the GR has been shown to be reduced by altering the suturing technique, suture material and knot position. In this section the effect of tendon repair and suture material on an injured tendon and their subsequent effect on the contact surface of the pulley following active motion will be studied.

4.2 Specimen Preparation

Fresh specimens of tendon, pulley and bone were dissected from the turkey feet (section 3.1 and section 3.2). After each experiment a 6/0 nylon suture was applied on the dorsal surface of all the flexor tendon specimens to allow the technician to identify and examine the volar surface of the tendon. To allow for visualisation of the inner most surface of the pulley a similar suture was applied on the opposite surface, avoiding injury to the deeper layers.

Specimens were delivered to the electron microscopy laboratory in phosphate buffered solution. All the specimens were initially fixed in buffered glutaraldehyde to stabilise them before the dehydration process, which was accomplished through

immersion in a series of increasing ethanol concentrations to remove all the water. The samples were then dried, either chemically using hexemethyldisilazane (HMDS), or via critical point drying (CPD). Drying them in preserved the integrity of the cells.

All the specimens were processed as followed:

Fixation and Initial Dehydration:

1. Fixed in 2.5% glutaraldehyde in 0.1M Sörensens buffer pH 7.2 overnight.
2. Washed in 0.1M buffer for 30 min (x2).
3. Washed in distilled deionised water for 30 min (x2).
4. Immersed in 70% ethanol for 30 min.
5. Immersed in 90% ethanol for 30 min.
6. Immersed in 100% analytical grade ethanol for 30 min (x2).
7. Immersed in 100% analytical grade ethanol for 90 min.

Chemical Dehydration using HMDS of the Pulleys:

1. Immersed in 3:1 analytical grade ethanol/HMDS for 60 min.
2. Immersed in 1:1 analytical grade ethanol/HMDS for 60 min.
3. Immersed in 1:3 analytical grade ethanol/HMDS for 60 min.
4. Immersed in HMDS for 30 min (x2).
5. Excess HMDS was removed and the specimen was left in a fume hood to allow all traces of HMDS to evaporate overnight.

Critical Point Drying of the Tendons:

1. Stored in 100% analytical grade ethanol overnight.
2. CPD using a Bal-Tec CPD 030.
3. Mounted and Sputter coat - 90secs @ 20mA.

Dried samples were mounted onto aluminium stubs with Araldite glue. Once the glue had set the samples were sputter coated with gold, using a Polaron SC7640 to improve the resolution of the sample, as well as helping to dissipate heat from the electron beam, resulting in less heat damage. Samples were viewed using a Hitachi S3000H Scanning Electron Microscope with an accelerating voltage of 10kV.

4.3 Fresh Tendons and Pulleys: Human versus Turkey

Freshly dissected tendons were noted as having a smooth surface at ×30 magnification and a glandular layer at ×100 and ×300 magnification. This layer is part of the synovial membrane and is responsible for producing HA (Figure 4.1, Figure 4.2). The most dorsal layer (deepest) of the pulley was found to be glandular and was responsible for the production of HA. This layer was most detailed at ×1000 magnification (Figure 4.3D).

A 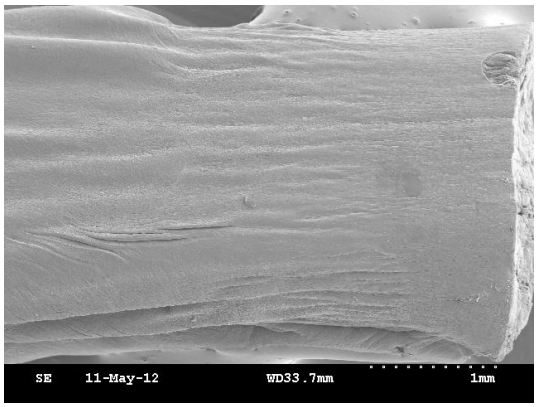

B 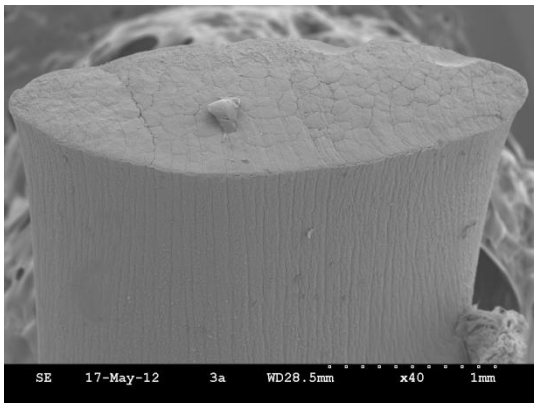

Figure 4.1: SEM of an intact flexor tendon

(A) Volar surface of fresh flexor tendon at ×30 magnification. (B) Cross section of the flexor tendon at ×40 magnification.

A 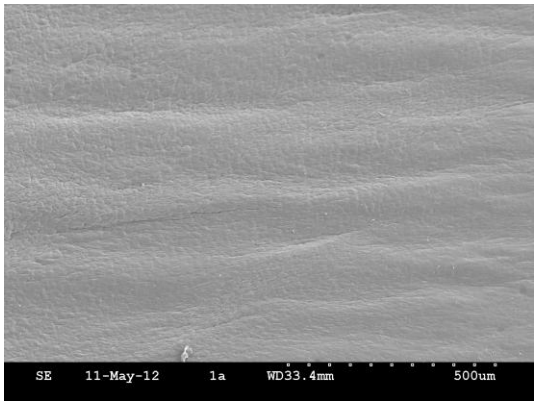

B 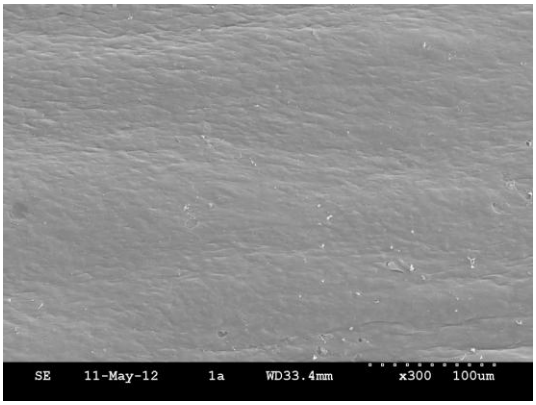

Figure 4.2: SEM of volar surface of a fresh flexor tendon

(A) ×30 magnification and (B) ×300 magnification.

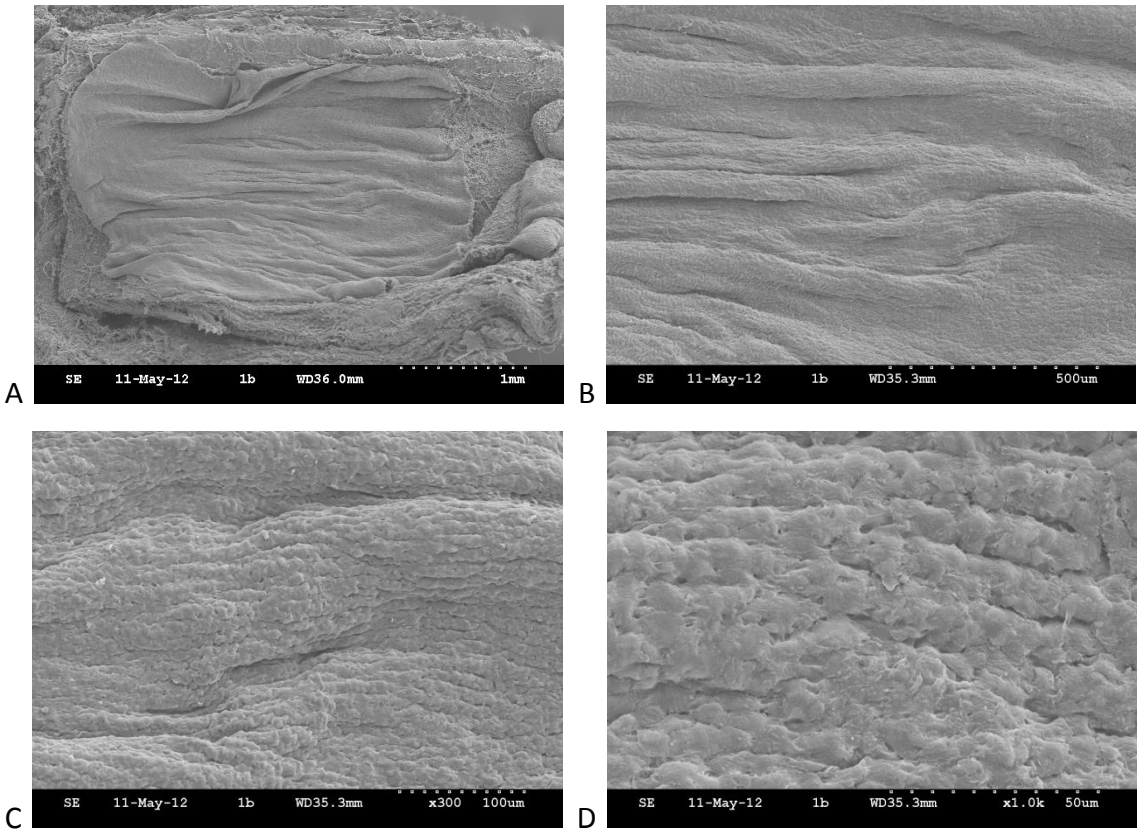

Figure 4.3: SEM of the deepest layer of the A2 pulley

(A) ×30 magnification, (B) ×100 magnification, (C) ×300 magnification, (D) ×1000 magnification.

Previous SEM studies by Sasaki et al. (1999) and Inoue et al. (1976) showed that the human flexor tendon and synovial sheath cells are similar in nature to those of the hen and appear similar to the turkey equivalent in this study (Figure 4.4 and Figure 4.5).

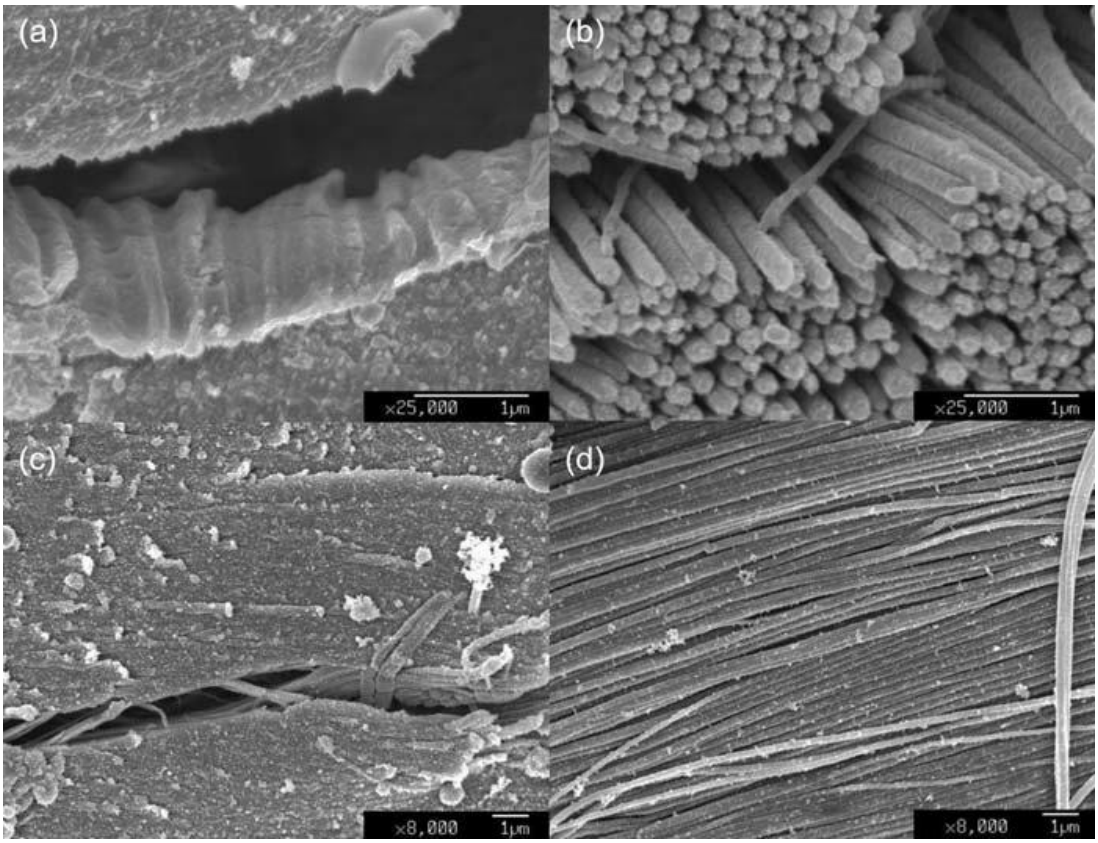

Figure 4.4: SEM views of an intact tendon

(A) and (B) Cross sections, (C) and (D) longitudinal sections, before and after cell-maceration (complete removal of the cellular elements and grinding) to allow visualisation of each collagen fibre.

With permission from: Sasaki et al. (1999).

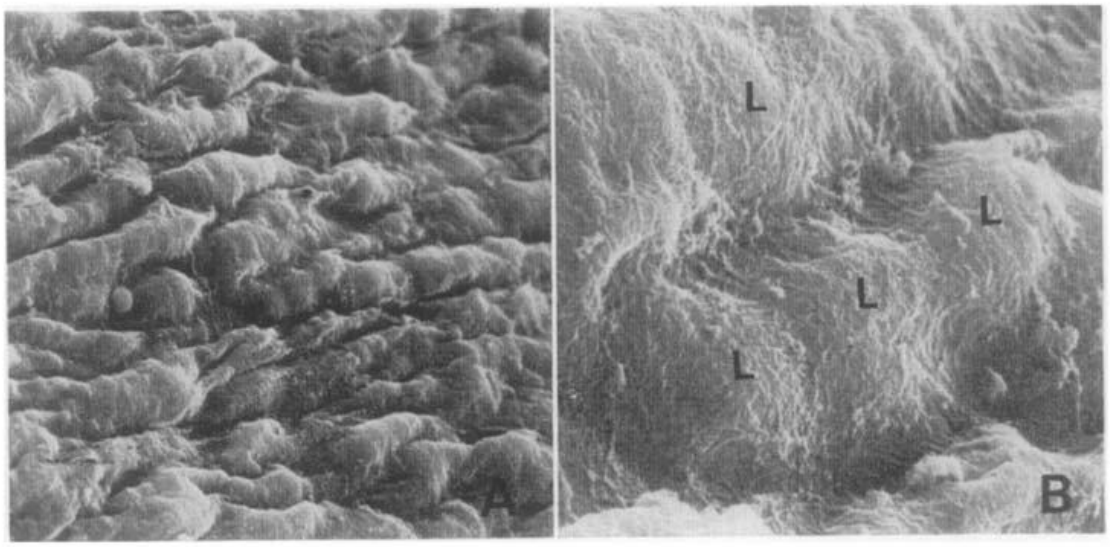

Figure 4.5: SEM of synovial cells in a human tendon sheath

With permission from: Inoue et al. (1976)

The surface structure of the flexor tendon and the A2 pulley remained unchanged after 10 minutes of simulated activity at 70° of flexion and 400g weight in the laboratory (Figure 4.6). This demonstrated that the tissues were not damaged during the dissection or handling, and therefore the subsequent procedures carried out on the tendons were solely responsible for the surface changes in the flexor tendon and the pulley.

A 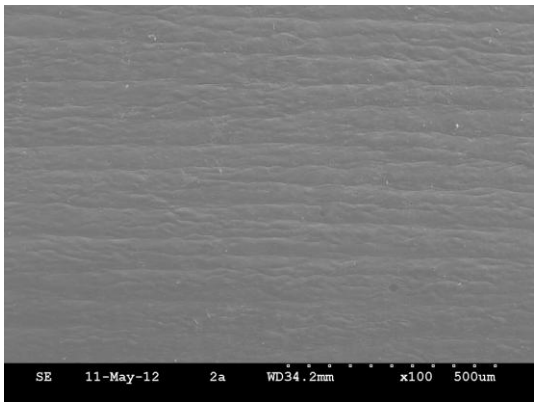

B 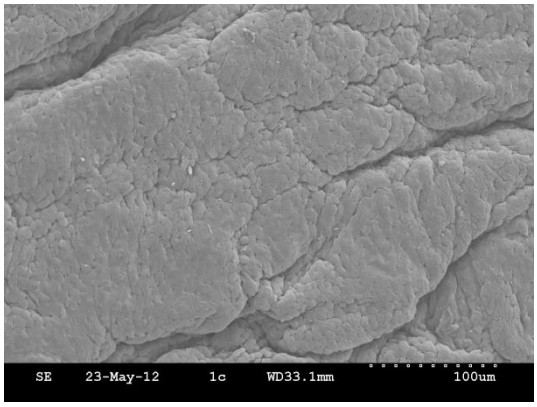

Figure 4.6: SEM following 10 minutes of simulated motion

(A) Flexor tendon surface ×100 magnification, (B) A2 pulley at ×1000 magnification

4.4 Pulleys and Tendons

4.4.1 Pulley Interaction with a Lacerated Flexor Tendon

A laceration of less than 50% was made to an intact tendon using a size 15 surgical blade. The lacerated tendon and the intact pulley were put though 10 minutes of simulated motion at 70° of flexion and 400 g weight, with normal saline lubrication, prior to the surface analysis.

During the simulated motion there was visible triggering of the partially lacerated tendon as the zone of injury entered under the pulley at each end. The zone of injury was observed to increase during the experiment (Figure 4.7) and this triggering led to tendon edge de-lamination at the level of the laceration (Figure 4.8A and B) and fraying below the centre of the laceration where the tendon had initially been intact (Figure 4.8C and D).

The effect of the lacerated tendon on the pulley was mild delamination at the entry and exit of the pulley where the triggering was most prominent. The central portion of the pulley remained relatively unaffected (Figure 4.9).

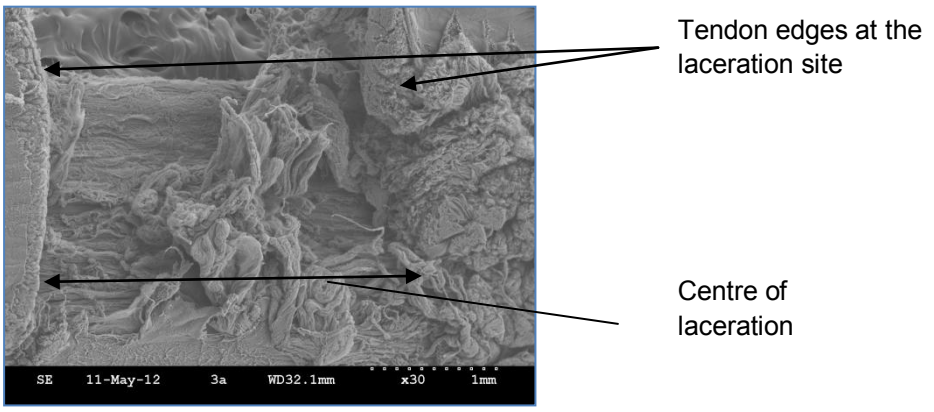

Figure 4.7: SEM of tendon laceration

At ×30 magnification

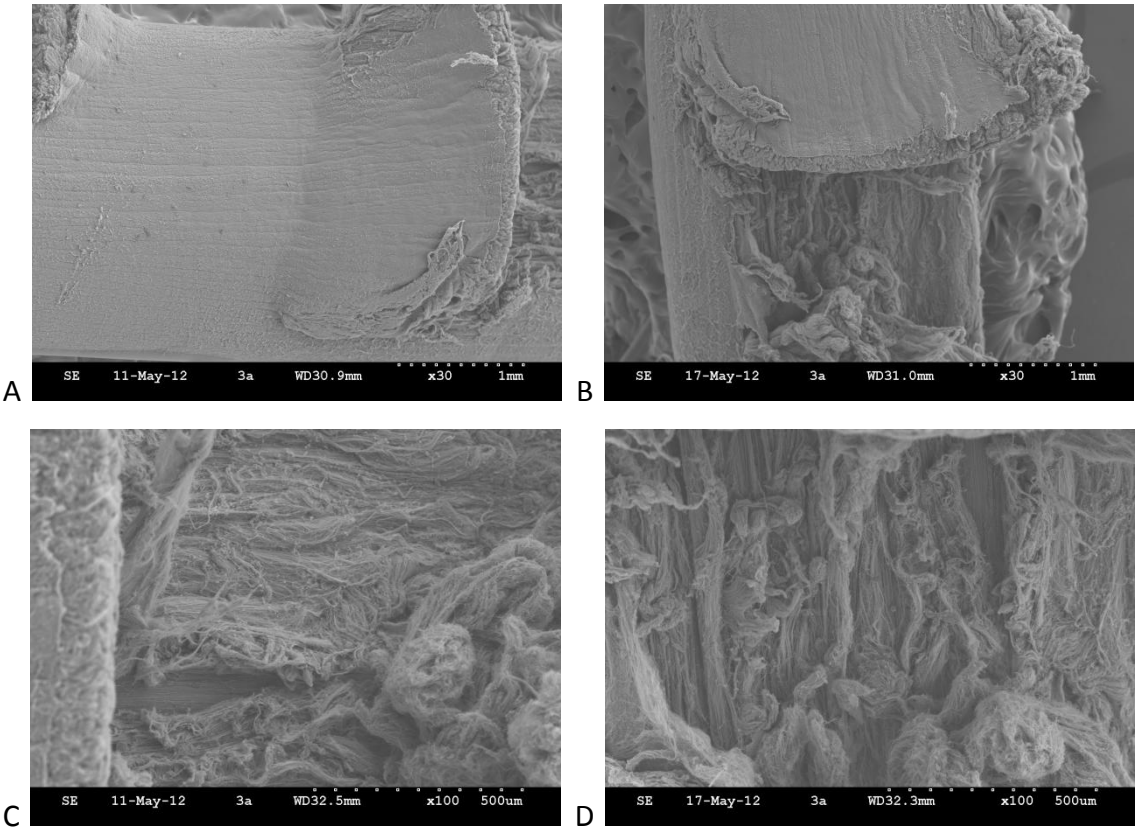

Figure 4.8: SEM showing de-lamination of the tendon edges at the laceration site

(A) and (B) ×30 magnification, (C) and (D) ×100 magnification.

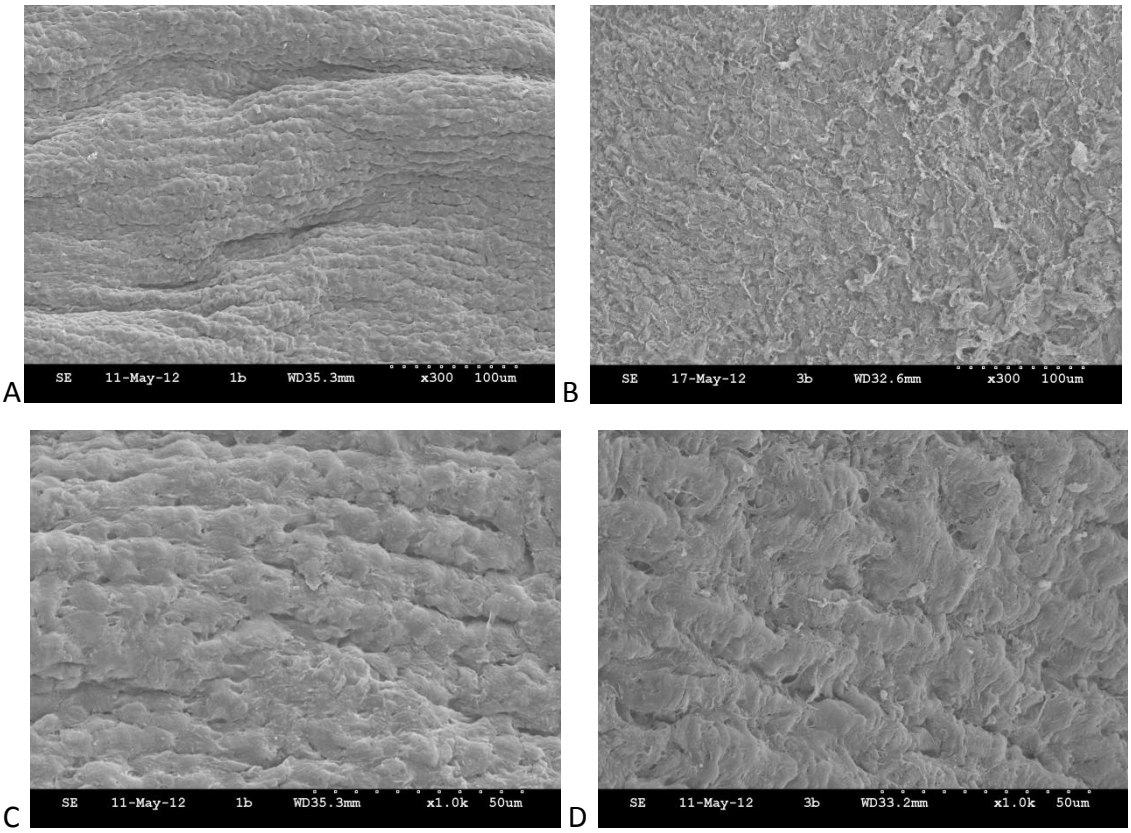

Figure 4.9: SEM of pulley following interaction with a lacerated tendon

Intact pulley (A and C) in comparison with the pulley following interaction with the lacerated tendon at the trigger point (B and D) at ×300 and ×1000 magnification, respectively.

4.4.2 Pulley Interaction with Circumferential Flexor Tendon Repair

A 6-0 Ethilon suture was used for a circumferential running suture on the volar aspect (gliding surface) of the flexor tendon in the absence of any laceration under ×3.5 magnification. The suture knot was positioned on the dorsal surface of the tendon and away from direct contact with the pulley. A simulated motion at 70° of flexion and 400 g weight was performed for 10 minutes with lubrication, prior to the surface analysis. This was in order to observe the effect of isolated suture material on the gliding surfaces.

At each needle entry site into the tendon, a V shape laceration was identified. Tensioning of the suture during the repair led to further longitudinal injury to the tendon in line with the suture tensioning, yielding a cauliflower appearance (Figure 4.10A) of the injured tendon at the final position of the suture material, and an overall Y-shaped laceration for each needle entry into the tendon (Figure 4.10B).

The suture material and iatrogenic injury to the tendon resulting from the needle and suture tensioning had very little effect on the pulley layer following simulated motion (Figure 4.11B) compared to the intact fresh pulley (Figure 4.11A).

A 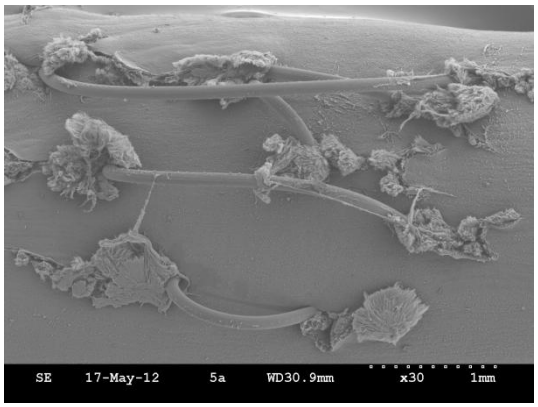

B 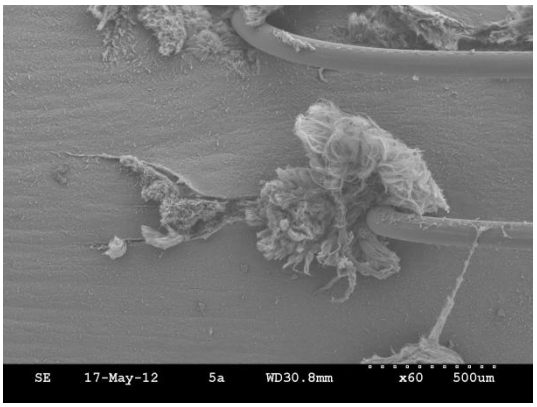

Figure 4.10: SEM following circumferential suturing

(A) ×30, (B) ×60 magnification.

A 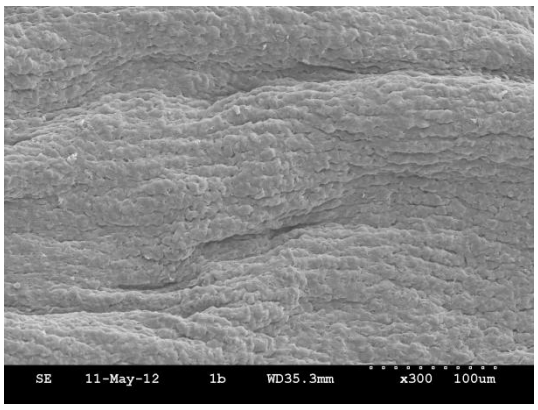

B 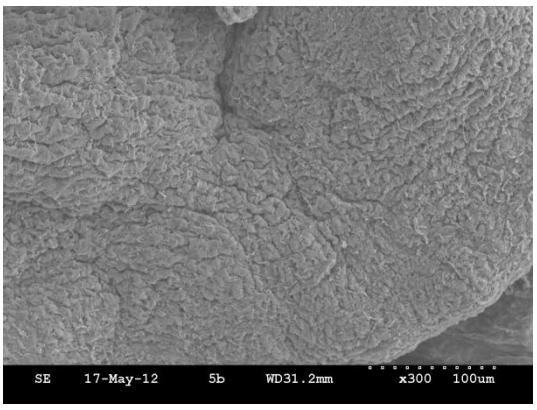

Figure 4.11: SEM of the pulley interaction with a circumferential suture

(A) intact fresh pulley, (B) pulley from a circumferential suture material specimen (x300 magnification).

4.4.3 Pulley Interaction with a Single Suture Knot

A single suture knot was applied on the volar surface of a tendon using a 6-0 Ethilon suture and five square knots; one surgeon's knot and three square throws.

A simulated motion at 70° of flexion and 400 g weight was performed for 10 minutes with lubrication, prior to the surface analysis.

The same findings were noted at the needle entry and exit sites as per previous experiment (Figure 4.12A); however, the presence of a prominent knot was noted to create areas of de-lamination on the corresponding section of the pulley (Figure 4.12A, B, C, D).

Ethilon is a monofilament suture but was found to have been made of heavily packed fibres (Figure 4.13C) that also fragmented during the simulated motion and when in contact with the pulley (Figure 4.13A). This was most prominent on the apex of the suture knot (Figure 4.13B). This progressive delamination of the suture material can lead to further pulley damage with prolonged motion.

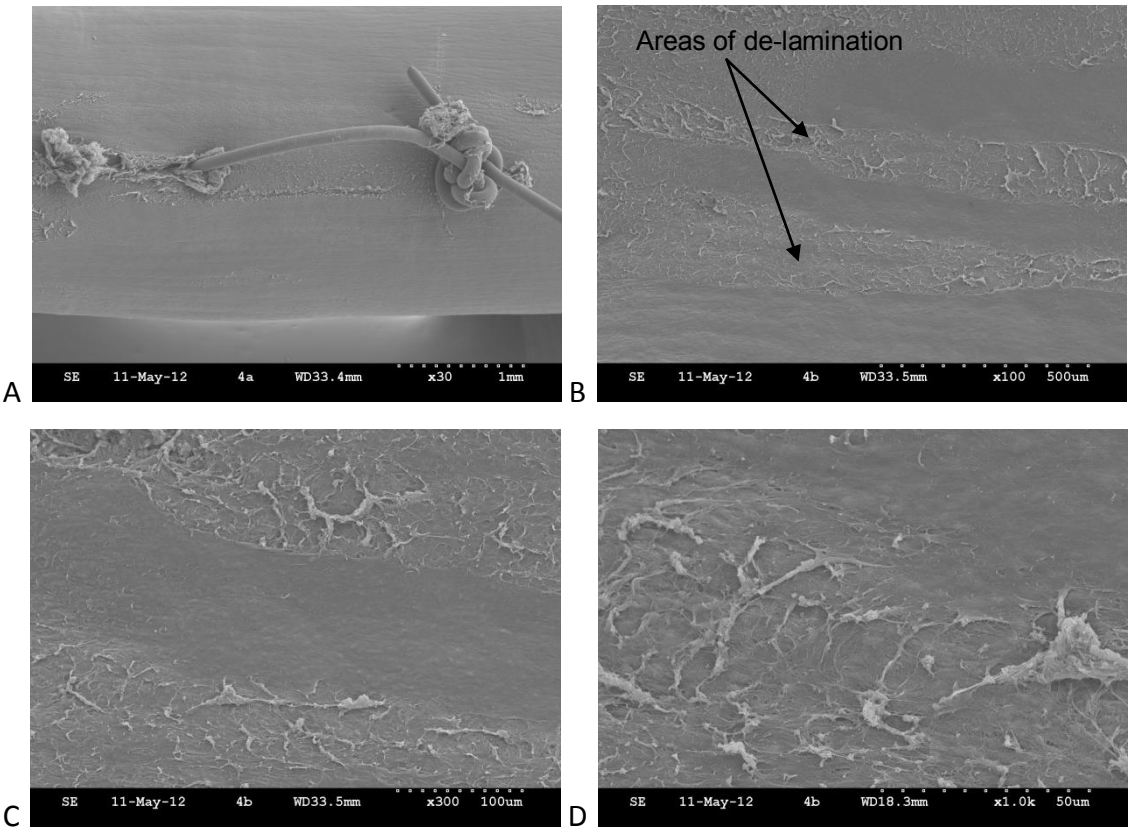

Figure 4.12: SEM of the suture knot and the effect on the pulley

(A) ×30, (B) ×100, (C) ×300, and (D) ×1000 magnification.

A 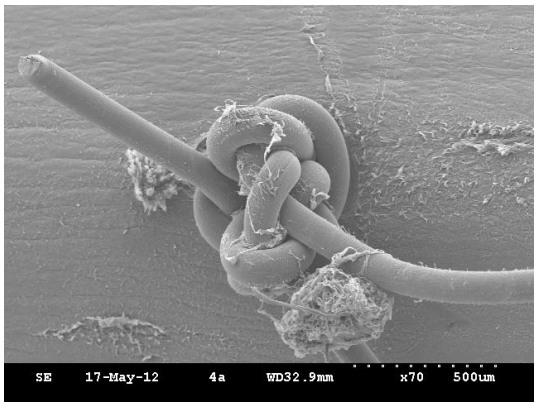

B 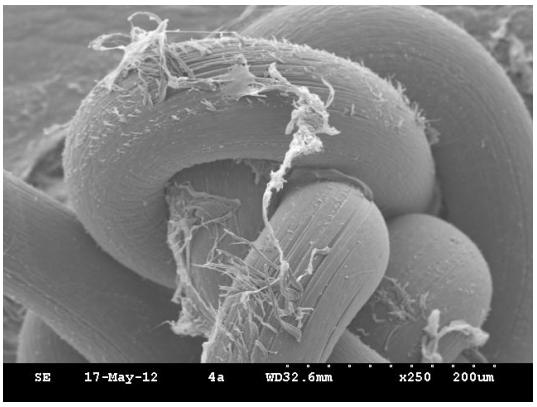

C 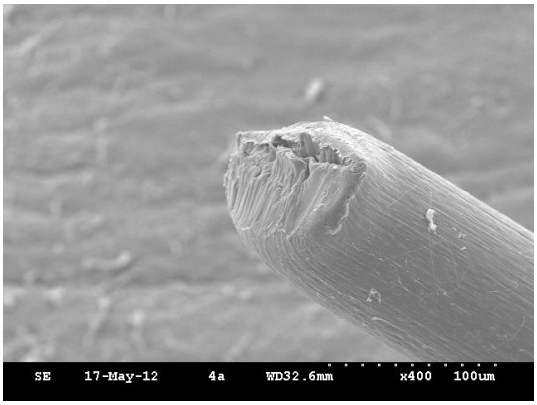

Figure 4.13: SEM of the suture knot

(A) ×30, (B) x250 and (C) ×400 magnification.

4.4.4 Pulley Interaction with a Fully Repaired Flexor Tendon Laceration

A fully lacerated flexor tendon was repaired with a core locked Kessler repair, using a 4-0 Ethibond suture, and a simple running circumferential repair using a 6-0 Ethilon suture, under ×3.5 magnification. The knot from the core suture was at the centre of the tendon with five square knots and was cut short at a distance approximately 3 mm from the knot to avoid the knot coming undone. The turkey flexor tendon was not thick enough to allow for the core suture knot to be buried inside the tendon ends. The knot from the circumferential suture was made by five square knots and was located on the dorsal surface of the tendon, away from the pulley.

A simulated motion at 70° of flexion and 400 g weight was performed for 10 minutes with lubrication, prior to the surface analysis.

Iatrogenic injury to the tendon from suturing was noted, similar to the previous experiments (Figure 4.14A). Dehydration and critical drying of these specimens led to

soft tissue shrinkage next to the suture material and relative elevation of the braided suture material from the tendon at the locking points (Figure 4.14C-D). The suture material, which was estimated to have been cut about 3 mm distal to the knot, was measured at 1.78 mm without corrections for the curved appearance of the fibres (Figure 4.14B).

Maximum pulley damage was observed in this specimen (Figure 4.15A-B), and was most likely due to the excess of suture material (braided suture), extensive tendon damage, and increased zone of tendon injury. De-roofing of the glandular layer of the pulley was noted at ×1000 magnification, indicating the loss of cellular integrity and therefore loss of the lubricating mechanism within the gliding surface of the pulley.

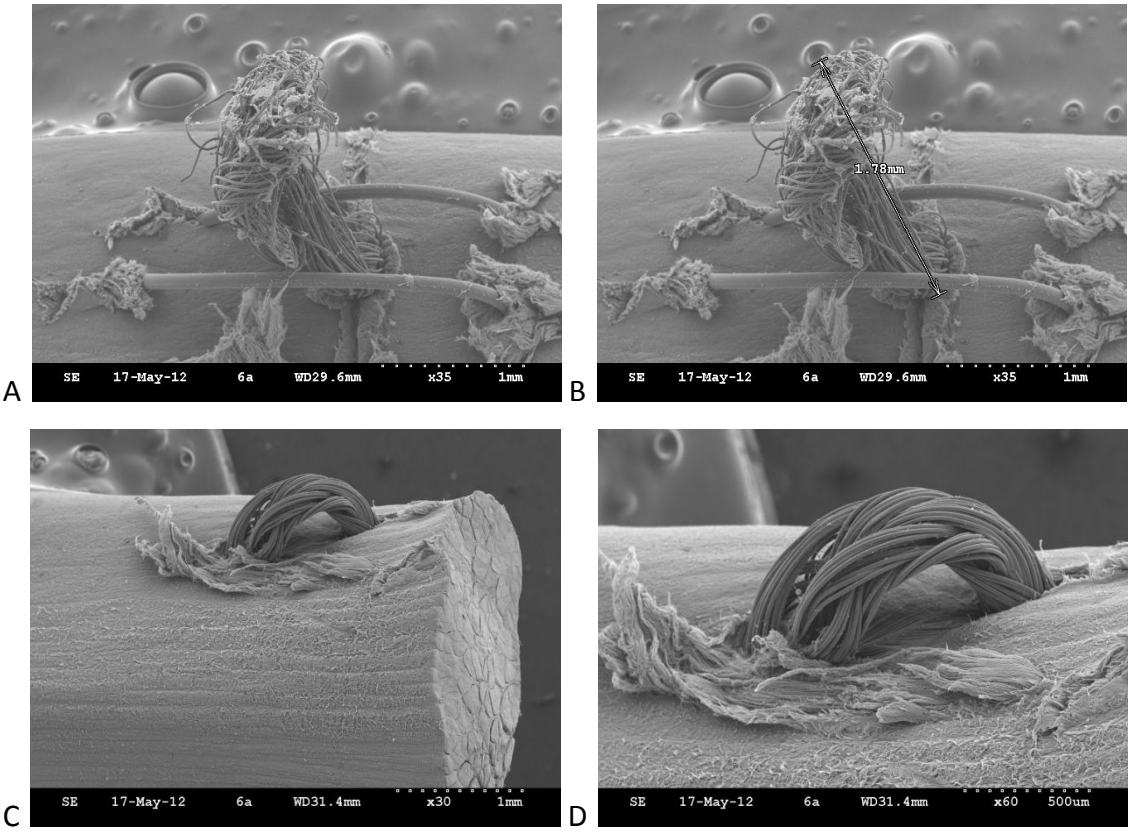

Figure 4.14: SEM of a full tendon repair

(A) ×35, (B) ×35, (C) ×30, (D) ×40 magnification.

A 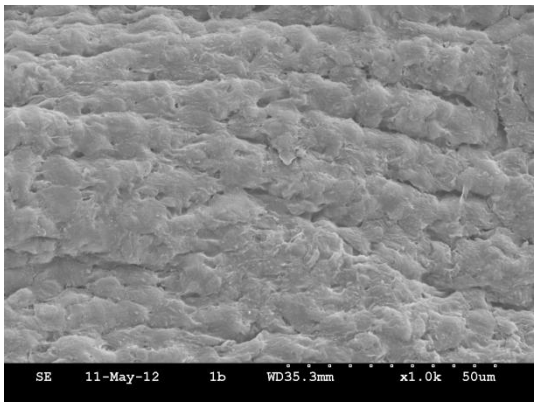

B 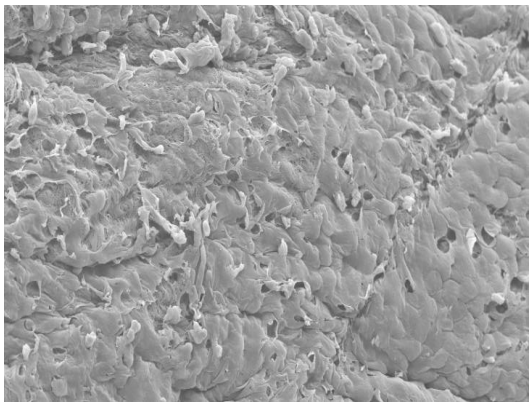

Figure 4.15: SEM of a pulley following full tendon laceration and repair

(A) x300, (B) x1000 magnification.

Chapter 5 - Effect of Tendon Repair and Pulley Resection on the Gliding Resistance and Co-efficient of Friction

5.1 Introduction

Paired studies have shown that the effect of tendon laceration on the gliding properties of a tendon are significantly influenced by the degree of tendon motion and the freedom of a repaired tendon within the A2 pulley (Tanaka et al., 2004). Whether these studies are valid in terms of the comparison of paired specimens remains debatable, as the paired specimens employed in these studies were not from the same subject. Research carried out by Kennedy (2011) confirmed that paired specimens from the same animal displayed similar properties, however further research by (Douglas, 2013) indicated the opposite, leaving this question unanswered.

Studies reported in the literature have looked at different treatment methods for flexor tendon repair in order to reduce gap formation and increase the strength of a repair such that early passive and active motion can be started after surgery. The effect of increasing weight (load) on the gliding properties of the flexor tendon in zone 2 have been investigated (Hajipour et al., 2010, Kennedy and Dias, 2013, Uchiyama et al., 1997). Uchiyama et al. (1997) demonstrated that increasing the load in a synovial tendon following tendon treatment and pulley resection does not lead to a significant change in the GR due to the presence of lubricating synovial fluid and surface structural properties. However, there is no clear evidence as to whether this is due to tendon treatment or pulley resection, as there was no comparison with a paired specimen. No studies are present in the literature that illustrate the effect of increasing weight or flexion angle in a repeated measure or multiple experiments.

5.2 Aim

The aim of this experiment was to answer the following five questions:

1. Do the paired feet show similar CF and GR during simulated tendon movement when completely intact (i.e. without any treatment to the tendon and the pulley)?

2. What is the effect of increasing the flexion angle and weight on an intact tendon?

3. Does the pulley resection have an effect on the CF and GR when a tendon is intact? Does the flexion angle or weight influence these parameters?

4. What is the effect of a tendon repair on the GR and CF? Does the flexion angle or weight influence these parameters?

5. Does a pulley resection have an effect on the CF and GR when a tendon has been fully repaired following 100% laceration? Does the flexion angle or weight influence these parameters?

5.3 Methods

Paired feet from the same animal were obtained from the turkey farm and then assessed in terms of their skin colour, size of foot and lower leg. This was part of the visual assessment to evaluate if the feet were actually paired in the slaughter house and if they were from the same animal. All the specimens were dissected as previously described (Section 3.1 and section 3.2), and specimens that were damaged during the dissection were disposed of as pairs.

All the specimens from the right legs were used in the control group and no procedure was carried out on the flexor tendons. Experiments were carried out at 10° and 70° of flexion (0.174533 and 1.22173 Radians respectively) and 200 g and 400 g weight; these experiments were recorded as control experiments with an intact pulley (right side). Following the experiments on the intact tendons and pulleys, all pulleys were measured and recorded using a digital calliper. Pulley measurements were carried out at this stage, as the soft tissues were flexible and relaxed after the first set of experiments. Experiments were then repeated at 10° and 70° of flexion and 200 g and 400 g weight following 25%, 50% and 75% sequential A2 pulley resection from distal to proximal direction (using a digital calliper and a sharp 15 surgical blade). These experiments were recorded as control experiments with pulley resection.

All the specimens from the left legs were used in the procedure group. In this group initial experiments were carried out at 10° and 70° of flexion and 200 g and 400 g weight with both the tendons and pulleys intact. These experiments were recorded as control experiments with an intact pulley (left side). The A2 pulleys were then

measured and recorded using a digital calliper. A 100% laceration was made to the flexor tendons for all specimens in this group. Tendons were then repaired using a 4-0 Ethibond locked Kessler core suture (2 strands) and a 6-0 Ethilon circumferential running suture, under ×3.5 magnification. Both suture sizes were chosen based on the relative size of the tendon. The experiments were repeated following tendon repair at 10° and 70° of flexion and 200 g and 400 g weight and then following 25%, 50% and 75% sequential A2 pulley resection. For each pulley resection interval the experiments were recorded at 10° and 70° of flexion and 200 g and 400 g weight. These experiments were recorded as repaired tendon experiments and repaired tendons with pulley resection, respectively.

All experiments were carried out following the system calibration as described in Section 3.3.13. There were no tendon ruptures in this study.

Each experiment was conducted for 1 minute and the data (F1 and F2) was collected in an Excel format for subsequent data analysis. A separate spreadsheet was constructed for each angle measurements with a formula to allow the CF and GR to be measured automatically using the CF formula described in Section 1.11.1.

The GR and CF for each experiment was then added to the Excel spreadsheet against the corresponding weight and angle for data comparison and statistical analysis.

5.4 Data Analysis

The collected data was not normally distributed, as there was evidence of both positive and negative skew (see Appendix 3). The Shapiro-Wilk W test for normal data showed that the majority of samples were not normally distributed (See Appendix 4). The CF was measured using the formula $\mu = Ln[(F2\ /\ F1)]/\varphi$. As there is natural logarithm within this formula, it was decided to use non-parametric tests for this data and avoid further logarithmic conversion of the data to achieve a normal distribution. This was a paired experimental design that required comparison of the results between different subjects, as well as before-and-after observations within the same subject. The experiments required repeated measures of the same subject (change of flexion angle and weight) and therefore the Wilcoxon matched pair statistical analyses

with a Bonferroni adjustment for multiple tests was used in addition to measuring the distribution of the median, in order to avoid type 1 errors (concluding there is a significant difference when it is not).

For a simple Bonferroni adjustment, the p value to be achieved for significance is divided by the number of paired comparisons to be made from a set of data. In this study, a set of data was compared for seven different settings and the significance of the p value in these experiments is therefore 0.05/7 = 0.007.

A randomisation test for the paired specimens was used to assess if the paired feet displayed similar gliding properties. The differences between the means of the actual paired specimens were measured against the differences between the means following 10000 times randomisation of the specimens. The null hypothesis was that the mean differences between the GR and CF of the randomised specimens were less than the mean differences of the GR and CF of the feet paired at the farm. As the randomisation test is a strong test for a paired comparison, the Wilcoxon Signed Rank test was not required for this part of the study.

IBM SPSS Statistics version 20 and Minitab 17 were used for the data analysis. Raw data, the average mean for CF and the CF of each tendon for different experimental measurements is recorded in Appendix 3.

5.5 Results

Pulley measurements, for all specimens are shown in Table 5.1. During each pulley resection, 1/4 length of the correspondent pulley was excised.

Table 5.1: Measurements of pulleys in all 20 specimens

Tendon Number	Right foot		Left foot	
	Full length (mm)	1/4 length (mm)	Full length (mm)	1/4 length (mm)
1	20.33	5.08	24.28	6.07
2	19.01	4.75	22.82	5.70
3	23.87	5.96	24.10	6.02
4	23.89	5.97	19.80	4.95
5	18.52	4.63	21.98	5.49
6	22.26	5.56	20.77	5.19
7	25.18	6.29	23.00	5.75
8	24.89	6.22	23.64	5.91
9	24.40	6.10	20.19	5.04
10	21.63	5.40	21.78	5.44

The results are presented are based on the research questions.

1. Do the paired feet show similar CF and GR during the simulated tendon movement when completely intact (i.e. without any treatment to the tendon and the pulley)?

The average differences between the right and left foot GR and CF were measured at two flexion angles and weights. The randomisation test assessed whether the paired legs were related to each other by measuring the average differences in GR and CF, and then following 10,000 times randomisation (see Appendix 5). The randomisation test showed no significant p value, confirming the null hypothesis that the randomised specimens had lower mean differences than those paired from the same animal.

This finding indicates that comparing the results between the right and left legs will lead to errors and although a comparison between the pairs is not possible, the data obtained from the sequential changes made in each leg individually remain valid for analysis.

2. What is the effect of increasing the flexion angle and weight on an intact tendon?

Increasing the flexion angle led to a significant decrease in the CF, but yielded no significant change in GR in control studies of both the right and left foot when the tendons were intact (Table 5.1).

Figure 5.1 and Figure 5.2 shows the GR median and CF median respectively, following the increase in the flexion angle.

Table 5.1: Change of flexion angle in control tendons from both feet

Wilcoxon Signed Rank tests at p=0.007

Intact control tendons (angle/weight)	Right foot		Left foot	
	GR (p-value)	CF (p-value)	GR (p-value)	CF (p-value)
10/200 vs. 70/200	0.878	**0.005**	0.285	**0.005**
10/400 vs. 70/400	0.093	**0.005**	0.386	**0.005**

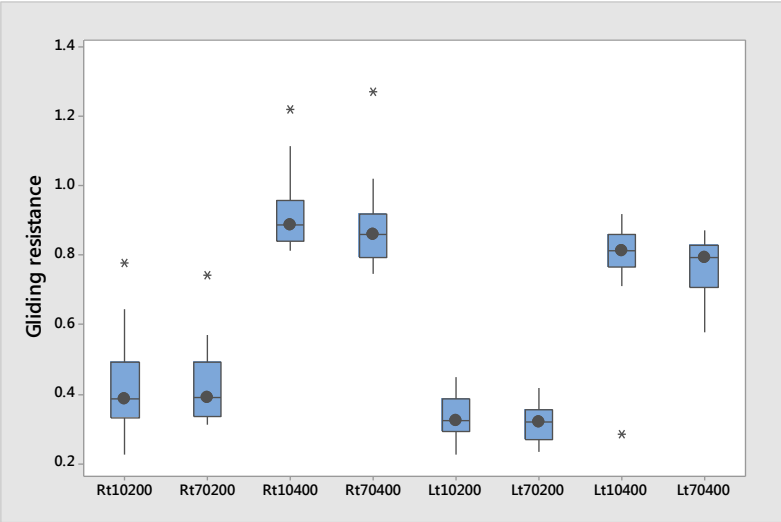

Figure 5.1: Effect of the flexion angle on the GR for intact tendons

Horizontal axis label codes: side - flexion angle - weight, for example Rt10200: right specimen, 10° flexion angle, 200 g weight

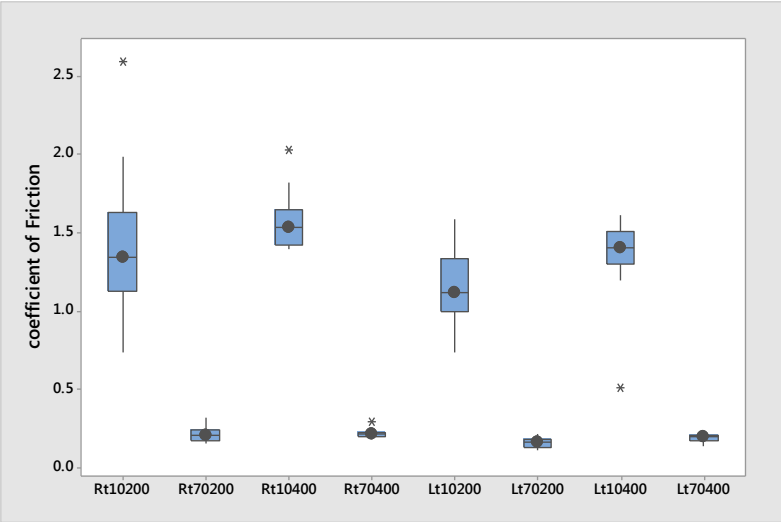

Figure 5.2: Effect of the flexion angle on the CF for intact tendons

Horizontal axis label codes: side - flexion angle - weight

Increasing the weight led to a significant increase in the GR for both sides but had no significant effect on the CF (Table 5.2). Figure 5.3 demonstrates a significant rise in the GR median from 200 g to 400 g weight in each flexion angle, but no major change in the CF median (Figure 5.4).

Table 5.2: Change of weight in control tendons of both sides

Wilcoxon Signed Rank tests (B) at p=0.007.

Intact control tendons (angle/weight)	Right foot		Left foot	
	GR (p-value)	CF (p-value)	GR (p-value)	CF (p-value)
10/200 vs. 10/400	**0.005**	0.139	**0.005**	0.022
70/200 vs. 70/400	**0.005**	0.386	**0.005**	0.009

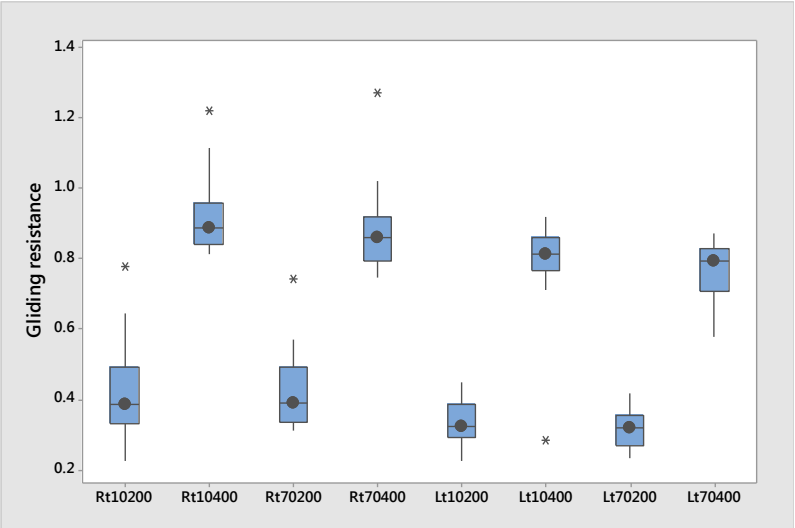

Figure 5.3: Effect of increasing weight on the GR for intact tendons

Horizontal axis label codes: side - flexion angle - weight

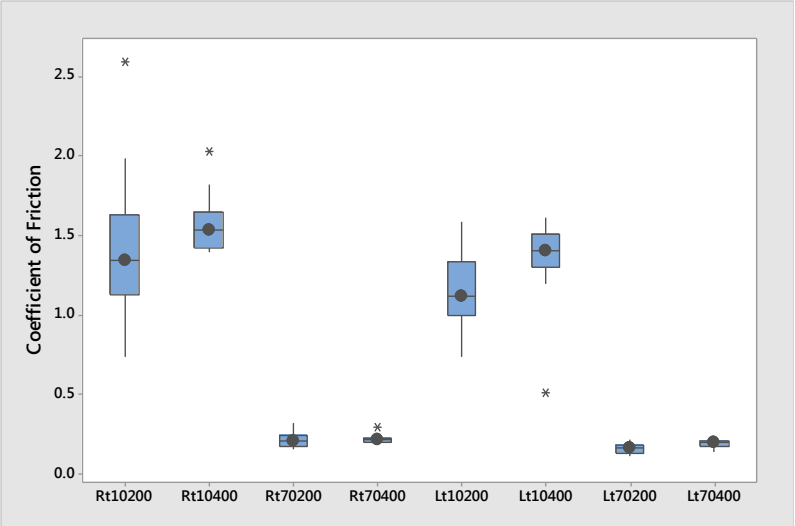

Figure 5.4: Effect of increasing weight on the CF for intact tendons

Horizontal axis label codes: side - flexion angle - weight

3. Does the pulley resection have an effect on the CF and GR when a tendon is intact? Does the flexion angle or weight influence these parameters?

Although the paired specimens were rendered dissimilar, it was still possible to look at the trend of change in the GR and CF for right foot specimens when the tendon was intact, and to investigate the effect of pulley resection and change in flexion angle and weight following pulley resection.

Looking at the right foot specimens where the tendon was intact and sequential pulley resection was carried out, there was no significant increase in the GR or CF for each individual angle and weight (Table 5.4). Pulley resection up to 75% had no effect on GR or CF.

Table 5.4: Effect of pulley resection on the right foot specimens for an intact tendon

Wilcoxon Signed Rank tests at p=0.007.

Angle (degrees)/ weight (g)	Pulley resection	GR (p-value)	CF (p-value)
10 / 200	100% vs. 25%	0.386	0.445
	100% vs. 50%	0.074	0.093
	100% vs. 75%	0.093	0.093
	From 25% to 50%	0.169	0.203
	From 50% to 75%	0.575	0.646
10 / 400	100% vs. 25%	0.878	0.959
	100% vs. 50%	0.333	0.333
	100% vs. 75%	0.646	0.445
	From 25% to 50%	0.241	0.203
	From 50% to 75%	0.878	0.878
70 / 200	100% vs. 25%	0.445	0.386
	100% vs. 50%	0.799	0.799
	100% vs. 75%	0.508	0.508
	From 25% to 50%	0.114	0.114
	From 50% to 75%	0.285	0.241
70 / 400	100% vs. 25%	0.203	0.285
	100% vs. 50%	0.959	0.959
	100% vs. 75%	0.575	0.575
	From 25% to 50%	0.333	0.333
	From 50% to 75%	0.386	0.445

A change in the flexion angle or weight during the three stages of the pulley resection showed similar results to the findings for question 1. At each pulley resection stage, increasing the flexion angle and weight, led to a significant decrease in the CF and a significant increase in the GR respectively (Table 5.3 and Table 5.4). Figure 5.5 and Figure 5.6 show these findings for the GR and CF medians.

Table 5.3: Change of flexion angle during the sequential pulley resection in the right foot
Wilcoxon Signed Rank tests at p=0.007.

Angle (degrees)/ weight (g)	Pulley resection	GR (p-value)	CF (p-value)
10 / 200 vs. 70 / 200	25%	0.086	**0.005**
	50%	0.508	**0.005**
	75%	0.445	**0.005**
10 / 400 vs. 70 / 400	25%	0.017	**0.005**
	50%	0.169	**0.005**
	75%	0.508	**0.005**

Table 5.4: Change of weight during the sequential pulley resection in the right foot
Wilcoxon Signed Rank tests at p=0.007.

Angle (degrees)/ weight (g)	Pulley resection	GR (p-value)	CF (p-value)
10 / 200 vs. 10 / 400	25%	**0.005**	0.139
	50%	**0.005**	0.047
	75%	**0.005**	0.093
70 / 200 vs. 70 / 400	25%	**0.005**	0.333
	50%	**0.005**	0.445
	75%	**0.005**	0.074

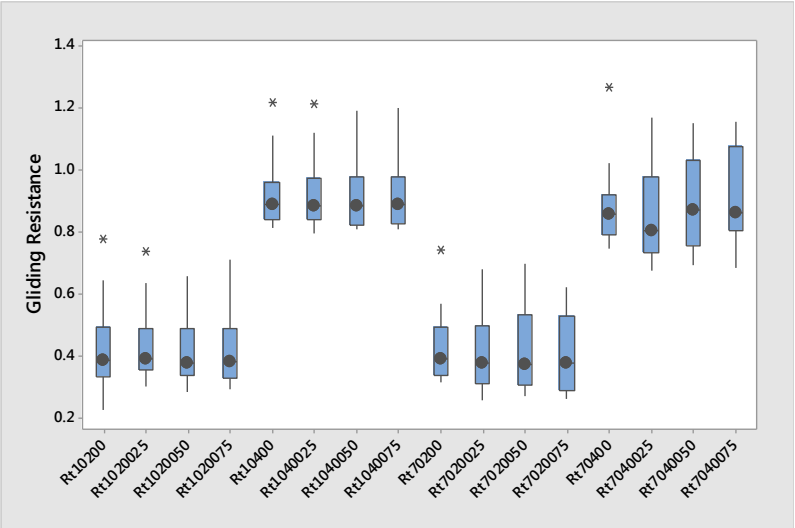

Figure 5.5: Effect of pulley resection on the GR in the right foot

Horizontal axis label codes: side - flexion angle - weight - % of pulley resection

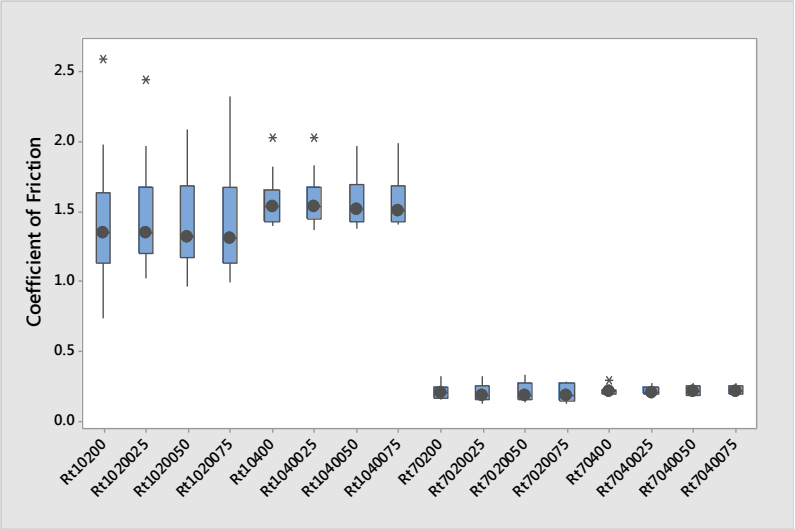

Figure 5.6: Effect of pulley resection on the CF in the right foot

Horizontal axis label codes: side - flexion angle - weight - % of pulley resection

F1 values at 70° and 400 g (Figure 5.7) confirm that the gliding forces, as the tendon is moved under the pulley during the experiment, show very little variation at each pulley resection.

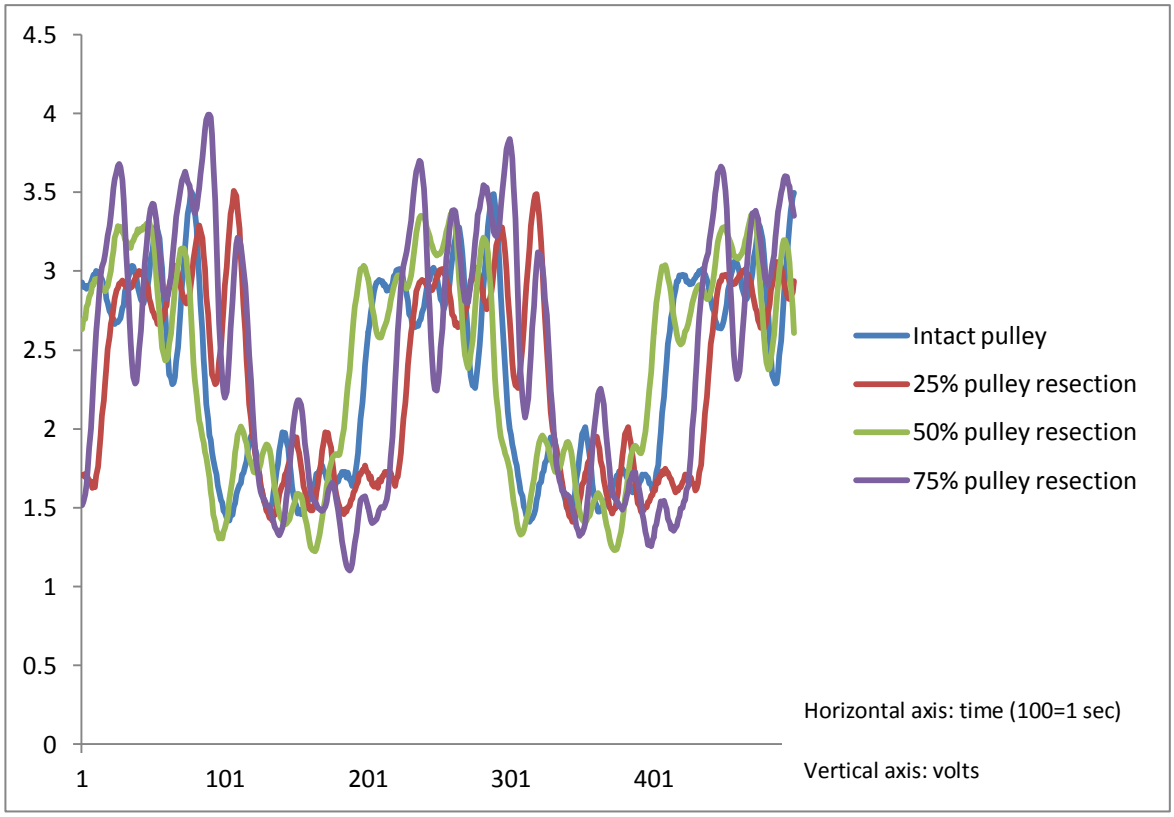

Figure 5.7: F1 values for pulley resection in the right foot at 70° flexion and 400 g weight

4. What is the effect of a tendon repair on the GR and CF? Does the flexion angle or weight influence these parameters?

Table 5.5 shows the results when comparing the intact and repaired tendons of the left foot. These results indicate that at low flexion angles, the GR and CF do not change significantly following tendon repair, regardless of the applied weight. During the experiments it was observed that at the low flexion angle the contact between the repaired tendon and the pulley was minimal with no evidence of triggering. At 70 degrees of flexion an increased level of contact was observed between the tendon and the pulley with moderate triggering at 400 g weight and there was very prominent triggering at 200 g weight. This was considered to be the main reason for the significant increase in the GR following the tendon repair when compared to the intact tendon for the 70° / 200 g group (Table 5.5 and Figure 5.8). The CF decreased significantly following the increase in the flexion angle but remained relatively unchanged at the lower flexion angle and weight (Figure 5.9).

Table 5.5: Tendon laceration and repair compared with an intact tendon in the left foot

Wilcoxon Signed Rank tests at p=0.007

Angle (degrees)/ weight (g)	GR (p-value)	CF (p-value)
10 / 200	0.721	0.799
10 / 400	0.959	0.799
70 / 200	**0.005**	**0.005**
70 / 400	0.059	**0.007**

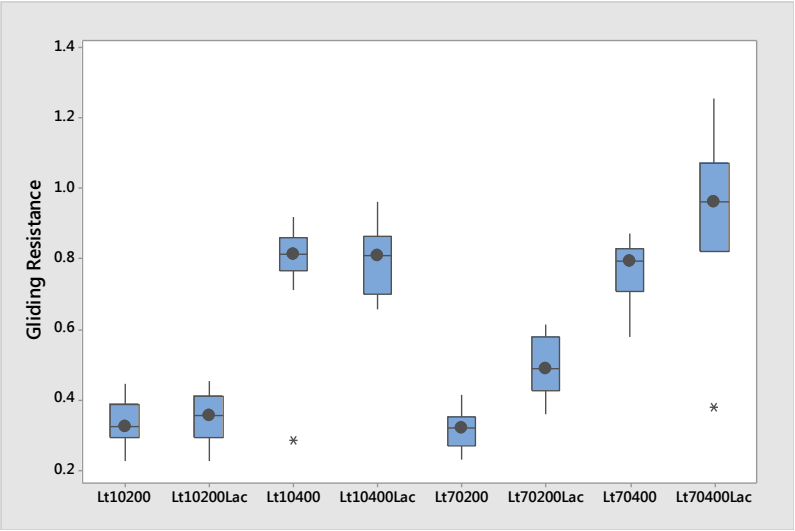

Figure 5.8: Effect of tendon laceration and repair on the GR in the left foot

Horizontal axis label codes: side - flexion angle - weight - intact vs. laceration

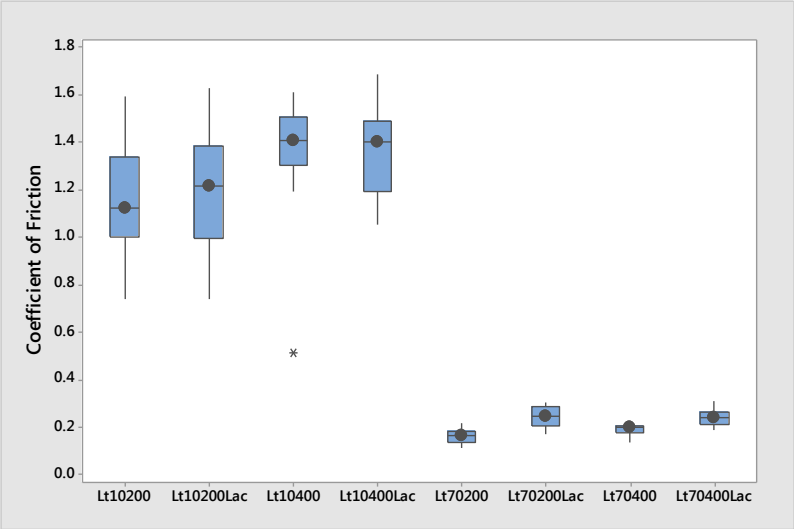

Figure 5.9: Effect of tendon laceration and repair on the CF in the left foot

Horizontal axis label codes: side - flexion angle - weight - intact vs. laceration

The F1 values before and after tendon repair at the lower flexion angle and weight (10° flexion and 200 g weight) showed very little variability and spiked from the baseline (Figure 5.10A). At 70° of flexion and 400 g weight it becomes apparent that higher forces were required to overcome the friction between the repaired tendon and the pulley on the volar side (Figure 5.10D).

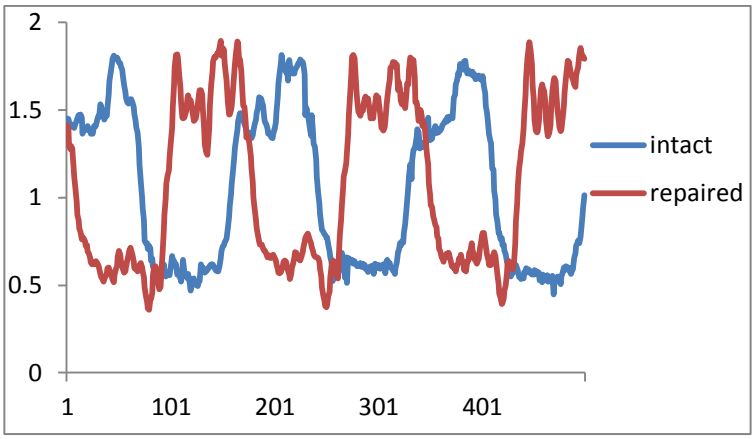

(A): 10° flexion and 200 g weight

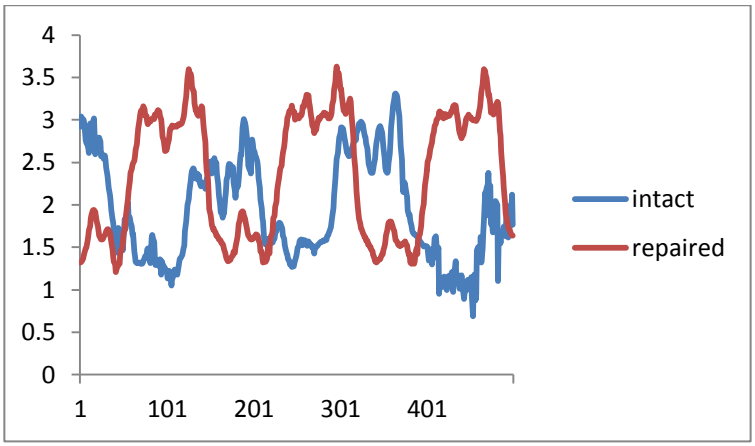

(B): 10° flexion and 400 g weight

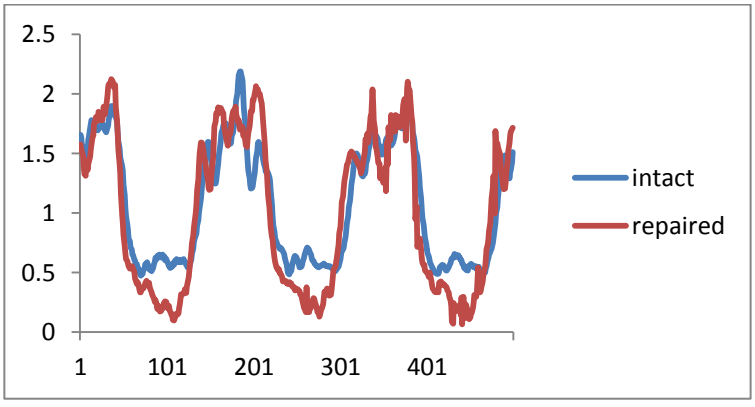

(C): 70° flexion and 200 g weight

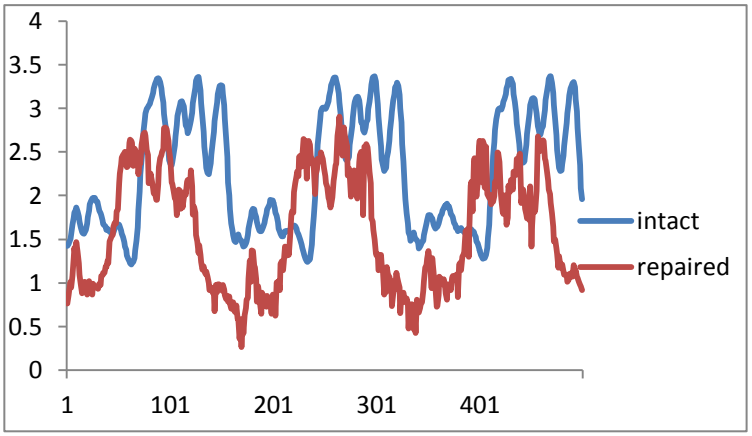

(D): 70° flexion and 400 g weight

Figure 5.10: F1 values in the left foot for an intact tendon and after tendon repair

Horizontal axis: time (100 = 1 sec), Vertical axis: Volts.

Table 5.6 shows the significant change in the CF and GR after increasing the flexion angle and weight. A significant cross over increase in the GR with the change of angle at 200 g weight was also noted. It is believed this change in GR is due to unexpected high level of triggering.

Table 5.6: Effect of flexion angle and load on the GR and CF following tendon repair

Wilcoxon Signed Rank tests at p=0.007.

Angle (degrees)/ weight (g)	**Wilcoxon Signed Rank tests**	
	GR (p-value)	**CF (p-value)**
10 / 200 vs. 10 / 400	**0.005**	0.047
10 / 200 vs. 10 / 400	**0.005**	0.047
10 / 200 vs. 70 / 200	**0.007**	**0.005**
10 / 400 vs. 70 / 400	0.059	**0.005**

5. Does a pulley resection have an effect on the CF and GR when a tendon has been fully repaired following 100% laceration? Does the flexion angle or weight influence these parameters?

Following tendon laceration and a full repair, pulley resections were carried out based on the original measurements for each pulley. Table 5.7A and B present a comparison

of the data obtained when the tendon was intact and then after repair with pulley resection. For example, intact vs. 25% indicates that the comparison is between the intact control experiments and those after tendon repair and 25% pulley resection. Each pulley resection was compared with the completely intact pulley and between each other.

Pulley resection following tendon repair when compared to the intact tendon and pulley mechanism did not lead to a significant change in the GR and CF. Pulley resection from 25% to 75%, 50% to 75% or 25% to 75% did not cause any significant change in the GR and CF at 10° flexion (Table 5.7A).

When intact tendon and pulley data was compared to a repaired tendon with pulley resection at 70° flexion, irrespective of the weight, there was a significant increase in the GR and a significant decrease in the CF. This indicates that the combination of tendon repair and pulley resection may be responsible for these changes (Table 5.7B).

At 70° flexion and 200 g weight, comparing the repaired tendon with an intact pulley to the sequential pulley resection showed no significant change in the GR and CF. This indicates that at this flexion angle the tendon repair is the main component leading to the changes in the GR and CF and not the pulley resection (Table 5.7B).

At 70° flexion and 400 g weight, comparing the repaired tendon with intact pulley to the sequential pulley resection showed a significant change in the GR and CF. This indicates that at this flexion angle the pulley resection is the main component leading to the changes in the GR and CF and not the tendon repair (Table 5.7B).

A comparison between each stage of pulley resection at 70° flexion and 200 g weight revealed a significant change in the GR and CF from 25% to 50% and from 50% to 75% pulley resection. However, at 70° flexion and 400 g weight there was no significant change in the GR and CF for the same analysis. Looking at the data shown in Figure 5.11 and Figure 5.12, the spread of data for Lt7040025, Lt7040050 and Lt7040075 was wider than in the other groups and this may be the reason for the lack of significance in these results.

There was no significant change in the GR and CF between 25% and 75% pulley resection following tendon repair at both weights and 70° flexion (Table 5.7B).

Table 5.7: Sequential pulley resection following tendon repair at 10° and at 70°

Wilcoxon Signed Rank tests at p=0.007.

(A): At 10 degrees of flexion

Angle (degrees)/ weight (g)	Tendon vs. Pulley resection	GR (p-value)	CF (p-value)
10 / 200	Intact vs. 25%	0.059	0.074
	Intact vs. 50%	0.093	0.241
	Intact vs. 75%	0.037	0.047
	Repaired vs. 25%	0.285	0.203
	Repaired vs. 50%	0.037	0.059
	Repaired vs. 75%	0.028	0.047
	From 25% to 50%	0.386	0.508
	From 50% to 75%	0.333	0.386
	From 25% to 75%	0.386	0.333
10 / 400	Intact vs. 25%	0.333	0.445
	Intact vs. 50%	0.445	0.386
	Intact vs. 75%	0.241	0.386
	Repaired vs. 25%	0.139	0.139
	Repaired vs. 50%	0.169	0.169
	Repaired vs. 75%	0.285	0.241
	From 25% to 50%	0.508	0.508
	From 50% to 75%	0.646	0.646
	From 25% to 75%	0.508	0.508

(B): At 70 degrees of flexion.

Angle (degrees)/ weight (g)	Tendon vs. Pulley resection	GR (p-value)	CF (p-value)
70 / 200	Intact vs. 25%	**0.005**	**0.005**
	Intact vs. 50%	**0.005**	**0.005**
	Intact vs. 75%	**0.005**	**0.005**
	Repaired vs. 25%	0.047	0.037
	Repaired vs. 50%	0.009	0.009
	Repaired vs. 75%	0.013	0.013
	From 25% to 50%	**0.005**	**0.005**
	From 50% to 75%	**0.005**	**0.005**
	From 25% to 75%	0.022	0.047
70 / 400	Intact vs. 25%	**0.005**	**0.005**
	Intact vs. 50%	**0.005**	**0.005**
	Intact vs. 75%	**0.005**	**0.005**
	Repaired vs. 25%	**0.005**	**0.005**
	Repaired vs. 50%	**0.005**	**0.005**
	Repaired vs. 75%	0.017	**0.005**
	From 25% to 50%	0.022	0.013
	From 50% to 75%	0.508	0.721
	From 25% to 75%	0.445	0.114

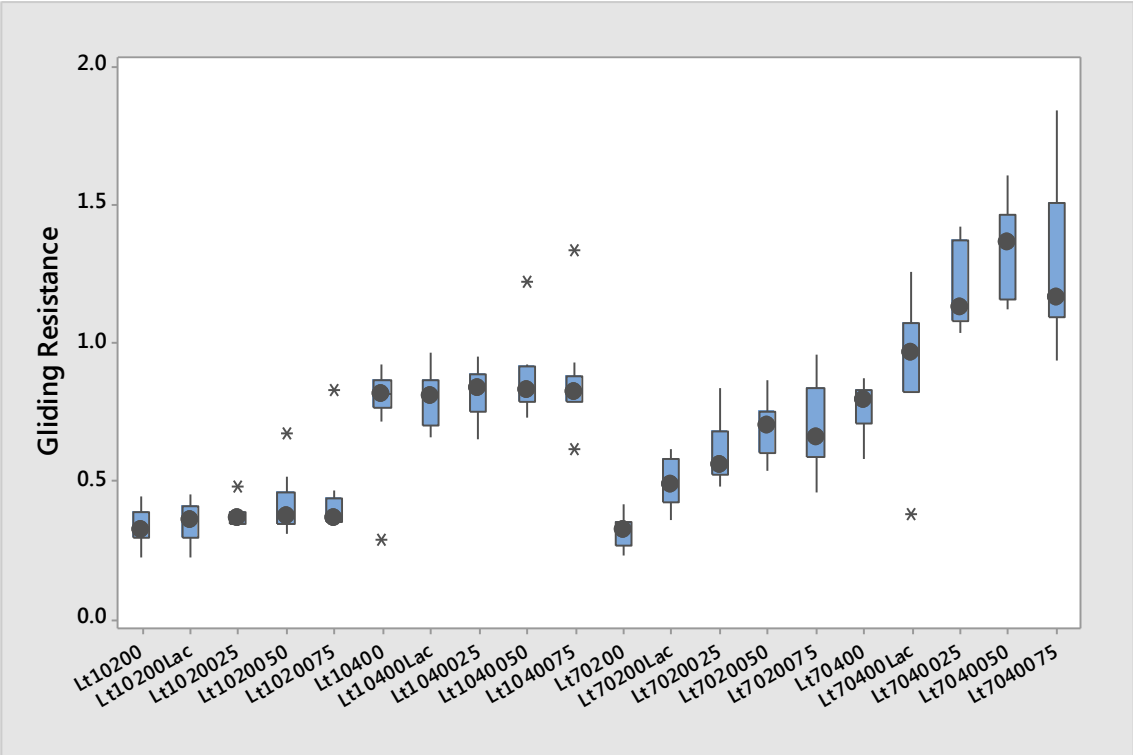

Figure 5.13: GR in intact, lacerated and following pulley resection in the left foot

Horizontal axis label codes: side - flexion angle - weight - intact vs. laceration-pulley resection%

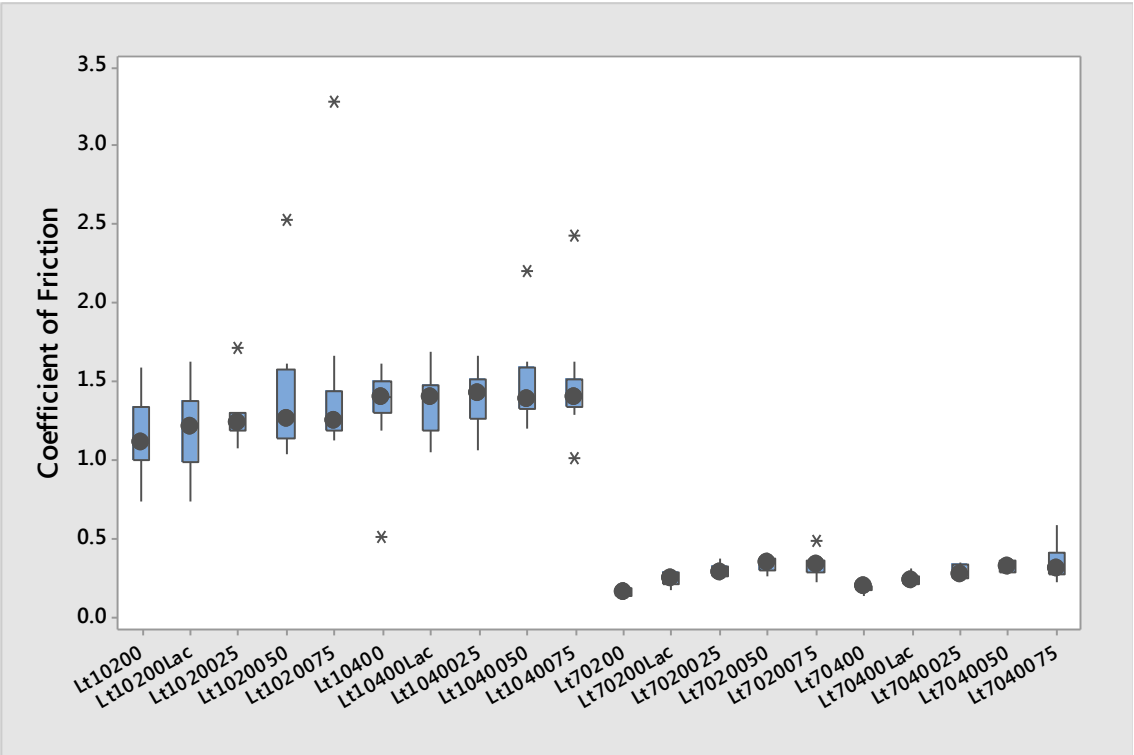

Figure 5.14: CF in intact, lacerated and following pulley resection in the left foot

Horizontal axis label codes: side - flexion angle - weight - intact vs. laceration-pulley resection

Figure 5.15 demonstrates the raw data for F1 (from tendon specimen number 1) as the pulley is resected at 70° flexion and 400 g weight. The peaks and troughs are evident, with a sharp rise from the complete intact pulley (red) to each pulley resection (25%, green; 50%, purple and 75%, blue).

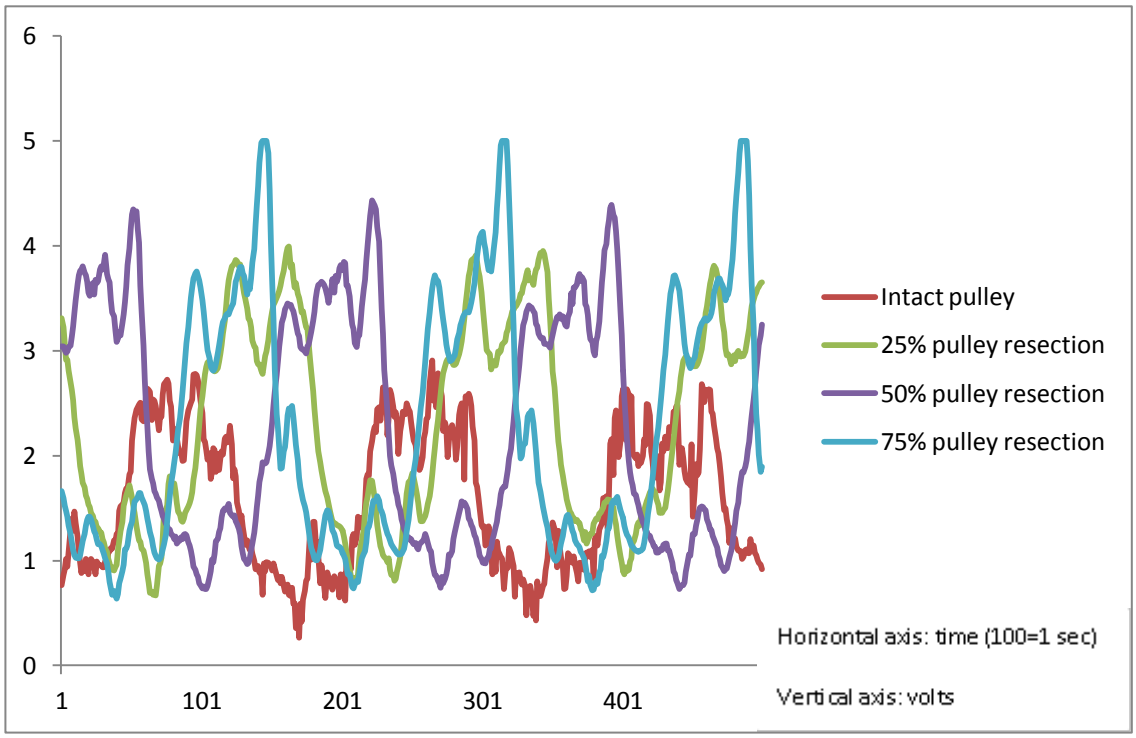

Figure 5.15: F1 data: tendon repair and pulley resections at 70° flexion and 400 g weight

Increasing the flexion angle during the pulley resection led to a significant increase and decrease in the GR and CF, respectively (Table 5.10), while increasing the weight led to a significant increase in the GR only (Table 5.11). The increase in the GR that resulted from increasing the flexion angle were most likely related to the triggering observed in this group.

Table 5.8: Tendon repair and sequential pulley resection with a change of flexion angle
Wilcoxon Signed Rank tests at p=0.007.

Angle (degrees)/ weight (g)	Pulley resection	GR (p-value)	CF (p-value)
10 / 200 vs. 70 / 200	25%	**0.005**	**0.005**
	50%	**0.005**	**0.005**
	75%	**0.005**	**0.005**
10 / 400 vs. 70 / 400	25%	**0.005**	**0.005**
	50%	**0.005**	**0.005**
	75%	**0.005**	**0.005**

Table 5.9: Tendon repair and sequential pulley resection with a change of weight
Wilcoxon Signed Rank tests at p=0.007.

Angle (degrees)/ weight (g)	Pulley resection	GR (p-value)	CF (p-value)
10 / 200 vs. 10 / 400	25%	**0.005**	0.047
	50%	**0.005**	0.386
	75%	**0.005**	0.445
70 / 200 vs. 70 / 400	25%	**0.005**	0.959
	50%	**0.005**	0.445
	75%	**0.005**	0.721

5.6 Discussion

Based on the five research questions this section will discuss each question individually.

1. Do the paired feet show similar CF and GR during the simulated tendon movement, when completely intact (i.e. without any treatment to the tendon and the pulley)?

The randomisation test identified that the paired tendon specimens from the same animal had significant differences in their GR and CF under the same experimental

settings. There was sufficient visual evidence, based on the size and skin colour, size of the proximal phalanx and the flexor tendon, that the turkey feet were paired as per instructions to the farm. However, the lack of similarity in the CF and GR between the feet could be related to:

- Within subject variability of the digits.
- Previous minor injuries to the digits (not detected macroscopically).
- The effect of dissection on each leg, which could lead to surface alterations to each specimen.

In previous studies where a treatment has been compared to an intact tendon specimen, the digits have been from the same animal or human cadaver but not paired in the same manner as in these experiments (Tanaka et al., 2004, Tang et al., 2009). Tanaka et al. (2004) looked at the effect of sequential pulley resection (proximal to distal and distal to proximal) in 32 cadaveric human fingers from 11 cadavers. The specimens were not paired and the results of the pulley resection were compared between the intact and repaired tendons of two different specimens, and so these comparisons were made between dissimilar subjects. As concluded from this experiment, there is a significant difference between the gliding properties of these paired specimens, and consequently between-subject comparisons will lead to errors.

It is therefore more important to analyse the trend in the CF and GR change within the same specimen before and after treatment, rather than to compare the treatment between paired groups.

2. What is the effect of increasing flexion angle and weight on an intact tendon?

Many studies in the past have shown that a change in flexion angle and weight do not affect the gliding properties of an intact tendon (Berschback et al., 2005, Hajipour et al., 2010, Kennedy and Dias, 2013). However, in this study a significant change in the CF and GR was noted with increasing flexion angle and weight, respectively, in the intact tendons of both feet (Table 5.1 and Table 5.2). The formula for the measurement of these values indicates that as the flexion angle (in radians) is part of the CF formula ($\mu = Ln[(F2 \,/\, F1)]/\varphi$) and the difference in weight is part of the GR formula, then an increase in the flexion angle and weight should lead to a change in

the CF and GR, respectively. All data from this experiment were calculated at 3 different occasions to exclude calculation errors. The significant decrease in CF while there is a significant increase in the GR for the same analysis could not be explained. It is difficult to clarify if the previous results are tendon batch dependent or if there has been an error in the calculations. These observations were made in intact tendons and are subject to variation when a tendon surface has been altered during treatment.

A significant increase in the GR and a significant decrease in the CF indicate that the friction forces had increased at the tendon pulley interface.

3. Does the pulley resection have an effect on the CF and GR when a tendon is intact? Does the flexion angle or weight influence these parameters?

The pulley resection at each specific weight and angle did not have a significant effect on the GR or CF despite the reduced contact surface, which leads to point loading over the remaining segment of the pulley (Table 5.4).

When comparing the 25% to 50%, 50% to 75%, or 25% to 75% resection, there was no significant change in the GR or the CF. These findings are different to those found by Tanaka et al. (2004) as in their study 75% resection of the pulley (from proximal to distal resection group) led to a significant increase in the GR when compared to 25% and 50% resection in the intact tendon group. The authors explained that as the FDS tendon is divided into two slips and glides within the A2 pulley distally, it reduces the antero-posterior height of the pulley. When the pulley is cut from the proximal toward the distal edge, the proximal FDS and FDP tendons also bowstring away from the curved proximal portion of the proximal phalanx, which further reduces the cross-sectional area. These anatomic factors may explain why the 25% distal pulley had a higher GR than under the other conditions. When the pulley was cut from the distal toward the proximal edge, the residual proximal portion of the pulley was less affected by this bowstringing effect. The authors also noted that the distal 25% of the A2 pulley was stiffer (Doyle, 1988, Tanaka et al., 2004) than the proximal portion and deformed less, leading to a higher GR in their experiments. However similar to Tanaka's study, distal to proximal sequential pulley resection has no significant effect on the GR at the tendon pulley interface.

Here, only the A2 pulley, proximal phalanx (with both PIPJ and DIPJ equivalents disarticulated) and the FDP tendon were used as the specimen and although the bowstring phenomenon was not demonstrated (due to proximal and distal joint disarticulation), the flexion angle of 70° did resemble the bowstring appearance as the tendon was flexed acutely at the edge of the pulley and away from the phalanx.

Increasing the flexion angle and weight led to a significant change in the frictional forces (decrease in the CF and increase in the GR) in the intact tendons of the right foot at each pulley resection interval (Table 5.3 and Table 5.4). This is consistent with the previous part of this study (question 2) and confirms the fact that friction is independent of the contact surface area between the two objects if both surfaces are made of the same material.

4. What is the effect of a tendon repair on the GR and CF? Does the flexion angle or weight influence these parameters?

Evidence in the literature suggests that the GR increases significantly following tendon laceration to twice the level of an intact tendon (Hajipour et al., 2010, Kennedy and Dias, 2013). Bunata et al. (2011) showed an average increase of 229% for the GR of a lacerated tendon that had been repaired compared to an intact tendon, and the GR was reduced by 15%, 25%, and 22%, when there was pulley venting of 50%, 66% and pulley enlargement, respectively.

In this study tendon repairs when compared to the intact tendon in the same foot did not lead to any significant change in the GR and CF until the flexion angles were increased to 70°. As the surface of the repaired tendon contains suture material, the interface between the tendon and the pulley is changed and therefore based on the definition of friction, the GR and CF should change following a tendon repair and pulley resection as the surface contact material and tendon size have changed. This was not observed for low flexion angles in this study for two possible reasons;

1. Turkey toes have three flexor tendons, and as the other two flexor tendons were absent in the specimen a large space was created within the pulley. At the low flexion angle, due to the large space under the A2 pulley, the contact surfaces had a soft contact that did not show any evidence of triggering despite the increased

tendon size at the repair site. At the higher flexion angle triggering at both ends of the pulley was observed and this is believed to be the reason why the GR and CF were only significantly affected at the higher flexion angles.

2. It must be clarified that following tendon repair *in vivo* pulley venting is usually performed at one end to allow the tendon repair site and zone of injury to move under the pulley without triggering. In these experiments the zone of injury was designed to move in and out of the intact pulley completely, in order to obtain sufficient data for analysis. Therefore these results are a magnified version of what happens *in vivo* as the zone of injury usually moves within one end of the pulley during tendon excursion.

The effect of increasing the flexion angle on the GR, in addition to the significant decrease on the CF was a new finding. This was attributed to the altered contact surfaces following the tendon repair and the triggering during tendon gliding.

5. Does a pulley resection have an effect on the CF and GR when a tendon has been fully repaired following 100% laceration? Does the flexion angle or weight influence these parameters?

Pulley resection up to 75% showed no significant change in the GR and CF at a low flexion angle. This was similar to the right foot specimens, indicating that the tendon repair at a lower flexion angle regardless of the pulley size does not increase the GR or CF. However, as explained in question 4, this may partly be due to the increased volume under the pulley from resection of the other flexor tendons. This is mainly due to the reduced contact area of the repaired tendon with the A2 pulley at this angle.

When the intact tendon and pulley data were compared to that for repaired tendon with pulley resection at 70° of flexion, the significant change in the GR and CF was attributed to the combination of tendon repair and pulley resection. However, at 70° flexion and 200 g weight, comparing the repaired tendon with intact pulley to the sequential pulley resection showed no significant change in the GR and CF. Therefore it was concluded that at this flexion angle, tendon repair is the main component leading to the changes in the GR and CF and that pulley resection had no significant role.

At 70° flexion and 400 g weight comparing the repaired tendon with intact pulley to the sequential pulley resection showed that the significant change in the GR and CF is mainly due to the pulley resection for this flexion angle.

Due to the spread of the data it was difficult to conclude the precise differences between each stage of pulley resections at 70° flexion and 400 g weight, but it was clear that at 70° flexion and 200 g there was a stepwise change in the GR and CF from 25% to 50% and 50% to 75% pulley resection. However, under both settings there was no significant change in the GR and CF between the 25% and 75% pulley resection. This is quite important, indicating that although the GR is raised after 75% pulley resection, there is no significant difference between 25% and 75% resection. This means that when in a clinical setting a tendon repair requires pulley resection, up to 75% resection may not influence the GR, although tendon bowstringing may still be an issue and should be carefully considered and assessed before pulley resection is carried out.

Tanaka et al. (2004) showed that the remaining 25% of the distal pulley has a higher GR when compared with the paired tendon. The authors showed a significant rise in friction from 50% to 75% pulley resection. This finding was not consistent with the results of this study and as explained in question 1 it may be due to the fact that paired specimens do not show similar gliding properties and therefore it is not accurate to compare paired specimens as it had been the case in their studies.

The effect of the flexion angle led to a significant change in the GR and CF at each pulley resection interval, which was consistent with the previous findings for question 4 and related to surface changes of the tendon. In this section the reduction in contact surface between the tendon and the pulley following sequential pulley resection may have contributed to the significant increase in the GR due to the progressive point loading in the remaining part of the pulley.

Increasing the weight however, led to a significant increase in the GR at each pulley resection interval, confirming the previous results of this study and other studies that in presence of tendon repair and injury increasing the load can significantly increase the GR of the tendon pulley complex (Hajipour et al., 2010). In clinical terms,

increasing the activity load after flexor tendon repairs can lead to increasing GR and failure of tendon repair.

These results are consistent throughout the experiments where the pulley-tendon-bone complex are one specimen and tendons are not harvested and used against a standard single bone-pulley complex, as in the study by Uchiyama et al. (1997). Specimens in this study were from one subject, were discarded at the end of each experiment, and were not reused in parts; and this may explain the different pattern of results that were observed.

Chapter 6 - Effect of a Peripheral Suture and Knot on the Gliding Resistance and Co-efficient of Friction

6.1 Introduction

Studies in the literature have focused mainly on the tensile strength of the peripheral suture and suture knot with an interest in the 2 mm gap formation and load to failure (Moriya et al., 2012, Wang and Tang, 2003). The effect of peripheral sutures or the suture knot on the GR and CF in isolation has not been studied.

6.2 Aim

The aim of this experiment was to answer three questions.

1. What is the effect of isolated circumferential suture material in the absence of tendon laceration on the CF and GR in comparison to a control group? Does the flexion angle or weight influence these parameters?

2. What is the effect of an isolated suture knot in the absence of tendon laceration on the CF and GR in comparison to a control group? Does the flexion angle or weight influence these parameters?

3. What component of the tendon injury and repair has the most significant effect on the CF and GR?

6.3 Method

Ten turkey feet were used for each experiment; all specimens were dissected as previously described (Section 3.1 and section 3.2) and specimens that were damaged during the dissection were excluded.

Ten specimens were used for the experiments in the running circumferential suture group and an additional 10 specimens in the single knot group. Before and after applying the running suture or the single knot the specimens were put through control experiments at 10° and 70° flexion and 200 g and 400 g weight. In the circumferential suture group a 6-0 Ethilon running suture was inserted on the volar surface of the

intact tendon, under ×3.5 magnification. The suture knot was applied on the dorsal aspect of the tendon away from the volar gliding surface.

In the knot group a suture knot (6-0 Ethilon) was applied on the volar surface of the intact tendon under ×3.5 magnification. The suture knot was made from a single surgeons knot and three additional throws. The suture was cut a 3 mm distance from the knot.

All experiments were carried out following the system calibration described previously in Section 3.3.13.

Each experiment was carried out for 1 minute and the data (F1 and F2) was collected in an Excel format for subsequent data analysis. A separate spreadsheet was constructed for each angle measurements with a formula to allow the CF and GR to be measured automatically using the CF formula described in Section 1.11.1. The GR and CF for each experiment was then added to an Excel spreadsheet against the corresponding weight and angle for data comparison and statistical analyses.

6.4 Data Analysis

As described in the previous chapter (Section 5.4), the data was not normally distributed and therefore Wilcoxon matched pair statistical analyses with a Bonferroni adjustment for multiple tests was used in addition to measuring the distribution of the median in order to avoid type 1 errors (i.e. concluding there is a significant difference when it is not).

In this study a set of data was compared at three different settings and the significance of the p value in these experiments will be 0.05/3=0.016.

Histograms to assess the distribution and the raw data (average mean for the CF and the CF of each tendon for different experimental measurements) are recorded in Appendix 3.

6.5 Results

1. What is the effect of isolated circumferential suture material in the absence of tendon laceration on the CF and GR in comparison to a control group? Does the flexion angle or weight influence these parameters?

Table 6.1 shows the p values when the results for the intact tendons were compared to those following insertion of a circumferential suture. The suture material on its own in the absence of tendon laceration had no significant effect on the GR or the CF, independent of change in flexion angle and weight.

Table 6.1: Comparison of the intact tendon and circumferential repair

Angle (Degrees)/ Weight (g)	Wilcoxon Signed Rank tests at p=0.01	
	GR	CF
10 / 200	0.028	0.047
10 / 400	0.878	0.575
70 / 200	0.241	0.203
70 / 400	0.508	0.445

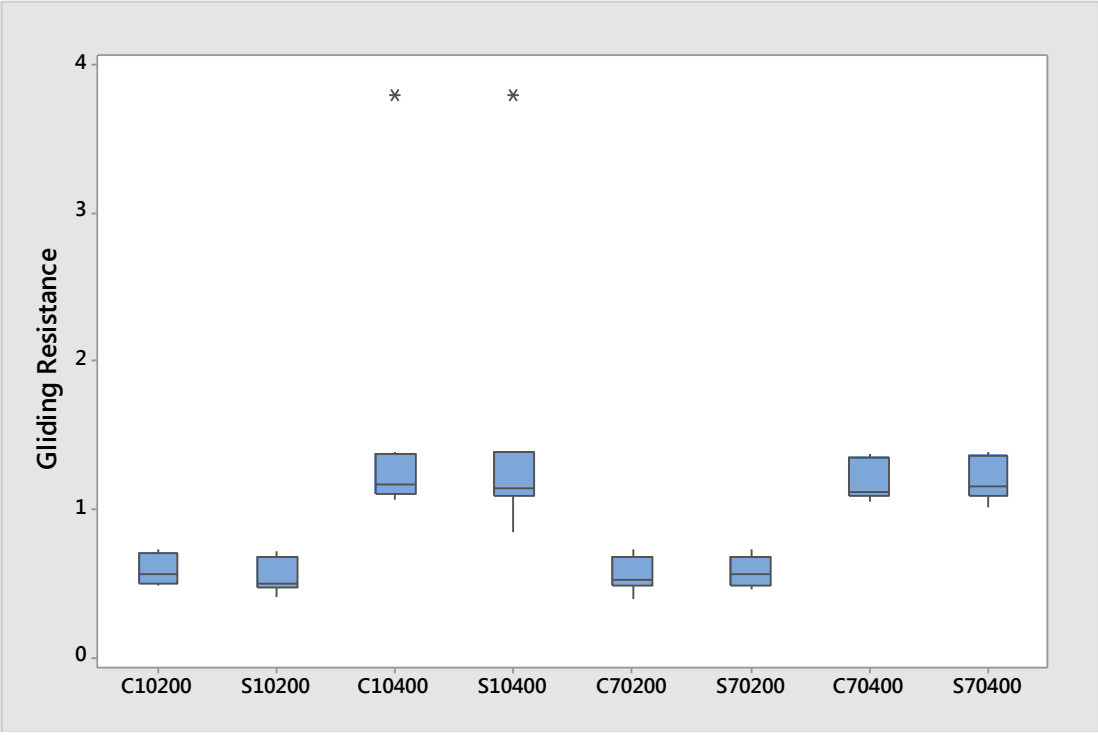

Figure 6.1: Effect of a circumferential tendon repair on the GR

Horizontal axis label codes: control vs. suture - flexion angle - weight

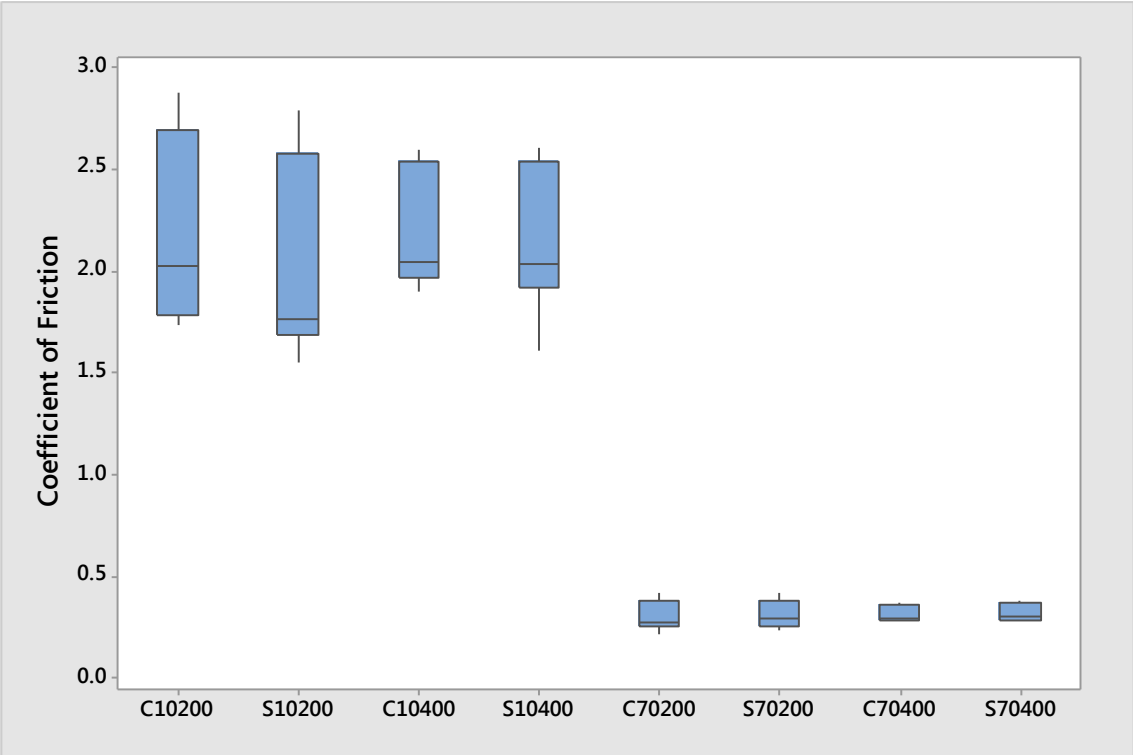

Figure 6.2: Effect of a circumferential tendon repair on the CF

Horizontal axis label codes: control vs. suture - flexion angle - weight

Figure 6.1 and Figure 6.2 show the distribution of the data and the median value for each group. There was no significant variation when the groups were compared for each flexion angle and weight.

Table 6.2 shows the effect of a change in the flexion angle on the intact tendon and following the insertion of a circumferential suture. Similar to previous studies, increasing the flexion angle led to a significant decrease in the CF.

Table 6.2: Effect of the flexion angle on an intact tendon vs. a circumferential tendon suture

Wilcoxon Signed Rank tests at p=0.016.

Angle (Degrees)/ Weight (g)	**Intact tendon**		**Circumferential tendon suture**	
	GR	**CF**	**GR**	**CF**
10/200 vs. 70/200	0.089	**0.000**	0.089	**0.000**
10/400 vs. 70/400	0.402	**0.000**	0.402	**0.000**

A change in the load (weight) led to a significant increase in the GR, similar to the previous studies, for both the intact and treated tendon (Table 6.3).

Table 6.3: Effect of change in weight on an intact tendon vs. a circumferential tendon suture

Wilcoxon Signed Rank tests at p=0.016.

Angle (Degrees)/ Weight (g)	Intact tendon		Circumferential tendon suture	
	GR	CF	GR	CF
10/200 vs. 10/400	**0.012**	0.341	**0.005**	0.721
70/200 vs. 70/400	**0.000**	0.958	**0.005**	0.508

Figure 6.3 and Figure 6.4 illustrate the change in median GR and CF following change in flexion angle and load. The CF decreases significantly after increasing the flexion angle to 70°.

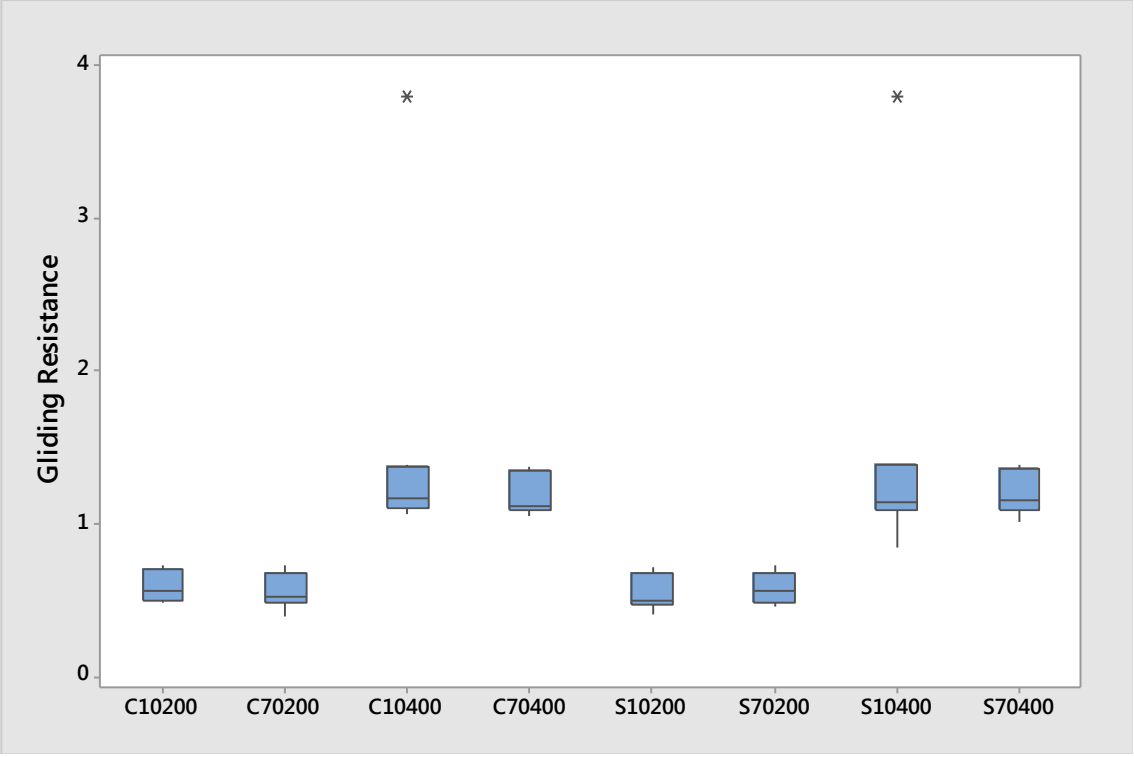

Figure 6.3: Effect of the flexion angle on the GR for an intact tendon vs. a circumferential tendon suture

Horizontal axis label codes: control vs. suture - flexion angle - weight

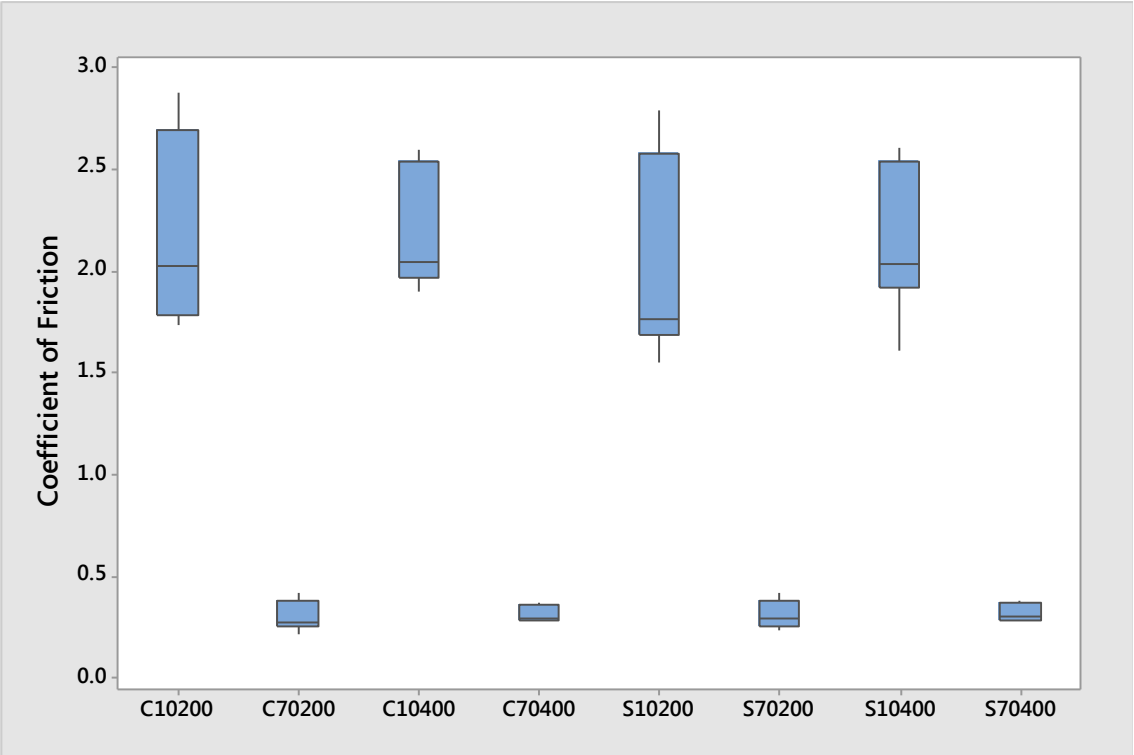

Figure 6.4: Effect of the flexion angle on the CF for an intact tendon vs. a circumferential tendon suture

Horizontal axis label codes: control vs. suture - flexion angle - weight

2. What is the effect of an isolated suture knot in the absence of tendon laceration on the CF and GR in comparison to a control group? Does the flexion angle or weight influence these parameters?

Table 6.4 shows the p-values when the results for the intact tendons were compared to those with a single knot. The isolated knot on its own had no significant effect on the GR or the CF independent of a change to the flexion angle and weight. This finding was also observed in the median distribution of the data for both the GR and CF (Figure 6.5 and Figure 6.6).

Table 6.4: Comparison of an intact tendon and a single knot

Wilcoxon Signed Rank tests at p=0.016.

Angle (Degrees)/ Weight (g)	Wilcoxon Signed Rank tests at p=0.016	
	GR	CF
10 / 200	0.257	0.280
10 / 400	0.650	0.464
70 / 200	0.214	0.188
70 / 400	0.565	0.533

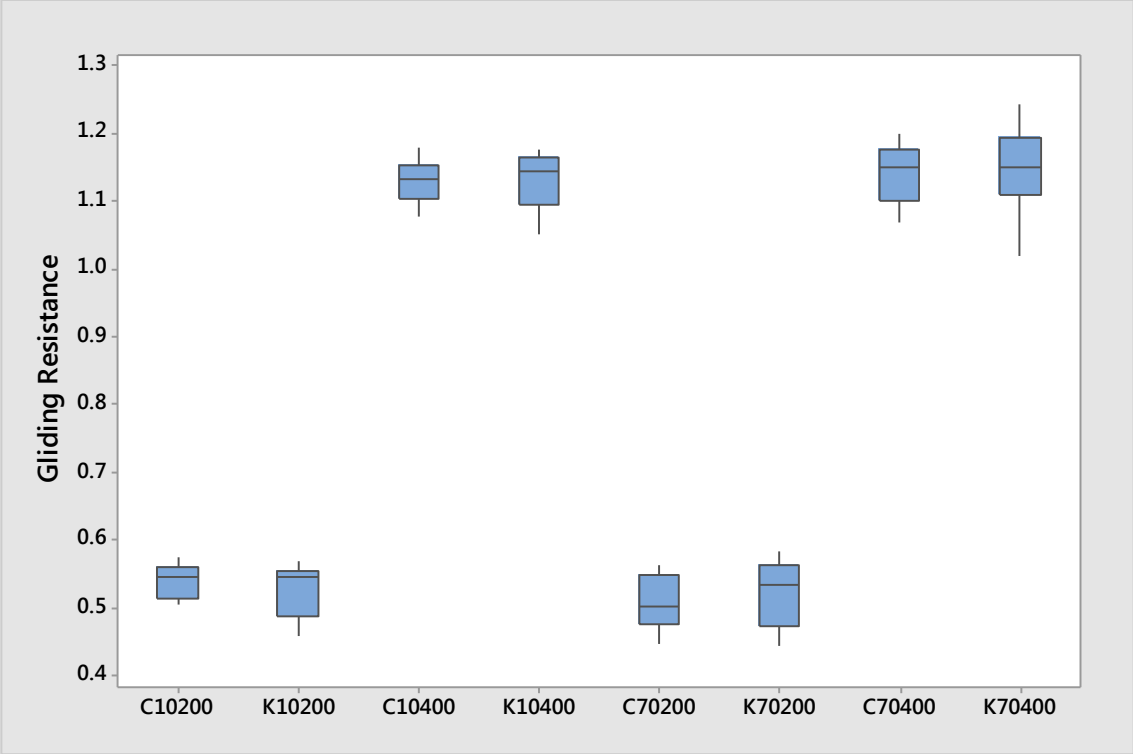

Figure 6.5: Effect of a suture knot on the GR

Horizontal axis label codes: control vs. knot - flexion angle - weight

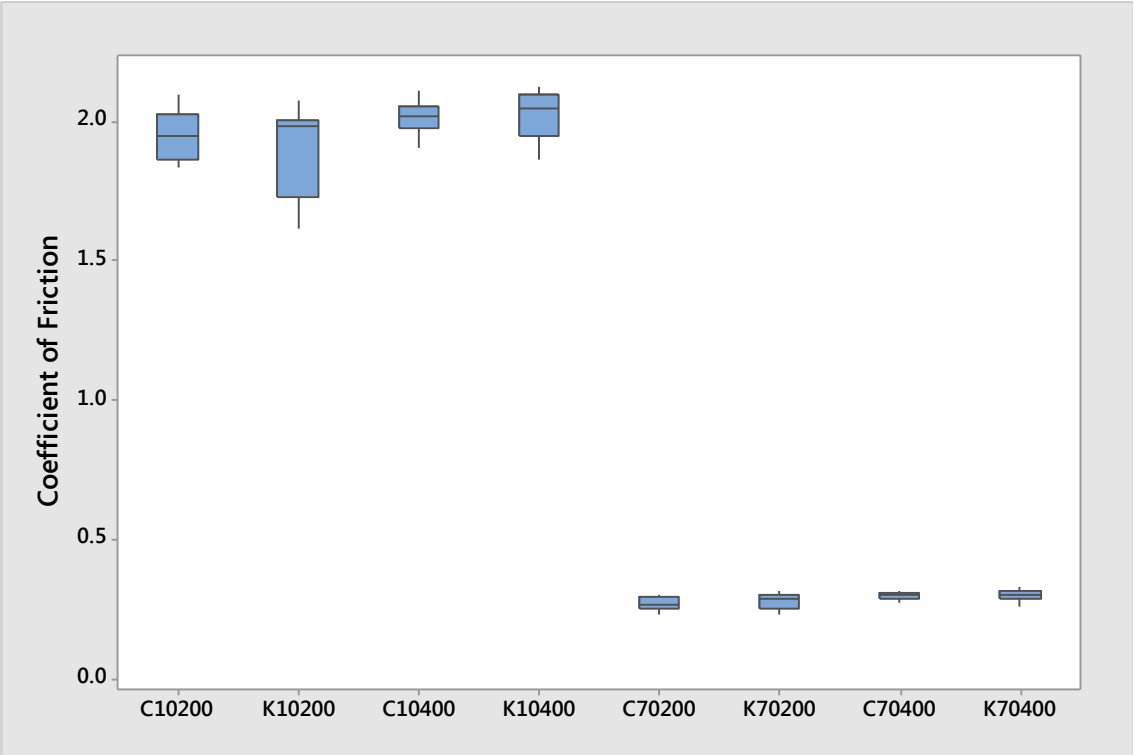

Figure 6.6: Effect of a suture knot on the CF

Horizontal axis label codes: control vs. knot - flexion angle - weight

Table 6.5 shows the effect of a change in the flexion angle on the intact tendon and following the insertion of a single knot. Increasing the flexion angle also led to a significant decrease in the CF, as in previous studies. This finding was also observed in the median distribution of the data for both the GR and CF (Figure 6.5 and Figure 6.6).

Table 6.5: Effect of the flexion angle for an intact tendon vs. a tendon with single knot

Wilcoxon Signed Rank tests at p=0.016.

Angle (Degrees)/ Weight (g)	**Intact tendon**		**Tendon with single knot**	
	GR	**CF**	**GR**	**CF**
10/200 vs. 70/200	0.017	**0.005**	0.799	**0.005**
10/400 vs. 70/400	0.074	**0.005**	0.139	**0.005**

A change in the load (weight) showed a significant change in the GR and CF for both intact tendons and those with a single knot (Table 6.6). This change in the CF with increasing weight was not consistent with the previous experiment on control subjects (Figure 6.7 and Figure 6.8).

Table 6.6: Effect of weight for an intact tendon vs. a tendon with single knot

Wilcoxon Signed Rank tests at p=0.016

Angle (Degrees)/ Weight (g)	Intact tendon		Tendon with single knot	
	GR	CF	GR	CF
10/200 vs. 10/400	**0.005**	0.047	**0.005**	**0.005**
70/200 vs. 70/400	**0.005**	**0.005**	**0.005**	**0.009**

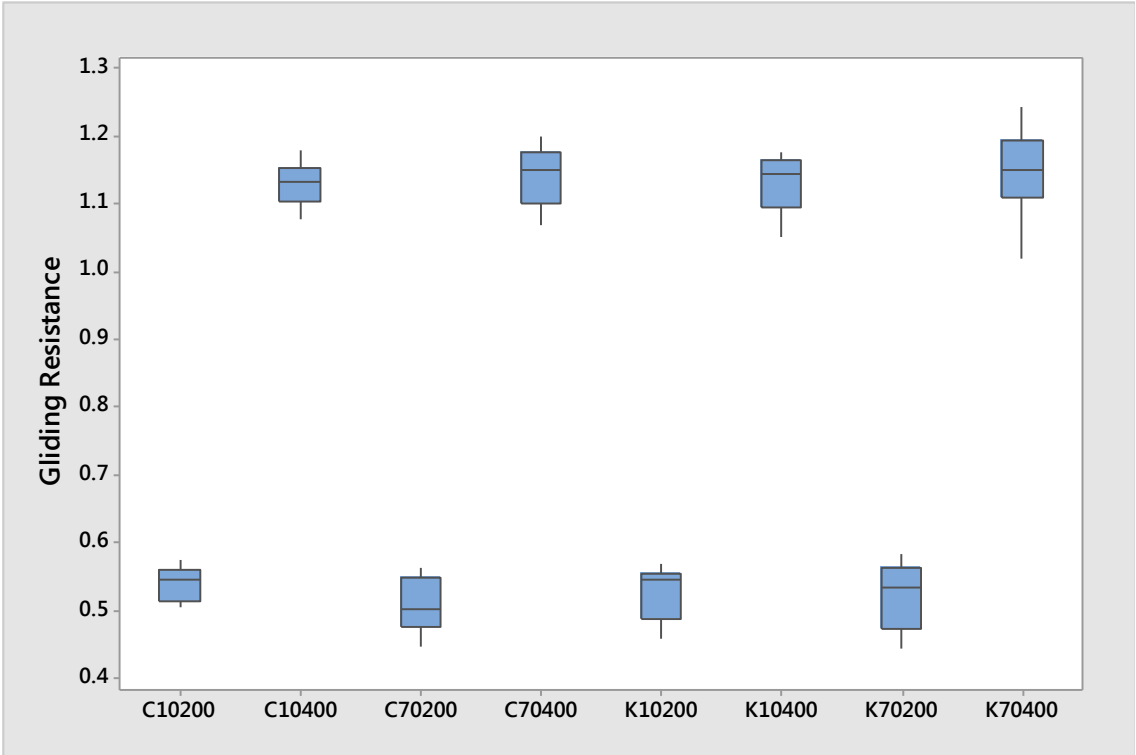

Figure 6.9: Effect of weight on the GR for an intact tendon vs. a tendon with a suture knot

Horizontal axis label codes: control vs. knot - flexion angle - weight

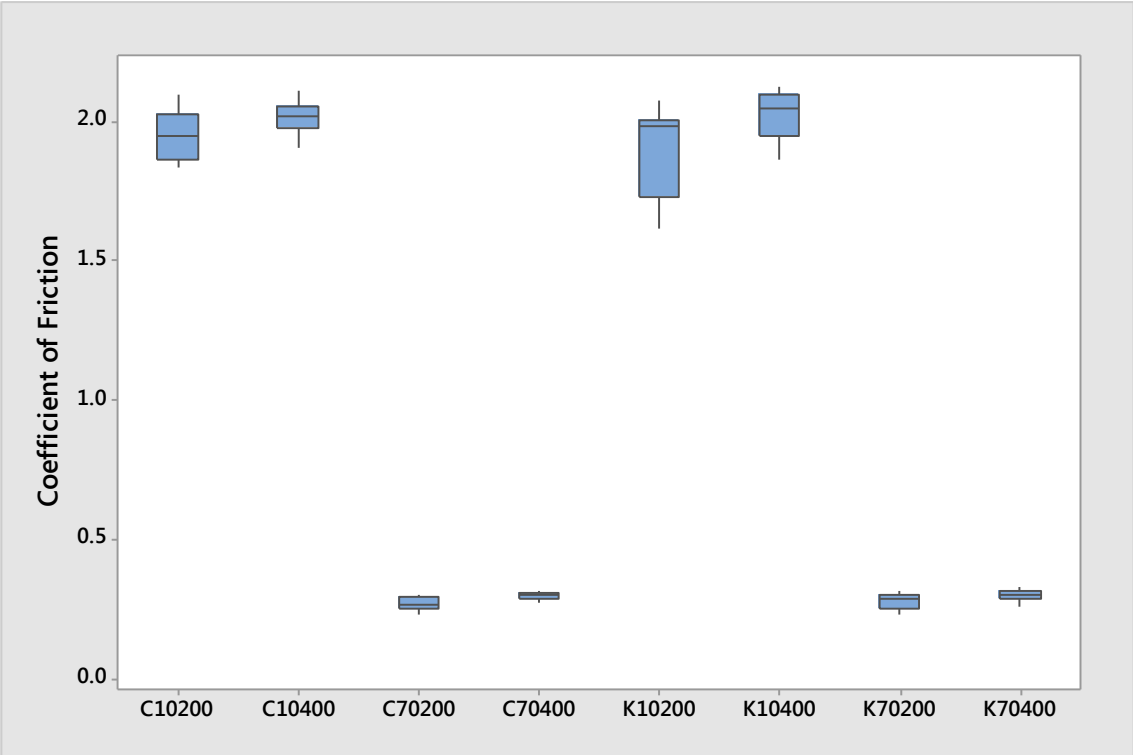

Figure 6.10: Effect of weight on the CF for an intact tendon vs. a tendon with suture knot

Horizontal axis label codes: control vs. knot - flexion angle - weight

It appears that this group of randomly allocated specimens demonstrated different properties compared to the previous groups.

By comparing the F1 values for the control tendons in each of the three experiments (Figure 6.11), it was noted that the F1 forces had significantly higher variation in the intact tendons where the tendons were treated with a circumferential suture and an isolated knot, compared to those from the first experiment (tendon repair and pulley resection). This was especially prominent in the knot group, which may be the reason why increasing the load in this group led to an unexpected increase in the CF before and after knot insertion. The different observations in the control specimens could be due to the variability in the size and the shape of the tendons, which were dissected and used a few months after the first experiment. The first experiment was carried out during the Christmas period and the specimens were considerably larger as the turkeys were older than average.

Although the baseline for these experiments are high, the effect of the knot insertion or circumferential suture in absence of tendon laceration did not lead to a significant change in the GR and CF when compared to the intact tendon of the same group.

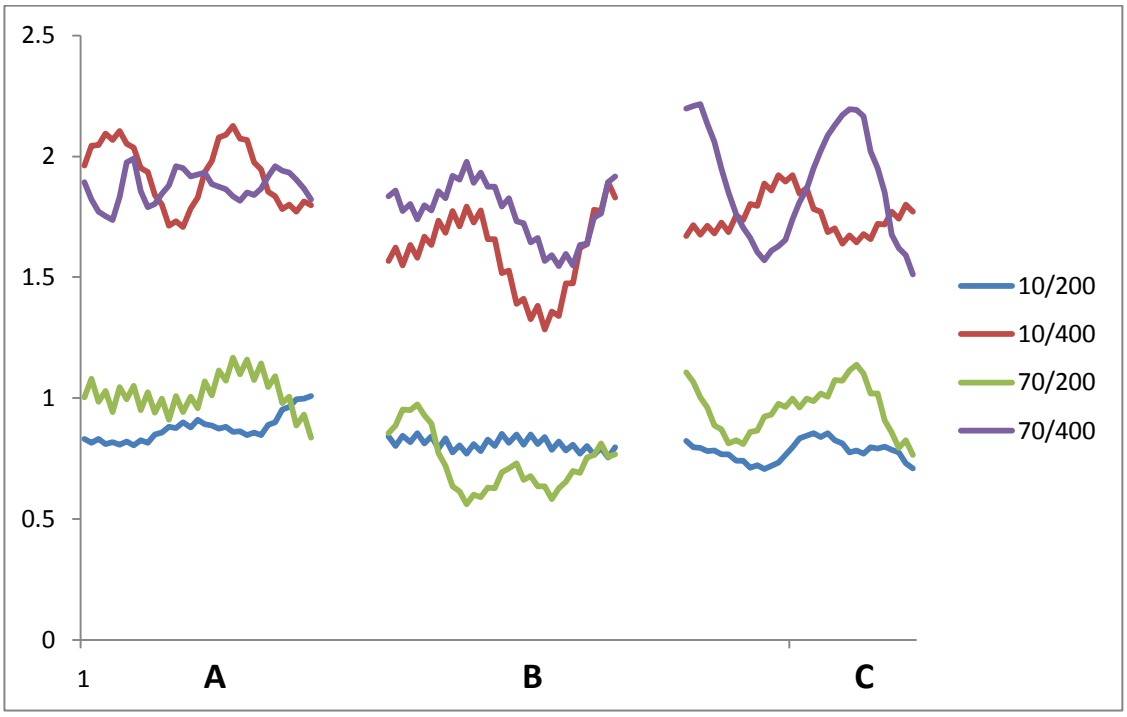

Figure 6.11: F1 forces for intact tendons in the three different experimental groups

(A) control specimens experiment 1, (right foot), (B) control specimens (circumferential suture), (C) control specimens (Knot). Vertical axis: Volts, Horizontal axis: time.

6.6 Discussion

1. What is the effect of isolated circumferential suture material in the absence of tendon laceration on the CF and GR in comparison to a control group? Does the flexion angle or weight influence these parameters?

Many studies in the literature have compared the strength of circumferential sutures in terms of their resistance to gap formation and load to failure (Moriya et al., 2012, Wang and Tang, 2003). In the last decade more complex peripheral repairs have been shown to be superior to simple running or simple cross-stitch patterns (Dona et al., 2003, Mishra et al., 2003, Moriya et al., 2010, Takeuchi et al., 2010); however, most of these studies have not looked at the gliding properties of the repaired tendons with different peripheral sutures. An ideal peripheral repair should minimise the gliding friction between the repaired tendon and the pulley. Gulihar et al. (2012) showed that

compared to the Halsted and Silfverskiold repair, a simple running suture had a lower GR following a 50% tendon laceration and full repair. Kubota et al (1996) also showed that a locking peripheral suture (Lin-locking) has a higher GR compared to other non-locking suture techniques. A simple running peripheral suture is still widely used because the complexity of many other techniques limits their clinical application (Tang et al., 2013). These suture techniques are difficult to insert and result in a large exposure of the suture material on the tendon surface.

In this study the running circumferential suture alone in the absence of a tendon injury had no significant effect on the GR or CF. A change in the flexion angle and weight led to a significant fall and rise in the CF and GR, respectively, showing the same pattern as in the previous experiment. This indicates that the peripheral suture material on its own does not increase the GR and that other factors are more important in the gliding properties of the tendon following tendon laceration and repair.

2. What is the effect of an isolated suture knot in the absence of tendon laceration on the CF and GR in comparison to a control group? Does the flexion angle or weight influence these parameters?

Joyce et al. (2014) and Peltz et al. (2014) showed that a knotless barbed core suture had good tensile strength, but required less load for a 2 mm gap formation. They also concluded that due to the lower cross sectional area at the repair site, the gliding properties must be better but did not assess the GR in their studies. The effects of cellular damage to the tendon from a single knot has been studied by Wong et al. (2006) but the effect of an isolated suture knot on the GR and CF is not known.

In this study, in the absence of tendon laceration the suture knot on the volar surface did not lead to a significant change in the GR and CF. A change in the flexion angle led to a significant decrease in the CF, consistent with previous experiments. However, a change in load led to a significant change in both the GR and CF, which was believed to be due to the increased zone of injury as the experiments progressed. The isolated knot was pulled under the pulley as it entered and exited the pulley, and this led to a longitudinal tear of the tendon substance and therefore higher gliding forces at 70° flexion and 400 g weight.

3. What component of the tendon injury and repair has the most significant effect on the CF and GR?

It is therefore concluded that as there was no significant change in the GR and CF following the insertion of an isolated running suture or suture knot, the combination of the initial tendon injury, insertion of the core suture, and the iatrogenic tendon injury from insertion of core suture, are responsible for the raised gliding properties of the flexor tendon following a tendon repair in zone 2.

Chapter 7 - Conclusions

To allow a clear understanding of the results, a summary of the current knowledge and the results will be discussed for each of the seven aims of the study.

1. Is the turkey animal model suitable with regards to flexor tendon experimentation?

Turkey toes are very similar to the human fingers. There are currently no evidence in the literature that clearly defines the anatomy of turkey feet or outlines the superficial and deep structures present. Previous experiments carried out on this animal originated in our Health and Science laboratory in Leicester.

The full anatomical assessment of the turkey toes confirmed that their tendon-pulley-bone structures are equivalent to those of humans. Although the size of each component is different, the biomechanical properties, macro and micro structures are similar.

The differences between the human fingers and turkey toes are:

- Three phalanxes in the human finger compared to four in the long turkey toe.
- Two flexor tendons to each human finger compared to three in the long turkey toe.

Turkey toes are therefore a suitable alternative to chicken and porcine tendons. They are easily available, cheap and closely resemble the anatomy of human fingers.

2. SEM study of the tendon surface and pulley when intact and following tendon repair.

Tendon laceration and subsequent tendon repair leads to a significant damage on the tendon surface which can be responsible for the changes in the GR.

There is evidence in the literature showing that following a tendon laceration and subsequent tendon repair, there is significant tissue damage around the zone of injury, first from the direct trauma, and secondly from the tissue handling and tendon repair. At a cellular level, cellular death is evident up to 14 days after a repair (Wu and Tang,

2013); this increased zone of injury subsequently leads to increased frictional forces. This knowledge has led to the use of lubricating factors following tendon repair to minimise the frictional forces at the tendon pulley interface during the early stages of rehabilitation. Although this is well understood, the tendon surface changes have not been fully studied.

Electron microscopy investigations in this study on the turkey tendons showed:

- Both the flexor tendon surface and pulley appeared to contain a glandular layer, responsible for the production of lubrication material and synovial fluid.
- Tendon laceration creates tendon flaps on each side of the laceration line and these flaps enlarge following triggering, as they interact with the pulley edge and therefore increase the zone of injury. However, the pulley only suffers mild delamination of its glandular layer.
- Tendon repair led to iatrogenic tendon injury. The cauliflower appearance of the tendon was observed as the suture needle entered and exited the tendon, both with the core suture and circumferential suture. However, these tendon changes led to very little delamination of the pulley following simulated tendon gliding.
- Tensioning the knot or the suture creates a longitudinal tear within a tendon. Suture knots, especially the prominent apex of the knot, leads to mild delamination of the pulley. However, a running suture in the absence of a knot had no significant effect on the pulley.
- The maximum amount of tendon damage was seen following a full tendon repair with core and circumferential suture in addition to maximum pulley damage.

These findings indicate that the tendon damage, from an initial injury and following a tendon repair, is responsible for the maximum pulley injury and potential subsequent increase in the GR. It is clear that a prominent suture knot can cause significant injury to the pulley and current surgical practice indicates that a suture knot should be positioned away from the gliding surfaces.

3. Do the paired specimens from the same animal behave the same in terms of their GR and CF when intact?

Paired specimens from the same animal did not display the same gliding properties.

Currently there are no studies in the literature looking at paired specimens from the same animal. Most studies compare the experimental settings to a control intact specimen but this is not from the same animal. This means that the specimens are not compared like for like.

In this study the specimens were paired in the farm following a prior agreement. They all appeared to be paired based on a visual inspection of the skin colour and size of the feet. However, based on the randomisation test the paired specimens showed a significant difference in their GR and CF under the same settings. It was concluded that even digits from the same animal may have different gliding properties or that the process of dissection and specimen preparation affects these properties more than was previously expected, and therefore paired experiments are not as accurate as previously thought.

4. To evaluate the effect of a full of tendon repair on the GR at the equivalent A2 pulley level when compared to an intact tendon for a paired specimen and to understand the effect of increasing the flexion angle and load.

Following a full tendon repair, GR is increased significantly only at higher load and flexion angles.

Current data in the literature indicates that the GR and CF increase 2-fold after a partial tendon laceration and 229% following a tendon repair; this is thought to be due to the tendon injury, tendon repair and suture material (Bunata et al., 2011, Hajipour et al., 2010, Kennedy and Dias, 2013).

This study confirms the previous studies, as the GR and CF changed significantly only at high flexion angles where the tendon contact with the pulley was at a maximum. This means that at the lower flexion angles motion leads to lower friction despite changes to the surface properties of the tendon. This is due to the fact that at lower flexion angles other tendons within the pulley are relaxed, leading to a wider pulley volume and less compression against the pulley as the tendon glides. Increasing the load leads to an increased GR, and increasing the flexion angle leads to an increase in the GR and

a decrease in the CF, both of which are related to the high resistance of the tendon and triggering at the intact pulley edge. These findings indicate that low flexion angle and load exercises immediately after surgery may be more appropriate.

5. To evaluate the effect of sequential pulley resection on the GR at the equivalent A2 pulley level when compared to the intact tendon in a paired specimen and to understand the effect of increasing the flexion angle and load.

At lower flexion angles and loads, up to 75% of pulley resection does not lead to any significant change in GR.

Tanaka et al. (2004) have shown that the distal 25% of the A2 pulley is more rigid, and when it is the only remaining part of the pulley (both in intact and repaired tendon groups), it leads to a higher GR due to the bowstringing effect of the tendon proximal to this section. The effect of increasing the flexion angle and load in these settings has not been studied previously.

In this study the GR and CF did not change significantly following pulley resection when the tendon was intact, which may be related to the fact the bowstringing phenomenon was not observed, as both the proximal and the distal joints in the specimens were disarticulated. Increasing the flexion angle and weight in each subgroup led to a significant decrease in the CF and an increase in the GR, respectively.

When the tendon was repaired, up to 75% pulley resection (distal to proximal direction) at a low flexion angle did not lead to any significant change in the GR and CF, similar to the intact tendons. However, at a higher flexion angle the pulley resection did cause a significant increase in friction. The main finding was that the resection from 50% to 75% did not lead to any significant change in the GR or CF. Increasing the flexion angle and load led to a significant increase in the GR and CF, similar to the repaired tendon experiment (without pulley resection), indicating persistent triggering of the tendon at the pulley edges. These findings indicate that up to 75% pulley resection did not have a significant effect on the GR and CF (when compared with 50% pulley resection) and can be cautiously considered during surgery if there is persistent triggering of the repaired tendon at the edge of the pulley.

6. To identify the individual effect of a suture knot and peripheral suture on the GR at the A2 pulley level and to understand the effect of increasing the flexion angle and load.

Isolated suture knot and isolated circumferential suture (without the knot) have no effect on the GR in absence of tendon laceration.

Previous studies have shown that a simple running suture has the lowest GR compared to other more complicated and locked peripheral sutures (Gulihar et al. 2012). There is also a general understanding that the presence of a prominent knot will lead to more triggering but the effect of this on the GR and CF has not been studied.

In this study a running circumferential suture or a single knot alone, in the absence of a tendon injury, had no significant effect on the GR or CF. A change in the flexion angle and load led to a significant change in the CF and GR respectively, which is the same finding as in the previous experiment; however, increasing the load led to a significant decrease in the CF related to the longitudinal increase in the zone of injury, as the knot came into repetitive contact with the pulley.

7. What component of the tendon injury and repair has the most significant effect on the CF and GR?

Currently there are no studies in the literature that can answer this question. In this study it has been clearly observed that the suture material, pulley resection and presence of a knot on their own has no effect on the gliding properties of a tendon in zone 2. It is the initial tendon injury and the extent of iatrogenic tendon damage from the insertion of a core and circumferential suture that are the most prominent factor affecting the gliding properties at this level.

7.1 Problems and Limitations

Avian influenza: The initial stage of this research coincided with a local avian influenza epidemic and therefore serious measures were put into place to avoid contracting or transmitting the virus. A health and safety application was completed and all infection protocols were followed.

Control board and the load cells: Both required fixation and replacement due to a short circuit in the laboratory, as both are sensitive to electrical current changes and temperature. Both load cells required calibration at the start of the experiments and hourly thereafter, with 15 minutes breaks every two hours to avoid overheating and inaccurate readings which were observed with temperature changes.

Anatomical variation: Due to the hardened mid-section of the tendons at the lower leg level, it was not possible to simulate a dynamic range of motion through flexion of the adjacent joints, which led to a static study only.

Freezing process: It was not possible to experiment on fresh specimens from the farm on the same day, as the initial dissection for each specimen took between 20-25 minutes. Access to the laboratory at night time was limited in the absence of another university member and therefore specimens were frozen following the initial dissection.

Uchiyama apparatus: This apparatus, while ideal for measuring the gliding properties for an isolated arc of contact, does not allow measurements of a dynamic arc of contact.

7.2 Strengths and Weaknesses

For the simplicity of the discussion, the strengths and weaknesses of each section of the research are discussed separately.

1. The anatomy of turkey feet

Strengths: The turkey toes were fully dissected under magnification by a single surgeon. All specimens for this part of the study were collected close to the Christmas period when turkeys were allowed to grow to a larger size and therefore larger specimens were used for accurate dissection.

Ethical approval or permission from the Home Office was not required for the use of the turkey feet and storage in the laboratory freezer did not impose a health and safety hazard.

Weaknesses: More proximal dissections showed that in the mid-section, proximal to the level of the foot, the flexor tendons become bone-like structures with different gliding properties, before their attachment to the muscle, and therefore dynamic studies were not possible. Flexor tendons are about half the size of the human equivalent (in terms of width and depth) and therefore their treatment required modification (suture size, suture material and applied load) for the purposes of this research.

2. Electron microscopy

Strengths: This part of the study was carried out in a staged manner; each factor affecting the flexor tendon repair was studied individually and accurately, leading to a better understanding of the flexor tendon repair and its effect on the already injured tendon and pulley. The electron microscopy department provided excellent specimen preparation and images at three to four different magnifications to allow better visualisation of the iatrogenic tendon injury and the suture material.

Weaknesses: It was difficult to quantify the degree of delamination of the suture material. It remains unclear as to how much of this damage was due to the processing of the specimens for electron microscopy and how much was related to the simulated gliding for 10 minutes. It was not possible to measure the extent of pulley damage in the form of a percentage of the surface area.

3. Specimen dissection and set-up

Strengths: All specimen dissections were carried out by one person (myself) under ×3.5 magnification to avoid iatrogenic injury to the specimens. The Uchiyama set-up (which has previously been approved) was used following multiple calibrations for accuracy.

Weaknesses: All the experiments were carried out on frozen specimens. Due to the time required for specimens to be collected from the farm, dissected and set up, it was logistically not possible to perform these experiments on fresh specimens.

4. **Effect of tendon repair, peripheral suture, suture knot and pulley resection on the GR and CF.**

Strengths:. All the experiments were carried out by one trained surgeon under ×3.5 magnification and the same technique was used for all the specimens for the purpose of a better comparison. A digital calliper was used for precise pulley measurements. All the results were analysed following statistical advice from two different statisticians.

Weaknesses: Due to the lack of similarity in the paired tendons it was not possible to compare the pairs as previously planned. The experiments that required pulley resection required two hours of experimentation. This could have led to a higher GR as a result of prolonged tendon exposure and experimentation. Due to the small size of the tendon it was not possible to increase the load to those experienced in active and passive human finger motions. Due to the prolonged periods of experimentation and the risk of tendon drying, only two flexion angles were employed.

7.3 Clinical Implications

1. **Turkey toes as experimental specimens**

The full understanding and similarity of the turkey toe anatomy to human fingers allows other researchers to consider this animal model for future studies of the flexor, extensor tendons and for bony experiments. These are better alternatives to chicken specimens which are smaller or porcine specimens which are larger than their human counterparts.

2. **Tendon repair**

Electron microscopy of the treated tendon illustrates the secondary damage to the tendon created by the tendon repair. This means that less soft tissue handling, careful use of needle type (non-cutting versus cutting tip), careful positioning of the suture knot and the use of a simple non-locking running suture can lead to less damage to the tendon and pulley following rehabilitation.

3. Pulley venting

Although in this study 75% pulley resection was not significantly different from 50% pulley resection in terms of the gliding properties, such extensive pulley venting has to be carefully and cautiously considered, as it can lead to bowstringing and a subsequent reduction in the functional range of motion of the affected joints. Pulley resection should be limited and only to allow trigger free motion.

4. Post-operative rehabilitation

As the higher flexion angles and loads lead to increased frictional forces at the tendon-pulley interface, it seems logical to modify rehabilitation protocols to lower flexion angles with the aid of a flexion block splint and lower loads at the start of therapy to facilitate tendon gliding and avoid excessive friction.

7.4 Impact Statement

The relevance of this research to the clinical application of zone 2 flexor tendon repairs are summarised as:

I. Minimal tissue handling.
II. Use of a non-cutting suture needle.
III. A strong two strand core suture.
IV. A simple running circumferential suture.
V. A suture knot away from the volar surface of the tendon.
VI. Minimal pulley resection (<75%).
VII. Early range of motion rehabilitation at lower flexion angles and loads with application of flexion block splint.

7.5 Future Directions

1. Experimental set-up

The experiment frame that was used in this study required manual elevation of the experiment plate to allow for 10° flexion from 70° in each experiment. An experimental frame that allows angular movement to be digitally controlled would reduce the experimental time and improve accuracy. It would also allow different

flexion angles at each end of the pulley, so that the tendon on one side of the pulley could have a different flexion angle compared to the other side, therefore simulating different IPJ flexion angles that are used during the rehabilitation programme. This could be achieved by an interlocking circular frame and a glider which controls the flexion angle on the frame.

2. Tendon repair

As the paired specimens do not share similar gliding properties it is more important to consider comparing the flexor tendon treatment modalities to the initial intact tendon before the repair has been performed, instead of comparing to another randomly selected intact tendon.

For a better understanding of the GR in zone 2 injuries, a multicentre trial based on flexor tendon repair of human fingers would be more appropriate. With a patient awake during surgery and the use of miniature pressure sensors, both the active and passive range of motion could be assessed at different flexion angles, allowing a more accurate and dynamic measurement of the CF and GR at the time of tendon repair.

3. Rehabilitation

This research indicates that lower flexion angles and loads lead to a lower GR of the tendon-pulley interval in zone 2, however further studies are required to determine the exact flexion angle and load that is safe to be used following flexor tendon repair without risking tendon rupture and while maintaining tendon motion. A flexion block splint may be more appropriate to avoid high flexion angles during early rehabilitation.

Appendix 1 – Web Figures

Figure W1:

http://www.swann-morton.com/product/16.php

Figure W2:

http://www.swann-morton.com/product_range/3.php

Figure W3:

http://www.rocialle.com/products/view/RSPU500-202

Figure W4:

http://www.swann-morton.com/product/26.php

Figure W5:

http://www.screwfix.com/p/dewalt-3mm-extreme-2-hss-drill-bit-pack-of-2/30294

Figure W6:

http://www.medline.com/jump/product/x/Z05-PF18900

Figure W7:

http://www.diy.com/departments/gardman-steel-garden-wire-l50m/312852_BQ.prd

Figure W8:

http://www.diy.com/departments/bq-6-pliers/171125_BQ.prd

Figure W9:

http://www.orientalmotor.com/products/rotary-linear-actuators/ezs2-series-linear-actuator-slides.html

Figure W10:

http://www.maplin.co.uk/p/electronic-digital-calliper-n48aa

Figure W11:

http://sensing.honeywell.com/honeywell-t&m-model-31-mid-miniature-load-cell-product-sheet-008630-1-en.pdf

Figure W12:

http://tracerdaq.software.informer.com/screenshot/236720/

Figure W13:

http://www.amazon.com/Dynaroll-Miniature-Precision-Shielded-Stainless/dp/B0064OUA3I

Figure W14:

http://www.pecheur.com/en/gb/buy-monofilament-shimano-antares-silk-shock-32083.html?af=393329&gclid=CI7LtNC4-8MCFYjLtAod_w4AjQ

Figure W15:

http://www.gamakatsu.com/fishing-hooks.php?category=All+Purpose

Figure W16:

http://www.buy-toys.co.uk/product/Sets-of-Masses-Slotted-50g-hanger-4-x-50g.html

Figure W17:

http://santamariamedicine.com/2013/04/saline-therapy-hydration-found-to-be-a-powerful-tool-in-treatment-of-dysautonomia-pots/

Figure W18:

https://www.esutures.com/product/0-in-date/1-ethicon-suture/5-ethibond/45681-ethibond-10-x-30-rb-1-taper-double-armed-10-sutures-per-packet-5-green-5-white-D8366/

Figure W19:

https://www.esutures.com/product/0-in-date/1-ethicon-suture/3-ethilon/1398-ethilon-black-18-pc-1-conventional-cutting-pliabilized-nylon-1956G/

Appendix 2 – Permissions

Figure 1.1:

JOHN WILEY AND SONS LICENSE

TERMS AND CONDITIONS

Jan 30, 2015

This Agreement between Ladan Hajipour ("You") and John Wiley and Sons ("John Wiley and Sons") consists of your license details and the terms and conditions provided by John Wiley and Sons and Copyright Clearance Center.

License Number	3558981357771
License date	Jan 30, 2015
Licensed Content Publisher	John Wiley and Sons
Licensed Content Publication	Scandinavian Journal of Medicine & Science In Sports
Licensed Content Title	Structure of the tendon connective tissue
Licensed Content Author	P. Kannus
Licensed Content Date	Jul 7, 2008
Pages	9
Type of use	Dissertation/Thesis
Requestor type	University/Academic
Format	Print
Portion	Figure/table
Number of figures/tables	1
Original Wiley figure/table number(s)	figure 1
Will you be translating?	No
Title of your thesis / dissertation	GLIDING PROPERTIES OF THE FLEXOR TENDON IN ZONE II: TENDON REPAIR AND PULLEY RESECTION
Expected completion date	Aug 2015
Expected size (number of pages)	160
Requestor Location	Ladan Hajipour

	no 9 pentland close hazel grove stockport, United Kingdom sk7 5bs Attn: Ladan Hajipour
Billing Type	Invoice
Billing Address	Ladan Hajipour no 9 pentland close hazel grove stockport, United Kingdom sk7 5bs Attn: Ladan Hajipour
Total	0.00 GBP

Terms and Conditions

Figure 1.3:

Re: permission for figure in an article

Nicola Maffulli (n.maffulli@keele.ac.uk)

Add to contacts

25/02/2015

To: Ladan HAJIPOUR

Dear Miss Hajipour

Many thanks for your email

There will be no problems

Permission granted

All the best

Nicola Maffulli MD, MS, PhD, FRCP, FRCS(Orth)

Professor of Sport and Exercise Medicine

Consultant Trauma and Orthopaedic Surgeon

On 24 February 2015 at 21:49, Ladan HAJIPOUR <lhajipour@hotmail.com> wrote:

Dear Miss Maffulli

I am writing to ask for permission to use a figure from your article on;

Biology of tendon injury: healing, modelling and remodelling.

As instructed by the publishers, you have the copy right for all the figures.

I will be grateful if you grant me permission to put figure 2 (stress-strain curve) in my thesis.

Regards

Miss Ladan Hajipour

MB ChB, FRCS (Tr&Orth)

Consultant Orthopaedic Surgeon

Honorary Senior Lecturer University of Salford

University Hospitals of South Manchester

Wythenshawe Hospital

Figures 1.4 and 1.14:

ELSEVIER LICENSE

TERMS AND CONDITIONS

Jan 30, 2015

This is a License Agreement between Ladan Hajipour ("You") and Elsevier ("Elsevier") provided by Copyright Clearance Center ("CCC"). The license consists of your order details, the terms and conditions provided by Elsevier, and the payment terms and conditions.

All payments must be made in full to CCC. For payment instructions, please see information listed at the bottom of this form.

Supplier	Elsevier Limited The Boulevard,Langford Lane Kidlington,Oxford,OX5 1GB,UK
Registered Company Number	1982084
Customer name	Ladan Hajipour
Customer address	no 9 pentland close stockport, sk7 5bs
License number	3559041302289
License date	Jan 30, 2015

Licensed content publisher	Elsevier
Licensed content publication	Hand Clinics
Licensed content title	Tendon Healing, Edema, and Resistance to Flexor Tendon Gliding Clinical Implications
Licensed content author	Ya Fang Wu,Jin Bo Tang
Licensed content date	May 2013
Licensed content volume number	29
Licensed content issue number	2
Number of pages	12
Start Page	167
End Page	178
Type of Use	reuse in a thesis/dissertation
Portion	figures/tables/illustrations
Number of figures/tables/illustrations	1
Format	print
Are you the author of this Elsevier article?	No
Will you be translating?	No
Original figure numbers	figure 1 and figure 5
Title of your thesis/dissertation	GLIDING PROPERTIES OF THE FLEXOR TENDON IN ZONE II: TENDON REPAIR AND PULLEY RESECTION
Expected completion date	Aug 2015
Estimated size (number of pages)	160
Elsevier VAT number	GB 494 6272 12
Permissions price	0.00 GBP
VAT/Local Sales Tax	0.00 GBP / 0.00 GBP
Total	0.00 GBP

Figure 1.5 and 1.8:

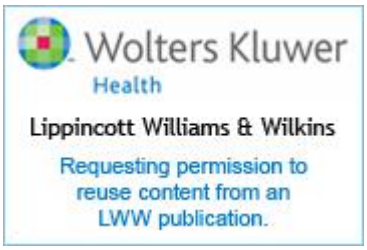

Book: Grabb and Smith's Plastic Surgery

Author: Charles H Thorne, Geoffrey C Gurtner,

Publisher: Wolters Kluwer Health

Date: 2013

Thesis / Dissertation Reuse

LWW grants permission for a maximum of 3 figures or tables without charge, provided that the material is for limited thesis/dissertation distribution. If you are required to post your thesis/dissertation on the university website/intranet/library reserve, access to it must be password-protected. Should you wish to publish your paper in the future, you will need to reapply for permission to use our material.

Figure 1.6A and 6B:

Thank you very much for your order.

This is a License Agreement between Ladan Hajipour ("You") and Elsevier ("Elsevier"). The license consists of your order details, the terms and conditions provided by Elsevier, and the

License Number	3663830691830
License date	Jul 07, 2015
Licensed content publisher	Elsevier
Licensed content publication	The Journal of Hand Surgery
Licensed content title	The second annular pulley: A histologic examination
Licensed content author	Frank D. Ellis,John Gray Seiler,C. Whitaker Sewell
Licensed content date	July 1995
Licensed content volume number	20

Licensed content issue number	4
Number of pages	4
Type of Use	reuse in a thesis/dissertation
Portion	figures/tables/illustrations
Number of figures/tables/illustrations	1
Format	print
Are you the author of this Elsevier article?	No
Will you be translating?	No
Original figure numbers	figure 1
Title of your thesis/dissertation	GLIDING PROPERTIES OF THE FLEXOR TENDON IN ZONE II: TENDON REPAIR AND PULLEY RESECTION
Expected completion date	Aug 2015
Estimated size (number of pages)	160
Elsevier VAT number	GB 494 6272 12
Permissions price	0.00 GBP
VAT/Local Sales Tax	0.00 GBP / 0.00 GBP
Total	0.00 GBP

Figure 1.7:

Title:	Scanning Electron Microscopic Findings of the Gliding Surface of the A1 Pulley in Trigger Fingers and Thumbs:
Author:	M. C. SBERNARDORI, V. MAZZARELLO, P. TRANQUILLI-LEALI
Publication:	Journal of Hand Surgery

Logged in as:

Ladan Hajipour

Account #:

3000883447

Publisher: SAGE Publications

Date: Aug 1, 2007

Gratis

Figure 1.9:

Title: Flexor Tendon Repair in Zone 2C:

Author: J. B. TANG

Publication: Journal of Hand Surgery

Publisher: SAGE Publications

Date: Feb 1, 1994

Gratis

Figure 1.10:

Title: An Evaluation of Suture Materials Used in Tendon Surgery:

Author: I. A. TRAIL, E. S. POWELL, J. NOBLE

Publication: Journal of Hand Surgery

Publisher: SAGE Publications

Date: Aug 1, 1989

Gratis

Figure 1.11:

	The Boulevard,Langford Lane Kidlington,Oxford,OX5 1GB,UK
Registered Company Number	1982084
Customer name	Ladan Hajipour
Customer address	no 9 pentland close stockport, sk7 5bs
License number	3559451380767
License date	Jan 31, 2015
Licensed content publisher	Elsevier
Licensed content publication	Hand Clinics
Licensed content title	Current Practice of Primary Flexor Tendon Repair A Global View
Licensed content author	Jin Bo Tang, Peter C. Amadio, Martin I. Boyer, Robert Savage, Chunfeng Zhao, Michael Sandow, Steve K. Lee, Scott W. Wolfe
Licensed content date	May 2013
Licensed content volume number	29
Licensed content issue number	2
Number of pages	11
Start Page	179
End Page	189
Type of Use	reuse in a thesis/dissertation
Intended publisher of new work	other
Portion	figures/tables/illustrations
Number of figures/tables/illustrations	1
Format	print
Are you the author of this	No

Elsevier article?	
Will you be translating?	No
Original figure numbers	figure 1
Title of your thesis/dissertation	GLIDING PROPERTIES OF THE FLEXOR TENDON IN ZONE II: TENDON REPAIR AND PULLEY RESECTION
Expected completion date	Aug 2015
Estimated size (number of pages)	160
Elsevier VAT number	GB 494 6272 12
Permissions price	0.00 GBP
VAT/Local Sales Tax	0.00 GBP / 0.00 GBP
Total	0.00 GBP

Figure 1.12:

Title:	The effect of core suture flexor tendon repair techniques on gliding resistance during static cycle motion and load to failure: a human cadaver study:
Author:	T. Moriya, M. C. Larson, C. Zhao, K.-N. An, P. C. Amadio
Publication:	Journal of Hand Surgery
Publisher:	SAGE Publications
Date:	May 1, 2012

Logged in as:

Ladan Hajipour

Account #:

3000883447

Gratis

Permission is granted at no cost for sole use in a Master's Thesis and/or Doctoral Dissertation.

Additional permission is also granted for the selection to be included in the printing of said scholarly work as part of UMI's "Books on Demand" program. For any further usage or publication, please contact the publisher.

Figure 1.13:

Logged in as:

Ladan Hajipour

Account #:

3000883447

Title:	The search for the ideal tendon repair in zone 2: strand number, anchor points and suture thickness:
Author:	R. Savage
Publication:	Journal of Hand Surgery
Publisher:	SAGE Publications
Date:	Jan 1, 2014

Copyright © 2014, The British Society for Surgery of the Hand

Gratis

Permission is granted at no cost for sole use in a Master's Thesis and/or Doctoral Dissertation. Additional permission is also granted for the selection to be included in the printing of said scholarly work as part of UMI's "Books on Demand" program. For any further usage or publication, please contact the publisher.

Figure 1.15:

SAGE

Title:	Flexor tendon pulley V–Y Plasty: an Alternative to Pulley Venting or Resection
Author:	E. DONA, W. R. WALSH
Publication:	Journal of Hand Surgery
Publisher:	SAGE Publications
Date:	04/01/2006

Copyright © 2006, © SAGE Publications

Logged in as:
Ladan Hajipour
Account #:
3000883447

LOGOUT

Figure 1.16:

ELSEVIER LICENSE

TERMS AND CONDITIONS

Jan 31, 2015

This is a License Agreement between Ladan Hajipour ("You") and Elsevier ("Elsevier") provided by Copyright Clearance Center ("CCC"). The license consists of your order details, the terms and conditions provided by Elsevier, and the payment terms and conditions.

All payments must be made in full to CCC. For payment instructions, please see information listed at the bottom of this form.

Supplier	Elsevier Limited The Boulevard,Langford Lane Kidlington,Oxford,OX5 1GB,UK
Registered Company Number	1982084
Customer name	Ladan Hajipour
Customer address	no 9 pentland close stockport, sk7 5bs
License number	3559461085286
License date	Jan 31, 2015
Licensed content publisher	Elsevier
Licensed content publication	Hand Clinics
Licensed content title	Current Flexor and Extensor Tendon Motion Regimens A Summary
Licensed content author	Sean P. Clancy,Daniel P. Mass
Licensed content date	May 2013

Licensed content volume number	29
Licensed content issue number	2
Number of pages	15
Start Page	295
End Page	309
Type of Use	reuse in a thesis/dissertation
Intended publisher of new work	other
Portion	figures/tables/illustrations
Number of figures/tables/illustrations	1
Format	print
Are you the author of this Elsevier article?	No
Will you be translating?	No
Original figure numbers	fig 2
Title of your thesis/dissertation	GLIDING PROPERTIES OF THE FLEXOR TENDON IN ZONE II: TENDON REPAIR AND PULLEY RESECTION
Expected completion date	Aug 2015
Estimated size (number of pages)	160
Elsevier VAT number	GB 494 6272 12
Permissions price	0.00 GBP
VAT/Local Sales Tax	0.00 GBP / 0.00 GBP
Total	0.00 GBP

Figure 1.17:

JOHN WILEY AND SONS LICENSE TERMS AND CONDITIONS

Jan 31, 2015

This Agreement between Ladan Hajipour ("You") and John Wiley and Sons ("John Wiley and

Sons") consists of your license details and the terms and conditions provided by John Wiley and Sons and Copyright Clearance Center.

License Number	3559471153709
License date	Jan 31, 2015
Licensed Content Publisher	John Wiley and Sons
Licensed Content Publication	Journal of Orthopaedic Research
Licensed Content Title	Method for the measurement of friction between tendon and pulley
Licensed Content Author	S. Uchiyama,J. H. Coert,L. Berglund,P. C. Amadio,K.-N. An
Licensed Content Date	Feb 18, 2005
Pages	7
Type of use	Dissertation/Thesis
Requestor type	University/Academic
Format	Print
Portion	Figure/table
Number of figures/tables	1
Original Wiley figure/table number(s)	fig 1
Will you be translating?	No
Title of your thesis / dissertation	GLIDING PROPERTIES OF THE FLEXOR TENDON IN ZONE II: TENDON REPAIR AND PULLEY RESECTION
Expected completion date	Aug 2015
Expected size (number of pages)	160
Requestor Location	Ladan Hajipour no 9 pentland close hazel grove

	stockport, United Kingdom sk7 5bs Attn: Ladan Hajipour
Billing Type	Invoice
Billing Address	Ladan Hajipour no 9 pentland close hazel grove stockport, United Kingdom sk7 5bs Attn: Ladan Hajipour
Total	0.00 GBP

Figure 1.18:

Title:	Flexor Tendon-Pulley Interaction afterTendon Repair:A biomechanical study
Author:	J. H. COERT, S. UCHIYAMA, P. C. AMADIO, L. J. BERGLUND, NK AN
Publication:	Journal of Hand Surgery
Publisher:	SAGE Publications
Date:	Oct 1, 1995

Logged in as:
Ladan Hajipour
Account #:
3000883447

scholarly work as part of UMI's "Books on Demand" program. For any further usage or publication, please contact the publisher.

Figure 2.1:

Re: image copyright

Thomas Roberts (thomas_roberts@brown.edu)

Add to contacts

02/02/2015

To: Ladan HAJIPOUR

Hello Ladan,

I'm happy that you would like to reproduce this image, you have my permission.

Tom Roberts

Sent from my iPad

On Feb 2, 2015, at 11:51 AM, Ladan HAJIPOUR <lhajipour@hotmail.com> wrote:

Hi

I am currently in the process of submitting my thesis. Our animal subject was turkey. I wanted to ask for your permission to put an image that has been created by you and published in the Scientific American in 2011. This is the link to the page if you need to refresh your memory.

http://blogs.scientificamerican.com/observations/2011/09/28/turkey-legs-tell-the-tale-of-our-unsung-tendons/

I wrote to the journal publisher and they directed me to you. I will really appreciate if you would give me permission, in writing, to print this image in my thesis.

Kind regards

Miss Ladan Hajipour

MB ChB, FRCS (Tr&Orth)

Consultant Orthopaedic Hand and Wrist Surgeon

Honorary Senior Lecturer University of Salford

University Hospitals of South Manchester

Wythenshawe Hospital

Figure 4.1:

Re: permission

James Kennedy

22:35

To: Ladan HAJIPOUR

Of course.

I will look for the original images on the pic to send over. Would probably be better quality and without annotations.

James

Yours Sincerely,

Dr James Kennedy

MBChB BSc(hons)

Sent from my iPad

On 24 Feb 2015, at 22:26, Ladan HAJIPOUR <lhajipour@hotmail.com> wrote:

Dear James

I hope you are well.

Can I please ask for your permission to use figure 15 from your MSC thesis on

Effect of Laceration and Trimming on Gliding Properties along the A2 Pulley:

In Vitro Study on Turkey Tendon?

Regards

ladan

Miss Ladan Hajipour

MB ChB, FRCS (Tr&Orth)

Consultant Orthopaedic Surgeon

Honorary Senior Lecturer University of Salford

University Hospitals of South Manchester

Figure 4.4:

OXFORD UNIVERSITY PRESS LICENSE

TERMS AND CONDITIONS

Jan 28, 2015

This is a License Agreement between Ladan Hajipour ("You") and Oxford University Press ("Oxford University Press") provided by Copyright Clearance Center ("CCC"). The license consists of your order details, the terms and conditions provided by Oxford University Press, and the payment terms and conditions.

All payments must be made in full to CCC. For payment instructions, please see information listed at the bottom of this form.

License Number	3557661240093
License date	Jan 28, 2015
Licensed content publisher	Oxford University Press
Licensed content publication	Journal of Electron Microscopy
Licensed content title	The role of collagen arrangement change during tendon healing demonstrated by scanning electron microscopy:
Licensed content author	Kaoru Sasaki, Naoto Yamamoto, Tomoharu Kiyosawa, Mitsuru Sekido
Licensed content date	10/01/2012
Type of Use	Thesis/Dissertation
Institution name	None
Title of your work	GLIDING PROPERTIES OF THE FLEXOR TENDON IN ZONE II: TENDON REPAIR AND PULLEY RESECTION
Publisher of your work	n/a
Expected publication date	Aug 2015
Permissions cost	0.00 GBP
Value added tax	0.00 GBP
Total	0.00 GBP

Total 0.00 GBP

Figure 4.5:

ELSEVIER LICENSE

TERMS AND CONDITIONS

Jan 31, 2015

This is a License Agreement between Ladan Hajipour ("You") and Elsevier ("Elsevier") provided by Copyright Clearance Center ("CCC"). The license consists of your order details, the terms and conditions provided by Elsevier, and the payment terms and conditions.

All payments must be made in full to CCC. For payment instructions, please see information listed at the bottom of this form.

Supplier	Elsevier Limited The Boulevard,Langford Lane Kidlington,Oxford,OX5 1GB,UK
Registered Company Number	1982084
Customer name	Ladan Hajipour
Customer address	no 9 pentland close stockport, sk7 5bs
License number	3559591205688
License date	Jan 31, 2015
Licensed content publisher	Elsevier
Licensed content publication	The Hand
Licensed content title	Surface study of tenosynovium in hens and humans by electron microscopy
Licensed content author	None
Licensed content date	October 1976
Licensed content volume number	8
Licensed content issue number	3
Number of pages	6

Start Page	222
End Page	227
Type of Use	reuse in a thesis/dissertation
Portion	figures/tables/illustrations
Number of figures/tables/illustrations	2
Format	Print
Are you the author of this Elsevier article?	No
Will you be translating?	No
Original figure numbers	fig6
Title of your thesis/dissertation	GLIDING PROPERTIES OF THE FLEXOR TENDON IN ZONE II: TENDON REPAIR AND PULLEY RESECTION
Expected completion date	Aug 2015
Estimated size (number of pages)	160
Elsevier VAT number	GB 494 6272 12
Permissions price	0.00 GBP
VAT/Local Sales Tax	0.00 GBP / 0.00 GBP
Total	0.00 GBP

Appendix 3 – Raw Data

Raw data: Effect of tendon repair and pulley resection on the gliding resistance and co-efficient of friction

Rt102000GR	Rt102000FC	Rt1020025GR	Rt1020025FC	Rt1020050GR	Rt1020050FC	Rt1020075GR	Rt1020075FC	Rt104000GR	Rt104000FC
0.2267	0.7428	0.4391	1.5791	0.4393	1.5747	0.4512	1.6019	0.8801	1.5329
0.6443	1.9832	0.638	1.9684	0.6362	2.0008	0.6077	1.906	1.1136	1.8265
0.7804	2.5921	0.7409	2.4478	0.6582	2.093	0.71	2.3228	1.2225	2.0322
0.4421	1.5159	0.3838	1.3	0.3915	1.3338	0.4062	1.3823	0.9034	1.5449
0.3745	1.2605	0.3599	1.1984	0.3645	1.2184	0.3774	1.2644	0.8488	1.4348
0.4113	1.4588	0.3985	1.4059	0.3872	1.3512	0.3892	1.3541	0.9095	1.5931
0.3583	1.2456	0.3619	1.2678	0.3449	1.1984	0.3381	1.176	0.8595	1.4984
0.3234	1.1067	0.3014	1.0257	0.3178	1.0805	0.2945	0.9944	0.8151	1.398
0.335	1.1397	0.3517	1.2005	0.2865	0.965	0.2994	1.0121	0.818	1.3971

Rt1040025G R	Rt1040025F C	Rt1040050G R	Rt1040050F C	Rt1040075G R	Rt1040075F C	Rt702000G R	Rt702000F C	Rt7020025G R	Rt7020025F C
0.9244	1.6187	0.9386	1.6588	0.9439	1.6626	0.3995	0.2151	0.4448	0.2366
1.1231	1.8354	1.1035	1.7863	1.082	1.7571	0.7432	0.3264	0.6652	0.3022
1.2179	2.0271	1.1939	1.9711	1.2036	1.9892	0.5703	0.2609	0.68	0.321
0.8873	1.5213	0.8811	1.5079	0.8921	1.522	0.4697	0.2399	0.3763	0.1897
0.8607	1.4524	0.9024	1.527	0.886	1.4929	0.3535	0.175	0.3759	0.1846
0.9161	1.6042	0.8916	1.5469	0.9034	1.5653	0.3807	0.1992	0.3985	0.2008
0.8422	1.4685	0.8388	1.4535	0.8117	1.4057	0.3413	0.1766	0.3162	0.1651
0.7988	1.3705	0.8114	1.3846	0.8244	1.4088	0.3243	0.1649	0.2593	0.132
0.8442	1.4472	0.8187	1.3995	0.8375	1.434	0.314	0.1577	0.2973	0.1511

Rt7020050GR	Rt7020050FC	Rt7020075GR	Rt7020075FC	Rt704000GR	Rt704000FC	Rt7040025GR	Rt7040025FC	Rt7040050GR	Rt7040050FC
0.4833	0.2611	0.5014	0.2685	0.86	0.2204	0.9261	0.2355	1.0122	0.2556
0.68	0.3098	0.6225	0.2826	1.2714	0.2965	1.1711	0.2751	1.0953	0.2566
0.6971	0.334	0.6209	0.2892	1.0228	0.2431	1.1412	0.2752	1.1555	0.2756
0.3842	0.1903	0.3975	0.1991	0.8288	0.2042	0.7516	0.1878	0.8885	0.2196
0.4208	0.2056	0.4464	0.2157	0.8679	0.2129	0.8485	0.2083	0.9106	0.2216
0.353	0.1844	0.3497	0.1801	0.8856	0.2255	0.8165	0.2079	0.8019	0.2046
0.3096	0.1604	0.2932	0.1513	0.7742	0.197	0.7647	0.1948	0.7317	0.1872
0.271	0.1379	0.2692	0.1362	0.7998	0.2002	0.6751	0.17	0.6947	0.1758
0.3045	0.1531	0.2631	0.1323	0.7467	0.1874	0.7939	0.1985	0.7679	0.1925

Rt7040075GR	Rt7040075FC	Lt102000GR	Lt102000FC	Lt10200LacGR	Lt10200LacFC	Lt1020025GR	Lt1020025FC	Lt1020050GR	Lt1020050FC
1.121	0.2777	0.2267	0.7428	0.4109	1.3054	0.3877	1.2372	0.5169	1.622
1.0638	0.2526	0.3831	1.3018	0.4104	1.3924	0.3854	1.3069	0.3733	1.2564
1.1565	0.2749	0.3116	1.0439	0.3615	1.2116	0.3567	1.2076	0.3641	1.2086
0.8788	0.2167	0.2628	0.8636	0.2271	0.743	0.337	1.0836	0.3299	1.0645
0.986	0.2369	0.3942	1.4042	0.3268	1.1478	0.3487	1.2241	0.3935	1.3784
0.8148	0.2057	0.3743	1.3189	0.3541	1.219	0.3618	1.2369	0.3745	1.2826
0.684	0.1751	0.3259	1.1188	0.2972	0.9979	0.3372	1.1254	0.3479	1.1637
0.8094	0.2017	0.3056	1.0487	0.2905	0.9842	0.3645	1.2598	0.3071	1.0375
0.7956	0.1988	0.448	1.5917	0.4542	1.6296	0.4797	1.7199	0.4388	1.5735

Lt1020075GR	Lt1020075FC	Lt104000GR	Lt104000FC	Lt10400LacGR	Lt10400LacFC	Lt1040025GR	Lt1040025FC	Lt1040050GR	Lt1040050FC
0.4277	1.3242	0.2846	0.5126	0.657	1.0526	0.6546	1.0703	0.8195	1.3503
0.3477	1.1624	0.85	1.4473	0.875	1.489	0.8547	1.4476	0.8317	1.4049
0.3695	1.2292	0.7945	1.3405	0.8577	1.4568	0.8605	1.4502	0.8212	1.389
0.3486	1.1307	0.7141	1.1945	0.6654	1.114	0.7393	1.2228	0.729	1.2019
0.3888	1.3666	0.8672	1.5155	0.782	1.3546	0.8126	1.41	0.9115	1.5882
0.3699	1.2775	0.8613	1.5059	0.8369	1.4466	0.8758	1.5042	0.8464	1.4576
0.3619	1.2186	0.817	1.4042	0.7741	1.3137	0.7586	1.2891	0.7997	1.3651
0.3542	1.2099	0.7862	1.3539	0.7131	1.2192	0.7579	1.3065	0.7498	1.2856
0.4682	1.6643	0.9216	1.6136	0.9634	1.6892	0.9467	1.6656	0.9215	1.6276

Lt1040075GR	Lt1040075FC	Lt702000GR	Lt702000FC	Lt70200LacGR	Lt70200LacFC	Lt7020025GR	Lt7020025FC	Lt7020050GR	Lt7020050FC
0.6126	1.0204	0.3175	0.1495	0.5296	0.2711	0.6706	0.3169	0.7199	0.3467
0.8118	1.3668	0.3378	0.1668	0.5107	0.2512	0.5326	0.262	0.5661	0.2766
0.8352	1.409	0.3201	0.1591	0.6022	0.2902	0.4774	0.2362	0.5387	0.2642
0.7816	1.2963	0.2553	0.1244	0.3595	0.1711	0.8376	0.3724	0.866	0.3979
0.833	1.4478	0.3501	0.1818	0.465	0.2376	0.5588	0.2875	0.7294	0.3709
0.8574	1.4777	0.3233	0.1686	0.5711	0.2883	0.6575	0.3241	0.7313	0.3622
0.8173	1.3915	0.2329	0.116	0.4421	0.2144	0.5621	0.2733	0.634	0.3053
0.7842	1.3508	0.2738	0.1402	0.3805	0.1908	0.4933	0.2519	0.6139	0.3034
0.9312	1.6316	0.4167	0.2206	0.4526	0.2419	0.5367	0.2859	0.6832	0.3577

Lt7020075G R	Lt7020075F C	Lt704000G R	Lt704000F C	Lt70400LacG R	Lt70400LacF C	Lt7040025G R	Lt7040025F C	Lt7040050G R	Lt7040050F C
0.8211	0.3689	0.5806	0.1377	0.8203	0.2287	1.0463	0.2453	1.3777	0.3201
0.4578	0.2247	0.8251	0.2031	0.9609	0.2348	1.0391	0.2532	1.163	0.2806
0.6654	0.3238	0.8504	0.2094	1.0308	0.249	1.1978	0.2877	1.1184	0.2718
0.9607	0.368	0.6609	0.1624	0.8236	0.1992	1.0864	0.2598	1.6056	0.3811
0.6673	0.3436	0.7882	0.1987	0.9628	0.2434	1.3749	0.3409	1.4571	0.3648
0.5699	0.2812	0.7852	0.1986	1.2578	0.311	1.419	0.3547	1.4762	0.3714
0.6251	0.2996	0.7229	0.1798	0.8944	0.2177	1.1155	0.2728	1.3484	0.325
0.5918	0.3003	0.8211	0.2066	0.3805	0.1908	1.0848	0.2728	1.2545	0.3096
0.6501	0.3445	0.8719	0.2224	1.0051	0.255	1.1471	0.2879	1.1387	0.2889

Lt7040075GR	Lt7040075FC
1.1253	0.2764
0.9348	0.2288
1.4537	0.3437
1.8404	0.4291
1.3449	0.3344
1.144	0.2857
0.9872	0.5949
1.1305	0.2803
1.1852	0.3013

Raw data: Effect of a circumferential suture on the gliding resistance and co-efficient of friction

1C10200GR	1C10200FC	1C10400GR	1C10400FC	1C70200GR	1C70200FC	1C70400GR	1C70400FC	1S10200GR	1S10200FC
0.5048	1.7951	1.0679	1.9047	0.533	0.2772	1.1061	0.283	0.4716	1.6566
0.5768	2.0779	1.1776	2.1059	0.5491	0.2966	1.1892	0.3113	0.5686	2.0875
0.5464	1.9725	3.7923	2.033	0.4936	0.2673	1.1259	0.2945	0.4653	1.7005
0.5815	2.1183	1.1511	2.0596	0.5277	0.2813	1.0491	0.2798	0.4067	1.5513
0.5074	1.8049	1.113	1.9805	0.3921	0.2169	1.0966	0.2879	0.5033	1.8031
0.4877	1.7369	1.1051	1.967	0.4695	0.2461	1.0807	0.2786	0.4787	1.7088
0.4902	1.7382	1.1123	1.9745	0.4955	0.2599	1.1053	0.2852	0.4916	1.7377
0.7128	2.7454	1.3659	2.542	0.7028	0.3994	1.3469	0.3625	0.7224	2.7891
0.7358	2.8809	1.3846	2.602	0.7271	0.4198	1.3769	0.3748	0.7131	2.7878

1S10400GR	1S10400FC	1S70200GR	1S70200FC	1S70400GR	1S70400FC
1.0893	1.9065	0.4633	0.2395	1.073	0.2759
0.8438	1.6099	0.6031	0.3299	1.2275	0.324
1.1259	2.0195	0.5485	0.2922	1.1266	0.2923
3.7936	2.0599	0.567	0.3062	1.1827	0.3101
1.1666	2.1066	0.5313	0.2862	1.0157	0.2739
1.0889	1.9267	0.4876	0.2573	1.137	0.2957
1.0919	1.9301	0.4757	0.2486	1.0989	0.2828
1.3833	2.5825	0.7348	0.4222	1.3766	0.3734
1.3824	2.6067	0.7259	0.4203	1.3838	0.3776

Raw data: Effect of a single suture knot on the gliding resistance and co-efficient of friction

1C10200GR	1C10200FC	1C10400GR	1C10400FC	1C70200GR	1C70200FC	1C70400GR	1C70400FC	1K10200GR	1K10200FC
0.5072	1.845	1.1109	1.9983	0.4756	0.2524	1.1232	0.2931	0.4835	1.724
0.5156	1.8696	1.1241	2.0023	0.4491	0.2324	1.1608	0.303	0.5177	1.8509
0.5301	1.8977	1.119	1.9932	0.4873	0.2553	1.101	0.2842	0.5476	1.9791
0.5644	2.0478	1.1411	2.0435	0.545	0.2923	1.1706	0.3065	0.5569	2.0262
0.5586	2.0185	1.141	2.0412	0.5388	0.2872	1.1713	0.3062	0.5567	2.0027
0.5765	2.0947	1.1517	2.0562	0.564	0.3034	1.1875	0.3118	0.5515	1.9908
0.5392	1.9289	1.1781	2.1126	0.5633	0.3016	1.199	0.3151	0.5696	2.0803
0.552	1.9761	1.1529	2.054	0.5188	0.2769	1.1388	0.2977	0.5482	1.9879
0.5529	1.9712	1.0864	1.9283	0.4781	0.2517	1.0984	0.2853	0.4585	1.6195

1K10400GR	1K10400FC	1K70200GR	1K70200FC	1K70400GR	1K70400FC
1.1099	1.9817	0.464	0.2438	1.112	0.2889
1.1466	2.0523	0.5288	0.281	1.242	0.3287
1.1373	2.0377	0.5144	0.2724	1.1408	0.2967
1.1419	2.0493	0.5701	0.3087	1.1505	0.3002
1.1557	2.065	0.5631	0.3037	1.1807	0.3093
1.1681	2.0982	0.5405	0.2888	1.1662	0.3055
1.1767	2.1259	0.584	0.317	1.2354	0.3277
1.1655	2.0997	0.5423	0.2924	1.1532	0.3024
1.0508	1.8621	0.4785	0.2522	1.0188	0.2612

Effect of tendon repair and pulley resection on the gliding resistance and co-efficient of friction

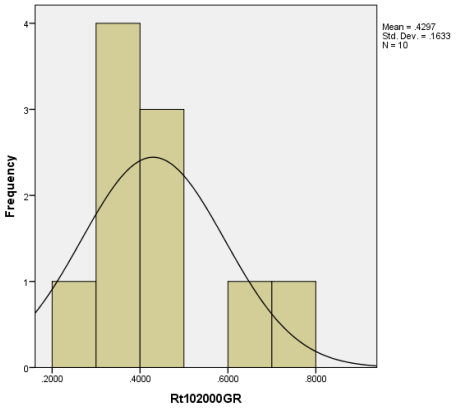

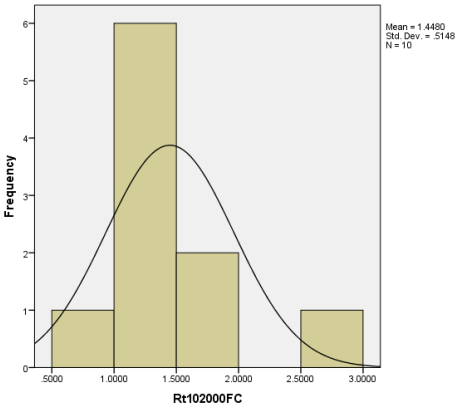

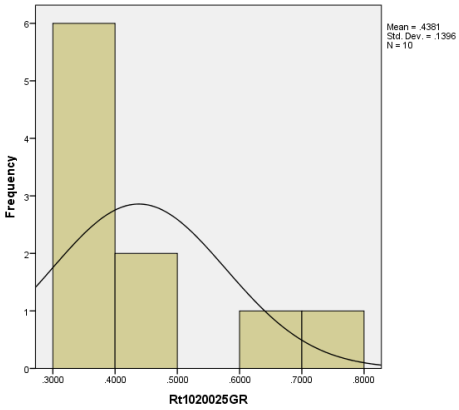

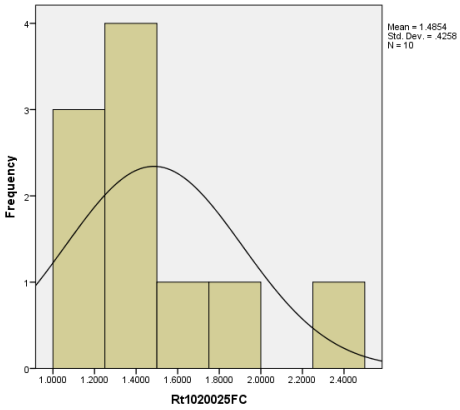

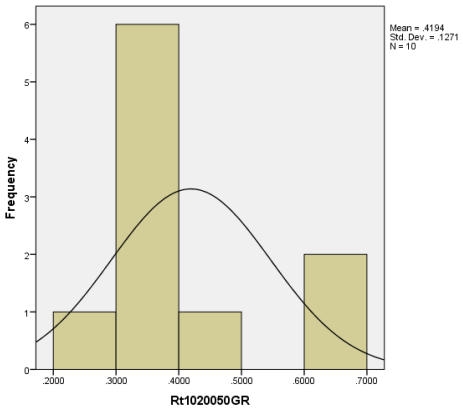

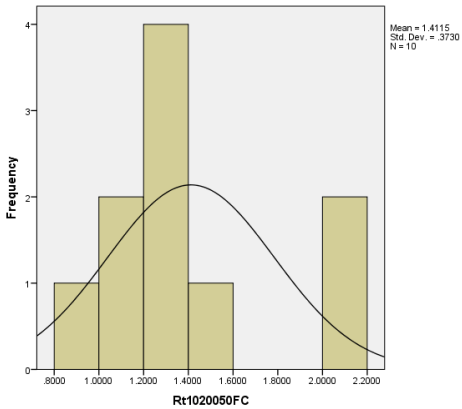

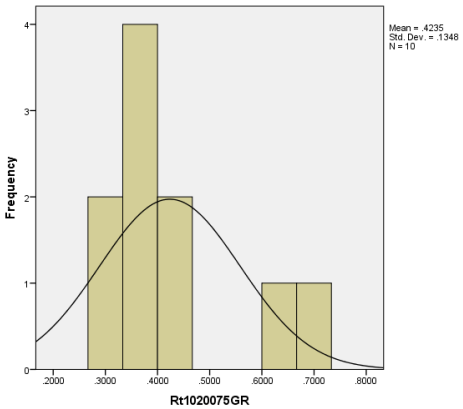

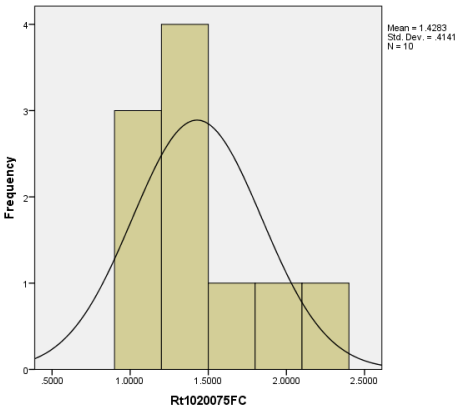

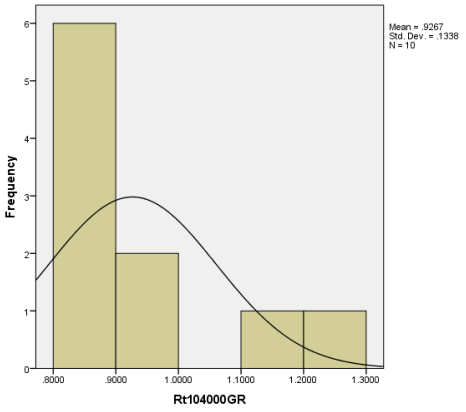
Mean = .9267
Std. Dev. = .1338
N = 10
Frequency
Rt104000GR

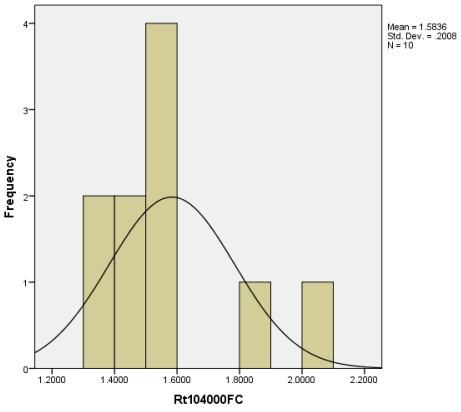
Mean = 1.5836
Std. Dev. = .2008
N = 10
Frequency
Rt104000FC

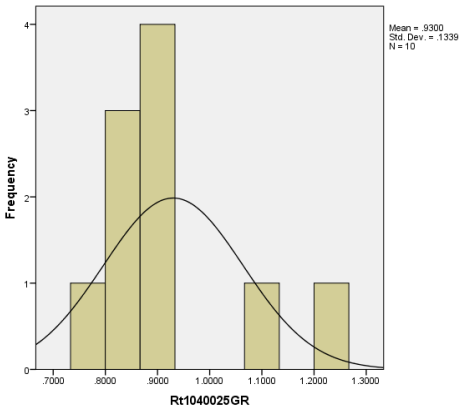
Mean = .9300
Std. Dev. = .1339
N = 10
Frequency
Rt1040025GR

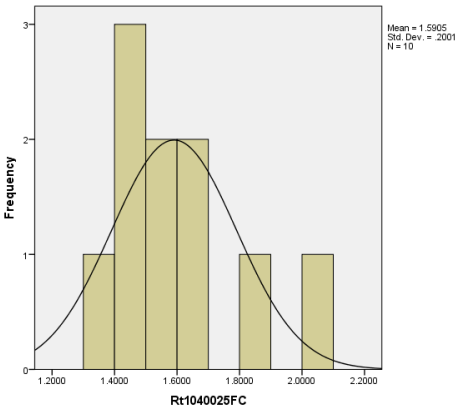
Mean = 1.5905
Std. Dev. = .2001
N = 10
Frequency
Rt1040025FC

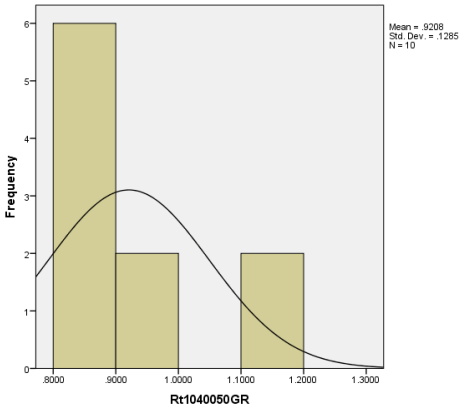
Mean = .9208
Std. Dev. = .1285
N = 10
Frequency
Rt1040050GR

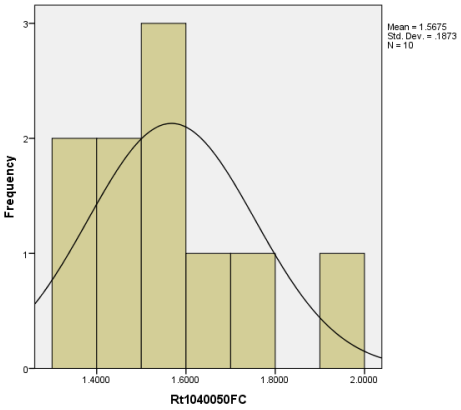
Mean = 1.5675
Std. Dev. = .1873
N = 10
Frequency
Rt1040050FC

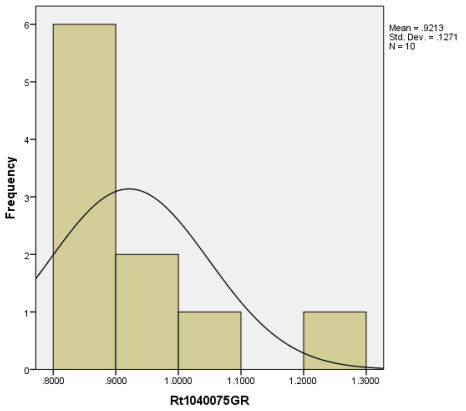
Mean = .9213
Std. Dev. = .1271
N = 10
Frequency
Rt1040075GR

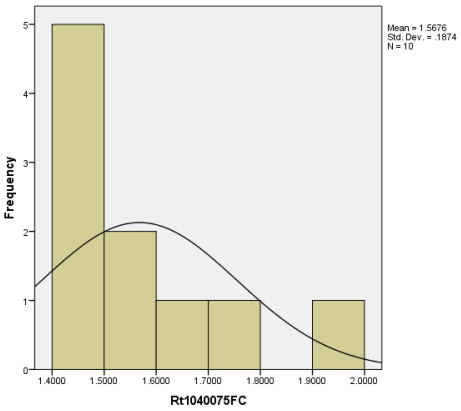
Mean = 1.5676
Std. Dev. = .1874
N = 10
Frequency
Rt1040075FC

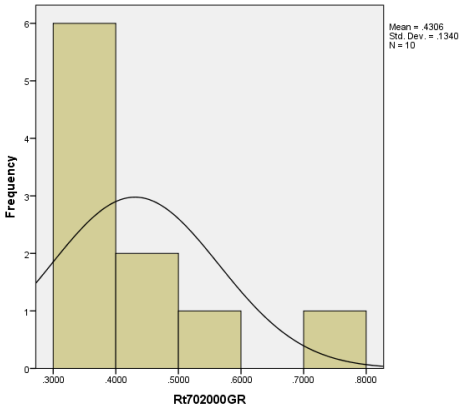
Mean = .4306
Std. Dev. = .1340
N = 10
Frequency
Rt702000GR

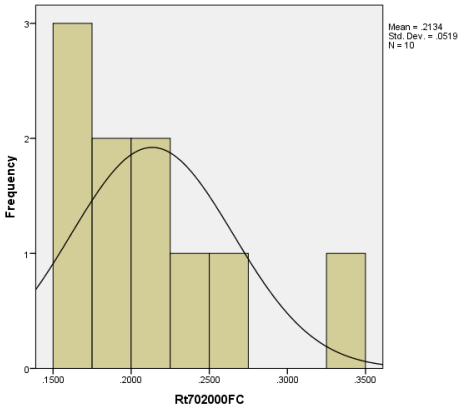
Mean = .2134
Std. Dev. = .0519
N = 10
Frequency
Rt702000FC

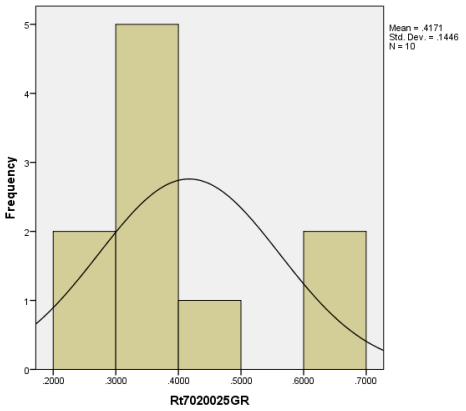
Mean = .4171
Std. Dev. = .1446
N = 10
Frequency
Rt7020025GR

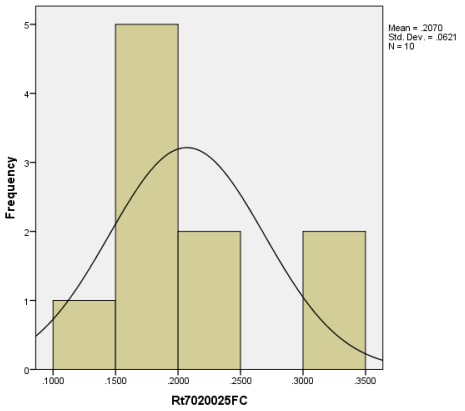
Mean = .2070
Std. Dev. = .0621
N = 10
Frequency
Rt7020025FC

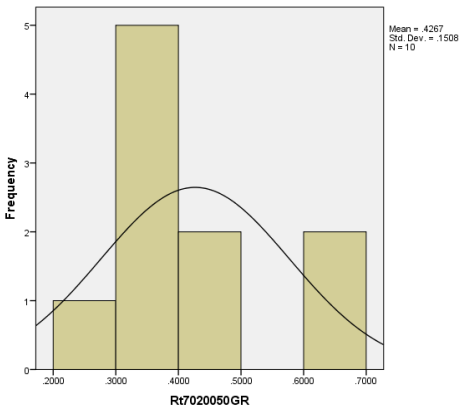
Mean = .4267
Std. Dev. = .1508
N = 10
Frequency
Rt7020050GR

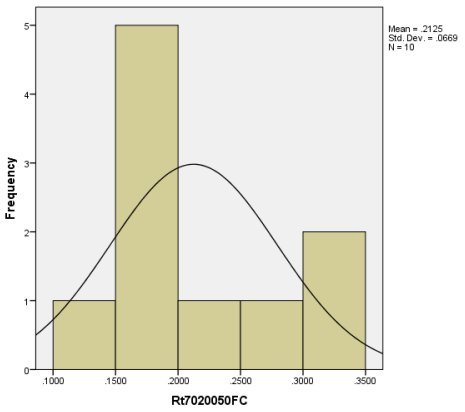
Mean = .2125
Std. Dev. = .0669
N = 10
Frequency
Rt7020050FC

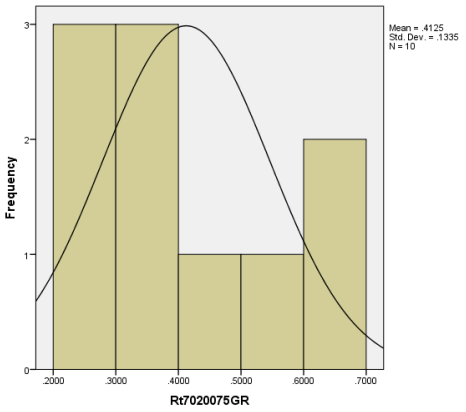
Mean = .4125
Std. Dev. = .1335
N = 10
Frequency
Rt7020075GR

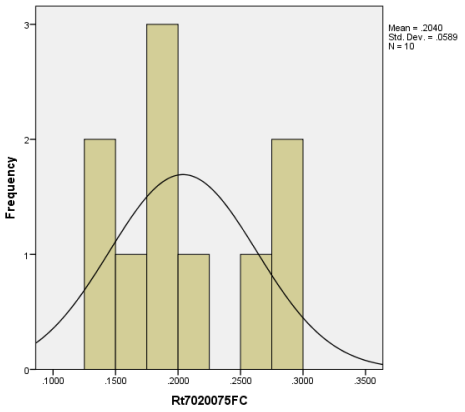
Mean = .2040
Std. Dev. = .0589
N = 10
Frequency
Rt7020075FC

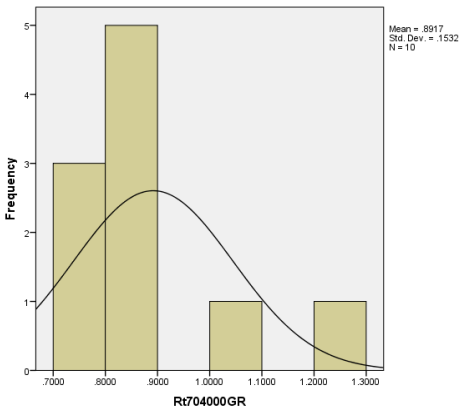
Mean = .8917
Std. Dev. = .1532
N = 10
Frequency
Rt704000GR

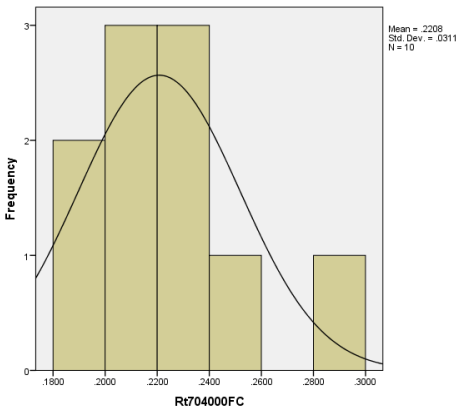
Mean = .2208
Std. Dev. = .0311
N = 10
Frequency
Rt704000FC

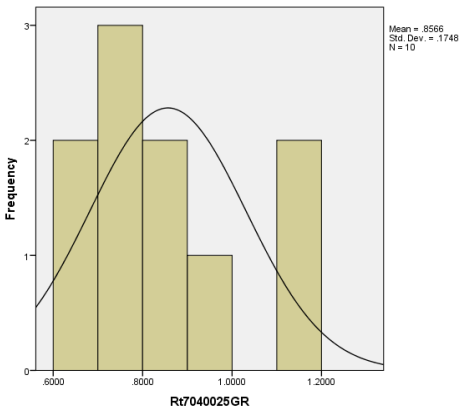
Mean = .8566
Std. Dev. = .1748
N = 10
Frequency
Rt7040025GR

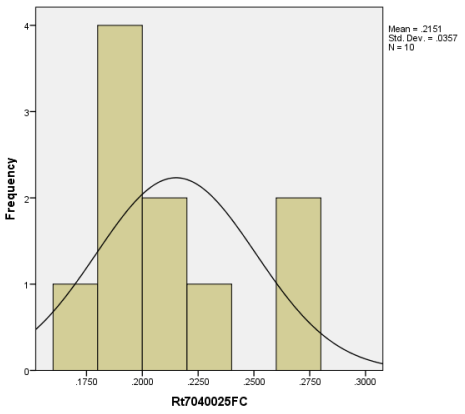
Mean = .2151
Std. Dev. = .0357
N = 10
Frequency
Rt7040025FC

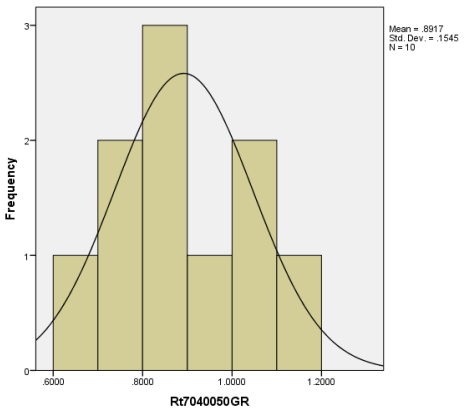
Mean = .8917
Std. Dev. = .1545
N = 10
Frequency
Rt7040050GR

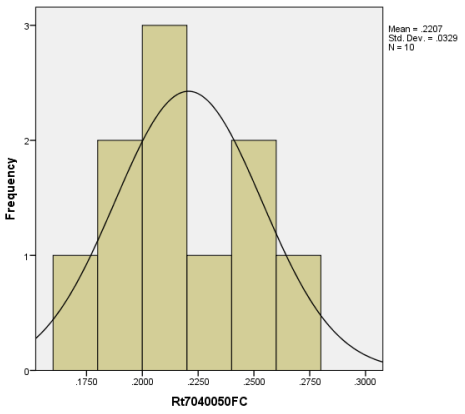
Mean = .2207
Std. Dev. = .0329
N = 10
Frequency
Rt7040050FC

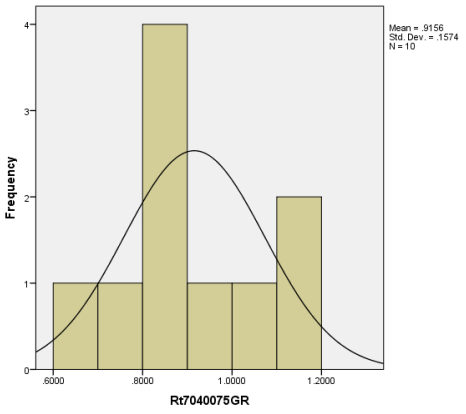
Mean = .9156
Std. Dev. = .1574
N = 10
Frequency
Rt7040075GR

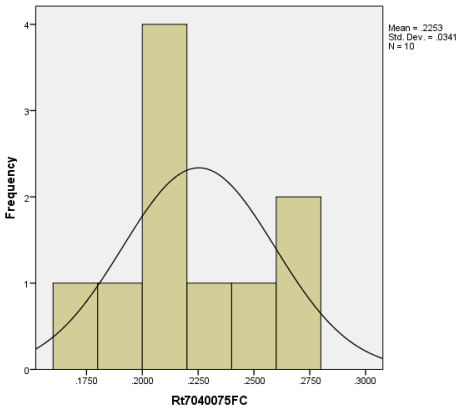
Mean = .2253
Std. Dev. = .0341
N = 10
Frequency
Rt7040075FC

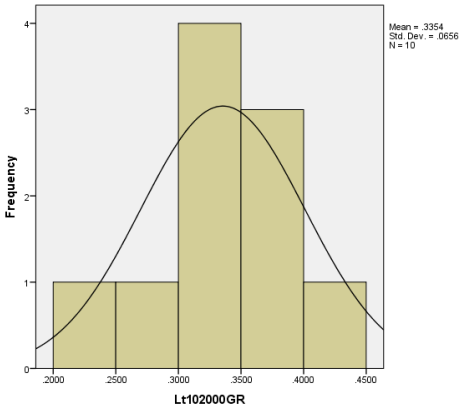
Mean = .3354
Std. Dev. = .0656
N = 10
Frequency
Lt102000GR

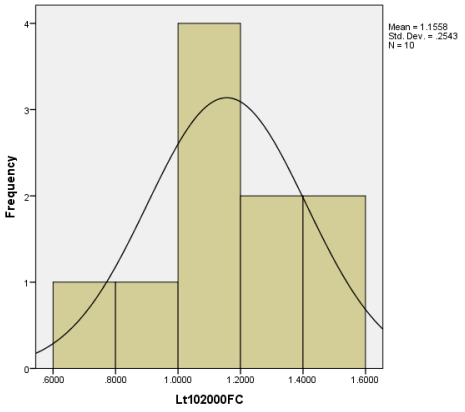
Mean = 1.1558
Std. Dev. = .2543
N = 10
Frequency
Lt102000FC

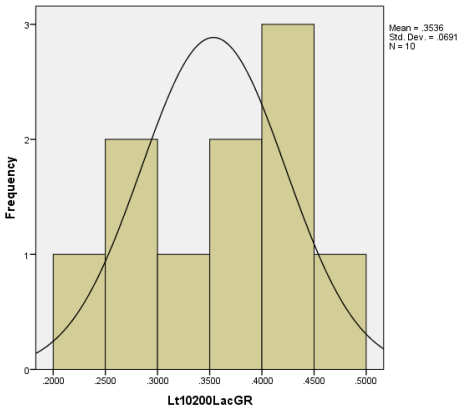
Mean = .3536
Std. Dev. = .0691
N = 10
Frequency
Lt10200LacGR

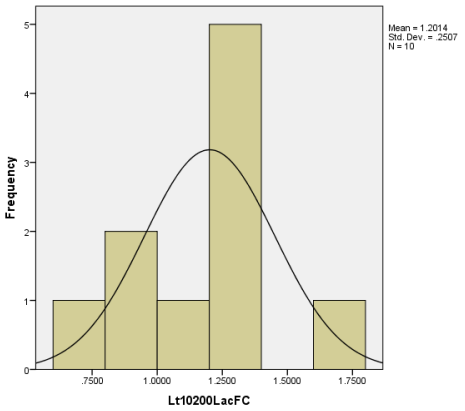
Mean = 1.2014
Std. Dev. = .2507
N = 10
Frequency
Lt10200LacFC

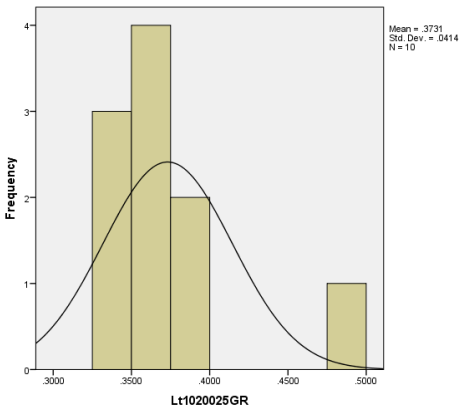
Mean = .3731
Std. Dev. = .0414
N = 10
Frequency
Lt1020025GR

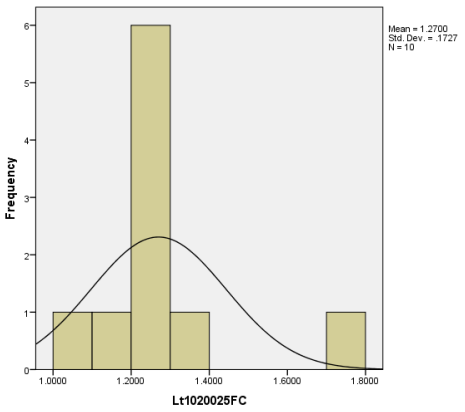
Mean = 1.2700
Std. Dev. = .1727
N = 10
Frequency
Lt1020025FC

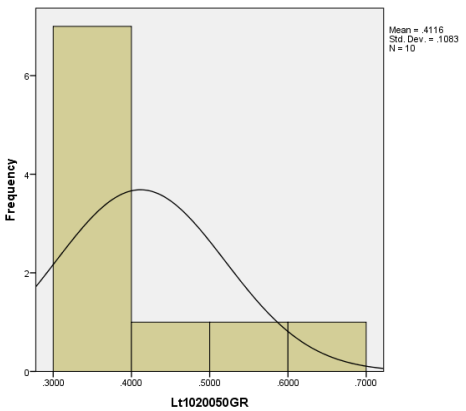
Mean = .4116
Std. Dev. = .1083
N = 10
Frequency
Lt1020050GR

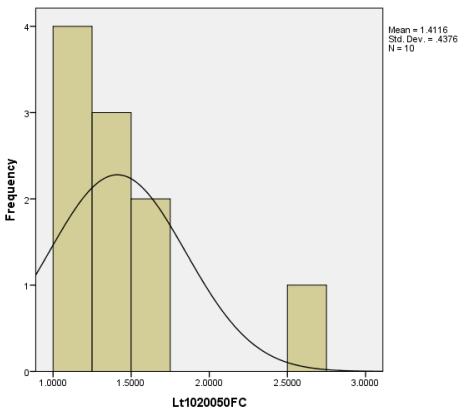
Mean = 1.4116
Std. Dev. = .4376
N = 10
Frequency
Lt1020050FC

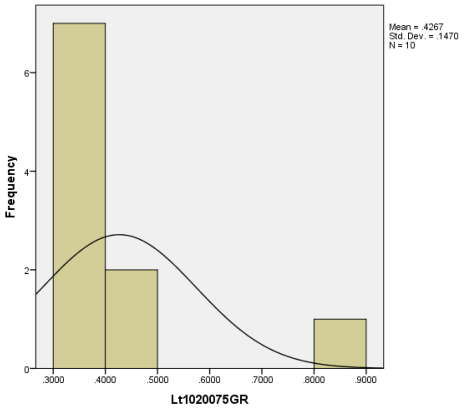
Mean = .4267
Std. Dev. = .1470
N = 10
Frequency
Lt1020075GR

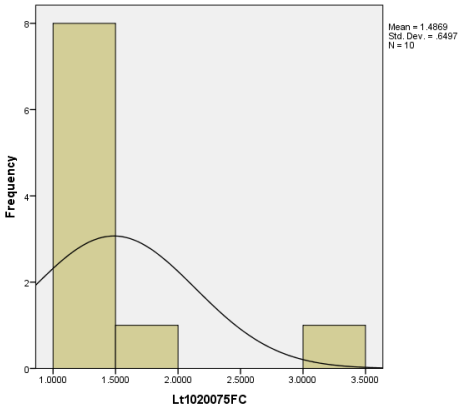
Mean = 1.4869
Std. Dev. = .6497
N = 10
Frequency
Lt1020075FC

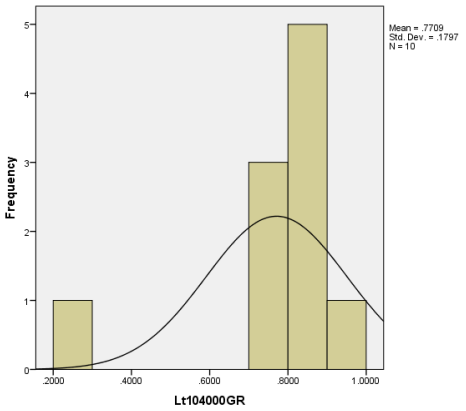
Mean = .7709
Std. Dev. = .1797
N = 10
Frequency
Lt104000GR

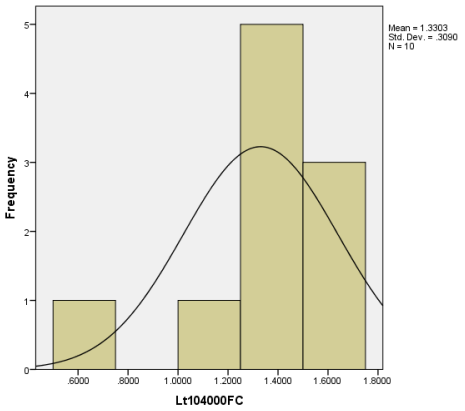
Mean = 1.3303
Std. Dev. = .3090
N = 10
Frequency
Lt104000FC

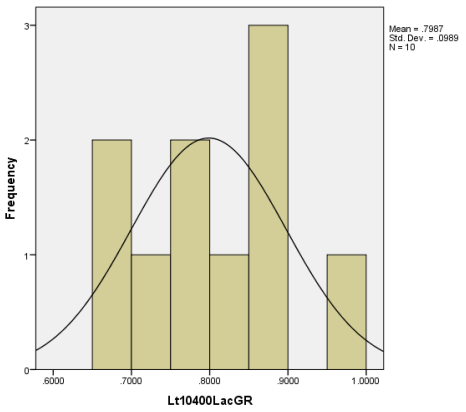
Mean = .7987
Std. Dev. = .0989
N = 10
Frequency
Lt10400LacGR

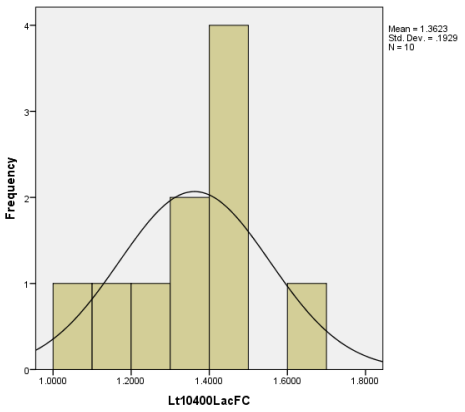
Mean = 1.3623
Std. Dev. = .1929
N = 10
Frequency
Lt10400LacFC

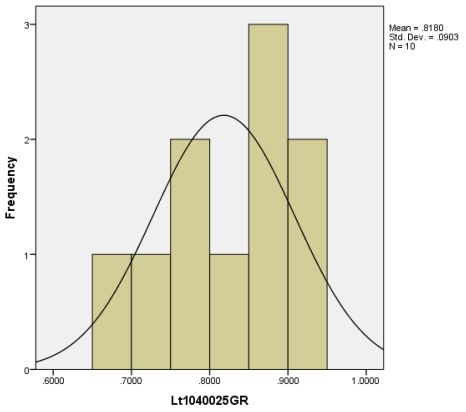
Mean = .8180
Std. Dev. = .0903
N = 10
Frequency
Lt1040025GR

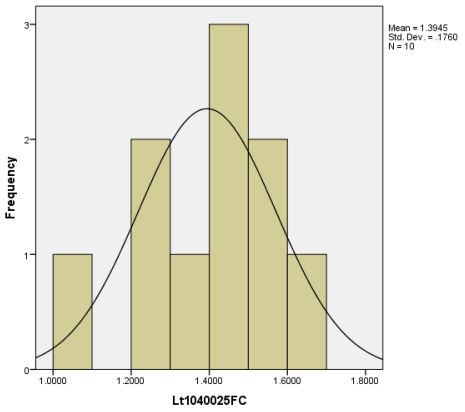
Mean = 1.3945
Std. Dev. = .1760
N = 10
Frequency
Lt1040025FC

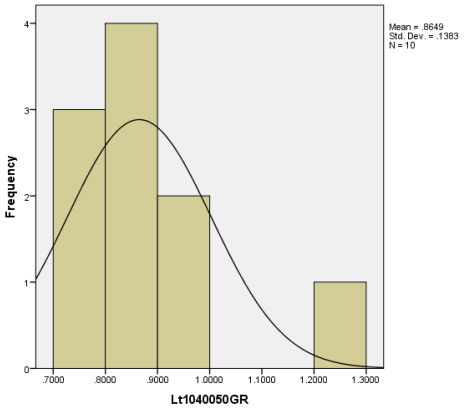
Mean = .8649
Std. Dev. = .1383
N = 10
Frequency
Lt1040050GR

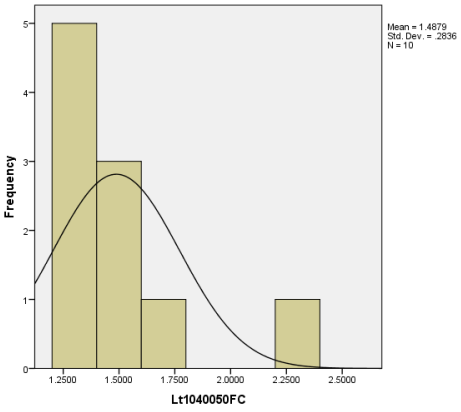
Mean = 1.4879
Std. Dev. = .2636
N = 10
Frequency
Lt1040050FC

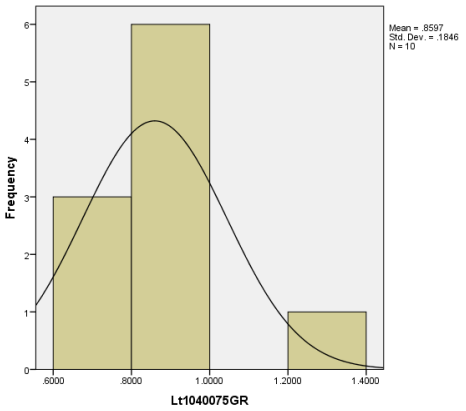
Mean = .8597
Std. Dev. = .1846
N = 10
Frequency
Lt1040075GR

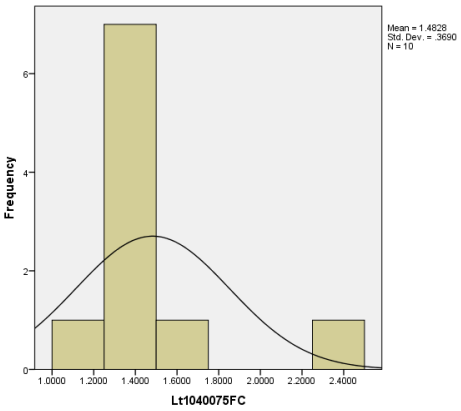
Mean = 1.4828
Std. Dev. = .3690
N = 10
Frequency
Lt1040075FC

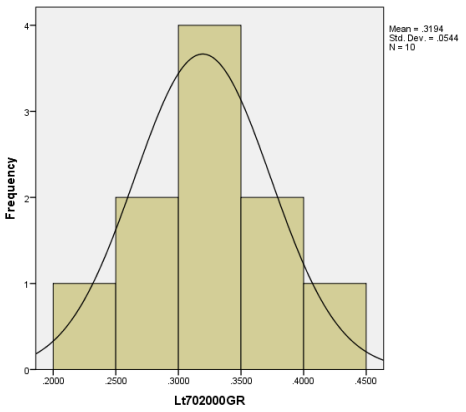
Mean = .3194
Std. Dev. = .0544
N = 10
Frequency
Lt702000GR

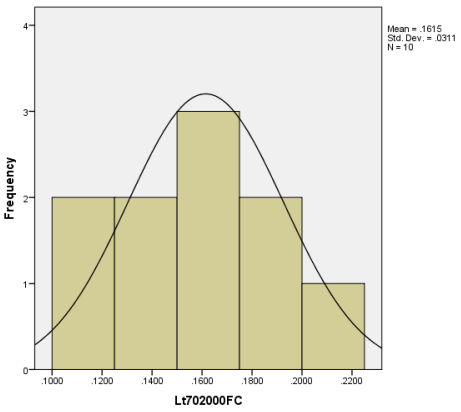
Mean = .1615
Std. Dev. = .0311
N = 10
Frequency
Lt702000FC

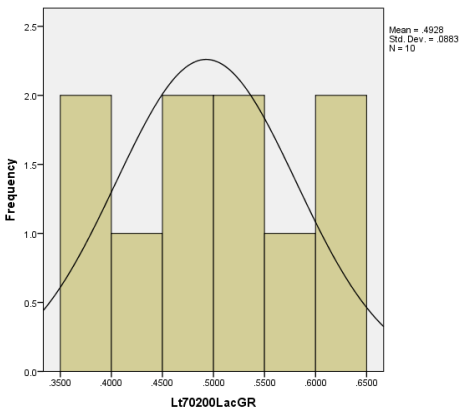
Mean = .4928
Std. Dev. = .0883
N = 10
Frequency
Lt70200LacGR

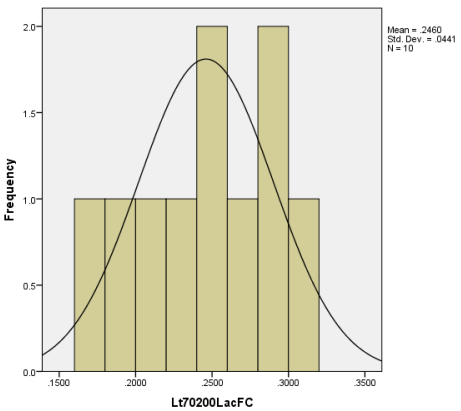
Mean = .2460
Std. Dev. = .0441
N = 10
Frequency
Lt70200LacFC

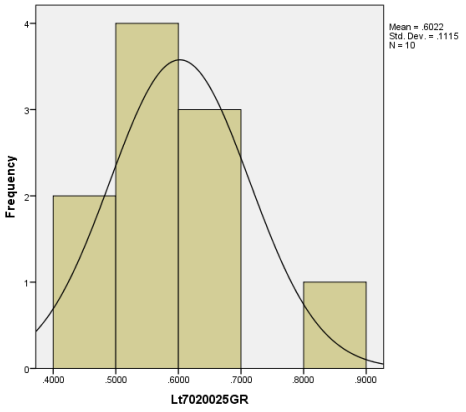
Mean = .6022
Std. Dev. = .1115
N = 10
Frequency
Lt7020025GR

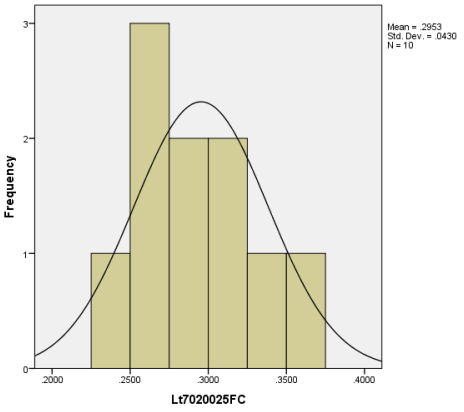
Mean = .2953
Std. Dev. = .0430
N = 10
Frequency
Lt7020025FC

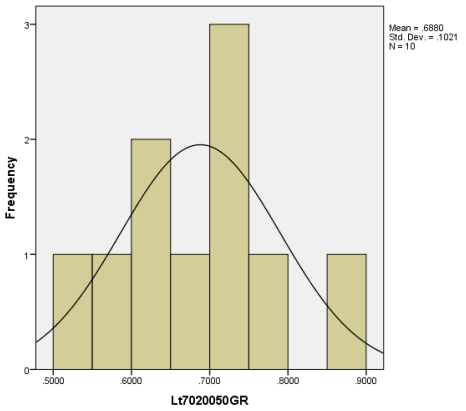
Mean = .6880
Std. Dev. = .1021
N = 10
Frequency
Lt7020050GR

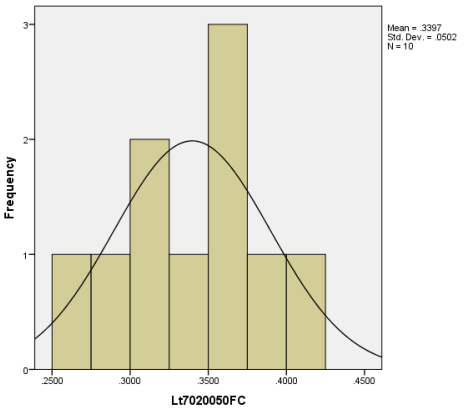
Mean = .3397
Std. Dev. = .0502
N = 10
Frequency
Lt7020050FC

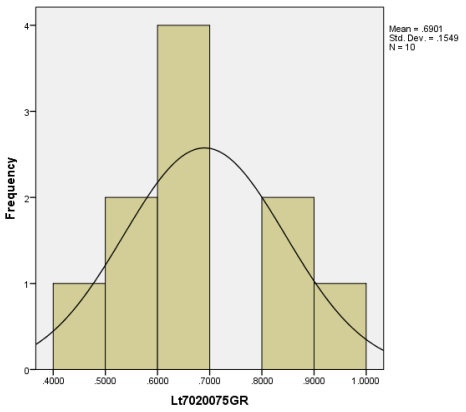
Mean = .6901
Std. Dev. = .1549
N = 10
Frequency
Lt7020075GR

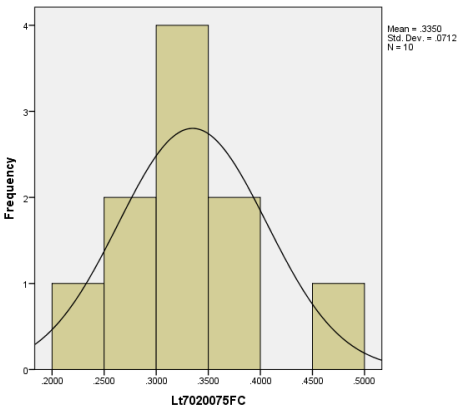
Mean = .3350
Std. Dev. = .0712
N = 10
Frequency
Lt7020075FC

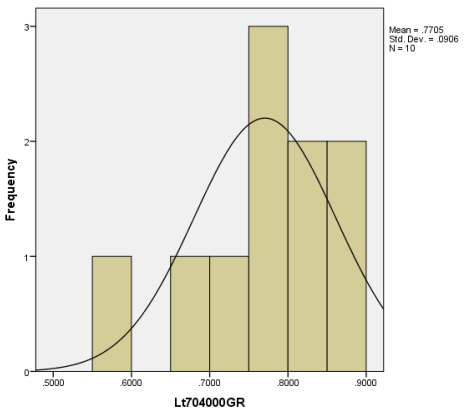
Mean = .7705
Std. Dev. = .0906
N = 10
Frequency
Lt704000GR

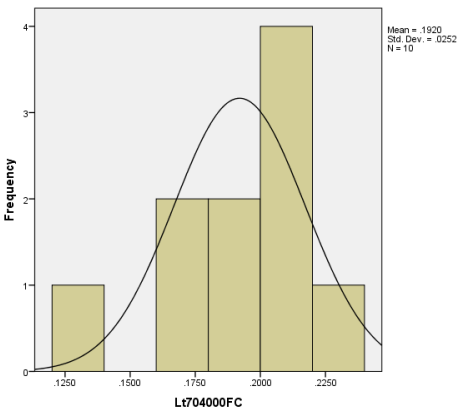
Mean = .1920
Std. Dev. = .0252
N = 10
Frequency
Lt704000FC

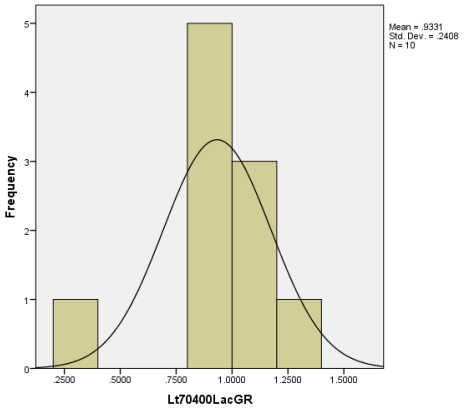
Mean = .9331
Std. Dev. = .2408
N = 10
Frequency
Lt70400LacGR

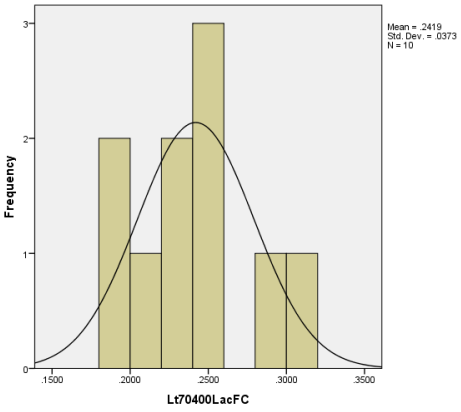
Mean = .2419
Std. Dev. = .0373
N = 10
Frequency
Lt70400LacFC

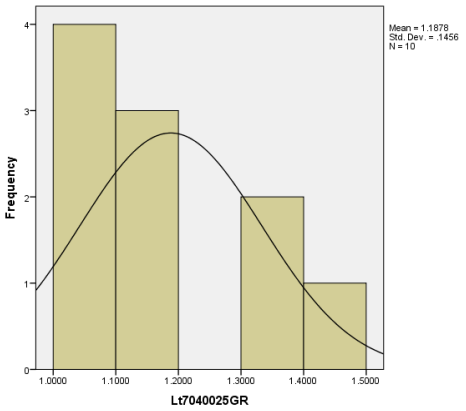
Mean = 1.1878
Std. Dev. = .1456
N = 10
Frequency
Lt7040025GR

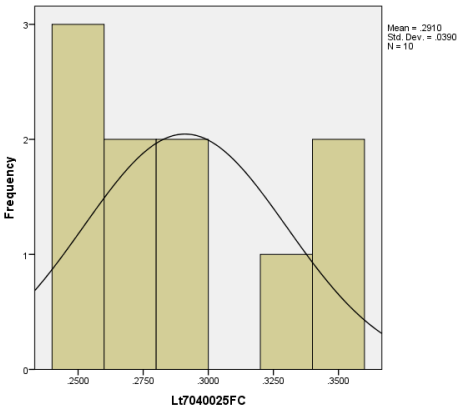
Mean = .2910
Std. Dev. = .0390
N = 10
Frequency
Lt7040025FC

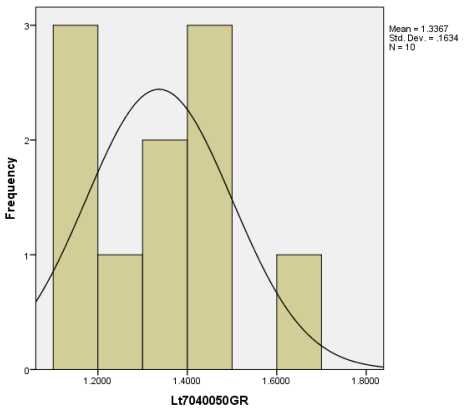
Mean = 1.3367
Std. Dev. = .1634
N = 10
Frequency
Lt7040050GR

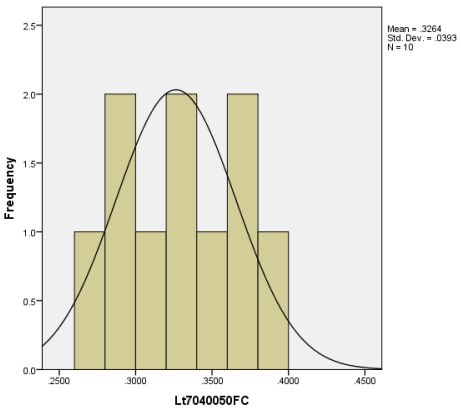
Mean = .3264
Std. Dev. = .0393
N = 10
Frequency
Lt7040050FC

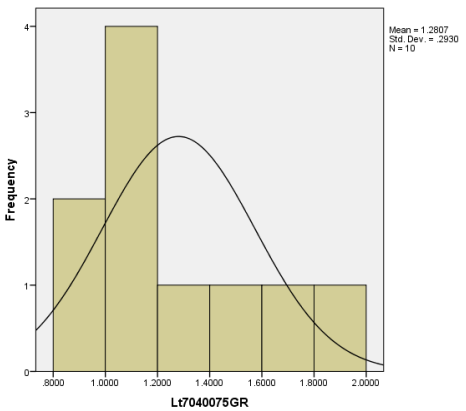
Mean = 1.2807
Std. Dev. = .2930
N = 10
Frequency
Lt7040075GR

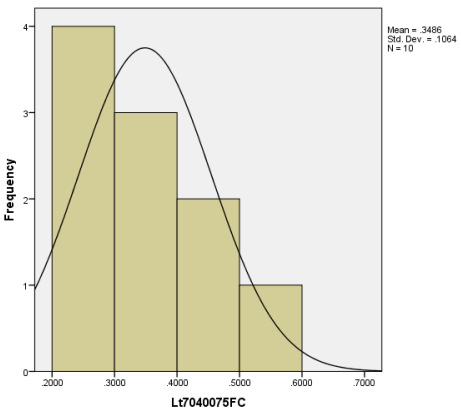
Mean = .3486
Std. Dev. = .1064
N = 10
Frequency
Lt7040075FC

Effect of a circumferential suture on the gliding resistance and co-efficient of friction

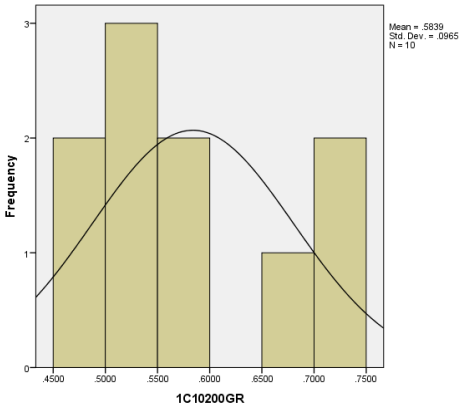

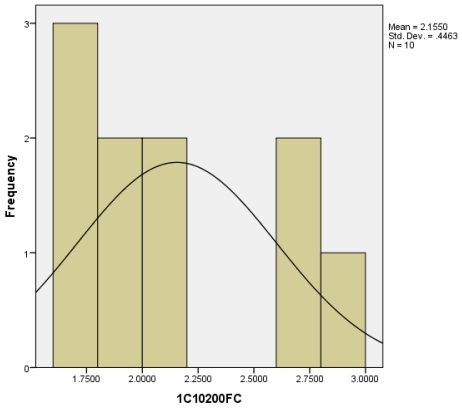

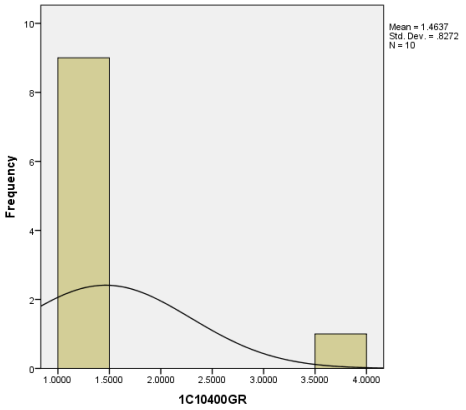

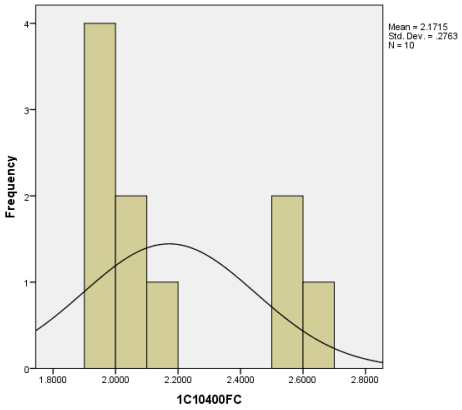

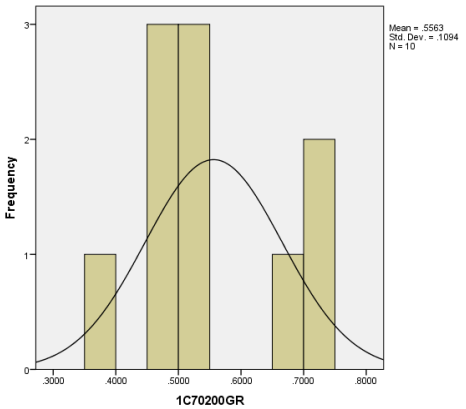

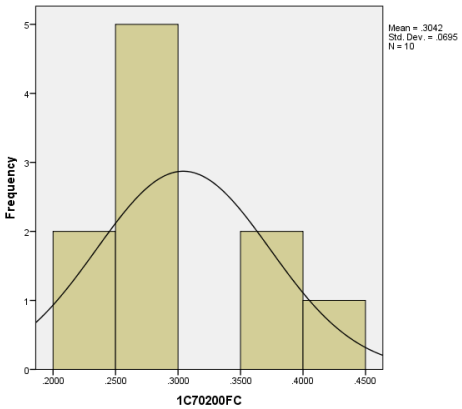

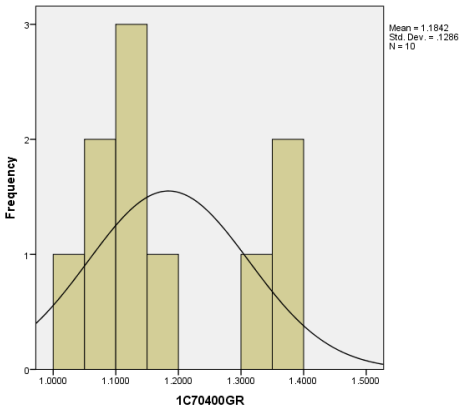

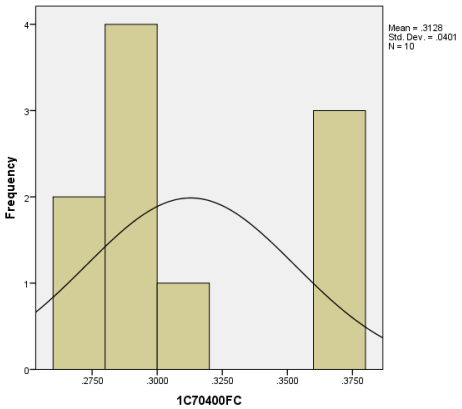

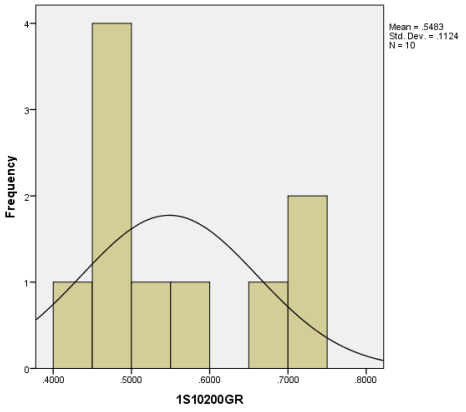
Mean = .5483
Std. Dev. = .1124
N = 10
Frequency
1S10200GR

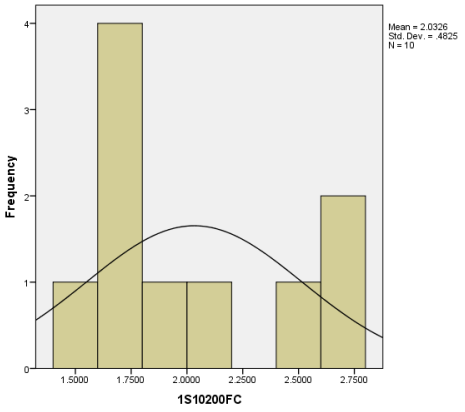
Mean = 2.0326
Std. Dev. = .4625
N = 10
Frequency
1S10200FC

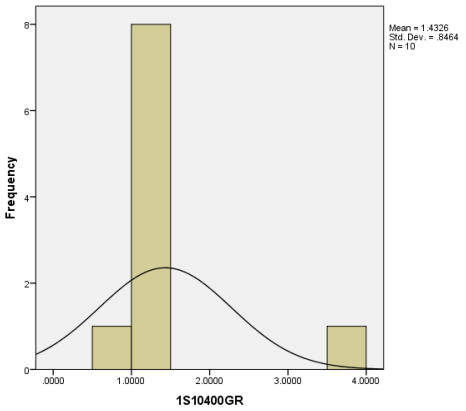
Mean = 1.4326
Std. Dev. = .8464
N = 10
Frequency
1S10400GR

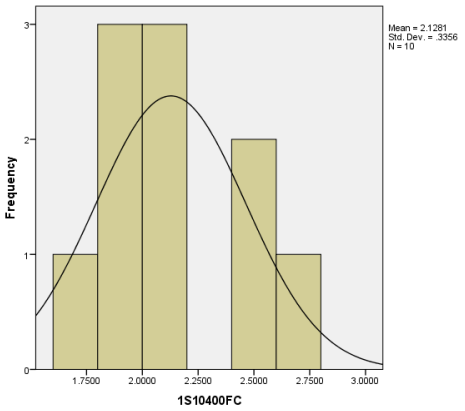
Mean = 2.1281
Std. Dev. = .3356
N = 10
Frequency
1S10400FC

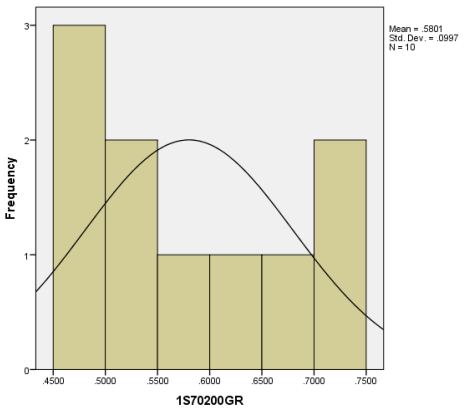
Mean = .5801
Std. Dev. = .0997
N = 10
Frequency
1S70200GR

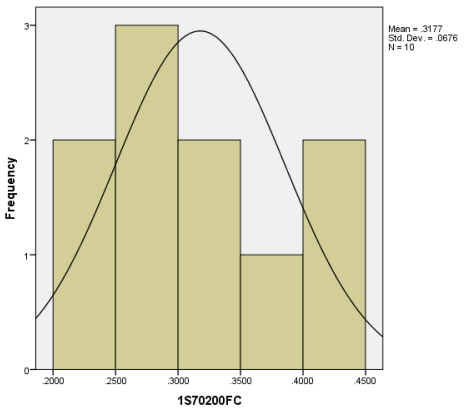
Mean = .3177
Std. Dev. = .0676
N = 10
Frequency
1S70200FC

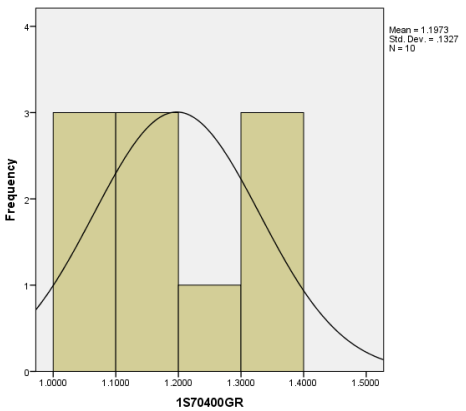
Mean = 1.1973
Std. Dev. = .1327
N = 10
Frequency
1S70400GR

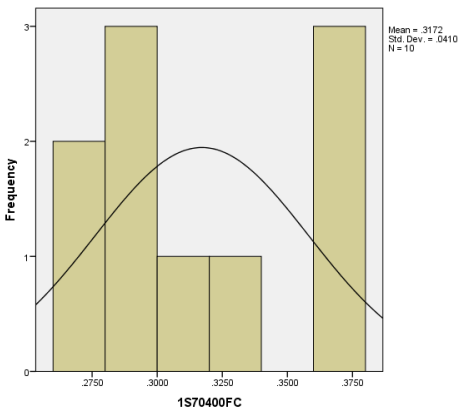
Mean = .3172
Std. Dev. = .0410
N = 10
Frequency
1S70400FC

Effect of a single knot on the gliding resistance and co-efficient of friction

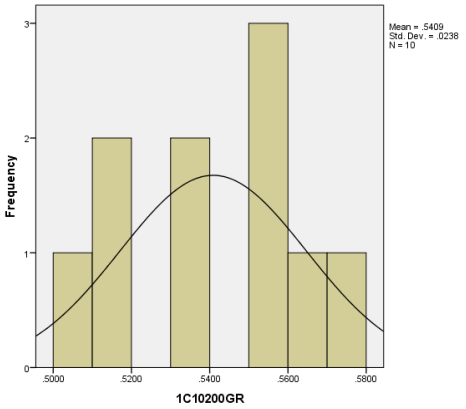

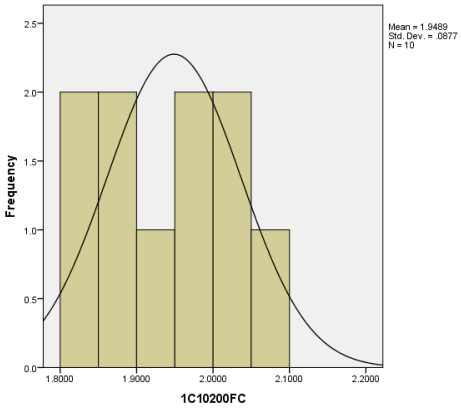

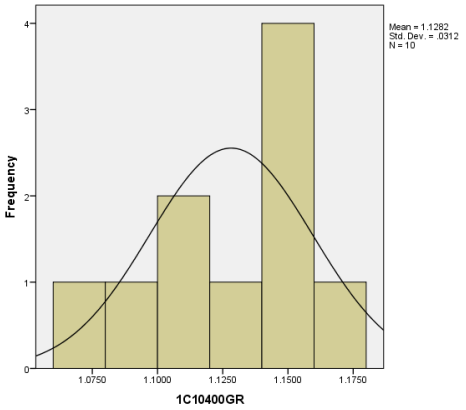

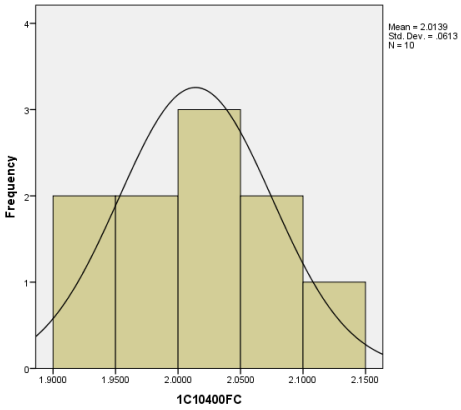

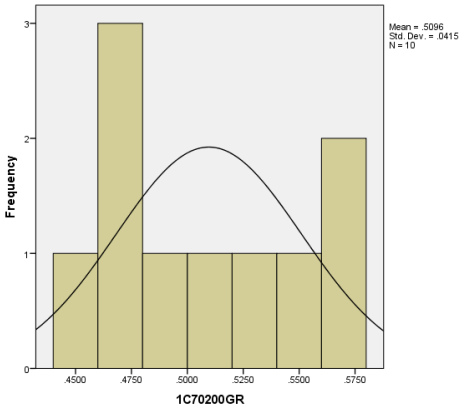

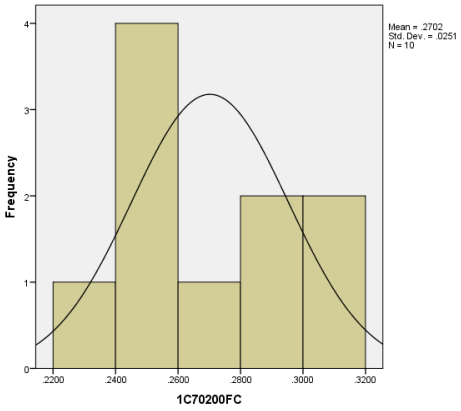

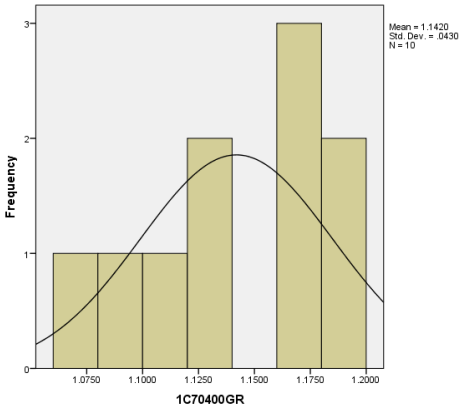

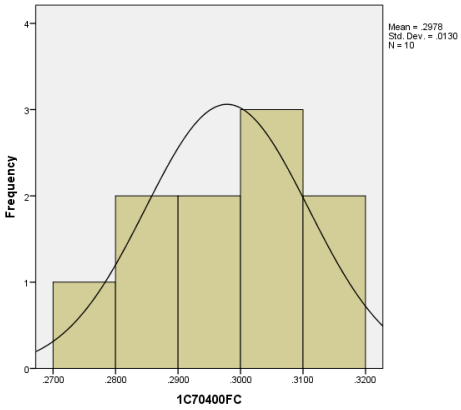

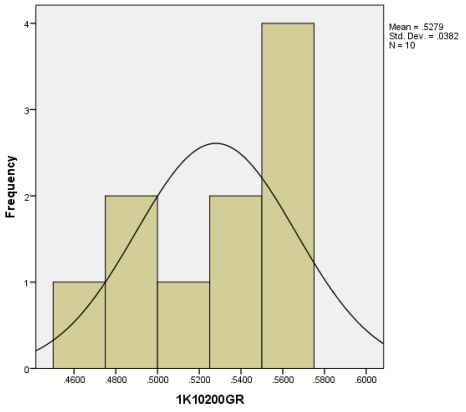
Mean = .5279
Std. Dev. = .0382
N = 10
Frequency
1K10200GR

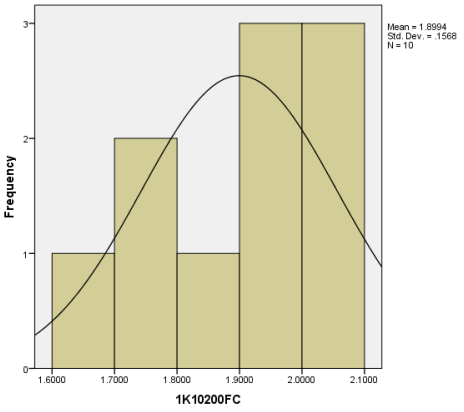
Mean = 1.8994
Std. Dev. = .1568
N = 10
Frequency
1K10200FC

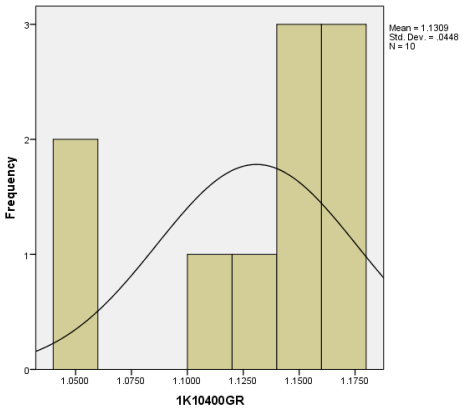
Mean = 1.1309
Std. Dev. = .0448
N = 10
Frequency
1K10400GR

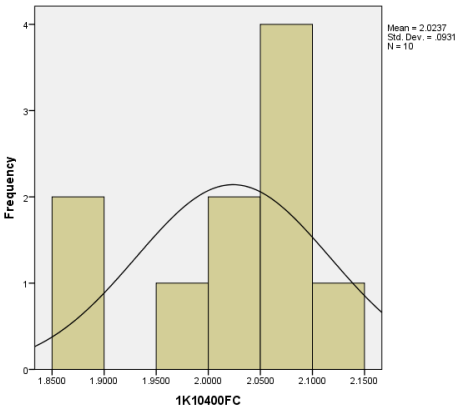
Mean = 2.0237
Std. Dev. = .0931
N = 10
Frequency
1K10400FC

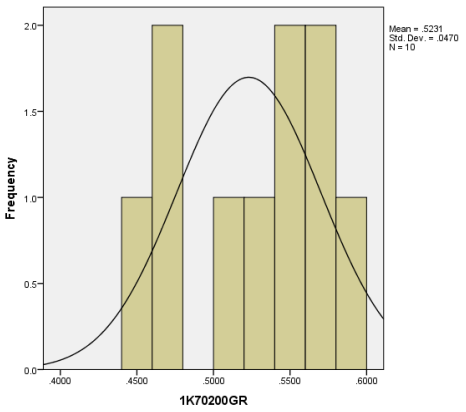
Mean = .5231
Std. Dev. = .0470
N = 10
Frequency
1K70200GR

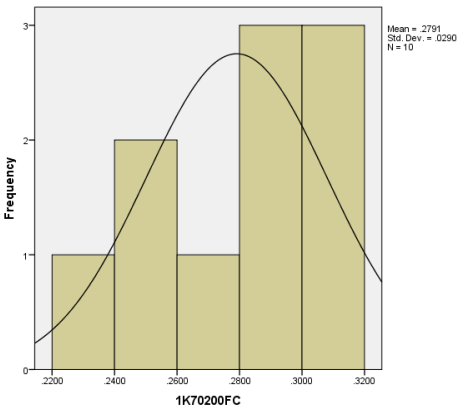
Mean = .2791
Std. Dev. = .0290
N = 10
Frequency
1K70200FC

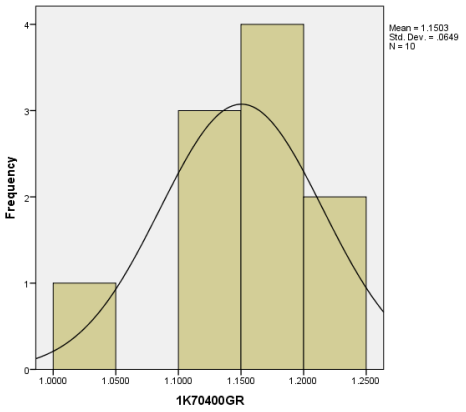
Mean = 1.1503
Std. Dev. = .0649
N = 10
Frequency
1K70400GR

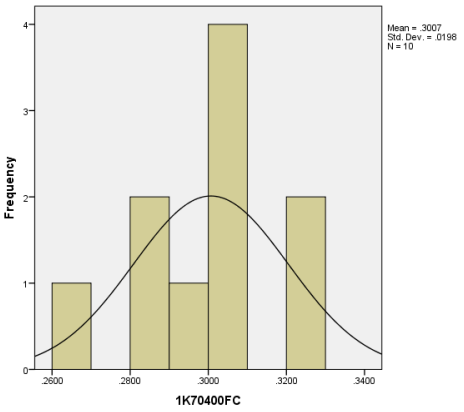
Mean = .3007
Std. Dev. = .0198
N = 10
Frequency
1K70400FC

Appendix 4 - Data Test for Normal Distribution

order rt102000gr rt1020025gr rt1020050gr rt1020075gr rt104000gr rt1040025gr rt1040050gr rt1040075gr rt702000gr rt7020025gr rt7020050gr rt7020075gr rt704000gr rt7040025gr rt704005

> 0gr rt7040075gr lt102000gr lt10200lacgr lt1020025gr lt1020050gr lt1020075gr lt104000gr lt10400lacgr lt1040025gr lt1040050gr lt1040075gr lt1040025gr lt1040050gr lt1040075gr lt70200

> 0gr lt70200lacgr lt7020025gr lt7020050gr lt7020075gr lt704000gr lt70400lacgr lt7040025gr lt7040050gr lt7040075gr

. foreach xvar of varlist rt102000gr- lt7040075fc {
2. swilk `xvar'
3. }

Shapiro-Wilk W test for normal data

Variable	Obs	W	V	z	Prob>z
rt102000gr	10	0.85788	2.190	1.461	0.07204

Shapiro-Wilk W test for normal data

Variable	Obs	W	V	z	Prob>z
rt1020025gr	10	0.77761	3.427	2.421	0.00774

Shapiro-Wilk W test for normal data

Variable	Obs	W	V	z	Prob>z
rt1020050gr	10	0.80596	2.990	2.117	0.01713

Shapiro-Wilk W test for normal data

Variable	Obs	W	V	z	Prob>z
rt1020075gr	10	0.83703	2.512	1.743	0.04065

Shapiro-Wilk W test for normal data

Variable	Obs	W	V	z	Prob>z

```
-------------+--------------------------------------------------
 rt104000gr |    10    0.76006     3.698     2.595    0.00473

            Shapiro-Wilk W test for normal data

   Variable |   Obs       W         V         z       Prob>z
-------------+--------------------------------------------------
 rt1040025gr |    10    0.78979     3.239     2.294    0.01089

            Shapiro-Wilk W test for normal data

   Variable |   Obs       W         V         z       Prob>z
-------------+--------------------------------------------------
 rt1040050gr |    10    0.80034     3.077     2.180    0.01464

            Shapiro-Wilk W test for normal data

   Variable |   Obs       W         V         z       Prob>z
-------------+--------------------------------------------------
 rt1040075gr |    10    0.80702     2.974     2.105    0.01764

            Shapiro-Wilk W test for normal data

   Variable |   Obs       W         V         z       Prob>z
-------------+--------------------------------------------------
 rt702000gr |    10    0.81287     2.884     2.038    0.02078

            Shapiro-Wilk W test for normal data

   Variable |   Obs       W         V         z       Prob>z
-------------+--------------------------------------------------
 rt7020025gr |    10    0.82935     2.630     1.840    0.03286

            Shapiro-Wilk W test for normal data

   Variable |   Obs       W         V         z       Prob>z
-------------+--------------------------------------------------
 rt7020050gr |    10    0.83914     2.479     1.716    0.04309

            Shapiro-Wilk W test for normal data

   Variable |   Obs       W         V         z       Prob>z
-------------+--------------------------------------------------
 rt7020075gr |    10    0.89910     1.555     0.792    0.21417

            Shapiro-Wilk W test for normal data

   Variable |   Obs       W         V         z       Prob>z
```

```
-------------+--------------------------------------------------
 rt704000gr |    10    0.78316     3.342     2.364    0.00905

            Shapiro-Wilk W test for normal data

   Variable |   Obs       W         V         z       Prob>z
-------------+--------------------------------------------------
 rt7040025gr |    10    0.85838     2.182     1.454    0.07303

            Shapiro-Wilk W test for normal data

   Variable |   Obs       W         V         z       Prob>z
-------------+--------------------------------------------------
 rt7040050gr |    10    0.94641     0.826    -0.322    0.62632

            Shapiro-Wilk W test for normal data

   Variable |   Obs       W         V         z       Prob>z
-------------+--------------------------------------------------
 rt7040075gr |    10    0.92889     1.096     0.158    0.43710

            Shapiro-Wilk W test for normal data

   Variable |   Obs       W         V         z       Prob>z
-------------+--------------------------------------------------
 lt102000gr |    10    0.97825     0.335    -1.697    0.95513

            Shapiro-Wilk W test for normal data

   Variable |   Obs       W         V         z       Prob>z
-------------+--------------------------------------------------
lt10200lacgr |    10    0.96589     0.526    -1.038    0.85039

            Shapiro-Wilk W test for normal data

   Variable |   Obs       W         V         z       Prob>z
-------------+--------------------------------------------------
 lt1020025gr |    10    0.76371     3.641     2.559    0.00524

            Shapiro-Wilk W test for normal data

   Variable |   Obs       W         V         z       Prob>z
-------------+--------------------------------------------------
 lt1020050gr |    10    0.81198     2.898     2.048    0.02027

            Shapiro-Wilk W test for normal data

   Variable |   Obs       W         V         z       Prob>z
```

```
-------------+--------------------------------------------------
 lt1020075gr |    10    0.57837     6.498     4.008    0.00003

                Shapiro-Wilk W test for normal data

    Variable |   Obs        W         V         z       Prob>z
-------------+--------------------------------------------------
 lt104000gr |    10    0.66257     5.200     3.422    0.00031

                Shapiro-Wilk W test for normal data

    Variable |   Obs        W         V         z       Prob>z
-------------+--------------------------------------------------
lt10400lacgr |    10    0.95047     0.763    -0.451    0.67405

                Shapiro-Wilk W test for normal data

    Variable |   Obs        W         V         z       Prob>z
-------------+--------------------------------------------------
 lt1040025gr |    10    0.96619     0.521    -1.051    0.85344

                Shapiro-Wilk W test for normal data

    Variable |   Obs        W         V         z       Prob>z
-------------+--------------------------------------------------
 lt1040050gr |    10    0.77497     3.468     2.448    0.00719

                Shapiro-Wilk W test for normal data

    Variable |   Obs        W         V         z       Prob>z
-------------+--------------------------------------------------
 lt1040075gr |    10    0.75525     3.772     2.641    0.00413

                Shapiro-Wilk W test for normal data

    Variable |   Obs        W         V         z       Prob>z
-------------+--------------------------------------------------
 lt702000gr |    10    0.97235     0.426    -1.352    0.91177

                Shapiro-Wilk W test for normal data

    Variable |   Obs        W         V         z       Prob>z
-------------+--------------------------------------------------
lt70200lacgr |    10    0.95373     0.713    -0.561    0.71272

                Shapiro-Wilk W test for normal data

    Variable |   Obs        W         V         z       Prob>z
```

```
-------------+--------------------------------------------------
 lt7020025gr |    10    0.90208     1.509     0.736    0.23090

                Shapiro-Wilk W test for normal data

    Variable |   Obs        W         V         z       Prob>z
-------------+--------------------------------------------------
 lt7020050gr |    10    0.97328     0.412    -1.402    0.91950

                Shapiro-Wilk W test for normal data

    Variable |   Obs        W         V         z       Prob>z
-------------+--------------------------------------------------
 lt7020075gr |    10    0.93442     1.011     0.018    0.49272

                Shapiro-Wilk W test for normal data

    Variable |   Obs        W         V         z       Prob>z
-------------+--------------------------------------------------
  lt704000gr |    10    0.88861     1.717     0.980    0.16358

                Shapiro-Wilk W test for normal data

    Variable |   Obs        W         V         z       Prob>z
-------------+--------------------------------------------------
lt70400lacgr |    10    0.89802     1.572     0.812    0.20837

                Shapiro-Wilk W test for normal data

    Variable |   Obs        W         V         z       Prob>z
-------------+--------------------------------------------------
 lt7040025gr |    10    0.84562     2.379     1.630    0.05152

                Shapiro-Wilk W test for normal data

    Variable |   Obs        W         V         z       Prob>z
-------------+--------------------------------------------------
 lt7040050gr |    10    0.94359     0.869    -0.237    0.59364

                Shapiro-Wilk W test for normal data

    Variable |   Obs        W         V         z       Prob>z
-------------+--------------------------------------------------
 lt7040075gr |    10    0.91271     1.345     0.524    0.30016

                Shapiro-Wilk W test for normal data

    Variable |   Obs        W         V         z       Prob>z
```

```
-------------+--------------------------------------------------
      animal |    10    0.97016      0.460   -1.239   0.89237

                    Shapiro-Wilk W test for normal data

    Variable |   Obs        W         V        z       Prob>z
-------------+--------------------------------------------------
 rt102000fc |    10    0.89745      1.580    0.823    0.20537

                    Shapiro-Wilk W test for normal data

    Variable |   Obs        W         V        z       Prob>z
-------------+--------------------------------------------------
rt1020025fc |    10    0.85070      2.301    1.561    0.05921

                    Shapiro-Wilk W test for normal data

    Variable |   Obs        W         V        z       Prob>z
-------------+--------------------------------------------------
rt1020050fc |    10    0.87751      1.888    1.164    0.12215

                    Shapiro-Wilk W test for normal data

    Variable |   Obs        W         V        z       Prob>z
-------------+--------------------------------------------------
rt1020075fc |    10    0.87982      1.852    1.127    0.12989

                    Shapiro-Wilk W test for normal data

    Variable |   Obs        W         V        z       Prob>z
-------------+--------------------------------------------------
 rt104000fc |    10    0.83181      2.592    1.810    0.03518

                    Shapiro-Wilk W test for normal data

    Variable |   Obs        W         V        z       Prob>z
-------------+--------------------------------------------------
rt1040025fc |    10    0.86521      2.077    1.354    0.08788

                    Shapiro-Wilk W test for normal data

    Variable |   Obs        W         V        z       Prob>z
-------------+--------------------------------------------------
rt1040050fc |    10    0.86609      2.064    1.341    0.08999

                    Shapiro-Wilk W test for normal data

    Variable |   Obs        W         V        z       Prob>z
```

```
-------------+--------------------------------------------------
 rt1040075fc |    10    0.83886     2.483     1.719    0.04276

              Shapiro-Wilk W test for normal data

    Variable |   Obs        W         V         z       Prob>z
-------------+--------------------------------------------------
 rt702000fc |    10    0.90421     1.476     0.695    0.24354

              Shapiro-Wilk W test for normal data

    Variable |   Obs        W         V         z       Prob>z
-------------+--------------------------------------------------
 rt7020025fc |    10    0.88908     1.709     0.972    0.16559

              Shapiro-Wilk W test for normal data

    Variable |   Obs        W         V         z       Prob>z
-------------+--------------------------------------------------
 rt7020050fc |    10    0.87984     1.852     1.127    0.12993

              Shapiro-Wilk W test for normal data

    Variable |   Obs        W         V         z       Prob>z
-------------+--------------------------------------------------
 rt7020075fc |    10    0.90691     1.435     0.642    0.26041

              Shapiro-Wilk W test for normal data

    Variable |   Obs        W         V         z       Prob>z
-------------+--------------------------------------------------
 rt704000fc |    10    0.84013     2.464     1.703    0.04428

              Shapiro-Wilk W test for normal data

    Variable |   Obs        W         V         z       Prob>z
-------------+--------------------------------------------------
 rt7040025fc |    10    0.86087     2.144     1.418    0.07813

              Shapiro-Wilk W test for normal data

    Variable |   Obs        W         V         z       Prob>z
-------------+--------------------------------------------------
 rt7040050fc |    10    0.94328     0.874    -0.228    0.59006

              Shapiro-Wilk W test for normal data

    Variable |   Obs        W         V         z       Prob>z
```

```
-------------+--------------------------------------------------
 rt7040075fc |    10    0.93138      1.057     0.096    0.46163

                    Shapiro-Wilk W test for normal data

    Variable |   Obs        W         V         z       Prob>z
-------------+--------------------------------------------------
 lt102000fc |    10    0.97973      0.312    -1.795    0.96370

                    Shapiro-Wilk W test for normal data

    Variable |   Obs        W         V         z       Prob>z
-------------+--------------------------------------------------
lt10200lacfc |    10    0.98160      0.284    -1.929    0.97315

                    Shapiro-Wilk W test for normal data

    Variable |   Obs        W         V         z       Prob>z
-------------+--------------------------------------------------
 lt1020025fc |    10    0.74972      3.857     2.693    0.00354

                    Shapiro-Wilk W test for normal data

    Variable |   Obs        W         V         z       Prob>z
-------------+--------------------------------------------------
 lt1020050fc |    10    0.76567      3.611     2.540    0.00554

                    Shapiro-Wilk W test for normal data

    Variable |   Obs        W         V         z       Prob>z
-------------+--------------------------------------------------
 lt1020075fc |    10    0.55335      6.883     4.167    0.00002

                    Shapiro-Wilk W test for normal data

    Variable |   Obs        W         V         z       Prob>z
-------------+--------------------------------------------------
 lt104000fc |    10    0.71629      4.372     2.991    0.00139

                    Shapiro-Wilk W test for normal data

    Variable |   Obs        W         V         z       Prob>z
-------------+--------------------------------------------------
lt10400lacfc |    10    0.96063      0.607    -0.817    0.79303

                    Shapiro-Wilk W test for normal data

    Variable |   Obs        W         V         z       Prob>z
```

```
-------------+--------------------------------------------------
 lt1040025fc |    10    0.98346      0.255    -2.074    0.98096

                Shapiro-Wilk W test for normal data

    Variable |   Obs        W         V         z       Prob>z
-------------+--------------------------------------------------
 lt1040050fc |    10    0.78390      3.330     2.356    0.00924

                Shapiro-Wilk W test for normal data

    Variable |   Obs        W         V         z       Prob>z
-------------+--------------------------------------------------
 lt1040075fc |    10    0.75264      3.812     2.666    0.00384

                Shapiro-Wilk W test for normal data

    Variable |   Obs        W         V         z       Prob>z
-------------+--------------------------------------------------
  lt702000fc |    10    0.97939      0.318    -1.772    0.96182

                Shapiro-Wilk W test for normal data

    Variable |   Obs        W         V         z       Prob>z
-------------+--------------------------------------------------
lt70200lacfc |    10    0.95397      0.709    -0.569    0.71548

                Shapiro-Wilk W test for normal data

    Variable |   Obs        W         V         z       Prob>z
-------------+--------------------------------------------------
 lt7020025fc |    10    0.96701      0.508    -1.088    0.86179

                Shapiro-Wilk W test for normal data

    Variable |   Obs        W         V         z       Prob>z
-------------+--------------------------------------------------
 lt7020050fc |    10    0.94880      0.789    -0.397    0.65431

                Shapiro-Wilk W test for normal data

    Variable |   Obs        W         V         z       Prob>z
-------------+--------------------------------------------------
 lt7020075fc |    10    0.91899      1.248     0.389    0.34863

                Shapiro-Wilk W test for normal data

    Variable |   Obs        W         V         z       Prob>z
```

```
-------------+--------------------------------------------------
 lt704000fc |    10    0.86870      2.023     1.302    0.09654

                Shapiro-Wilk W test for normal data

    Variable |    Obs       W          V          z       Prob>z
-------------+--------------------------------------------------
lt70400lacfc |    10    0.95793      0.648    -0.713    0.76208

                Shapiro-Wilk W test for normal data

    Variable |    Obs       W          V          z       Prob>z
-------------+--------------------------------------------------
 lt7040025fc |    10    0.88833      1.721     0.985    0.16237

                Shapiro-Wilk W test for normal data

    Variable |    Obs       W          V          z       Prob>z
-------------+--------------------------------------------------
 lt7040050fc |    10    0.93723      0.967    -0.057    0.52259

                Shapiro-Wilk W test for normal data

    Variable |    Obs       W          V          z       Prob>z
-------------+--------------------------------------------------
 lt7040075fc |    10    0.86602      2.065     1.342    0.08982
```

Appendix 5 - Randomisation Test

```
> source("pair.test.v1.r.txt")
> pair.test
function(leg.l, leg.r, n.sims, rand.seed)
  set.seed(rand.seed);
  leg.l.len <- length(leg.l);
  leg.r.len <- length(leg.r);
  stopifnot(leg.l.len==leg.r.len);
#   t.legs <- cbind(leg.l, leg.r)
  lr.diff <- mean(abs(leg.l - leg.r));
  array.v.lr.diff <- rep(NA, n.sims)
  for (i in 1:n.sims)
     v.leg.r <- sample(leg.r, leg.r.len, replace=FALSE);
     v.leg.l <- sample(leg.l, leg.l.len, replace=FALSE);
     v.lr.diff <- mean(abs(v.leg.l - v.leg.r));
     array.v.lr.diff[i] <- v.lr.diff;
  xx <- 1*(lr.diff > array.v.lr.diff);
#   print(cbind(v.leg.l, v.leg.r, v.lr.diff);
  print(paste("lr.diff = ", lr.diff, sep=""));
  print(paste("mean(array.v.lr.diff) = ", mean(array.v.lr.diff), sep=""));
  print(paste("p.value = ", sum(xx)/n.sims, sep=""));
> pair.test(data1$Lt102000GR, data1$Rt102000GR, n.sims=10, rand.seed=1)
[1] "lr.diff = 0.1207632668"
[1] "mean(array.v.lr.diff) = 0.13528392306"
[1] "p.value = 0"
> pair.test(data1$Lt102000GR, data1$Rt102000GR, n.sims=10000, rand.seed=1)
[1] "lr.diff = 0.1207632668"
[1] "mean(array.v.lr.diff) = 0.1346281824275"
[1] "p.value = 0.1673"
> pair.test(data1$Lt702000GR, data1$Rt702000GR, n.sims=10000, rand.seed=1)
[1] "lr.diff = 0.1317293511"
```

[1] "mean(array.v.lr.diff) = 0.12444312802326"

[1] "p.value = 0.7672"

> pair.test(data1$Lt104000GR, data1$Rt104000GR, n.sims=10000, rand.seed=1)

[1] "lr.diff = 0.1801948604"

[1] "mean(array.v.lr.diff) = 0.17074731879768"

[1] "p.value = 0.8639"

> pair.test(data1$Lt704000GR, data1$Rt704000GR, n.sims=10000, rand.seed=1)

[1] "lr.diff = 0.150540982"

[1] "mean(array.v.lr.diff) = 0.14322858723688"

[1] "p.value = 0.7348"

> pair.test(data1$Lt102000FC, data1$Rt102000FC, n.sims=10000, rand.seed=1340110512)

[1] "lr.diff = 0.4113236391"

[1] "mean(array.v.lr.diff) = 0.4522894226443"

[1] "p.value = 0.2204"

> pair.test(data1$Lt702000FC, data1$Rt702000FC, n.sims=10000, rand.seed=1341110512)

[1] "lr.diff = 0.0658689187"

[1] "mean(array.v.lr.diff) = 0.05981349849666"

[1] "p.value = 0.8584"

> pair.test(data1$Lt104000FC, data1$Rt104000FC, n.sims=10000, rand.seed=1342110512)

[1] "lr.diff = 0.3127672142"

[1] "mean(array.v.lr.diff) = 0.28777843546306"

[1] "p.value = 0.8939"

> pair.test(data1$Lt704000FC, data1$Rt704000FC, n.sims=10000, rand.seed=1343110512)

[1] "lr.diff = 0.037032217"

[1] "mean(array.v.lr.diff) = 0.03416747446264"

[1] "p.value = 0.839"

References

Abrahamsson SO. Matrix metabolism and healing in the flexor tendon. Experimental studies on rabbit tendon. Scand J Plast Reconstr Surg Hand Surg Suppl. 1991, 23: 1-51.

Abrahamsson SO, Lundborg G, Lohmander LS. Tendon healing in vivo. An experimental model. Scand J Plast Reconstr Surg Hand Surg. 1989, 23: 199-205.

Ackermann PW, Li J, Finn A, Ahmed M, Kreicbergs A. Autonomic innervation of tendons, ligaments and joint capsules. A morphologic and quantitative study in the rat. J Orthop Res. 2001, 19: 372-8.

Al-Qattan MM, Al-Turaiki TM. Flexor tendon repair in zone 2 using a six-strand 'figure of eight' suture. J Hand Surg Eur Vol. 2009, 34: 322-8.

Amiel D, Frank CB, Harwood FL, Akeson WH, Kleiner JB. Collagen alteration in medial collateral ligament healing in a rabbit model. Connect Tissue Res. 1987, 16: 357-66.

An KN, Berglund L, Uchiyama S, Coert JH. Measurement of friction between pulley and flexor tendon. Biomed Sci Instrum. 1993, 29: 1-7.

Angeles JG, Heminger H, Mass DP. Comparative biomechanical performances of 4-strand core suture repairs for zone II flexor tendon lacerations. J Hand Surg Am. 2002, 27: 508-17.

Aoki M, Manske PR, Pruitt DL, Larson BJ. Work of flexion after tendon repair with various suture methods. A human cadaveric study. J Hand Surg Br. 1995, 20: 310-3.

Archambault JM, Wiley JP, Bray RC. Exercise loading of tendons and the development of overuse injuries. A review of current literature. Sports Med. 1995, 20: 77-89.

Astrom M. Laser Doppler flowmetry in the assessment of tendon blood flow. Scand J Med Sci Sports. 2000, 10: 365-7.

Bailey AJ, Robins SP, Balian G. Biological significance of the intermolecular crosslinks of collagen. Nature. 1974, 251: 105-9.

Barr M, Kiernan J. *The Human Nervous System – An Anatomical Viewpoint.* London, JB Lippincott Company, 1988.

Becker W, Krahl H. *Die Tendopathien. Grundlagen, Klinik, Therapie*. Stuttgart, Georg Thieme, 1978.

Benazzo F, Zanon G, Maffulli N. An operative approach to Achilles tendinopathy. Sports Med Arthroscopy Rev 2000: 96-101.

Benjamin M, Ralphs JR. Fibrocartilage in tendons and ligaments--an adaptation to compressive load. J Anat. 1998, 193 (Pt 4): 481-94.

Berschback JC, Amadio PC, Zhao C, Zobitz ME, An KN. Providing quantitative feedback when teaching tendon repair: a new tool. J Hand Surg Br. 2005, 30: 626-32.

Best T, Garrett W. Basic science of soft tissue: muscle and tendon. *In: DeLee JC, Drez D (eds) Orthopaedic Sports Medicine: Principles and Practice*. Philadelphia, USA, WB Saunders, 1994: 24-5.

Bestwick CS, Maffulli N. Reactive oxygen species and tendinopathy: do they matter? Br J Sports Med. 2004, 38: 672-4.

Bilos ZJ, Hui PW, Stamelos S. Trigger finger following partial flexor tendon laceration. Hand. 1977, 9: 232-3.

Birch HL, Wilson AM, Goodship AE. The effect of exercise-induced localised hyperthermia on tendon cell survival. J Exp Biol. 1997, 200: 1703-8.

Bourne RB, Bitar H, Andreae PR, Martin LM, Finlay JB, Marquis F. In-vivo comparison of four absorbable sutures: Vicryl, Dexon Plus, Maxon and PDS. Can J Surg. 1988, 31: 43-5.

Boushel R, Langberg H, Green S, Skovgaard D, Bulow J, Kjaer M. Blood flow and oxygenation in peritendinous tissue and calf muscle during dynamic exercise in humans. J Physiol. 2000, 524 Pt 1: 305-13.

Boyes JH. *Bumaell's surgery of the hand*, 5th ed. Philadelphia, USA, JB Lippincott, 1970.

Brain SD, Williams TJ, Tippins JR, Morris HR, MacIntyre I. Calcitonin gene-related peptide is a potent vasodilator. Nature. 1985, 313: 54-6.

Branford OA, Lee DA, Bader DL, Grobbelaar AO. The mechanics of flexor tendon adhesions. J Hand Surg Eur Vol. 2011, 37: 555-63.

Bunata RE, Simmons S, Roso M, Kosmopoulos V. Gliding resistance and triggering after venting or A2 pulley enlargement: a study of intact and repaired flexor tendons in a cadaveric model. J Hand Surg Am. 2011, 36: 1316-22.

Bunnell S. *Surgery of the hand*, 3rd ed. Philadelphia, USA, JB Lippincott, 1956: 712.

Butler DL, Grood ES, Noyes FR, Zernicke RF. Biomechanics of ligaments and tendons. Exerc Sport Sci Rev. 1978, 6: 125-81.

Cao Y, Chen CH, Wu YF, Xu XF, Xie RG, Tang JB. Digital oedema, adhesion formation and resistance to digital motion after primary flexor tendon repair. J Hand Surg Eur Vol. 2008, 33: 745-52.

Cao Y, Zhu B, Xie RG, Tang JB. Influence of core suture purchase length on strength of four-strand tendon repairs. J Hand Surg Am. 2006, 31: 107-12.

Carlstedt CA. Mechanical and chemical factors in tendon healing. Effects of indomethacin and surgery in the rabbit. Acta Orthop Scand Suppl. 1987, 224: 1-75.

Carr AJ, Norris SH. The blood supply of the calcaneal tendon. J Bone Joint Surg Br. 1989, 71: 100-1.

Chansky HA, Iannotti JP. The vascularity of the rotator cuff. Clin Sports Med. 1991, 10: 807-22.

Clancy SP, Mass DP. Current flexor and extensor tendon motion regimens: a summary. Hand Clin. 2013, 29: 295-309.

Clark TA, Skeete K, Amadio PC. Flexor tendon pulley reconstruction. J Hand Surg Am. 2010, 35: 1685-9.

Clayton RA, Court-Brown CM. The epidemiology of musculoskeletal tendinous and ligamentous injuries. Injury. 2008, 39: 1338-44.

Courage KH. Turkey Legs Tell the Tale of Our Unsung Tendons. Scientific American. 2011.

Curwin S. Biomechanics of tendon and the effects of immobilization. Foot Ankle Clin. 1997: 371-89.

Curwin S, Stanish W. *Tendinitis: Its Etiology and Treatment*. Lexington, USA, Collamore Press, 1984.

Diamant J, Keller A, Baer E, Litt M, Arridge RG. Collagen; ultrastructure and its relation to mechanical properties as a function of ageing. Proc R Soc Lond B Biol Sci. 1972, 180: 293-315.

Diao E, Hariharan JS, Soejima O, Lotz JC. Effect of peripheral suture depth on strength of tendon repairs. J Hand Surg Am. 1996, 21: 234-9.

Dias JJ, Garcia-Elias M. Hand injury costs. Injury. 2006, 37: 1071-7.

Dinopoulos HT, Boyer MI, Burns ME, Gelberman RH, Silva MJ. The resistance of a four- and eight-strand suture technique to gap formation during tensile testing: an experimental study of

repaired canine flexor tendons after 10 days of in vivo healing. J Hand Surg Am. 2000, 25: 489-98.

Dona E, Turner AW, Gianoutsos MP, Walsh WR. Biomechanical properties of four circumferential flexor tendon suture techniques. J Hand Surg Am. 2003, 28: 824-31.

Dona E, Walsh WR. Flexor tendon pulley V-Y plasty: an alternative to pulley venting or resection. J Hand Surg Br. 2006, 31: 133-7.

Douglas A. Effect of repair techniques and freezing on tendon gliding properties. Leicester, UK, University of Leicester, 2013, Vol. Bachelor of Science.

Doyle JR. Anatomy of the finger flexor tendon sheath and pulley system. J Hand Surg Am. 1988, 13: 473-84.

Doyle JR. Anatomy of the flexor tendon sheath and pulley system: a current review. J Hand Surg Am. 1989, 14: 349-51.

Drake R, Vogl AW. Gray's Anatomy for Students Flash Cards: with STUDENT CONSULT Online Access, 3e Cards. 3rd ed, Churchill Livingstone, 2014.

Drape JL, Silbermann-Hoffman O, Houvet P et al. Complications of flexor tendon repair in the hand: MR imaging assessment. Radiology. 1996, 198: 219-24.

Duran R, Houser R. Controlled passive motion following flexor tendon repairing zones 2 and 3. In: Hunter J, Schneider L (Eds.) *AAOS symposium on tendon surgery in the hand*. St Louis (MO), CV Mosby, 1975: 105-14.

Dy CJ, Daluiski A. Flexor pulley reconstruction. Hand Clin. 2013, 29: 235-42.

Ejeskar A. Finger flexion force and hand grip strength after tendon repair. J Hand Surg Am. 1982, 7: 61-5.

Elliot D, Giesen T. Primary flexor tendon surgery: the search for a perfect result. Hand Clin 2013: 191-206.

Elliott DH. Structure and function of mammalian tendon. Biol Rev 1965, 40: 392-421.

Ellis FD, Seiler JG, Sewell CW. The second annular pulley: a histological examination. J Hand Surg 1995, 20A: 632-5.

Evans CH. Cytokines and the role they play in the healing of ligaments and tendons. Sports Med. 1999, 28: 71-6.

Evans EJ, Benjamin M, Pemberton DJ. Fibrocartilage in the attachment zones of the quadriceps tendon and patellar ligament of man. J Anat. 1990, 171: 155-62.

Evans TJ, Buttery LD, Carpenter A, Springall DR, Polak JM, Cohen J. Cytokine-treated human neutrophils contain inducible nitric oxide synthase that produces nitration of ingested bacteria. Proc Natl Acad Sci U S A. 1996, 93: 9553-8.

Fan L, Sarkar K, Franks DJ, Uhthoff HK. Estimation of total collagen and types I and III collagen in canine rotator cuff tendons. Calcif Tissue Int. 1997, 61: 223-9.

Farkas LG, Thomson HG, Martin R. Some practical notes on the anatomy of the chicken toe for surgeon investigators. Plast Reconstr Surg. 1974, 54: 452-8.

Field PL. Tendon fibre arrangement and blood supply. Aust N Z J Surg. 1971, 40: 298-302.

Franko OI, Lee NM, Finneran JJ et al. Quantification of partial or complete A4 pulley release with FDP repair in cadaveric tendons. J Hand Surg Am. 2011, 36: 439-45.

Fujita M, Hukuda S, Doida Y. [Experimental study of intrinsic healing of the flexor tendon: collagen synthesis of the cultured flexor tendon cells of the canine]. Nihon Seikeigeka Gakkai Zasshi. 1992, 66: 326-33.

Fyfe I, Stanish WD. The use of eccentric training and stretching in the treatment and prevention of tendon injuries. Clin Sports Med. 1992, 11: 601-24.

Gelberman RH, Boyer MI, Brodt MD, Winters SC, Silva MJ. The effect of gap formation at the repair site on the strength and excursion of intrasynovial flexor tendons. An experimental study on the early stages of tendon-healing in dogs. J Bone Joint Surg Am. 1999, 81: 975-82.

Gelberman RH, Manske PR, Akeson WH, Woo SL, Lundborg G, Amiel D. Flexor tendon repair. J Orthop Res. 1986, 4: 119-28.

Gelberman RH, Manske PR, Vande Berg JS, Lesker PA, Akeson WH. Flexor tendon repair in vitro: a comparative histologic study of the rabbit, chicken, dog, and monkey. J Orthop Res. 1984, 2: 39-48.

Gelberman RH, Nunley JA, 2nd, Osterman AL, Breen TF, Dimick MP, Woo SL. Influences of the protected passive mobilization interval on flexor tendon healing. A prospective randomized clinical study. Clin Orthop Relat Res. 1991: 189-96.

Gelse K, Poschl E, Aigner T. Collagens--structure, function, and biosynthesis. Adv Drug Deliv Rev. 2003, 55: 1531-46.

Gill RS, Lim BH, Shatford RA, Toth E, Voor MJ, Tsai TM. A comparative analysis of the six-strand double-loop flexor tendon repair and three other techniques: a human cadaveric study. J Hand Surg Am. 1999, 24: 1315-22.

Goodship AE, Birch HL, Wilson AM. The pathobiology and repair of tendon and ligament injury. Vet Clin North Am Equine Pract. 1994, 10: 323-49.

Gordon SL. Late rupture of one slip on the floor digitorum superficialis: an unusual cause of triggering. Clin Orthop Relat Res. 1981: 142-3.

Gratton P. Early active mobilization after flexor tendon repairs. J Hand Ther. 1993, 6: 285-9.

Greenwald D, Shumway S, Albear P, Gottlieb L. Mechanical comparison of 10 suture materials before and after in vivo incubation. J Surg Res. 1994, 56: 372-7.

Greiling D, Clark RA. Fibronectin provides a conduit for fibroblast transmigration from collagenous stroma into fibrin clot provisional matrix. J Cell Sci. 1997, 110 (Pt 7): 861-70.

Gulihar A, Hajipour L, Dias JJ. Comparison of three different peripheral suturing techniques for partial flexor tendon lacerations: a controlled in-vitro biomechanical study. Hand Surg. 2012, 17: 155-60.

Haddad RJ, Jr., Kester MA, McCluskey GM, Brunet ME, Cook SD. Comparative mechanical analysis of a looped-suture tendon repair. J Hand Surg Am. 1988, 13: 709-13.

Hajipour L, Gulihar A, Dias J. Effect of laceration and trimming of a tendon on the coefficient of friction along the A2 pulley: an in vitro study on turkey tendon. J Bone Joint Surg Br. 2010, 92: 1171-5.

Harris SB, Harris D, Foster AJ, Elliot D. The aetiology of acute rupture of flexor tendon repairs in zones 1 and 2 of the fingers during early mobilization. J Hand Surg Br. 1999, 24: 275-80.

Hess GP, Cappiello WL, Poole RM, Hunter SC. Prevention and treatment of overuse tendon injuries. Sports Med. 1989, 8: 371-84.

Hirpara KM, Sullivan PJ, Raheem O, O'Sullivan ME. A biomechanical analysis of multistrand repairs with the Silfverskiold peripheral cross-stitch. J Bone Joint Surg Br. 2007, 89: 1396-401.

Hooley CJ, McCrum NG, Cohen RE. The viscoelastic deformation of tendon. J Biomech. 1980, 13: 521-8.

Inoue H, Takasugi H, Akahori O. Surface study of tenosynovium in hens and humans by electron microscopy. Hand. 1976, 8: 222-7.

Inoue H, Takasugi H, Akahori O. Surface Study of Tenosynovium in Hens and Humans By Electron Microscopy. The Hand. 1976, 8: 222-7.

Joyce CW, Whately KE, Chan JC, Murphy M, O'Brien FJ, Carroll SM. Flexor tendon repair: a comparative study between a knotless barbed suture repair and a traditional four-strand monofilament suture repair. J Hand Surg Eur Vol. 2014, 39: 40-5.

Jozsa L, Balint B. The architecture human of tendons. II. The peritenonium and so-called surface phenomenon. Traumatologia. 1978: 293-7.

Jozsa L, Balint JB, Reffy A, Demel Z. Histochemical and ultrastructural study of adult human tendon. Acta Histochem. 1979, 65: 250-7.

Jozsa L, Kannus P. Tendons. Anatomy, Physiology, and Pathology. *Champaign, IL: Human Kinetics*, 1997: 47-8; 54–5; 6–7; 9; 76–7; 80–1; 104.

Jozsa L, Kannus P, Balint JB, Reffy A. Three-dimensional ultrastructure of human tendons. Acta Anat (Basel). 1991, 142: 306-12.

Jozsa L, Lehto M, Kvist M, Balint JB, Reffy A. Alterations in dry mass content of collagen fibers in degenerative tendinopathy and tendon-rupture. Matrix. 1989, 9: 140-6.

Kadler KE, Baldock C, Bella J, Boot-Handford RP. Collagens at a glance. J Cell Sci. 2007, 120: 1955-8.

Kannus P. Structure of the tendon connective tissue. Scand J Med Sci Sports. 2000, 10: 312-20.

Kannus P, Jozsa L. Histopathological changes preceding spontaneous rupture of a tendon. A controlled study of 891 patients. J Bone Joint Surg Am. 1991, 73: 1507-25.

Kannus P, Jozsa L, Jarvinen TA et al. Location and distribution of non-collagenous matrix proteins in musculoskeletal tissues of rat. Histochem J. 1998, 30: 799-810.

Kannus P, Jozsa L, Jarvinnen M. Basic science of tendons. In: Garrett W, Speer K, Kirkendall D (Eds.) *Principles and Practice of Orthopaedic Sports Medicine*. Philadelphia, USA, Lippincott Williams & Wilkins, 2000: 21-37.

Kannus P, Jozsa L, Natri A, Jarvinen M. Effects of training, immobilization and remobilization on tendons. Scand J Med Sci Sports. 1997, 7: 67-71.

Karpakka J. Effects of physical activity and inactivity on collagen synthesis in rat skeletal muscle and tendon. Oulu, Finland, University of Oulu, 1991: 1-52.

Kastelic J, Galeski A, Baer E. The multicomposite structure of tendon. Connect Tissue Res. 1978, 6: 11-23.

Kennedy JA. Effect of laceration and trimming on gliding properties along the A2 pulley. Leicester, Uk, University of Leicester, 2011, Vol. MSc.

Kennedy JA, Dias JJ. Effect of triggering and entrapment on tendon gliding properties following digital flexor tendon laceration: in vitro study on turkey tendon. J Hand Surg Eur Vol. 2013, 39: 708-13.

Khan KM, Cook JL, Bonar F, Harcourt P, Astrom M. Histopathology of common tendinopathies. Update and implications for clinical management. Sports Med. 1999, 27: 393-408.

Kirkendall DT, Garrett WE. Function and biomechanics of tendons. Scand J Med Sci Sports. 1997, 7: 62-6.

Kleinert H, Forshew F, Cohen M. Repair of zone 1 flexor tendon injuries. In: AAOS symposium on tendon surgery in the hand. St Louis Mosby, 1975: 115-22.

Komanduri M, Phillips CS, Mass DP. Tensile strength of flexor tendon repairs in a dynamic cadaver model. J Hand Surg Am. 1996, 21: 605-11.

Komi PV, Fukashiro S, Jarvinen M. Biomechanical loading of Achilles tendon during normal locomotion. Clin Sports Med. 1992, 11: 521-31.

Koob TJ. Biomimetic approaches to tendon repair. Comp Biochem Physiol A Mol Integr Physiol. 2002, 133: 1171-92.

Koob TJ, Summers AP. Tendon--bridging the gap. Comp Biochem Physiol A Mol Integr Physiol. 2002, 133: 905-9.

Korstanje JW, Soeters JN, Schreuders TA et al. Ultrasonographic assessment of flexor tendon mobilization: effect of different protocols on tendon excursion. J Bone Joint Surg Am. 2012, 94: 394-402.

Kusano N, Yoshizu T, Maki Y. Experimental study of two new flexor tendon suture techniques for postoperative early active flexion exercises. J Hand Surg Br. 1999, 24: 152-6.

Kvist M. Achilles tendon injuries in athletes. Sports Med. 1994, 18: 173-201.

Kvist M, Jozsa L, Jarvinen M, Kvist H. Fine structural alterations in chronic Achilles paratenonitis in athletes. Pathol Res Pract. 1985, 180: 416-23.

Kvist M, Jozsa L, Jarvinen MJ, Kvist H. Chronic Achilles paratenonitis in athletes: a histological and histochemical study. Pathology. 1987, 19: 1-11.

Kvist M, Jozsa L, Kannus P et al. Morphology and histochemistry of the myotendineal junction of the rat calf muscles. Histochemical, immunohistochemical and electron-microscopic study. Acta Anat (Basel). 1991, 141: 199-205.

Kwai Ben I, Elliot D. "Venting" or partial lateral release of the A2 and A4 pulleys after repair of zone 2 flexor tendon injuries. J Hand Surg Br. 1998, 23: 649-54.

Lappalainen R, Knuuttila M, Lammi S, Alhava EM, Olkkonen H. Zn and Cu content in human cancellous bone. Acta Orthop Scand. 1982, 53: 51-5.

Lee H. Double loop locking suture: a technique of tendon repair for early active mobilization. Part I: Evolution of technique and experimental study. J Hand Surg Am. 1990, 15: 945-52.

Lephart SM, Pincivero DM, Giraldo JL, Fu FH. The role of proprioception in the management and rehabilitation of athletic injuries. Am J Sports Med. 1997, 25: 130-7.

Leversedge FJ, Ditsios K, Goldfarb CA, Silva MJ, Gelberman RH, Boyer MI. Vascular anatomy of the human flexor digitorum profundus tendon insertion. J Hand Surg Am. 2002, 27: 806-12.

Lieber RL, Amiel D, Kaufman KR, Whitney J, Gelberman RH. Relationship between joint motion and flexor tendon force in the canine forelimb. J Hand Surg Am. 1996, 21: 957-62.

Lin GT, Amadio PC, An KN, Cooney WP. Functional anatomy of the human digital flexor pulley system. J Hand Surg Am. 1989, 14: 949-56.

Lin GT, An KN, Amadio PC, Cooney WP, 3rd. Biomechanical studies of running suture for flexor tendon repair in dogs. J Hand Surg Am. 1988, 13: 553-8.

Lin GT, Cooney WP, Amadio PC, An KN. Mechanical properties of human pulleys. J Hand Surg Br. 1990, 15: 429-34.

Lister GD, Kleinert HE, Kutz JE, Atasoy E. Primary flexor tendon repair followed by immediate controlled mobilization. J Hand Surg Am. 1977, 2: 441-51.

Lui PP, Cheuk YC, Hung LK, Fu SC, Chan KM. Increased apoptosis at the late stage of tendon healing. Wound Repair Regen. 2007, 15: 702-7.

Lundborg G, Myrhage R. The vascularization and structure of the human digital tendon sheath as related to flexor tendon function. An angiographic and histological study. Scand J Plast Reconstr Surg. 1977, 11: 195-203.

Macaluso A, De Vito G. Muscle strength, power and adaptations to resistance training in older people. Eur J Appl Physiol. 2004, 91: 450-72.

Mackie EJ, Ramsey S. Expression of tenascin in joint-associated tissues during development and postnatal growth. J Anat. 1996, 188 (Pt 1): 157-65.

Maffulli N, Barrass V, Ewen SW. Light microscopic histology of achilles tendon ruptures. A comparison with unruptured tendons. Am J Sports Med. 2000, 28: 857-63.

Maffulli N, King JB. Effects of physical activity on some components of the skeletal system. Sports Med. 1992, 13: 393-407.

Maganaris CN, Narici MV, Reeves ND. In vivo human tendon mechanical properties: effect of resistance training in old age. J Musculoskelet Neuronal Interact. 2004, 4: 204-8.

Maganaris CN, Reeves ND, Rittweger J et al. Adaptive response of human tendon to paralysis. Muscle Nerve. 2006, 33: 85-92.

Manchio JV, Shashikant MP, Shrivastava A, Weinzweig J, Vernadakis AJ. Evaluation of a new 4-strand flexor tendon repair in a cadaveric porcine model. J Hand Surg Am. 2009, 34: 102-7.

Manske PR, Gelberman RH, Lesker PA. Flexor tendon healing. Hand Clin. 1985, 1: 25-34.

Matthews P, Richards H. Factors in the adherence of flexor tendon after repair: an experimental study in the rabbit. J Bone Joint Surg Br. 1976, 58: 230-6.

McGrouther DA, Ahmed MR. Flexor tendon excursions in "no-man's land". Hand. 1981, 13: 129-41.

McLarney E, Hoffman H, Wolfe SW. Biomechanical analysis of the cruciate four-strand flexor tendon repair. J Hand Surg Am. 1999, 24: 295-301.

Merrell GA, Wolfe SW, Kacena WJ, Gao Y, Cholewicki J, Kacena MA. The effect of increased peripheral suture purchase on the strength of flexor tendon repairs. J Hand Surg Am. 2003, 28: 464-8.

Minor RR. Collagen metabolism: a comparison of diseases of collagen and diseases affecting collagen. Am J Pathol. 1980, 98: 225-80.

Mishra V, Kuiper JH, Kelly CP. Influence of core suture material and peripheral repair technique on the strength of Kessler flexor tendon repair. J Hand Surg Br. 2003, 28: 357-62.

Mitsionis G, Bastidas JA, Grewal R, Pfaeffle HJ, Fischer KJ, Tomaino MM. Feasibility of partial A2 and A4 pulley excision: effect on finger flexor tendon biomechanics. J Hand Surg Am. 1999, 24: 310-4.

Molloy T, Wang Y, Murrell G. The roles of growth factors in tendon and ligament healing. Sports Med. 2003, 33: 381-94.

Momose T, Amadio PC, Zhao C, Zobitz ME, An KN. The effect of knot location, suture material, and suture size on the gliding resistance of flexor tendons. J Biomed Mater Res. 2000, 53: 806-11.

Moriya T, Larson MC, Zhao C, An KN, Amadio PC. The effect of core suture flexor tendon repair techniques on gliding resistance during static cycle motion and load to failure: a human cadaver study. J Hand Surg Eur Vol. 2012, 37: 316-22.

Moriya T, Zhao C, Yamashita T, An KN, Amadio PC. Effect of core suture technique and type on the gliding resistance during cyclic motion following flexor tendon repair: a cadaveric study. J Orthop Res. 2010, 28: 1475-81.

Moro-oka T, Miura H, Mawatari T et al. Mixture of hyaluronic acid and phospholipid prevents adhesion formation on the injured flexor tendon in rabbits. J Orthop Res. 2000, 18: 835-40.

Mosler E, Folkhard W, Knorzer E, Nemetschek-Gansler H, Nemetschek T, Koch MH. Stress-induced molecular rearrangement in tendon collagen. J Mol Biol. 1985, 182: 589-96.

Muffly TM, Cook C, Distasio J, Bonham AJ, Blandon RE. Suture end length as a function of knot integrity. J Surg Educ. 2009, 66: 276-80.

Murphy PG, Loitz BJ, Frank CB, Hart DA. Influence of exogenous growth factors on the synthesis and secretion of collagen types I and III by explants of normal and healing rabbit ligaments. Biochem Cell Biol. 1994, 72: 403-9.

Murrell GA, Szabo C, Hannafin JA et al. Modulation of tendon healing by nitric oxide. Inflamm Res. 1997, 46: 19-27.

Myllyharju J, Kivirikko KI. Collagens and collagen-related diseases. Ann Med. 2001, 33: 7-21.

Naito M, Ogata K. The blood supply of the tendon with a paratenon. An experimental study using hydrogen washout technique. Hand. 1983, 15: 9-14.

Nakamura-Craig M, Smith TW. Substance P and peripheral inflammatory hyperalgesia. Pain. 1989, 38: 91-8.

Nelson GN, Potter R, Ntouvali E et al. Intrasynovial flexor tendon repair: a biomechanical study of variations in suture application in human cadavera. J Orthop Res. 2012, 30: 1652-9.

O'Brien M. Structure and metabolism of tendons. Scand J Med Sci Sports. 1997, 7: 55-61.

Oakes B. Tissue healing and repair: tendons and ligaments. *In: Frontera WR (ed) Rehabilitation of Sports Injuries: Scientific Basis*. Oxford, UK, Blackwell Science, 2003: 56-98.

Ochiai N, Matsui T, Miyaji N, Merklin RJ, Hunter JM. Vascular anatomy of flexor tendons. I. Vincular system and blood supply of the profundus tendon in the digital sheath. J Hand Surg Am. 1979, 4: 321-30.

Peltz TS, Haddad R, Scougall PJ, Gianoutsos MP, Bertollo N, Walsh WR. Performance of a knotless four-strand flexor tendon repair with a unidirectional barbed suture device: a dynamic ex vivo comparison. J Hand Surg Eur Vol. 2014, 39: 30-9.

Peterson WW, Manske PR, Bollinger BA, Lesker PA, McCarthy JA. Effect of pulley excision on flexor tendon biomechanics. J Orthop Res. 1986, 4: 96-101.

Pettengill KM. The evolution of early mobilization of the repaired flexor tendon. J Hand Ther. 2005, 18: 157-68.

Phillips GF, McGrouther DA, Andrews BJ. Finger mobility following flexor tendon repair. J Hand Surg Br. 1985, 10: 337-9.

Potenza AD. CRITICAL EVALUATION OF FLEXOR-TENDON HEALING AND ADHESION FORMATION WITHIN ARTIFICIAL DIGITAL SHEATHS. J Bone Joint Surg Am. 1963, 45: 1217-33.

Reeves ND, Narici MV, Maganaris CN. Strength training alters the viscoelastic properties of tendons in elderly humans. Muscle Nerve. 2003, 28: 74-81.

Reynolds NL, Worrell TW. Chronic achilles peritendinitis: etiology, pathophysiology, and treatment. J Orthop Sports Phys Ther. 1991, 13: 171-6.

Riederer-Henderson MA, Gauger A, Olson L, Robertson C, Greenlee TK, Jr. Attachment and extracellular matrix differences between tendon and synovial fibroblastic cells. In Vitro. 1983, 19: 127-33.

Riley GP, Curry V, DeGroot J et al. Matrix metalloproteinase activities and their relationship with collagen remodelling in tendon pathology. Matrix Biol. 2002, 21: 185-95.

Rispler D, Greenwald D, Shumway S, Allan C, Mass D. Efficiency of the flexor tendon pulley system in human cadaver hands. J Hand Surg Am. 1996, 21: 444-50.

Rosberg HE, Carlsson KS, Hojgard S, Lindgren B, Lundborg G, Dahlin LB. What determines the costs of repair and rehabilitation of flexor tendon injuries in zone II? A multiple regression analysis of data from southern Sweden. J Hand Surg Br. 2003, 28: 106-12.

Rowe RW. The structure of rat tail tendon fascicles. Connect Tissue Res. 1985, 14: 21-30.

Sandow MJ, McMahon M. Active mobilisation following single cross grasp four-strand flexor tenorrhaphy (Adelaide repair). J Hand Surg Eur Vol. 2011, 36: 467-75.

Sasaki N, Shukunami N, Matsushima N, Izumi Y. Time-resolved X-ray diffraction from tendon collagen during creep using synchrotron radiation. J Biomech. 1999, 32: 285-92.

Savage R. In vitro studies of a new method of flexor tendon repair. J Hand Surg Br. 1985, 10: 135-41.

Savage R. The mechanical effect of partial resection of the digital fibrous flexor sheath. J Hand Surg Br. 1990, 15: 435-42.

Savage R. The search for the ideal tendon repair in zone 2: strand number, anchor points and suture thickness. J Hand Surg Eur Vol. 2014, 39: 20-9.

Sbernardori MC, Mazzarello V, Tranquilli-Leali P. Scanning electron microscopic findings of the gliding surface of the A1 pulley in trigger fingers and thumbs. J Hand Surg Eur Vol. 2007, 32: 384-7.

Schlenker JD, Lister GD, Kleinert HE. Three complications of untreated partial laceration of flexor tendon--entrapment, rupture, and triggering. J Hand Surg Am. 1981, 6: 392-8.

Schor RA, Prussin SG, Jewett DL, Ludowieg JJ, Bhatnagar RS. Trace levels of manganese, copper, and zinc in rib cartilage as related to age in humans and animals, both normal and dwarfed. Clin Orthop Relat Res. 1973: 346-55.

Schuind F, Garcia-Elias M, Cooney WP, 3rd, An KN. Flexor tendon forces: in vivo measurements. J Hand Surg Am. 1992, 17: 291-8.

Selvanetti A, Cipolla M, Puddu G. Overuse tendon injuries: basic science and classification. Oper Tech Sports Med. 1997: 110-7.

Seyfer AE, Bolger WE. Effects of unrestricted motion on healing: a study of posttraumatic adhesions in primate tendons. Plast Reconstr Surg. 1989, 83: 122-8.

Shadwick RE. Elastic energy storage in tendons: mechanical differences related to function and age. J Appl Physiol (1985). 1990, 68: 1033-40.

Shaieb MD, Singer DI. Tensile strengths of various suture techniques. J Hand Surg Br. 1997, 22: 764-7.

Sharma P, Maffulli N. Tendon injury and tendinopathy: healing and repair. J Bone Joint Surg Am. 2005, 87: 187-202.

Sharma P, Maffulli N. Biology of tendon injury: healing, modeling and remodeling. J Musculoskelet Neuronal Interact. 2006, 6: 181-90.

Shoulders MD, Raines RT. Collagen structure and stability. Annu Rev Biochem. 2009, 78: 929-58.

Silfverskiold KL, Andersson CH. Two new methods of tendon repair: an in vitro evaluation of tensile strength and gap formation. J Hand Surg Am. 1993, 18: 58-65.

Silfverskiold KL, May EJ. Flexor tendon repair in zone II with a new suture technique and an early mobilization program combining passive and active flexion. J Hand Surg Am. 1994, 19: 53-60.

Silfverskiold KL, May EJ, Tornvall AH. Gap formation during controlled motion after flexor tendon repair in zone II: a prospective clinical study. J Hand Surg Am. 1992, 17: 539-46.

Small JO, Brennen MD, Colville J. Early active mobilisation following flexor tendon repair in zone 2. J Hand Surg Br. 1989, 14: 383-91.

Smith AM, Forder JA, Annapureddy SR, Reddy KS, Amis AA. The porcine forelimb as a model for human flexor tendon surgery. J Hand Surg Br. 2005, 30: 307-9.

Srugi S, Adamson JE. A comparative study of tendon suture materials in dogs. Plast Reconstr Surg. 1972, 50: 31-5.

Strick MJ, Filan SL, Hile M, McKenzie C, Walsh WR, Tonkin MA. Adhesion formation after flexor tendon repair: a histologic and biomechanical comparison of 2- and 4-strand repairs in a chicken model. J Hand Surg Am. 2004, 29: 15-21.

Strickland J. Flexor tendons: acute injuries. In: Green D, Hotchkiss R, Pedersen W (Eds.) *Green's Operative Hand Surgery*. New York, USA, Churchill Livingstone, 1997: 1851-97.

Strickland JW. The scientific basis for advances in flexor tendon surgery. J Hand Ther. 2005, 18: 94-110; quiz 1.

Strickland JW, Glogovac SV. Digital function following flexor tendon repair in Zone II: A comparison of immobilization and controlled passive motion techniques. J Hand Surg Am. 1980, 5: 537-43.

Sun YL, Yang C, Amadio PC, Zhao C, Zobitz ME, An KN. Reducing friction by chemically modifying the surface of extrasynovial tendon grafts. J Orthop Res. 2004, 22: 984-9.

Syed M, Frew Q, Sood M. Use of porcine trotters as models for flexor tendon repair—the pulley system. Eur J Plast Surg 2013: 449-52.

Taguchi M, Sun YL, Zhao C et al. Lubricin surface modification improves extrasynovial tendon gliding in a canine model in vitro. J Bone Joint Surg Am. 2008, 90: 129-35.

Takeuchi N, Mitsuyasu H, Hotokezaka S, Miura H, Higaki H, Iwamoto Y. Strength enhancement of the interlocking mechanism in cross-stitch peripheral sutures for flexor tendon repair: biomechanical comparisons by cyclic loading. J Hand Surg Eur Vol. 2010, 35: 46-50.

Takeuchi N, Mitsuyasu H, Kikuchi K, Shimoto T, Higaki H, Iwamoto Y. The biomechanical assessment of gap formation after flexor tendon repair using partial interlocking cross-stitch peripheral sutures. J Hand Surg Eur Vol. 2011, 36: 584-9.

Tan J, Tang JB. Locking repairs for obliquely cut tendons: Effects of suture purchase and directions of locking circles. J Hand Surg Am. 2004, 29: 891-7.

Tanaka T, Amadio PC, Zhao C, Zobitz ME, An KN. Gliding resistance versus work of flexion--two methods to assess flexor tendon repair. J Orthop Res. 2003, 21: 813-8.

Tanaka T, Amadio PC, Zhao C, Zobitz ME, An KN. The effect of partial A2 pulley excision on gliding resistance and pulley strength in vitro. J Hand Surg Am. 2004, 29: 877-83.

Tanaka T, Amadio PC, Zhao C, Zobitz ME, An KN. Flexor digitorum profundus tendon tension during finger manipulation. J Hand Ther. 2005, 18: 330-8; quiz 8.

Tanaka T, Zhao C, Sun YL, Zobitz ME, An KN, Amadio PC. The effect of carbodiimide-derivatized hyaluronic acid and gelatin surface modification on peroneus longus tendon graft in a short-term canine model in vivo. J Hand Surg Am. 2007, 32: 876-81.

Tang J. Flexor tendon repair. In: Neligan P, Chang J (Eds.) *Plastic surgery*. Philadelphia, Elsevier Saunders, 2012, Vol. 6: 178-205.

Tang JB. Subdivision of ''no man's land''. *Presented at the Fourth Meeting of Chinese Society for Surgery of the Hand*. Wuxi, Jiangsu, 1990.

Tang JB. The double sheath system and tendon gliding in zone 2C. J Hand Surg Br. 1995, 20: 281-5.

Tang JB. Outcomes and evaluation of flexor tendon repair. Hand Clin. 2013, 29: 251-9.

Tang JB, Amadio PC, Boyer MI et al. Current practice of primary flexor tendon repair: a global view. Hand Clin. 2013, 29: 179-89.

Tang JB, Cao Y, Wu YF, Wang GH. Effect of A2 pulley release on repaired tendon gliding resistance and rupture in a chicken model. J Hand Surg Am. 2009, 34: 1080-7.

Tang JB, Gu YT, Rice K, Chen F, Pan CZ. Evaluation of four methods of flexor tendon repair for postoperative active mobilization. Plast Reconstr Surg. 2001, 107: 742-9.

Tang JB, Ishii S, Usui M. Surviving processes of free grafted tendon sheath. Chinese Journal of Surgery. 1990, 28: 473-5.

Tang JB, Wang YH, Gu YT, Chen F. Effect of pulley integrity on excursions and work of flexion in healing flexor tendons. J Hand Surg Am. 2001, 26: 347-53.

Tang JB, Xie RG, Cao Y, Ke ZS, Xu Y. A2 pulley incision or one slip of the superficialis improves flexor tendon repairs. Clin Orthop Relat Res. 2007, 456: 121-7.

Tang JB, Zhang QG, Ishii S. Autogenous free sheath grafts in reconstruction of injured digital flexor tendon sheath at the delayed primary stage. J Hand Surg Br. 1993, 18: 31-2.

Tang JB, Zhang Y, Cao Y, Xie RG. Core suture purchase affects strength of tendon repairs. J Hand Surg Am. 2005, 30: 1262-6.

Taras JS, Raphael JS, Marczyk SC, Bauerle WB. Evaluation of suture caliber in flexor tendon repair. J Hand Surg Am. 2001, 26: 1100-4.

Territo MC, Cline MJ. Mononuclear phagocyte proliferation, maturation and function. Clin Haematol. 1975, 4: 685-703.

Tillman LJ, Chasan NP. Properties of dense connective tissue and wound healing. In: Hertling D, Kessler R (Eds.) *Management of common musculoskeletal disorders: physical therapy principles and methods*, 3rd ed. Philadelphia, Lippincott, 1996: 8-21.

Tipton C, Vailas A, Laughlin H, Diana J. Aerobic characteristics of isolated ligaments and tendons. Physiologist. 1975b, 14: 422-30.

Tipton CM, Matthes RD, Maynard JA, Carey RA. The influence of physical activity on ligaments and tendons. Med Sci Sports. 1975, 7: 165-75.

Tomaino M, Mitsionis G, Basitidas J, Grewal R, Pfaeffle J. The effect of partial excision of the A2 and A4 pulleys on the biomechanics of finger flexion. J Hand Surg Br. 1998, 23: 50-2.

Trail IA, Powell ES, Noble J. An evaluation of suture materials used in tendon surgery. J Hand Surg Br. 1989, 14: 422-7.

Trail IA, Powell ES, Noble J. The mechanical strength of various suture techniques. J Hand Surg Br. 1992, 17: 89-91.

Uchiyama S, Amadio PC, Berglund LJ, An KN. Analysis of the gliding pattern of the canine flexor digitorum profundus tendon through the A2 pulley. J Biomech. 2008, 41: 1281-8.

Uchiyama S, Amadio PC, Coert JH, Berglund LJ, An KN. Gliding resistance of extrasynovial and intrasynovial tendons through the A2 pulley. J Bone Joint Surg Am. 1997, 79: 219-24.

Uchiyama S, Coert JH, Berglund L, Amadio PC, An KN. Method for the measurement of friction between tendon and pulley. J Orthop Res. 1995, 13: 83-9.

Vailas AC, Tipton CM, Laughlin HL, Tcheng TK, Matthes RD. Physical activity and hypophysectomy on the aerobic capacity of ligaments and tendons. J Appl Physiol Respir Environ Exerc Physiol. 1978, 44: 542-6.

Verdan CE. Half a century of flexor-tendon surgery. Current status and changing philosophies. J Bone Joint Surg Am. 1972, 54: 472-91.

Viidik A. Tendons and ligaments. In: Comper W, Sharma P, Maffulli N (Eds.) *Tendon injury and healing Extracellular Matrix*. Amsterdam, Netherlands, Harwood Academic Publishers, 1996, Vol. 1: 303-27.

Viinikainen A, Goransson H, Huovinen K, Kellomaki M, Tormala P, Rokkanen P. The strength of the 6-strand modified Kessler repair performed with triple-stranded or triple-stranded bound suture in a porcine extensor tendon model: an ex vivo study. J Hand Surg Am. 2007, 32: 510-7.

Wade PJ, Wetherell RG, Amis AA. Flexor tendon repair: significant gain in strength from the Halsted peripheral suture technique. J Hand Surg Br. 1989, 14: 232-5.

Wagner WF, Jr., Carroll Ct, Strickland JW, Heck DA, Toombs JP. A biomechanical comparison of techniques of flexor tendon repair. J Hand Surg Am. 1994, 19: 979-83.

Wang B, Tang JB. Embedded cross-stitch suture: An alternative to current cross-stitch peripheral suture. J Hand Surg 2003: 471-4.

Williams JG. Achilles tendon lesions in sport. Sports Med. 1986, 3: 114-35.

Wong JK, Cerovac S, Ferguson MW, McGrouther DA. The cellular effect of a single interrupted suture on tendon. J Hand Surg Br. 2006, 31: 358-67.

Woo SL, Debski RE, Zeminski J, Abramowitch SD, Saw SS, Fenwick JA. Injury and repair of ligaments and tendons. Annu Rev Biomed Eng. 2000, 2: 83-118.

Wu YF, Tang JB. Effects of tension across the tendon repair site on tendon gap and ultimate strength. J Hand Surg Am. 2012, 37: 906-12.

Wu YF, Tang JB. Tendon healing, edema, and resistance to flexor tendon gliding: clinical implications. Hand Clin. 2013, 29: 167-78.

Xie RG, Cao Y, Xu XF, Zhu B. The gliding force and work of flexion in the early days after primary repair of lacerated flexor tendons: an experimental study. J Hand Surg Eur Vol. 2008, 33: 192-6.

Xie RG, Tang JB. Investigation of locking configurations for tendon repair. J Hand Surg Am. 2005, 30: 461-5.

Xie RG, Xue HG, Gu JH, Tan J, Tang JB. Effects of locking area on strength of 2- and 4-strand locking tendon repairs. J Hand Surg Am. 2005, 30: 455-60.

Xu Y, Tang JB. Effects of superficialis tendon repairs on lacerated profundus tendons within or proximal to the A2 pulley: an in vivo study in chickens. J Hand Surg Am. 2003, 28: 994-1001.

Yamamoto E, Hayashi K, Yamamoto N. Mechanical properties of collagen fascicles from stress-shielded patellar tendons in the rabbit. Clin Biomech (Bristol, Avon). 1999, 14: 418-25.

Yanagishita M. Function of proteoglycans in the extracellular matrix. Acta Pathol Jpn. 1993, 43: 283-93.

Yuan J, Wang MX, Murrell GA. Cell death and tendinopathy. Clin Sports Med. 2003, 22: 693-701.

Zhao C, Amadio PC, Momose T, Zobitz ME, Couvreur P, An KN. Remodeling of the gliding surface after flexor tendon repair in a canine model in vivo. J Orthop Res. 2002, 20: 857-62.

Zhao C, Amadio PC, Paillard P et al. Digital resistance and tendon strength during the first week after flexor digitorum profundus tendon repair in a canine model in vivo. J Bone Joint Surg Am. 2004, 86-A: 320-7.

Zhao C, Amadio PC, Zobitz ME, An KN. Gliding characteristics of tendon repair in canine flexor digitorum profundus tendons. J Orthop Res. 2001, 19: 580-6.

Zhao CF, Amadio PC, Berglund L, An KN. The A3 pulley. J Hand Surg Am. 2000, 25: 270-6.

Ziche M, Morbidelli L, Masini E et al. Nitric oxide mediates angiogenesis in vivo and endothelial cell growth and migration in vitro promoted by substance P. J Clin Invest. 1994, 94: 2036-44.

Zidel P. Tendon healing and flexor tendon surgery. In: Thorne CH (Ed.) *Grabb and Smith's Plastic surgery*, 6th ed, Lippincott Williams & Wilkins, 2007: 803-9.